Final report

Assessment of communication masking in Antarctic marine mammals by underwater sound from airguns

by:

Dr. Benno Wölfing, Prof. Dr. Marianne Rasmussen, Dr. Tobias Schaffeld,
Dr. Joseph Schnitzler, Prof. Prof. h. c. Dr. Ursula Siebert
Stiftung Tierärztliche Hochschule Hannover (TiHo), Institut für Terrestrische und
Aquatische Wildtierforschung (ITAW), Büsum (Germany)

Dr. Peter Stilz
Freelance Biologist (Germany)

Prof. Dr. Alexander Gavrilov, Prof. Dr. Christine Erbe, Prof. Dr. Robert McCauley
Curtin University, Centre for Marine Science and Technology (CMST), Bentley
(Western Australia)

Prof. Dr. Magnus Wahlberg
University of Southern Denmark (SDU), Odense (Denmark)

Matthias Fischer, Max Schuster, Dr. Dietrich Wittekind
DW-ShipConsult GmbH (DWSC), Schwentinental (Germany)

German Environment Agency

Umwelt Bundesamt

Assessment of communication masking in Antarctic marine mammals by underwater sound from airguns

by
Dr. Benno Wölfing, Prof. Dr. Marianne Rasmussen, Dr. Tobias Schaffeld,
Dr. Joseph Schnitzler, Prof. Prof. h. c. Dr. Ursula Siebert
Stiftung Tierärztliche Hochschule Hannover (TiHo), Institut für Terrestrische
und Aquatische Wildtierforschung (ITAW), Büsum (Germany)

Dr. Peter Stilz
Freelance Biologist (Germany)

Prof. Dr. Alexander Gavrilov, Prof. Dr. Christine Erbe, Prof. Dr. Robert McCauley
Curtin University, Centre for Marine Science and Technology (CMST) , Bentley
(Western Australia)

Prof. Dr. Magnus Wahlberg
University of Southern Denmark (SDU), Odense (Denmark)

Matthias Fischer, Max Schuster, Dr. Dietrich Wittekind
DW-ShipConsult GmbH (DWSC), Schwentinental (Germany)

Abstract: Assessment of communication masking in Antarctic marine mammals by underwater sound from airguns

Airguns used in seismic explorations and scientific surveys produce high-intensity impulsive sounds with most energy concentrated in the low frequency band. Apart from the potential to induce permanent and temporary shifts of hearing threshold and to trigger disturbance reactions, airgun noise can mask the perception of acoustic environmental cues. This frequency range overlaps with many marine mammal vocalizations, especially the songs and calls of baleen whales. Airguns may therefore mask marine mammal communication signals even at large distances from the airgun location. This study assesses the communication masking potential of airgun noise in the Southern Ocean using a modelling approach.

A parabolic equation approximation was used to model the propagation of airgun pulses in the Southern Ocean. The propagation models were verified based on recordings of two seismic surveys in the Southern Ocean. Model predictions are consistent with the measurement results within a few decibels for the sound exposure and energy spectral levels. Multiple ray paths arise from the point source with a three-dimensional spreading and resulting reflections from the water surface and seabed. These rays, which connect the source with the receiver differ in length. Ray arrival of a short impulsive signal at the receiver is therefore not simultaneous. Accordingly, the length of the received signal increases with distance from the source. The amount of this so-called signal stretching was slightly underestimated by the propagation model. Airguns operating over the Australian continental shelf were found to be best correlated with the sound fixing and ranging (SOFAR) channel when the water depth was in the range of 300 to 700 meters, leading to much further propagation distances. Sound scattering by the surface due to surface wind-waves was found to be an important cause of transmission loss in the region south of the polar front.

The verified propagation models allowed for predicting the received levels of airgun pulses and animal vocalization signals at the animal's ear for any distance to the airgun as well as to the vocalizing conspecific. A psychophysical model based on a spectrogram correlation receiver was developed in order to reflect temporal and spectral resolving properties of the animal' auditory system. It predicts that communication ranges of blue and fin whales can still be severely reduced at distances between 1000 and 2000 kilometres from an airgun survey. For example, the model predicts that airgun operations at a distance of 2000 km from the listening individual can reduce the detection range for Antarctic blue whale z-calls from 40 km (natural communication range under high ambient noise conditions) to 15 km. The context in which blue whale z-calls and fin whale 20 Hz calls are produced indicates that these calls have important functions for mating and possibly foraging, which both necessitate long-range communication. For species with high-frequency or broadband vocalizations such as killer whales and Weddell seals, the extent of communication masking depends on the degree animals rely on the low frequency part of the vocalizations to extract biologically relevant information, which remains unknown to date.

Kurzbeschreibung: Bewertung der Kommunikationsmaskierung bei antarktischen Meeressäugern durch Unterwasserschall von Airguns

Airguns werden bei seismischen Erkundungen und wissenschaftlichen Untersuchungen eingesetzt und erzeugen impulshafte Schallsignale mit hoher Intensität im tieffrequenten Bereich. Abgesehen von der Möglichkeit, permanente oder temporäre Hörschädigungen zu induzieren oder Verhaltensreaktionen auszulösen, können Airgungsignale die Wahrnehmung relevanter akustischer Signale in der Umwelt maskieren. Dieser Frequenzbereich überschneidet sich mit vielen Vokalisationen von Meeressäugern, insbesondere den Gesängen und Rufen von Bartenwalen. Auf Grund der hohen Quellschallpegel besitzen Airguns das Potential Kommunikationssignale von Meeressäugern auch noch in großen Entfernungen zu maskieren. Dieses Potential zur Maskierung von Kommunikationssignalen im Südpolarmeer wird in dieser Studie mithilfe eines Modellierungsansatzes bewertet.

Um die Ausbreitung von Airgunimpulsen im Südpolarmeer zu modellieren, wurde eine parabolische Gleichungsnäherung verwendet,. Die Ausbreitungsmodelle wurden anhand von Aufzeichnungen zweier seismischer Vermessungen im Südpolarmeer validiert. Die Modellvorhersagen zeigen eine große Übereinstimmung in den empfangenen Schallpegel und den Frequenzspektren mit den Messergebnissen und weichen nur um wenige Dezibel ab. Durch die von einer Punktquelle ausgehende dreidimensionale Schallsusbreitung und den resultierenden Reflektionen an der Wasseroberfläche und dem Meeresboden ergeben sich mehrere Strahlengänge. Diese Strahlengänge, die Schallquelle und Empfänger verbinden, besitzen unterschiedliche Längen, so dass Signale über die verschiedenen Wege den Empfänger nicht gleichzeitig erreichen. Die Dauer der empfangenen Signale nimmt entsprechend mit der Entfernung von der Schallquelle zu. Das Ausmaß dieser sogenannten Signalstreckung wurde vom Ausbreitungsmodell leicht unterschätzt. Für Airguns, die über dem australischen Festlandsockel eingesetzt wurden, wurde die höchste Korrelation mit dem SOFAR-Kanal (Sound Fixing and Ranging) gefunden, wenn die Wassertiefe im Bereich von 300 bis 700 Metern lag, woraus sich sehr große Ausbreitungsdistanzen ergeben. Es wurde festgestellt, dass Übertragungsverluste in der Region südlich der Polarfront maßgeblich durch die Schallstreuung an der Oberfläche, ausgelöst durch Windwellen beeinflusst wird.

Die validierten Ausbreitungsmodelle ermöglichen es, die empfangenen Schallpegel der Airgun- und Vokalisierungssignale am Ohr des Tieres für jede Entfernung zur Airgun sowie zu vokalisierenden Artgenossen vorherzusagen. Ein psychophysisches Modell basierend auf einem Spektrogramm-Korrelationsempfänger wurde entwickelt, um die zeitlichen und spektralen Auflösungseigenschaften des tierischen Hörvermögens widerzuspiegeln. Das Modell sagt vorher, dass Kommunikationsreichweiten von Blau- und Finnwalen in Entfernungen zwischen 1000 und 2000 Kilometern von dem Airgunmessungen, noch erheblich beeinträchtigt sein können. Für den Einsatz von Airguns in einer Entfernung von 2000 km vom hörenden Individuum modelliert es eine Reduzierung der Detektionsreichweite für Z-Rufe von Blauwalen in der Antarktis von 40 km (natürliche Kommunikationsreichweite unter Bedingungen mit hohem Umgebungsgeräusch) auf 15 km. Der Kontext, in dem Blauwal-Z-Rufe und Finnwal-20-Hz-Rufe erzeugt werden, zeigt, dass diese Rufe wichtige Funktionen für die Paarung und möglicherweise Nahrungssuche haben und somit eine Langstreckenkommunikation erfordern. Bei Arten mit hochfrequenten oder breitbandigen Lautäußerungen wie Schwertwalen und Weddellrobben hängt das Ausmaß der Kommunikationsmaskierung davon ab, wie stark Tiere von dem tieffrequenten Anteil der Lautäußerungen abhängig sind, um biologisch relevante Informationen zu extrahieren. Diese Abhängigkeit wurde bislang jedoch noch nicht untersucht.

Acknowledgment

Table of Contents

List of Figures

List of Tables

List of Abbreviations

KOPRI	Korea Polar Research Institute
AAD	Australian Antarctic Division
CMST	Centre for Marine Science and Technology
CSIRO	Commonwealth Scientific and Industrial Research Organisation
ESD	Energy Spectral Level
ETOPO2	Earth TOPOgraphy of 2 min resolution
PE	Parabolic Equation
SEL	Sound Exposure Level
SOFAR	SOund Fixing And Ranging channel
PGS	Petroleum Geo-Services
ESD, ESD_R, ESD_S	Energy spectral density level, $_R$ receiver, $_S$ source

Summary

Concern about the effects of underwater noise on marine ecosystems is growing. The importance of the acoustic sense has been documented in a wide variety of behavioural contexts. Vocalizations play a role in finding and competing for mating partners. Another important function of vocalizations is that they facilitate the reunion of mothers with their young and can serve to maintain cohesion between members of larger groups that forage or migrate together.

The Antarctic is protected by stringent environmental protection regulations. The Antarctic Treaty manifests the intention to use the Antarctic for peaceful purposes only. Additionally, the Protocol on Environmental Protection to the Antarctic Treaty has been ratified by 33 states. This protocol implements the strictest and most comprehensive environmental regulations, which have ever been developed for any region of the world in an international agreement. Germany is a Party to the Antarctic Treaty and thus assumes responsibility for the Antarctic. The German Environment Agency (UBA) is the national competent authority and issues permits for German activities in the Antarctic. These activities include scientific marine seismic surveys, which typically apply sound sources consisting of small airgun arrays. Airguns produce a high-intensity impulsive sound by suddenly releasing highly pressurized air into the water and represent one of the loudest anthropogenic noise sources in the ocean. The scientific basis for evaluating the effects of airgun operations on marine mammals still has gaps in knowledge. Evidence of auditory effects on the hearing of marine mammals due to intensive or chronic noise exposure serve as a very important regulatory tool for mitigating effects of underwater noise. Existing studies show that airgun noise can induce temporary shifts of the hearing threshold in marine mammals (Kastelein et al. 2017, Sills et al. 2020). Noise exposures of high energy can even lead to a permanent threshold shift, as it has been accidentally shown for a harbour seal (Reichmuth et al. 2019). In addition to hearing impairment, airgun pulses can also trigger disturbance or displacement reactions (Castellote et al. 2012, Nowacek et al. 2015). Knowledge on the extent of communication masking caused by airgun noise and on the effects of communication masking at the level of the individual and the population is still limited. This study seeks to assess the extent of communication masking by airgun noise for selected Antarctic marine mammals and discusses effects on an individual and population level building on and refining models developed in a preceding project (Siebert et al. 2014).

The importance of the acoustic sense has been documented in a wide variety of behavioural contexts. Here we list behavioural contexts and provide examples with a focus on marine mammal species that occur in the Antarctic Ocean. Fin whale songs (sequences of 20 Hz calls) recorded in a fin whale breeding ground were exclusively produced by males (Croll et al. 2002). The behavioural context strongly suggests that these acoustic cues serve to attract females from great distances (Croll et al. 2002). Song sequences of Antarctic blue whale Z-calls have also been proposed to be male reproductive display signals (Thomisch et al. 2016, Croll et al. 2002). Male Weddell seal calls during the breeding season are likely important for the establishment of underwater territories (Rouget et al. 2007) and for attracting females (Opzeeland et al. 2010) and may serve as honest signals of male fitness as studied for leopard seals (Rogers et al. 2017). Moreover, calls can advertise feeding opportunities. The fin whale songs discussed above have e.g. been suggested to serve two functions: Males call to attract females, while females move towards the callers to take advantage of good feeding opportunities (Croll et al. 2002).

Another important function of vocalizations is that they facilitate the reunion of mothers with their young. In Weddell seals airborne calls of mothers and pups facilitate successful reunions after foraging excursions of the mother (Collins et al. 2005, Collins et al. 2011, Opzeeland et al. 2012). These studies have shown that there is substantial inter-individual variation between the calls of mothers as well as pups. Despite this variation in vocalizations between individuals, playback experiments suggest that acoustic cues alone are not sufficient for individual recognition between a pup and its mother (Collins et al. 2005, Opzeeland et al. 2012). In baleen whales, contact calls are likely important to maintain or re-establish the mother-calf bond (e.g. after deep dives of the mother). Similar to the function of

maintaining the union between a mother and its young, acoustic cues can serve to maintain cohesion between members of larger groups that forage or migrate together.

Communication of marine mammals can be masked by noise, especially if the frequency range of noise and vocalizations overlap. In order to evaluate if a marine mammal is affected by noise, it is important to know the spectral, temporal and amplitude characteristics of the species vocalizations. Indeed, since even individuals at distances as far as several thousand kilometres away from the airgun location may suffer from acoustic masking (Nieukirk et al. 2012, Siebert et al. 2014), masking may be the most pervasive effect of airgun noise. Marine mammals may respond to increased noise levels by increasing the amplitude, altering the frequency content or increasing the repetition rate of their vocalizations (Erbe et al. 2016). **Chapter two** presents a **pilot study** that assesses the occurrence of such antimasking strategies in blue whales off Iceland. We investigated the call rate and its relation to time or number of boats. Although the call rate was quite variable, we found indications that the anthropogenic noise level might affect the blue whale call rate. The blue whales were calling more often under noisier conditions, although this trend was not significant. A similar phenomenon was found by Di Iorio and Clark (2010), who observed that blue whales emitted significantly more calls during seismic activities (noisy) than in periods when the seismic sound source was not operating. Effects on the blue whale calling rate were only found for noise exposures in the frequency range of their vocalisations (48-102 Hz). Noise exposures at a higher frequency band (150 -500 Hz), which do not overlap with the frequency band of blue whale calls, seem not to affect the blue whale calling rate. Most energy of airgun pulses is concentrated in the low frequency band. This frequency range overlaps with many marine mammal vocalizations, especially the songs and calls of baleen whales. While acoustic cues are not limited to vocalizations of conspecifics, but also include cues for predator presence (Cure et al. 2015) as well as cues important for orientation (Clark et al. 2009), masking of communication signals may have severe negative effects on baleen whales.

To gain insight into the spatial extent of masking, sound propagation in the focal environment in the Antarctic has to be understood. In **chapter three** sound **propagation models** are developed for the Antarctic Ocean. In this project two different data sets of airgun noise from two surveys in the Antarctic **(Figure 1)** were used to verify model predictions.

This first dataset (referred to as the "**ARAGORN dataset**") was recorded in the Southern Ocean in 2006 while PGS Geophysical was conducting an offshore seismic survey over the Australian continental shelf and slope in the western part of the Bass Strait. The investigations were recorded using three autonomous underwater sound recorders deployed at three different locations: southwest of Tasmania (at ~500 km distance from airguns), within the Antarctic Convergence zone (at ~1600 km distance from airguns) and near the Antarctic continental shelf (at ~2900 km distance from airguns).

The second dataset (denoted as "**ARAON dataset**") was recorded in February 2015 during the Tangaroa 2015 Research Voyage at Ross Sea. HIDAR sonobuoys were deployed to track marine mammal presence. 28 sonobuoys were deployed while a nearby seismic survey (at distances between 50 and 500 km from airguns) was conducted from R/V Araon.

For each of the two datasets a corresponding modelling strategy was used. A numerical approach was used to model the sound emission and propagation from the airgun array used in the Aragorn survey to the most distant underwater sound recorder on the continental slope in Antarctica (at location 3 shown on the map in Figure 1). The model tested with the ARAON dataset allowed to model the time domain representation of a received signal from a source signal. Even short pulses will experience pronounced stretching when traveling long distances. A comparison with respect to magnitude and signal stretching could be made for selected sonobuoys at different distances from the airguns. The expected signal stretching is higher for sonobuoys situated further away from the airguns due to the longer propagation distance. The far field representation of the source (waveform, time series) needs indeed to assess time related propagation phenomena, such as signal stretching, which is a result of frequency-dependent

sound propagation. The sound propagation models allow estimating the received signal (including stretching and level) at the position of the listener (received signal at distances ranging from 100 m to up to 3000 km) from the source signal.

Figure 1 **Left)** The "**ARAGORN dataset**" was recorded in the Southern Ocean in 2006 using three autonomous underwater sound recorders deployed at three locations at ~500 km, at ~1600 km and ~2900 km distance from the airguns. **Right)** The "**ARAON dataset**" was recorded on 28 sonobuoys deployed 50 to 500 km from a nearby seismic survey. The seismic transects are shown by red lines and location of the deployed sonobuoys (blue circles).

Both modelling approaches are validated by a comparison of modelled signals with measurements of the respective recordings of airgun noise of two seismic surveys conducted in the Southern Ocean. Signals change in level, frequency content and duration (or more specifically "temporal structure") as they radiate from the sound source. The validated models provide insight into how physical phenomena affect sound propagation in the Southern Ocean and help us to understand the physical parameters, which affect the propagation of sound signals (airgun as well as animal vocalizations (i.e. communication signals) and therefore the received signal that arrives at a listener.

Our analysis of recordings of seismic surveys as well as the sound propagation models (chapter three) illustrates that low-frequency airgun noise could affect intraspecific communication at distances exceeding 2000 km from the source location. For seismic surveys conducted at the northern edges of the Southern Ocean, the best coupling of the airgun sound source with the SOFAR underwater sound channel and thus the highest potential for masking in Antarctic waters occurs, when the airgun is located over the continental slope (chapter three). Ambient noise can reduce the audible range for airgun noise and accordingly the range at which airgun noise can mask communication signals. In **chapter four** we analysed **ambient noise** at three different locations in the eastern part of the Southern Ocean in 2006. In addition to noise arising from abiotic sound sources, three characteristic features can be distinguished in the long-time average spectrogram: intense broadband noise between 15 and 30 Hz arising from multiple calls from fin whales (*Balaenoptera physalus*), chorus of Z-shaped calls from Antarctic blue whales with a frequency around 20 Hz and slightly below 30 Hz and relatively narrowband noise at 300-350 Hz visibly formed by multiple sounds from Antarctic seals.

In **chapter five** a **psychophysical model (masking model)** is developed that predicts if a receiving animal can detect a conspecific's vocalization in various scenarios (variation of ocean, source and receiver depth, as well as ambient noise levels). The ability of an animal to detect a signal in the presence of noise depends on the absolute sensitivity of its auditory system. Signal detection depends on the frequency tuning characteristics of the system, which is defined as the resolution of the auditory system to separate a sound into its individual frequency components. The temporal processing characteristics of the system, which correspond to the auditory integration time, determine the auditory perception (Erbe et al. 2016). For signals with a characteristic frequency and intensity pattern over time, a hearing system that searches for these patterns and thus make use of the combined time-frequency-intensity structure of a signal (this project: "Masking II") will be much more sensitive than a hearing system that only analyses the total energy accumulating within a time interval and frequency band (previous project: "Masking I"[1]). The "Masking II" project is based on the previous project "Masking I" and represents a refinement of the developed model, which aims at assessing masking potential from airguns in the Antarctic.

The psychophysical model basically consists of three components **(Figure 2)**:

1. For every scenario the signal arriving at the animal's ear is modelled first by mixing the propagated airgun and/or vocalization with ocean noise. Based on the validated **propagation models** developed in chapter three, the airgun noise that a listener receives can be inferred for any distance between the listener and the airgun source. Moreover, the propagation models can be used to infer the vocalization that a listener receives for any distance between the listener and the vocalizing conspecific. Overall, mixing of the received airgun noise, the received vocalization and the ambient noise allows inference of the sound arriving at the receiver animal's ear for any given distance to the airgun location and the location of the vocalizing conspecific. Sound samples are generated in which the propagated vocalization signal is either present or not and challenge the receiver model to detect a vocalisation.

2. Based on the receiver models "leaky integrator" or "spectrogram correlator", the signal detector representing the auditory hearing system is modelled. The receiver model is challenged with sound samples and has to decide whether or not a propagated vocalization signal is present in a sound sample.

    a) The receiver model of the earlier airgun project (Siebert et al. 2014) consisted of a **leaky integrator** model, which integrated the received energy within the frequency band of the focal vocalization in a temporally lossy manner. The maximum levels of the leaky integrator output of vocalization and interference noise are analysed and compared (in an alternative analysis, only over a certain time slice), and it is postulated on the basis of this comparison whether communication is possible or not.

    b) In the current project, we developed also a **spectrogram correlator,** which represents a phase-insensitive receiver. The receiver matches a representation of the incoming sound sample (as generated in component 1) with a spectral representation (a characteristic frequency and intensity pattern) of the search signal over time and evaluates their similarity over time. This principle functionally corresponds to the comparison of the stimulation pattern of the cochlear output over time with a search pattern of the signal. The spectrogram correlation receiver model is a very sensitive receiver, because it makes use of the full time-frequency information in the signal and the masker.

3. To determine the detection success and ranges a fundamentally different approach was applied within this project as compared to Siebert et al. 2014. Both for spectrogram correlator model as well

---

[1] https://www.umweltbundesamt.de/sites/default/files/medien/378/publikationen/texte_16_2014_0.pdf)

as the leaky integrator model implemented in this project, the evaluation of whether a sufficiently successful classification was possible in the focal scenario was performed according to standardized classification theory (receiver operating characteristic curve (ROC AUC)). Based on Branstetter et al. (2016) we assumed that detection of vocalizations was sufficiently precise to allow communication if the area under the ROC (in short: ROC AUC) exceeded 0.9.

Figure 2   Schematic representation of the general setup of the psychophysical model. For every scenario the signal arriving at the animal's ear is modelled first (by mixing the propagated airgun and/or vocalization with ocean noise). Next the auditory system is modelled by a signal detector, that decides based on an adjustable threshold if a vocalization is present or not.
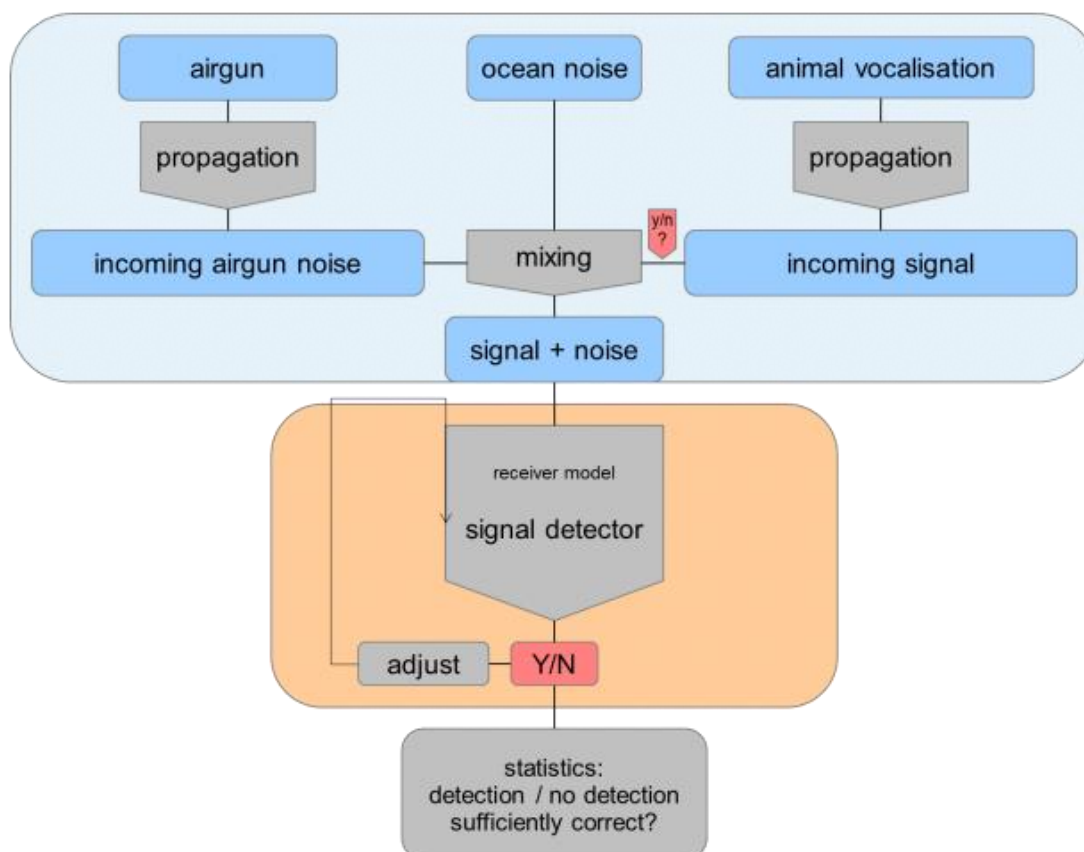
Different transmission scenarios have been modelled depending on the water depth (500 m and 4000 m), the sender depths (5 m and 50 m) and the receiver depths (10 m, 50 m and 200 m) for all 5 vocalisation types (Blue whale Z-call, fin whale call, Killer whale multi-harmonic call, Weddell seal long sound and Weddell seal sound sequence). For better visualization the output of the models for all scenarios have been visualized with an interactive multimedia application, which provides a summary overview, explanations and individual illustrations (https://tschaffeld.shinyapps.io/UBA_mask/).

The superpositions of different reflections from sea floor, water surface and direct transmission path cause conspicuous irregularities. The transmission loss in the **shallow ocean** is distinctly higher than in the **deep ocean**, due to the monotonic decreasing behaviour of the sound propagation. Consequently, the effect ranges of airguns in the shallow ocean scenarios are generally distinctly smaller than in the deep ocean for communication distances of blue whales and fin whales (see example in **Figure 3**).

The most striking differences between the respective sound propagations for different **receiver depths** are that the influence of surface effects cause larger irregularities in propagation close to the source at shallow receiver depths (10 m). For blue whales and fin whales, which have long communication ranges, the differences between different receiver depths are not substantial and no clear systematic difference

between different receiver depths is obvious. The effect ranges of airguns for 200 m receiver depth are generally distinctly higher than for 10 m or 50 m receiver depth for communication distances of blue whales and fin whales (see example in **Figure 4**).

The level of the propagated sound originating from a depth of 5 m, is more attenuated than the sound originating from a **vocalization depth** of 50 m for the low-frequency transmission loss at long ranges. Thus, an increase in communication ranges is expected for blue and fin whale if these species vocalize at greater depths (50 m versus 5 m sender depth). Regarding overall attenuation for the remaining species using wideband vocalizations (with full frequency band analysis), there is no striking difference in the signal attenuation for vocalisation depths of 5 and 50 m. Thus, communication ranges do not differ significantly (see example in **Figure 5**).

Quantitative predictions of communication ranges depend on the vocalization, environmental conditions (natural ambient noise and sound propagation conditions / assumptions) and the **psychophysical model** (spectrogram correlator model or bandpass leaky integrator model). The spectrogram correlator detects vocalizations with higher precision than the leaky integrator, particularly if vocalizations have a characteristic spectral / frequency / intensity structure over the signal course, provided that the incoming signals are not distorted strongly and were not temporally stretched. For narrow-band signals, without a strong temporal signature (e.g. fin whale), the advantage can be only minor.

Due to the fact that several parts of the model were refined as compared to the previous project, a direct comparison between the model predictions from Masking I and II proves to be difficult. Main changes include (1) Sound propagation modeling (spherical spreading vs. new numerical model) 2) Auditory model (band pass leaky integrator vs. new spectrogram correlation) and 3) Detection model (signal> noise vs. AUC receiver operating characteristic)) at the same time. This means that the potential causes of variations cannot be clearly identified. Nevertheless, the results of the Masking II modeling support the core message of the Masking I report which indicated that airgun sounds can lead to a significant loss in communication range for blue and fin whales at 2000 km from the source.

In the following table 1 we present acoustic communication distances for Blue whales in quiet ambient noise conditions (80 dB), moderate ambient noise conditions (94 dB), medium ambient noise conditions (102 dB) and high ambient noise conditions (112 dB). As expected, the distance range in which an airgun causes interference is generally larger in low ocean noise scenarios than in higher ocean noise scenarios.

Table 1   Acoustic communication distances for Blue whales in quiet ambient noise conditions (80 dB), moderate ambient noise conditions (94 dB), medium ambient noise conditions (102 dB) and high ambient noise conditions (112 dB). The quiet ambient noise conditions (80 dB) correspond to the noise situation of the earlier report (Masking I) and permits comparisons between Models

Case	Receiver depth (m)	Distance Airgun-Receiver (km)	Water Depth (m)	Loss in acoustic communication distances [%]					
				"80 dB noise" = the noise situation of the earlier report (Masking I)			"94 dB noise" = moderate levels of ocean noise	"102 dB noise" = medium levels of ocean noise	"112 dB noise" = high levels of ocean noise
				leaky integrator (Masking I)	leaky integrator (Masking II)	spectrogram correlator	spectrogram correlator	spectrogram correlator	spectrogram correlator
1	10	500	4000	98%	97%	94%	36%	36%	0%
2	10	1000	4000	98%	90%	94%	36%	36%	0%
3	10	2000	4000	96%	84%	88%	36%	0%	0%
4	50	500	4000	99%	97%	92%	65%	80%	61%
5	50	1000	4000	99%	92%	92%	65%	65%	61%
6	50	2000	4000	99%	77%	88%	65%	65%	61%
7	200	500	4000	99%	97%	88%	74%	75%	68%
8	200	1000	4000	99%	90%	82%	74%	75%	0%
9	200	2000	4000	98%	81%	65%	68%	60%	0%
10	10	500	500	97%	89%	79%	0%	0%	0%
11	10	1000	500	93%	78%	64%	0%	0%	0%
12	10	2000	500	89%	67%	50%	0%	0%	0%
13	50	500	500	99%	70%	87%	29%	38%	0%
14	50	1000	500	98%	87%	40%	7%	19%	0%
15	50	2000	500	97%	91%	27%	0%	13%	0%
16	200	500	500	99%	98%	53%	0%	44%	0%
17	200	1000	500	99%	94%	33%	0%	0%	0%
18	200	2000	500	97%	77%	27%	0%	0%	0%

The output of the models shows that such seismic surveys, which are conducted in lower latitudes (Australia) may even have masking potential in distant areas in higher latitudes (Antarctic). As expected, masking generally decreases (and communication ranges generally increase) with distance from the

airgun source (all models in chapter five). However, as the transmitted total (airgun) energy does not decline monotonously over distance to the source, our models indicate local deviations from the general trend. Following, we present the predicted communication ranges obtained in chapter five for several targeted species and we interpret the effects of airgun noise on the **individual and population level**, which is discussed in **chapter six**.

Antarctic blue whales generally feed at higher latitudes during austral summer and migrate to breed at lower latitudes during winter. Acoustic recordings of Antarctic blue whale calls document that Antarctic blue whales are present in low latitudes of the Indian Ocean, the eastern Pacific Ocean and the South Atlantic Ocean during the austral winter but are absent during the austral summer (Stafford et al. 2004, Samaran et al. 2013, Shabangu et al. 2019). At high latitudes, Antarctic blue whale calls are detected year-round with a peak in call detections between January and April (Thomisch et al. 2016), in accordance with the occurrence pattern of Z-calls at the Antarctic recording station analysed in this report (Chapter three).

Under quiet ambient noise conditions below 90 dB and in the absence of airgun noise, the auditory model predicts communication ranges exceeding 1000 km. It is unknown if communication over such vast ranges is biologically relevant. Moreover, it is likely that these distant calls are masked by calls that are more proximal. The predicted communication range rapidly decreases as **ambient noise** level increases.

Blue whale scenario 1 (Figure 3, left):

Parameter settings: Blue whale Z-call, water depth=500 m, vocalization depth=50 m, receiver depth=50 m, Spectrogram correlator, 102 dB ambient noise

For medium ambient noise levels (102 dB) and in the absence of airgun noise, the auditory model predicts communication ranges of 320 km in the shallow ocean scenarios (**water depth of 500 m**). In presence of an airgun, the communication range is significantly affected up to a distance of 500 km from the airgun and the communication distance is reduced to 200 km (which corresponds to a loss in communication distance of 38% (in ratio of loss in communication distance to natural communication distance)). As the airgun-receiver distance decreases, the estimated communication range decreases strongly to 140 km (66% loss) for an airgun at a distance of 200 km and severely to 60 km (81% loss) for an airgun at a distance of 100 km. The communication ranges in the shallow ocean scenarios are generally distinctly higher than communication ranges in the deep ocean for communication of blue whales and fin whales and therefore the masking potential varies also in deep ocean scenarios.

Blue whale scenario 2 (Figure 3, right):

Parameter settings: Blue whale Z-call, water depth=4000 m, vocalization depth=50 m, receiver depth=50 m, Spectrogram correlator, 102 dB ambient noise

For 102 dB ambient noise levels and in the absence of airgun noise, the auditory model predicts communication ranges of 200 km in deep ocean scenarios (**water depth of 4000 m**). In presence of an airgun, the communication range is already strongly affected up to a distance of 2000 km from the airgun and the communication distance is reduced to 70 km (which corresponds to a loss in communication distance of 65% (in ratio of loss in communication distance to natural communication distance)). As the airgun-receiver distance decreases, the estimated communication range decreases severely to 40 km (80% loss) for an airgun at a distance of 500 km. The masking potential of airguns are thus higher if the communicating blue whales are in deep ocean. It seems plausible that a reduction of the detection range from 200 km to 70 km (by an airgun in 2000 km distance) will affect an individual's vital rates. The auditory model for the **Antarctic blue whale Z-call** shows that noise from an airgun at a distance of 2000 km (the maximal distance analysed) from the blue whale reduces its detection range for a conspecific's call to 35% of the range achieved in the absence of airgun noise.

Figure 3   Overview illustrations showing masking of Antarctic blue whale z-calls by airgun noise. Graphs show the percentage loss in communication distance relative to equivalent scenarios with no airgun present and apply to medium ambient noise levels of 102 dB. The effect ranges of airguns in the shallow ocean scenarios are generally lower than in the deep ocean scenario.
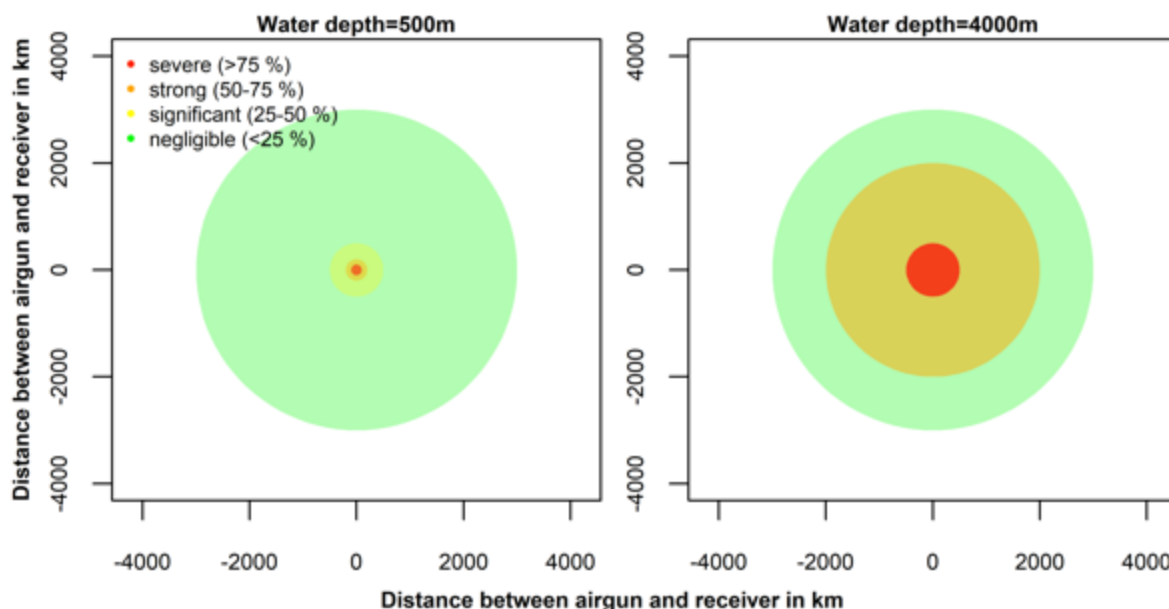
Antarctic blue whales often repeat **Z-calls** multiple times. This results in patterned sequences that can last for hours (Erbe et al. 2017). These songs are believed to origin from males trying to attract females by advertising male quality and/or good foraging opportunities (Croll et al. 2002). Therefore, masking of these Z-calls may lead to missed foraging opportunities, may interfere with female mate choice and may even lead to missed mating opportunities for the calling male as well as a female receiving animal. Selection of a mate of high genetic quality whose genetic makeup is compatible with that of the choosing female should increase offspring fitness and can mediate adaptation to changing environmental conditions (Jones & Ratterman 2009). Since Antarctic blue whale abundance is still below 1% of the pre-exploitation levels (Branch et al. 2004), communication over extended distances may be necessary for a male to attract females and for a female to find and evaluate males.

We conclude that it is likely that blue whale Z-calls are masked by airguns even if the distance between receiver animal and airgun is large and that this has an impact on individual vital rates. Quantifying the effects of communication masking on individual vital rates is still challenging, since we have only limited knowledge on the biological functions of the calls. The importance of mate choice in blue whales and the extent an individual can compensate for a missed mating or foraging opportunity have not been assessed to date.

Similar to Antarctic blue whales, the Southern hemisphere **fin whale** subspecies *Balaenoptera physalus quoyi* has a circumpolar distribution during the austral summer months. In comparison to blue whales, fin whales are less closely associated with the ice edge and mostly occur in more northern latitudes. Their distribution in the summer feeding grounds is likely driven by the distribution of specific krill species (Herr et al. 2016). In winter, fin whales migrate to lower latitudes where they breed (Aguilar et al. 2009, Leroy et al. 2018, Shabangu et al. 2019). Fin whales have been reported to vocalize more during the winter months and less in summer (Sirovic et al. 2009, Thomisch et al. 2016). The most prominent and loudest fin whale vocalization is the 20 Hz call. It has been observed that only male fin whales produce stereotypic repetitions of the **20 Hz call** (Croll et al. 2002).

Our model results suggest that detection ranges for this call strongly depend on natural ambient and airgun noise levels. When ambient noise levels are low (<90 dB), detection ranges can be in the order of 1000 km in the absence of airgun noise, while detection ranges may only reach a few kilometres under higher ambient noise levels (112 dB), which are typical of the Southern Ocean.

Fin whale scenario 1: (Figure 4, left):

Parameter settings: Fin whale 20 Hz call, water depth=4000 m, vocalization depth=50 m, receiver depth=50 m, Spectrogram correlator, 102 dB ambient noise

For 102 dB ambient noise levels and in the absence of airgun noise, the auditory model predicts communication ranges of 140 km in deep ocean scenarios (**receiver depth of 50 m**). In presence of an airgun, the communication range is significantly affected up to a distance of 2000 km from the airgun and the communication distance is reduced to 100 km (which corresponds to a loss in communication distance of 29% (in ratio of loss in communication distance to natural communication distance)). As the airgun-receiver distance decreases, the estimated communication range decreases strongly to 50 km (64% loss) for an airgun at a distance of 1000 km and severely to 1 km (99% loss) for an airgun at a distance of 500 km.

Fin whale scenario 2: (Figure 4, right):

Parameter settings: Fin whale 20 Hz call, water depth=4000 m, vocalization depth=50 m, receiver depth=200 m, Spectrogram correlator, 102 dB ambient noise

The communication ranges for 200 m receiver depth are distinctly shorter than for 50 m receiver depth. So, if the receiver fin whale is at a depth of 200 m, for 102 dB ambient noise levels and in the absence of airgun noise, the auditory model predicts communication ranges of 200 km for the deep ocean scenarios (**receiver depth of 200 m**). In presence of an airgun, the communication range is severely affected up to a distance of 2000 km from the airgun and the communication distance is reduced to 50 km (which corresponds to a loss in communication distance of 75% (in ratio of loss in communication distance to natural communication distance)). As the airgun-receiver distance decreases, the estimated communication range decreases to 18 km (91% loss) for an airgun at a distance of 1000 km and to 3 km (99% loss) for an airgun at a distance of 500 km. The masking effect of airguns is thus higher if the receiver fin whales is at 200 m depth compared to the situation at 50 m depth.

Figure 4　　　　Overview illustrations showing how communication ranges of **fin whale 20 Hz call** are reduced in medium ambient noise levels (102 dB) typical of the Southern Ocean. The effect ranges of airguns of a receiver at 200 m depth are generally higher than for a receiver at 50 m depth.
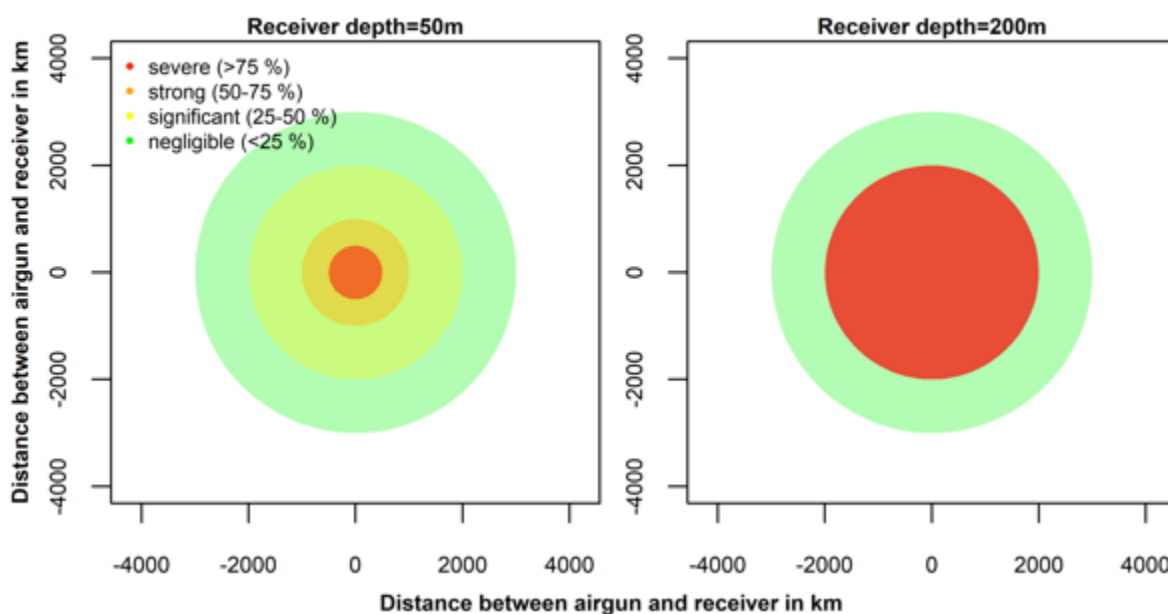
The **fin whale 20 Hz call** is believed to serve similar biological functions like the Z-call in blue whales (finding and comparing mates, advertising good foraging opportunities) with only males producing stereotypic repetitions of the call (Croll et al. 2002). The call only has a short duration in comparison to the blue whale Z-call and lacks a very characteristic pattern, so that it is strongly masked by airgun noise but also by ambient noise. Airguns cause particularly dramatic reductions in communication range under relatively quiet ambient noise conditions. Fin whales may use windows of quiet ambient noise conditions for long-range communication. Our model results indicate that even distant airguns (in order of 500 km between receiving animal and airgun) can totally block these "long range communication windows" (by reducing communication ranges to less than 1 km).

In summary, there is substantial spatiotemporal overlap between seismic surveys and Antarctic blue whale as well as fin whale distribution. In high latitudes seismic survey as well as blue and fin whale activity peak during the austral summer. In low latitudes, there is continued seismic survey activity during the austral winter when blue and fin whales migrate northward. The results of the auditory model show that potentially fitness-relevant masking of blue whale Z-calls occurs even in distances exceeding 2000 km from the airgun location. The areas potentially affected by a single survey are huge (compared to the distance between Australia and the Antarctic continent, which is approximately 3000 km). For fin whale 20 Hz calls the auditory model suggests that masking by airgun noise is most relevant if ambient noise levels are moderate to low (under high ambient noise levels detection ranges are mainly ambient noise limited and airgun noise causes little additional reduction). When ambient noise levels are low, airguns at a distance of 500 km can cause potentially fitness-relevant masking of fin whale calls. It remains unknown to date how the migratory behaviour differs between sex and age groups, reproductive state and between populations for blue and fin whales. Filling this gap of knowledge is important since effects of masking on individual vital rates likely depend on these parameters (e.g. an immature or non-breeding individual may not suffer a reduction in vital rates when a mating call is masked).

Killer whale and Weddell seal are discussed in the same subchapter, because these species produce high frequency or broadband vocalizations (Erbe et al. 2017). Only some of their vocalizations overlap with the frequency range of airgun noise (< 500 Hz) and these vocalizations typically also contain substantial energy in frequency bands > 500 Hz. The auditory models have confirmed that airgun noise has little effect on communication ranges if animals have the ability to focus on frequencies above 500 Hz by high pass filtering.

For killer whale and Weddell seal broadband calls, low frequency airgun noise only has the potential to affect fitness, if 1) the auditory system of the receiving animal cannot analyse low and high frequency parts of the vocalization separately or 2) biologically relevant information (e.g. information for individual recognition) is coded in the low frequency part of the vocalization. In case 1) signal recognition in the high frequency part is hampered by low frequency noise, whereas in 2) animals rely on the low-frequency part of the calls for communication (the low-frequency part of the calls may be especially important for communication over long distances over which high frequencies are severely attenuated).

Weddell seal scenario 1: (Figure 5, left):

Parameter settings: Weddell seal, sound sequence, water depth=500 m, vocalization depth=5 m, receiver depth=50 m, Spectrogram correlator, 80 dB ambient noise

For the Weddell seal sound sequence (**vocalization depth of 5 m**), when ambient noise levels are low (80 dB), detection ranges can be in the order of 100 km in the absence of airgun noise. In presence of an airgun, the communication range is already strongly affected for a fullband-analysis up to a distance of 2000 km from the airgun and the communication distance is reduced to 40 km (which corresponds to a loss in communication distance of 60% (in ratio of loss in communication distance to natural communication distance)). As the airgun-receiver distance decreases, the estimated communication range decreases severely to 14 km (86% loss) for an airgun at a distance of 1000 km**.** The levels of the propagated sound originating from 5 m, is more attenuated than the sound originating from 50 m **vocalization depth** for the low-frequency transmission loss at long ranges.

Weddell seal scenario 2: (Figure 5, right):

Parameter settings: Weddell seal, sound sequence, water depth 500 m, vocalization depth=50 m, receiver depth=50 m, Spectrogram correlator, 80 dB ambient noise

For the Weddell seal sound sequence (**vocalization depth of 50 m**), when ambient noise levels are low (80 dB), detection ranges can be in the order of 100 km in the absence of airgun noise. In presence of an airgun, the communication range is already strongly affected up to a distance of 2000 km from the airgun and the communication distance is reduced to 50 km (which corresponds to a loss in communication distance of 50% (in ratio of loss in communication distance to natural communication distance)). As the airgun-receiver distance decreases, the estimated communication range decreases severely to 14 km (86% loss) for an airgun at a distance of 500 km. The masking potential of airguns are thus higher if the communicating Weddell seal vocalizes at 5 m depth compared to 50 m depth.

Figure 5   Overview illustrations showing how the levels of the propagated sound originating from 5 m, is more attenuated than the sound originating from **50 m vocalization depth** for the low-frequency transmission loss at long ranges.
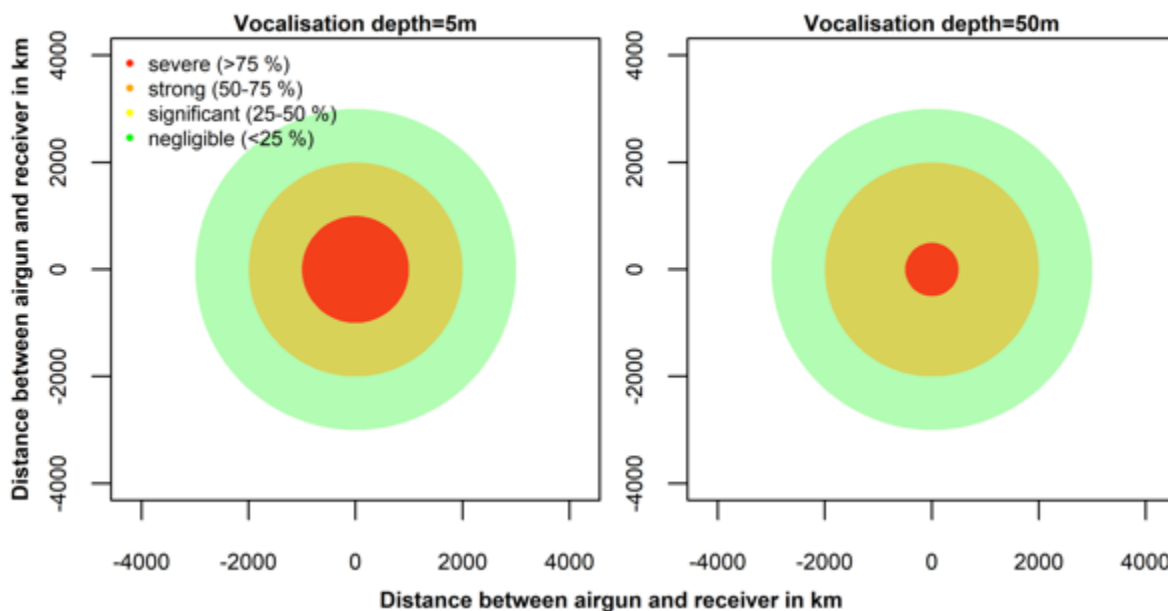
Communication masking by airgun noise only affects the low frequency part of killer whale and Weddell seal calls. If the detection of calls alone is sufficient, communication ranges in Weddell seals and killer whales are unlikely to be affected by airgun noise. However, if the low frequency part contains biologically relevant information or if individuals listen specifically for the low frequency part of the vocalizations to obtain information on distant callers, airguns can cause communication masking. While communication masking by airgun noise is predicted to be less relevant for Weddell seals and killer whales than for the two baleen whale species discussed above, it remains difficult to quantify the risk of exposure to communication masking by airguns for these species.

We do not know to what extent **Weddell seals** and **killer whales** depend on the masked low frequency part of their vocalizations, so that the extent to which these species suffer from communication masking by airgun noise is unclear. Male Weddell seal calls are produced during the breeding season and are likely important for the establishment of underwater territories (Rouget et al. 2007) and for attracting females (Opzeeland et al. 2010). Rogers (2017) suggested a mechanism by which calls can serve as honest signals of male quality: The production of repetitive sequences of underwater calls may indicate the breath-holding ability of the caller. In leopard seals, only large males were able to maintain consistent rhythmic calling patterns throughout the breeding season, whereas the number of inter-vocalizing rests increased over the breeding season in small males (Rogers 2017). Similar mechanisms may allow Weddell seal females to evaluate male quality based on vocalizations. Although Weddell seal vocalization activity peaks during the breeding season, vocalizations are not restricted to this time of the year. Weddell seals produce a wide variety of different calls (Erbe et al. 2017). Functions of in-air calls include mother-pup contact calls. Depending on the importance of the low frequency part of the vocalizations for biological functionality, airgun noise may interfere with maintenance of underwater territories, mate finding, female mate choice and still unknown functions of the rich Weddell seal vocal repertoire.

The acoustic sense is typically most important for receiving information about distant objects in real time. The evolution of sophisticated auditory systems and biosonar (Au and Hastings 2008) constitutes a powerful proof that natural selection on the auditory system is strong in marine mammals: The ability

to gather detailed information from acoustic signals provides a fitness advantage. The importance of the acoustic sense has been documented in a wide variety of behavioural contexts. In this report, we list behavioural contexts and provide examples with a focus on marine mammal species that occur in the Antarctic Ocean.

Marine mammals have evolved to use sound as their primary sensory modality. Any interference of acoustic communication can have severe effects on both sender and receiver leading to effects on fitness, for example if masking impedes signal detection (Branstetter et al. 2016). Behavioural responses can be highly variable and may not be fully predictable with simple acoustic exposure metrics e.g. like the received sound exposure level. Rather, differences among species and individuals along with contextual aspects of exposure like the behavioural state appear to affect response probability (Southall et al. 2016).

To validate our results, experimental studies on masking are needed. While disturbance responses have been studied in the field, this is much more challenging with masking. This is because disturbance responses are often associated with sudden changes in behaviour, which can be observed in the field. Studying masking based on behavioural observations requires knowledge on how the animal behaves in the presence and absence of the biological cue. This has been only shown for animals in human care, which are trained to respond to a cue in order to receive a reward. Such experiments have been conducted with dolphins (Branstetter et al. 2016) and recently also pinnipeds (Sills et al. 2017), but are impossible to conduct with baleen whales. Sills et al. (2017) studied how well two individuals of two Arctic seal species (one male spotted seal and one female ringed seal) were able to detect test signals (linear upsweeps from 95 to 105 Hz in 500 ms) in the presence of airgun noise recorded at distances of 1 and 30 km from an airgun array. Since only two individuals have been studied, it is unknown how well the results transfer to other individuals of the same species and whether or not they can be transferred to other species. Such experimental studies provide an excellent opportunity for future validation of the psychophysical model developed in this report. As more such studies become available, the listening situation of the experimental animals should be simulated and the predictions of the psychophysical model should be compared to the performance of the experimental animals.

Finally, we discuss the available knowledge on the modelled Antarctic populations for each of the main steps of a PCoD-model (Population Consequences of Disturbance model). The rational of the PCoD framework can be summarized as follows: if an individual is exposed to a stressor, its physiological state and its behaviour change. Physiological and behavioural changes can directly ("acute effects") or indirectly ("chronic effects") affect the individual's vital rates, for example by affecting the survival rate or fecundity. This relationship is modulated by environmental conditions. Based on modelling the exposure risk of an individual and basic population parameters, the population dynamics can then be modelled. We use the PCoD framework to structure our discussion of the masking effects at the population level and to identify knowledge gaps.

A bullet point list of the main conclusions of this report can be found in **chapter seven**. The models developed in this study for the Antarctic Ocean indicate that airgun noise is likely to mask marine mammal calls - in particular low frequency calls of baleen whales: Noise from airguns in a distance of 1000 - 2000 km from the receiving animal can severely reduce communication ranges of blue and fin whales. For species with high-frequency or broadband vocalisations the masking effect is limited if mere detection of a call is sufficient. Reductions in operation time and airgun source levels can reduce the areas in which masking occurs. A 10 dB reduction of the airgun source level roughly reduces the affected area to a tenth of its original size. The behavioural context of call production together with the time and energy animals invest in calling indicates that Antarctic blue whale Z-calls and fin whale 20 Hz calls have important functions in mating and possibly also foraging contexts. Declines in individual vital rates (that entail effects at the population level) are therefore likely when calls are masked.

Zusammenfassung

Die Sorge über die Auswirkungen von Unterwasserlärm auf marine Ökosysteme wächst. Die Bedeutung der akustischen Wahrnehmung wurde in verschiedenen Verhaltenskontexten dokumentiert. Vokalisierungen spielen eine Rolle beim Finden und Konkurrieren um Paarungspartner. Eine weitere wichtige Funktion von Vokalisierungen ist, dass sich Muttertiere und ihre Jungtiere leichter wiederfinden und der Zusammenhalt zwischen Mitgliedern größerer Gruppen, die gemeinsam auf Nahrungssuche gehen oder migrieren, aufrechterhalten wird.

Die Antarktis wird durch strenge Umweltschutzbestimmungen geschützt. Der Antarktisvertrag wurde mit der Absicht beschlossen, die Antarktis nur zu friedlichen Zwecken zu nutzen. Zusätzlich wurden mit dem Umweltschutzprotokoll zum Antarktisvertrag die strengsten und umfassendsten Umweltbestimmungen umgesetzt, die jemals für eine Region der Erde in einem internationalen Abkommen entwickelt wurden. Deutschland ist Vertragspartner des Antarktisvertrages und übernimmt damit Verantwortung für die Antarktis. Das Umweltbundesamt (UBA) ist die national zuständige Behörde und erteilt Genehmigungen für Tätigkeiten in der Antarktis. Zu diesen Tätigkeiten gehören wissenschaftliche seismische Untersuchungen im Meer, bei denen Airgun-Arrays als Schallquellen verwendet werden. Airguns erzeugen Schallimpulse von hoher Intensität, indem sie unter hohem Druck stehende Luft schlagartig in das Wasser freisetzen und stellen eine der lautesten anthropogenen Lärmquellen im Ozean dar. Die wissenschaftliche Grundlage zur Bewertung der Auswirkungen vom Einsatz von Airguns auf Meeressäuger weist noch Wissenslücken auf. Bisherige Studien zeigen, dass Airgunsignale zu temporären Verschiebungen der Hörschwelle bei marinen Säugetieren führen können (Kastelein et al. 2017, Sills et al. 2020). Lärmbelastungen mit sehr hoher Schallenergie können sogar zu einer dauerhaften Hörschwellenverschiebung führen, wie es unbeabsichtigt für einen Seehund gezeigt werden konnte (Reichmuth et al. 2019). Neben der Hörbeeinträchtigung können Airgun-Impulse auch Stör- oder Vertreibungsreaktionen auslösen (Castellote et al. 2012, Nowacek et al. 2015). Das Wissen über das Ausmaß der Maskierung von Kommunikationslauten durch Lärm von Airguns und deren Auswirkungen auf Individuen- und Populationsebene ist noch begrenzt. Diese Studie versucht, das Ausmaß der Maskierung der Kommunikation durch Airgunsignale für ausgewählte antarktische Meeressäuger abzuschätzen und diskutiert die Auswirkungen auf Individuen- und Populationsebene, aufbauend auf Modellen, die in einem vorherigen Projekt erstellt wurden (Siebert et al. 2014).

Die Bedeutung der akustischen Wahrnehmung wurde in verschiedensten Verhaltenskontexten dokumentiert. In diesem Bericht werden Verhaltenskontexte aufgelistet und Beispiele mit Fokus auf Meeressäugerarten, die im Südlichen Ozean vorkommen, aufgezeigt. Aufgezeichnete Finnwalgesänge (Sequenzen von 20-Hz-Rufe) aus einem-Kalbungsgebiet wurden ausschließlich von Männchen produziert (Croll et al. 2002). Der Verhaltenskontext deutet stark darauf hin, dass diese akustischen Signale dazu dienen, Weibchen aus großer Entfernung anzulocken (Croll et al. 2002). Sequenzen von sogenannten Z-Rufe des antarktischen Blauwals werden ebenfalls als Paarungssignale der Männchen interpretiert (Thomisch et al. 2016, Croll et al. 2002). Die Vokalisierungen männlicher Weddellrobben während der Fortpflanzungszeit sind vermutlich wichtig für die Etablierung von Unterwasserterritorien (Rouget et al. 2007) das Anlocken von Weibchen (Opzeeland et al. 2010) und können als Anzeiger für die männliche Fitness dienen, was für Seeleoparden untersucht wurde (Rogers et al. 2017). Außerdem können Vokalisierungen signalisieren, wo sich Nahrungsmöglichkeiten bieten. Die bereits erwähnten Finnwalgesänge z.B. deuten auf zwei Funktionen hin: Die Männchen vokalisieren, um Weibchen anzulocken, während die Weibchen sich auf die vokalisierenden Männchen zubewegen, um gute Futtergelegenheiten zu nutzen (Croll et al. 2002).

Eine weitere wichtige Funktion von Lautäußerungen ist, dass sich Muttertiere und ihre Jungtiere leichter wiederfinden. Bei Weddellrobben begünstigen die Vokalisierungen von Muttertieren und Jungtieren an Luft die erfolgreiche Wiedervereinigung nach Futtersuchgängen der Mutter (Collins et al. 2005, Collins et al. 2011, Opzeeland et al. 2012). Diese Studien haben gezeigt, dass es eine erhebliche

Variation zwischen den Individuen bei den Vokalisierungen von Müttern sowie von Jungtieren gibt. Trotz dieser Variation in den Vokalisierungen deuten Playback-Experimente darauf hin, dass akustische Signale allein nicht für die individuelle Erkennung zwischen einem Jungtier und seiner Mutter ausreichen (Collins et al. 2005, Opzeeland et al. 2012). Bei Bartenwalen sind Vokalisierungen zu Kontaktaufnahme vermutlich wichtig, um die Bindung zwischen Mutter und Kalb aufrechtzuerhalten oder wiederherzustellen (z.B. nach tiefen Tauchgängen der Mutter). Ähnlich wie beim Aufrechterhalten der Bindung zwischen Mutter und Jungtier können akustische Signale dazu dienen, den Zusammenhalt zwischen Mitgliedern größerer Gruppen, die gemeinsam auf Nahrungssuche gehen oder migrieren, zu gewährleisten.

Die Kommunikation von Meeressäugern kann durch Lärm maskiert werden, insbesondere wenn sich der Frequenzbereich von Lärm und Vokalisierungen überschneidet. Um zu beurteilen, ob ein Meeressäuger durch Lärm beeinträchtigt wird, ist es relevant, die spektralen, zeitlichen und Amplituden-Eigenschaften der Vokalisierungen einer Art zu kennen. Da sogar Individuen in Entfernungen von bis zu mehreren tausend Kilometern vom Airgun-Standort unter akustischer Maskierung leiden können (Nieukirk et al. 2012, Siebert et al. 2014), ist Maskierung möglicherweise der am weitesten verbreiteten Effekt von Lärm durch Airguns. Meeressäuger können auf erhöhte Lärmpegel reagieren, indem sie die Amplitude eigener Kommunikationssignale erhöhen, die Frequenzanteile der Signale ändern oder die Wiederholungsrate ihrer Vokalisierungen erhöhen (Erbe et al. 2016). **Kapitel zwei** enthält eine **Pilotstudie**, die das Auftreten solcher Antimaskierungs-Strategien bei Blauwalen vor Island abschätzt. Hierfür wurde die Vokalisationsrate in Abhängigkeit von der Tageszeit oder der Anzahl der Boote untersucht. Obwohl die Vokalisationsrate recht variabel war, wurden Hinweise darauf gefunden, dass der anthropogene Lärmpegel die Vokalisationsrate der Blauwale beeinflussen könnte. Unter lauteren Bedingungen produzierten die Blauwale häufiger Signale, aber dieser Trend war nicht signifikant. Ein ähnliches Phänomen wurde von Di Iorio und Clark (2010) beobachtet, wo Blauwale während seismischer Aktivitäten signifikant mehr vokalisierten als in Zeiten, in denen die seismische Schallquelle nicht in Betrieb war. Effekte auf die Vokalisationsrate der Blauwale wurden nur festgestellt, wenn die Lärmbelastungen im Frequenzbereich ihrer Vokalisierungen (48 – 102 Hz) lag. Schallexpositionen in einem höheren Frequenzband (150 – 500 Hz), das sich nicht mit dem Frequenzband der Blauwalvokalisierungen überschneidet, scheinen die Vokalisationsrate der Blauwale nicht zu beeinflussen. Die meiste Energie der Airgun-Impulse ist im niedrigen Frequenzband konzentriert. Dieser Frequenzbereich überschneidet sich mit vielen Vokalisierungen von Meeressäugern, insbesondere mit den Gesängen und Vokalisierungen von Bartenwalen. Da akustische Signale nicht auf die Vokalisierungen von Artgenossen beschränkt sind, sondern auch Hinweise auf die Anwesenheit von Prädatoren (Cure et al. 2015) sowie für die Orientierung wichtige Signale (Clark et al. 2009) enthalten können, kann die Maskierung von Kommunikationssignalen besonders negative Auswirkungen auf Bartenwale haben.

Um einen Einblick in das räumliche Ausmaß der Maskierung zu erhalten, muss zunächst die Schallausbreitung im Untersuchungsgebiet ermittelt werden. In **Kapitel drei** werden **Schallausbreitungsmodelle** für den Südlichen Ozean entwickelt. In diesem Projekt wurden zwei verschiedene Datensätze von Airgunsignalen aus zwei Untersuchungen in der Antarktis (**Abbildung 1**) verwendet, um die Modellvorhersagen zu überprüfen.

Der erste Datensatz (bezeichnet als „**ARAGORN-Datensatz**") wurde 2006 im Südlichen Ozean aufgezeichnet, in dem PGS Geophysical eine seismische Offshore-Untersuchung über dem australischen Kontinentalschelf und dem Hang im westlichen Teil der Bass-Straße durchführte. Die Untersuchungen wurden mit drei eigenständigen Unterwasserschallrekordern vorgenommen, die an drei verschiedenen Standorten eingesetzt wurden: südwestlich von Tasmanien (in ~500 km Entfernung von den Airguns), innerhalb der antarktischen Konvergenzzone (in ~1600 km Entfernung von den Airguns) und in der Nähe des antarktischen Kontinentalschelfs (in ~2900 km Entfernung von den Airguns).

Der zweite Datensatz (bezeichnet als „**ARAON-Datensatz**") wurde im Februar 2015 während der Forschungsreise Tangaroa 2015 im Rossmeer aufgenommen. HIDAR-Sonobojen wurden ausgebracht, um die Anwesenheit von Meeressäugern zu verfolgen. 28 Sonobojen wurden eingesetzt, während eine nahegelegene seismische Untersuchung (in Entfernungen zwischen 50 und 500 km von den Airguns) von der R/V Araon durchgeführt wurde.

Für jeden der beiden Datensätze wurde eine entsprechende Modellierungsstrategie angewandt. Ein numerischer Ansatz wurde verwendet, um die Schallemission und -ausbreitung vom Airgun-Array der Aragorn-Untersuchung bis zum am weitesten entfernten Unterwasserschallrekorder am Kontinentalhang in der Antarktis (an der auf der Karte in Abbildung 1 dargestellten Position 3) zu modellieren. Das mit dem ARAON-Datensatz getestete Modell ermöglichte die Modellierung der Zeitbereichsdarstellung eines empfangenen Signals aus einem Signal der Schallquelle. Selbst kurze Pulse erfahren eine ausgeprägte Dehnung, wenn sie lange Strecken zurücklegen. Für ausgewählte Sonobojen in unterschiedlichen Entfernungen zu den Airguns konnte ein Vergleich hinsichtlich der Magnitude und der Signaldehnung durchgeführt werden. Die zu erwartende Signalstreckung ist bei weiter von den Airguns entfernten Sonobojen aufgrund der längeren Ausbreitungsstrecke höher. Die Fernfelddarstellung der Quelle (Wellenform, Zeitreihen) muss in der Tat zeitbezogene Ausbreitungsphänomene, wie z.B. die Signaldehnung, die eine Folge der frequenzabhängigen Schallausbreitung ist, bewerten. Die Schallausbreitungsmodelle ermöglichen die Abschätzung des empfangenen Signals (einschließlich Dehnung und Pegel) an der Position des Zuhörers (empfangenes Signal in Entfernungen von 100 m bis zu 3000 km) vom Signal der Schallquelle.

Abbildung 1:   **Links)** Der „**ARAGORN-Datensatz**" wurde 2006 im Südlichen Ozean mit drei eigenständigen Unterwasserschallrekordern aufgezeichnet, die an drei Standorten in ~500 km, ~1600 km und ~2900 km Entfernung von den Airguns eingesetzt wurden. **Rechts)** Der „**ARAON-Datensatz**" wurde mit 28 Sonobojen aufgezeichnet, die in 50 bis 500 km Entfernung von einer nahegelegenen seismischen Untersuchung ausgebracht wurden. Die seismischen Transekte sind durch rote Linien und die Position der ausgebrachten Sonobojen durch blaue Kreise dargestellt.
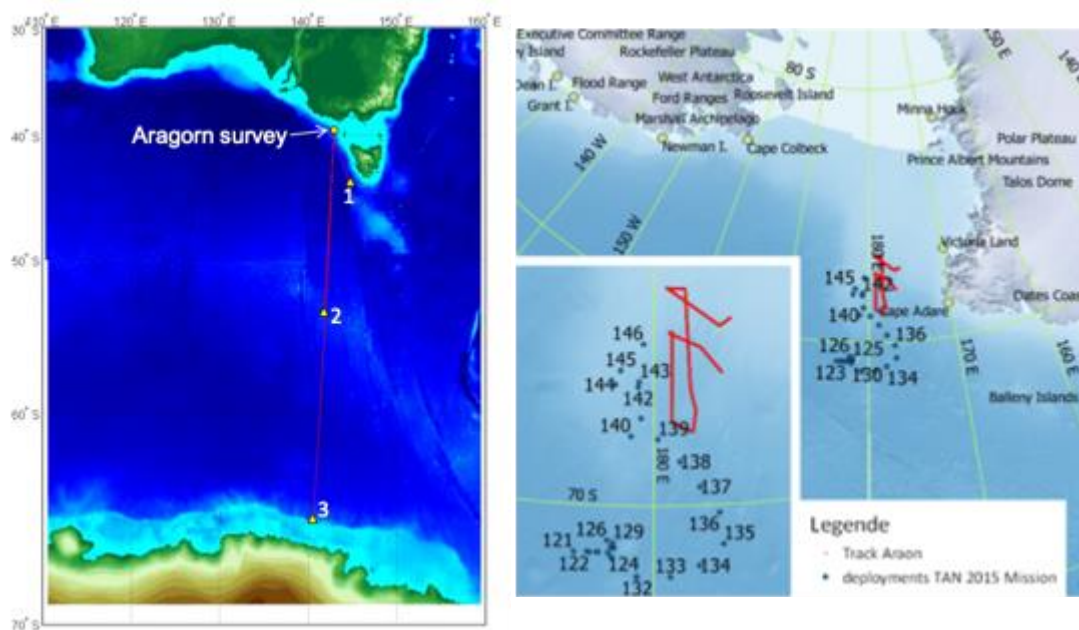
Beide Modellierungsansätze werden durch einen Vergleich von modellierten Signalen mit Messungen der jeweiligen Aufzeichnungen des Airgunsignals von zwei seismischen Untersuchungen im Südlichen Ozean validiert. Die Signale ändern sich in Pegel, Frequenzgehalt und Dauer (oder genauer gesagt „zeitlicher Struktur"), während sie von der Schallquelle abstrahlen. Die validierten Modelle geben

Aufschluss darüber, wie physikalische Phänomene die Schallausbreitung im Südlichen Ozean beeinflussen und helfen dabei, die physikalischen Parameter zu verstehen, die die Ausbreitung von Schallsignalen (sowohl Airgun- als auch Kommunikationssignale durch Tiervokalisierungen) und damit das empfangene Signal, das bei einem Empfänger ankommt, beeinflussen.

Die Analyse von Aufzeichnungen seismischer Untersuchungen sowie der Schallausbreitungsmodelle (Kapitel drei) zeigt, dass tieffrequente Airgunsignale die intraspezifische Kommunikation in Entfernungen von mehr als 2000 km vom Quellort beeinträchtigen könnten. Bei seismischen Untersuchungen, die an den nördlichen Rändern des Südlichen Ozeans durchgeführt werden, tritt die beste Kopplung der Airgun-Schallquelle mit dem SOFAR-Unterwasserschallkanal und damit das höchste Potential für Maskierung in antarktischen Gewässern auf, wenn sich die Airgun über dem Kontinentalhang befindet (Kapitel drei). Der Umgebungslärm kann den hörbaren Bereich für Airgunsignale und damit auch den Bereich verringern, in dem Airgunsignale Kommunikationssignale maskieren können. In **Kapitel vier** wurde der **Umgebungslärm** an drei verschiedenen Orten im östlichen Teil des Südlichen Ozeans im Jahr 2006 analysiert. Zusätzlich zum Lärm, der von abiotischen Schallquellen stammt, können drei charakteristische Merkmale im langzeitgemittelten Spektrogramm unterschieden werden: intensives Breitbandrauschen zwischen 15 und 30 Hz, das von mehreren Vokalisierungen von Finnwalen ausgeht, ein Chor Z-förmiger Signale von antarktischen Blauwalen mit einer Frequenz um 20 Hz und etwas unter 30 Hz und relativ schmalbandiges Rauschen bei 300 – 350 Hz, das sichtbar von mehreren Vokalisierungen antarktischer Robben verursacht wird.

In **Kapitel fünf** wird ein **psychophysisches Modell (Maskierungsmodell)** entwickelt, das vorhersagt, ob ein empfangendes Tier die Vokalisierung eines Artgenossen in verschiedenen Szenarien (Variation der Meeres-, der Quell- und Empfängertiefe sowie der Umgebungslärmpegel) erkennen kann. Die Fähigkeit eines Tieres, ein Signal in Anwesenheit von Lärm zu erkennen, hängt von der absoluten Empfindlichkeit seines Gehörs ab. Die Signaldetektion hängt von den Frequenzabstimmungseigenschaften des Systems ab, die als das Auflösungsvermögen des Gehörs definiert ist, den Schall in seine einzelnen Frequenzkomponenten aufzuspalten. Die zeitlichen Verarbeitungseigenschaften des Systems, die der auditiven Integrationszeit entsprechen, bestimmen die auditive Wahrnehmung (Erbe et al., 2016). Bei Signalen mit einem charakteristischen Frequenz- und Intensitätsmuster über die Zeit ist ein Hörsystem, das nach diesen Mustern sucht und damit die kombinierte Zeit-Frequenz-Intensitätsstruktur eines Signals verwendet (dieses Projekt: „Masking II"), wesentlich empfindlicher als ein Hörsystem, das nur die Gesamtenergie analysiert, die sich innerhalb eines Zeitintervalls und Frequenzbands ansammelt (Vorgängerprojekt: „Masking I"[2]). Das Projekt „Masking II" basiert auf dem Vorgängerprojekt „Masking I" und stellt eine Weiterentwicklung des Modells dar, mit dem das Maskierungspotential von Airguns in der Antarktis abgeschätzt werden soll.

Das psychophysische Modell besteht im Wesentlichen aus drei Komponenten (**Abbildung 2**):

1. Für jedes Szenario wird zunächst das am Ohr des Tieres ankommende Signal modelliert, indem das sich ausbreitende Airgun-Signal und/oder die Tiervokalisierung mit dem Meeresrauschen gemischt wird. Basierend auf den validierten Ausbreitungsmodellen, die in Kapitel 3 entwickelt wurden, kann das Airgunsignal, das ein Hörer empfängt, für jede Entfernung zwischen dem Hörer und dem Airgun-Standort abgeleitet werden. Darüber hinaus können die Ausbreitungsmodelle verwendet werden, um auf die Vokalisierung zu schließen, die ein Empfänger, für jede Entfernung zwischen dem Hörer und dem vokalisierenden Artgenossen empfängt. Insgesamt ermöglicht das Mischen der empfangenen Airgunsignale, der empfangenen Vokalisierung und des Umgebungslärms den Rückschluss auf den Schall, der am Ohr des Empfängers ankommt, für jede beliebige Entfernung zum Airgun-Standort und zum Ort des vokalisierenden Artgenossen. Es werden Stichproben von

---

[2] https://www.umweltbundesamt.de/sites/default/files/medien/378/publikationen/texte_16_2014_0.pdf)

Schall erzeugt, in denen das übertragene Vokalisationssignal entweder vorhanden ist oder nicht und das Empfängermodell gestellt, ob es eine Vokalisierung erkennt.

2. Basierend auf den Empfängermodellen „leaky integrator" oder „spectrogram correlator" wird der Signaldetektor modelliert, der das auditorische Hörsystem repräsentiert. Das Empfängermodell wird mit Stichproben des Schalls konfrontiert und muss entscheiden, ob ein propagiertes Vokalisationssignal in einer Stichprobe vorhanden ist oder nicht.

   a) Das Empfängermodell der vorherigen Airgun-Studie (Siebert et al., 2014) bestand aus einem **Leaky-Integrator**-Modell, das die empfangene Energie innerhalb des Frequenzbands der fokalen Vokalisierung zeitlich verlustbehaftet integriert. Die maximalen Pegel des Leaky-Integrator-Ergebnis fürVokalisierungen und Störgeräusche werden analysiert und verglichen (in einer alternativen Analyse nur über einen bestimmten Zeitbereich). Auf Grundlage dieses Vergleichs kann vorhergesagt werden, ob eine Kommunikation möglich ist oder nicht.

   b) Im aktuellen Projekt wurde zusätzlich ein **Spektrogrammkorrelator** entwickelt, der einen phasenunempfindlichen Empfänger darstellt. Der Empfänger vergleicht eine Repräsentation des eintreffenden Schallmusters (wie in Komponente 1 erzeugt) mit einer spektralen Repräsentation (ein charakteristisches Frequenz- und Intensitätsmuster) des gesuchten Signals über die Zeit und wertet deren Ähnlichkeit über die Zeit aus. Dieses Prinzip entspricht funktionell dem Vergleich des Stimulationsmusters des Cochlea-Ausgangs über die Zeit mit einem Suchmuster des Signals. Das Spektrogramm-Korrelationsempfängermodell ist sehr empfindlich, da es die gesamte Zeit-Frequenz-Information im Signal und im Maskierer nutzt.

3. Zur Bestimmung des Detektionserfolgs und der -distanzen wurde in diesem Projekt ein grundsätzlich anderer Ansatz verfolgt als bei Siebert et al. (2014). Sowohl für das Spektrogramm-Korrelator-Modell als auch für das in diesem Projekt implementierte Leaky-Integrator-Modell wurde die Bewertung, ob eine hinreichend erfolgreiche Klassifikation im Fokusszenario möglich war, nach der standardisierten Grenzwertoptimierungskurve (Receiver Operating Characteristic Kurve (ROC-Kurve)) durchgeführt. In Anlehnung an Branstetter et al. (2016) wurde vermutet, dass die Erkennung von Vokalisierungen hinreichend genau war, um eine Kommunikation zu ermöglichen, wenn die Fläche unter der ROC-Kurve (kurz: AUROC) 0,9 überstieg.

Abbildung 2   Schematische Darstellung des allgemeinen Aufbaus des psychophysischen Modells. Für jedes Szenario wird zunächst das am Ohr des Tieres ankommende Signal modelliert (durch Mischen des sich ausbreitenden Airgun-Signals und/oder der Vokalisierung mit Meeresrauschen). Als nächstes wird das auditorische System durch einen Signaldetektor modelliert, der anhand einer einstellbaren Schwelle entscheidet, ob eine Vokalisierung vorliegt oder nicht.
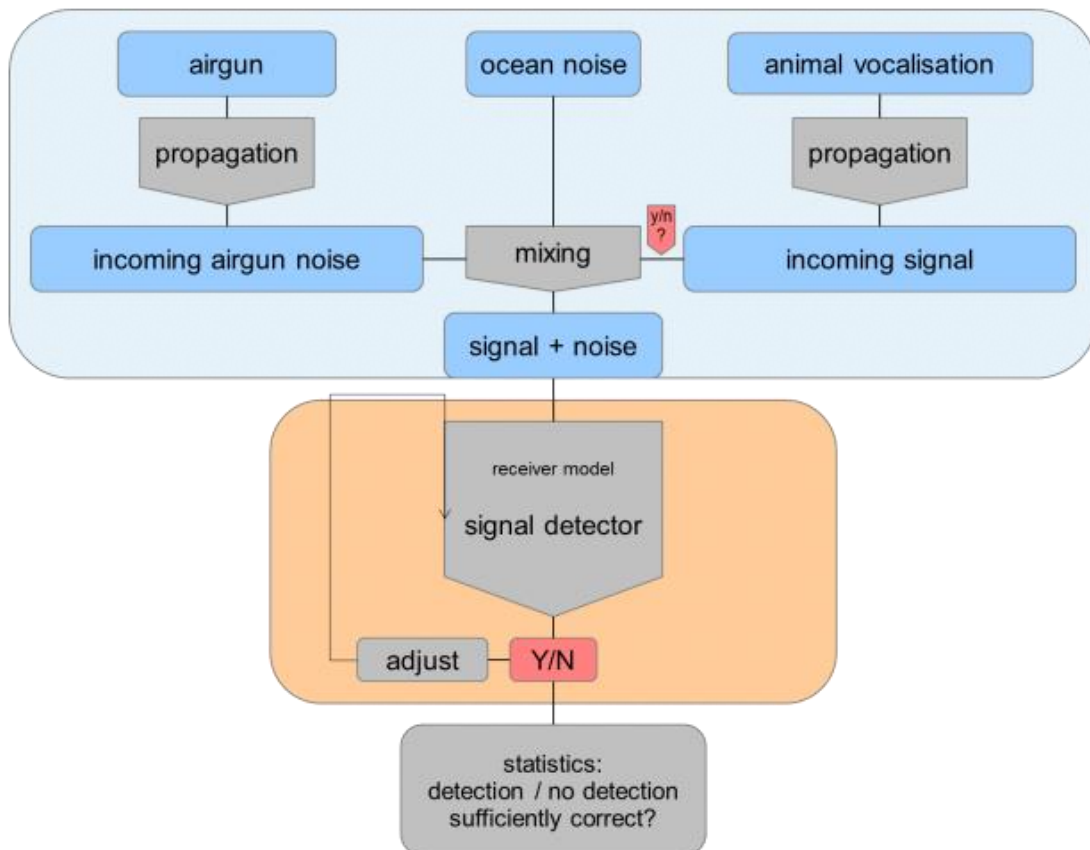
Es wurden verschiedene Übertragungsszenarien in Abhängigkeit von der Wassertiefe (500 m und 4000 m), den Sendertiefen (5 m und 50 m) und den Empfängertiefen (10 m, 50 m und 200 m) für alle fünf Vokalisationstypen (Blauwal-Z-Ruf, Finnwal-20Hz-Ruf, multiharmonischer Call eines Schwertwals, Weddellrobben-Langton und Weddellrobben-Tonfolge) modelliert. Zur besseren Veranschaulichung wurden die Ergebnisse der Modelle für alle Szenarien mit einer interaktiven Multimedia-Anwendung visualisiert, die eine erklärende Übersicht und einzelne Abbildungen bietet (https://tschaffeld.shinyapps.io/UBA_mask/).

Die Überlagerungen unterschiedlicher Reflexionen von Meeresboden, Wasseroberfläche und direktem Übertragungsweg verursachen auffällige Unregelmäßigkeiten. Die Übertragungsverluste im **flachen Ozean** sind deutlich höher als im **tiefen Ozean**, bedingt durch das monoton abfallende Verhalten der Schallausbreitung. Folglich sind die Wirkungsbereiche von Airguns für Kommunikationsdistanzen von Blau- und Finnwalen in den Szenarien des flachen Ozeans in der Regel deutlich kleiner als im tiefen Ozean (siehe Beispiel in **Abbildung 3**).

Die auffälligsten Unterschiede zwischen den jeweiligen Schallausbreitungen für **verschiedene Empfängertiefen** bestehen darin, dass der Einfluss von Oberflächeneffekten bei flachen Empfängertiefen (10 m) größere Unregelmäßigkeiten in der Ausbreitung nahe der Quelle verursacht. Für Blau- und Finnwale, die große Kommunikationsreichweiten haben, sind die Unterschiede zwischen verschiedenen Empfängertiefen nicht wesentlich und es ist kein klarer systematischer Unterschied

zwischen verschiedenen Empfängertiefen erkennbar. Die Wirkungsbereiche der Airguns für 200 m Empfängertiefe sind im Allgemeinen deutlich höher als für 10 m oder 50 m Empfängertiefe für Kommunikationsreichweiten von Blau- und Finnwalen (siehe Beispiel in **Abbildung 4**).

Der Pegel des sich ausbreitenden Schalls, der aus einer Tiefe von 5 m stammt, ist für den tieffrequenten Übertragungsverlust bei großen Reichweiten stärker gedämpft als der Schall, der aus einer **Vokalisationstiefe** von 50 m kommt. Daher wird für Blau- und Finnwale eine Erhöhung der Kommunikationsreichweite erwartet, wenn diese Arten in größeren Tiefen (50 m versus 5 m Sendertiefe) vokalisieren. Hinsichtlich der Gesamtdämpfung für die übrigen Arten, die breitbandige Vokalisierungen (mit vollständiger Frequenzbandanalyse) produzieren, gibt es keinen auffälligen Unterschied in der Signaldämpfung für Vokalisationstiefen von 5 und 50 m. Daher unterscheiden sich die Kommunikationsreichweiten nicht signifikant (siehe Beispiel in **Abbildung 5**).

Quantitative Vorhersagen von Kommunikationsdistanzen sind abhängig von der Vokalisierung, den Umweltbedingungen (natürlicher Umgebungslärm und Schallausbreitungsbedingungen / -annahmen) und dem **psychophysischen Modell** (Spektrogramm-Korrelator-Modell oder Bandpass-Leaky-Integrator-Modell). Der Spektrogramm-Korrelator detektiert Vokalisierungen mit einer höheren Präzision als der Leaky-Integrator, vor allem wenn Vokalisierungen eine charakteristische Spektral-/Frequenz-/Intensitätsstruktur über den Signalverlauf aufweisen. Dies trifft jedoch nur zu, wenn die eingehenden Signale sind nicht stark verzerrt und zeitlich gestreckt wurden. Bei schmalbandigen Signalen, ohne starke zeitliche Signatur (z.B. Finnwal), kann der Vorteil nur gering sein.

Da einige Teile des Modells im Vergleich zum Vorgängerprojekt weiterentwickelt wurden, erweist sich ein direkter Vergleich zwischen den Modellvorhersagen aus Masking I und II als schwierig. Die wichtigsten Änderungen betreffen 1) die Modellierung der Schallausbreitung (sphärische Ausbreitung vs. neues numerisches Modell), 2) das auditorische Modell (Bandpass-Leaky-Integrator vs. neue Spektrogramm-Korrelation) und 3) das Detektionsmodell (Signal>Rauschen vs. AUC- Receiver Operating Characteristic). Das bedeutet, dass die möglichen Ursachen für die Abweichungen nicht eindeutig identifiziert werden können. Dennoch unterstützen die Ergebnisse der Masking-II-Modellierung die Kernaussage des Masking-I-Berichts, der darauf hinweist, dass Airgun-Signale zu einem signifikanten Verlust der Kommunikationsreichweite für Blau- und Finnwale in 2000 km Entfernung von der Quelle führen können.

In der folgenden Tabelle 1 sind die akustischen Kommunikationsentfernungen für Blauwale bei leisem Umgebungslärm (80 dB), mäßigem Umgebungslärm (94 dB), mittlerem Umgebungslärm (102 dB) und hohem Umgebungslärm (112 dB) dargestellt. Wie erwartet, ist der Entfernungsbereich, in dem eine Airgun Störungen verursacht, in Szenarien mit geringem Meeresrauschen generell größer als in Szenarien mit höherem Meeresrauschen.

Tabelle 1   Akustische Kommunikationsdistanzen für Blauwale bei leisem Umgebungslärm (80 dB), mäßigem Umgebungslärm (94 dB), mittleren Umgebungslärm (102 dB) und starkem Umgebungslärm (112 dB). Die ruhigen Umgebungslärmbedingungen (80 dB) entsprechen der Geräuschsituation des früheren Berichts (Maskierung I) und ermöglichen Vergleiche zwischen den Modellen.

Fall	Empfänger-Tiefe (m)	Entfernung Airgun-Empfänger (km)	Wasser tiefe (m)	Verlust der akustischen Kommunikationsdistanzen [%]					
				"80 dB Umgebungslärm" = die Situation des vorherigen Projektes (Masking I)			"94 dB Umgebungslärm" = moderate Pegel von Meeresrauschen	"102 dB Umgebungslärm" = medium Pegel von Meeresrauschen	"112 dB Umgebungslärm" = hohe Pegel von Meeresrauschen
				leaky integrator (Masking I)	leaky integrator (Masking II)	Spectrogram Korrelator	Spectrogram Korrelator	Spectrogram Korrelator	Spectrogram Korrelator
1	10	500	4000	98%	97%	94%	36%	36%	0%
2	10	1000	4000	98%	90%	94%	36%	36%	0%
3	10	2000	4000	96%	84%	88%	36%	0%	0%
4	50	500	4000	99%	97%	92%	65%	80%	61%
5	50	1000	4000	99%	92%	92%	65%	65%	61%
6	50	2000	4000	99%	77%	88%	65%	65%	61%
7	200	500	4000	99%	97%	88%	74%	75%	68%
8	200	1000	4000	99%	90%	82%	74%	75%	0%
9	200	2000	4000	98%	81%	65%	68%	60%	0%
10	10	500	500	97%	89%	79%	0%	0%	0%
11	10	1000	500	93%	78%	64%	0%	0%	0%
12	10	2000	500	89%	67%	50%	0%	0%	0%
13	50	500	500	99%	70%	87%	29%	38%	0%
14	50	1000	500	98%	87%	40%	7%	19%	0%
15	50	2000	500	97%	91%	27%	0%	13%	0%
16	200	500	500	99%	98%	53%	0%	44%	0%
17	200	1000	500	99%	94%	33%	0%	0%	0%
18	200	2000	500	97%	77%	27%	0%	0%	0%

Das Ergebnis der Modelle zeigt, dass solche seismischen Untersuchungen, die in niedrigeren Breitengraden (Australien) durchgeführt werden, sogar in entfernten Gebieten in höheren Breitengraden (Antarktis) Maskierungspotential haben können. Wie erwartet, nimmt die Maskierung im Allgemeinen mit der Entfernung von der Airgun-Quelle ab (und die Kommunikationsreichweite nimmt im Allgemeinen zu) (alle Modelle in Kapitel fünf). Da jedoch die übertragene Gesamtenergie (Airgun) nicht monoton über die Entfernung zur Quelle abnimmt, zeigen die hier dargestellten Modelle lokale Abweichungen vom allgemeinen Trend. Im Folgenden werden die in Kapitel fünf ermittelten Kommunikationsreichweiten für mehrere Zielarten vorgestellt und die Auswirkungen der Airgunsignale auf **Individuen- und Populationsebene**, welche in **Kapitel sechs** diskutiert werden, interpretiert.

Antarktische Blauwale ernähren sich im Allgemeinen während des australischen Sommers in höheren Breitengraden und migrieren im Winter zum Kalben in niedrigere Breitengrade. Akustische Aufzeichnungen von Vokalisierungen antarktischer Blauwale dokumentieren, dass antarktische Blauwale in niedrigen Breiten des Indischen Ozeans, des östlichen Pazifiks und des Südatlantiks während des australischen Winters anwesend sind, aber während des australischen Sommers fehlen (Stafford et al. 2004, Samaran et al. 2013, Shabangu et al. 2019). In hohen Breitengraden werden antarktische Blauwalvokalisierungen das ganze Jahr über detektiert, mit einem Maximum in den Detektionen zwischen Januar und April (Thomisch et al. 2016), in Übereinstimmung mit dem Muster des Auftretens von Z-Rufen an der in diesem Bericht analysierten antarktischen Aufzeichnungsstation (Kapitel drei).

Unter ruhigen Umgebungslärmbedingungen mit weniger als 90 dB und in Abwesenheit von Airgunsignalen sagt das Hörmodell Kommunikationsreichweiten von über 1000 km voraus. Es ist nicht bekannt, ob die Kommunikation über so große Reichweiten biologisch relevant ist. Außerdem ist es wahrscheinlich, dass diese weit entfernten Vokalisierungen durch andere Vokalisierungen maskiert werden, die in der näheren Umgebung auftreten. Die vorhergesagte Kommunikationsreichweite nimmt schnell ab, wenn der Umgebungslärmpegel steigt.

Blauwalszenario 1 (Abbildung 3, links):

Parametereinstellungen: Blauwal Z-Ruf, Wassertiefe=500 m, Vokalisationstiefe=50 m, Empfängertiefe=50 m, Spektrogramm-Korrelator, 102 dB Umgebungslärm

Für mittlere Umgebungslärmpegel (102 dB) und in Abwesenheit von Airgunsignalen sagt das Hörmodell Kommunikationsreichweiten von 320 km in den Szenarien im flachen Ozean (**Wassertiefe von 500 m**) voraus. In Anwesenheit einer Airgun wird die Kommunikationsreichweite bis zu einer Entfernung von 500 km von der Airgun erheblich beeinträchtigt und die Kommunikationsreichweite auf 200 km reduziert (was einem Verlust der Kommunikationsreichweite von 38% entspricht (im Verhältnis von verlorener Kommunikationsreichweite zu natürlicher Kommunikationsreichweite)). Mit abnehmender Airgun-Empfänger-Distanz sinkt die geschätzte Kommunikationsreichweite stark auf 140 km (66% Verlust) für eine Airgun in 200 km Entfernung und auf 60 km (81% Verlust) für eine Airgun in 100 km Entfernung. Die Kommunikationsreichweiten in den Szenarien im flachen Ozean sind im Allgemeinen deutlich höher als die Kommunikationsreichweiten im tiefen Ozean für die Kommunikationen von Blau- und Finnwalen und daher variiert das Maskierungspotential auch in den Szenarien im tiefen Ozean.

Blauwalszenario 2 (Abbildung 3, rechts):

Parametereinstellungen: Blauwal-Z-Ruf, Wassertiefe=4000 m, Vokalisationstiefe=50 m, Empfängertiefe=50 m, Spektrogramm-Korrelator, 102 dB Umgebungsgeräusch

Für 102 dB Umgebungslärm und in Abwesenheit von Airgunsignalen sagt das Hörmodell Kommunikationsreichweiten von 200 km in Tiefseeszenarien (**Wassertiefe von 4000 m**) voraus. In Anwesenheit einer Airgun wird die Kommunikationsreichweite bereits bis zu einer Entfernung von

2000 km von der Airgun stark beeinträchtigt und die Kommunikationsreichweite reduziert sich auf 70 km (was einem Verlust der Kommunikationsreichweite von 65% entspricht (im Verhältnis von Verlust der Kommunikationsreichweite zu natürlicher Kommunikationsreichweite)). Mit abnehmender Airgun-Empfänger-Distanz sinkt die geschätzte Kommunikationsreichweite stark auf 40 km (80% Verlust) für eine Airgun in 500 km Entfernung. Das Maskierungspotential von Airguns ist also höher, wenn sich die kommunizierenden Blauwale in der Tiefsee befinden. Es erscheint plausibel, dass eine Verringerung der Erfassungsreichweite von 200 km auf 70 km (durch eine Airgun in 2000 km Entfernung) die Vitalraten eines Individuums beeinflusst. Das Hörmodell für den **Z-Ruf des antarktischen Blauwals** zeigt, dass Airgunsignale in einer Entfernung von 2000 km (die maximale analysierte Entfernung) vom Blauwal seine Erkennungsreichweite für die Vokalisierung eines Artgenossen auf 35% der Reichweite reduzieren, die in Abwesenheit von Airgunsignalen erreicht wird.

Abbildung 3 Übersichtsdarstellungen, die die Maskierung von Z-Rufen des antarktischen Blauwals durch Airgunsignale zeigen. Die Diagramme zeigen den prozentualen Verlust der Kommunikationsdistanz im Vergleich zu äquivalenten Szenarien ohne Airgun und gelten für mittlere Umgebungslärmpegel von 102 dB. Die Wirkungsbereiche der Airguns in den Szenarien im flachem Ozean sind im Allgemeinen geringer als im Szenario im tiefem Ozean.
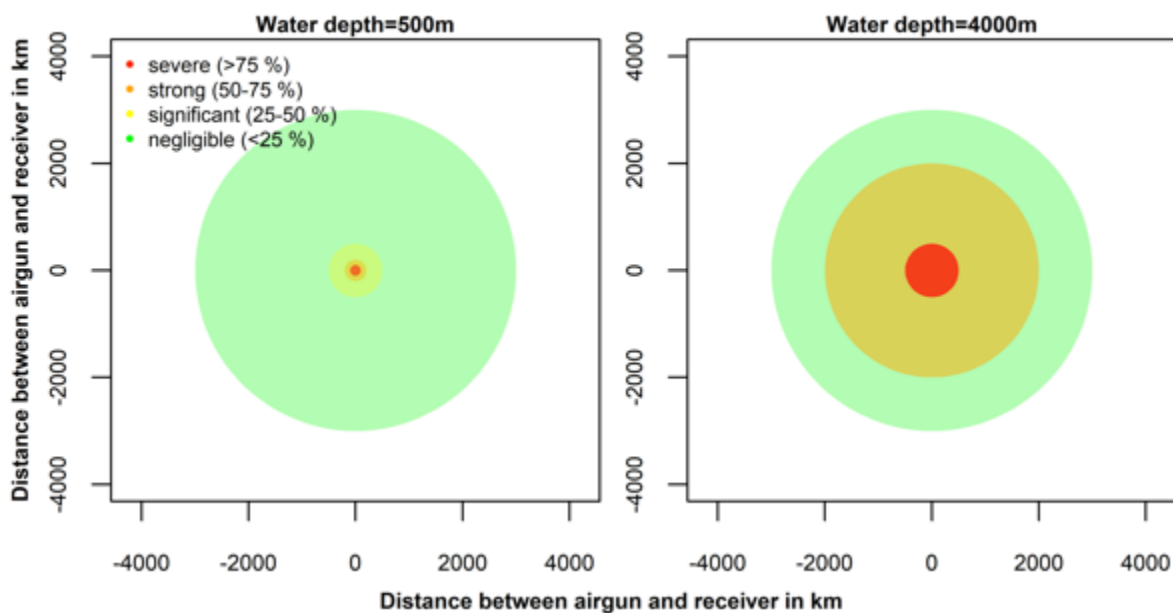
Antarktische Blauwale wiederholen **Z-Rufe** oft mehrfach. Dies führt zu Sequenzenmustern, die stundenlang andauern können (Erbe et al. 2017). Es wird angenommen, dass diese Gesänge von Männchen stammen, die versuchen, Weibchen anzulocken, indem sie die Qualität des Männchens und/oder gute Futtergelegenheiten ankündigen (Croll et al. 2002). Daher kann das Maskieren dieser Z-Rufe zu verpassten Gelegenheiten derNahrungsaufnahme führen, die Partnerwahl der Weibchen beeinträchtigen und sogar zu verpassten Paarungschancen für das vokalisierende Männchen sowie für das weibliche empfangende Tier führen. Die Auswahl eines Partners von hoher genetischer Qualität, dessen genetische Veranlagung mit der des auswählenden Weibchens vereinbar ist, sollte die Fitness der Nachkommen erhöhen und kann die Anpassung an veränderte Umweltbedingungen fördern (Jones & Ratterman 2009). Da die Abundanz der antarktischen Blauwale immer noch unter 1% des Niveaus vor der Ausbeutung liegt (Branch et al. 2004), könnte die Kommunikation über weite Entfernungen notwendig sein, damit ein Männchen Weibchen anlocken und ein Weibchen Männchen finden und bewerten kann.

Blauwal-Z-Rufe werden vermutlich durch Airguns maskiert, selbst wenn der Abstand zwischen Empfängertier und Airgun groß ist, was einen Einfluss auf die individuellen Vitalraten hat. Die Quantifizierung der Auswirkungen von einer Maskierung der Kommunikation auf die individuellen Vitalraten stellt jedoch noch immer eine große Herausforderung dar, da die biologischen Funktionen der Vokalisierungen nur in begrenztem Maße bekannt sind. Die Bedeutung der Partnerwahl bei Blauwalen und das Ausmaß, in dem ein Individuum eine verpasste Gelegenheiten zur Paarungs oder Nahrungsaufnahme kompensieren kann, wurden bisher nicht untersucht.

Ähnlich wie die antarktischen Blauwale hat die **Finnwal**-Unterart *Balaenoptera physalus quoyi* auf der Südhalbkugel eine zirkumpolare Verbreitung während der australischen Sommermonate. Im Vergleich zu Blauwalen sind Finnwale weniger eng mit der Eiskante verbunden und kommen meist in nördlicheren Breiten vor. Ihre Verteilung in den sommerlichen Nahrungsgründen wird wahrscheinlich durch die Verteilung bestimmter Krillarten bestimmt (Herr et al. 2016). Im Winter migrieren Finnwale in niedrigere Breitengrade, wo sie ihre Jungen gebähren (Aguilar et al. 2009, Leroy et al. 2018, Shabangu et al. 2019). Es wurde dokumentiert, dass Finnwale in den Wintermonaten mehr vokalisieren und im Sommer weniger (Sirovic et al. 2009, Thomisch et al. 2016). Die auffälligste und lauteste Vokalisierung der Finnwale ist der 20-Hz-Ruf. Es wurde beobachtet, dass nur männliche Finnwale stereotype Wiederholungen des **20-Hz-Rufs** produzieren (Croll et al. 2002).

Die Modellergebnisse deuten darauf hin, dass die Detektionsbereiche für diesen Vokalisationstyp stark von den natürlichen Umgebungs- und Airgunsignalpegeln abhängen. Wenn der Umgebungslärm niedrig ist (<90 dB), können die Detektionsreichweiten in der Größenordnung von 1000 km ohne Airgunsignale liegen, während die Detektionsreichweiten bei höherem Umgebungslärm (112 dB), die typisch für den Südlichen Ozean sind, nur wenige Kilometer erreichen.

Finnwalszenario 1: (Abbildung 4, links):

Parametereinstellungen: Finnwal 20-Hz-Ruf, Wassertiefe=4000 m, Vokalisationstiefe=50 m, Empfängertiefe=50 m, Spektrogramm-Korrelator, 102 dB Umgebungslärm

Für 102 dB Umgebungslärmpegel und in Abwesenheit von Airgunsignalen sagt das Hörmodell Kommunikationsreichweiten von 140 km in Tiefseeszenarien (**Empfängertiefe von 50 m**) voraus. In Anwesenheit einer Airgun wird die Kommunikationsreichweite bis zu einer Entfernung von 2000 km von der Airgun erheblich beeinträchtigt und die Kommunikationsreichweite auf 100 km reduziert (was einem Verlust der Kommunikationsreichweite von 29% entspricht (im Verhältnis von verlorener Kommunikationsreichweite zu natürlicher Kommunikationsreichweite)). Mit abnehmender Airgun-Empfänger-Distanz sinkt die geschätzte Kommunikationsreichweite stark auf 50 km (64% Verlust) für eine Airgun in 1000 km Entfernung und auf 1 km (99% Verlust) für eine Airgun in 500 km Entfernung.

Finnwalszenario 2: (Abbildung 4, rechts):

Parametereinstellungen: Finnwal 20-Hz-Ruf, Wassertiefe=4000 m, Vokalisationstiefe=50 m, Empfängertiefe=200 m, Spektrogramm-Korrelator, 102 dB Umgebungslärm

Die Kommunikationsreichweiten für 200 m Empfängertiefe sind deutlich kürzer als für 50 m Empfängertiefe. Wenn sich also der Empfänger-Finnwal in 200 m Tiefe befindet, sagt das Hörmodell für einen 102 dB Umgebungslärmpegel und in Abwesenheit von Airgunsignalen Kommunikationsreichweiten von 200 km für die Tiefseeszenarien (**Empfängertiefe 200 m**) voraus. In Anwesenheit einer Airgun wird die Kommunikationsreichweite bis zu einer Entfernung von 2000 km von der Airgun stark beeinträchtigt und die Kommunikationsreichweite auf 50 km reduziert (was einem Verlust der Kommunikationsreichweite von 75% entspricht (im Verhältnis von verlorener Kommunikationsreichweite zu natürlicher Kommunikationsreichweite)). Mit abnehmender Entfernung zwischen Airgun und Empfänger sinkt die geschätzte Kommunikationsreichweite auf 18 km (91% Verlust) für eine Airgun in einer Entfernung von 1000 km und auf 3 km (99% Verlust) für eine Airgun

in einer Entfernung von 500 km. Der Maskierungseffekt von Airguns ist also höher, wenn sich die empfangenden Finnwale in 200 m Tiefe befinden, verglichen mit der Situation in 50 m Tiefe.

Abbildung 4: Übersichtsdarstellungen, die zeigen, wie die Kommunikationsreichweiten des **20-Hz-Rufs der Finnwale** bei mittleren Umgebungslärmpegeln (102 dB), die für den Südlichen Ozean typisch sind, reduziert werden. Die Wirkungsbereiche von Airguns eines Empfängers in 200 m Tiefe sind generell höher als bei einem Empfänger in 50 m Tiefe.
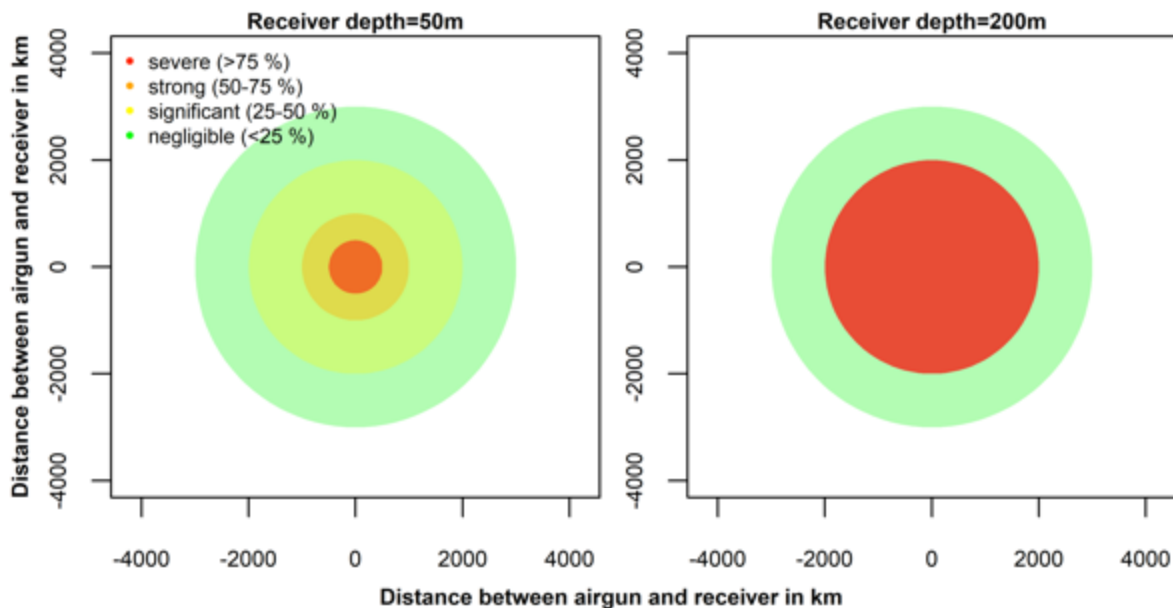
Es wird angenommen, dass der **20-Hz-Ruf des Finnwals** ähnliche biologische Funktionen wie der Z-Ruf bei Blauwalen erfüllt (Finden und Vergleichen von Partnern, Anzeigen guter Nahrungsgründe), wobei nur Männchen stereotypische Wiederholungen dieses Vokalisationstyps produzieren (Croll et al. 2002). Diese Vokalisierung hat im Vergleich zum Blauwal-Z-Ruf nur eine kurze Dauer und besitzt kein sehr charakteristisches Muster, sodass diese durch Airgunsignale, aber auch durch Umgebungslärm stark maskiert werden kann. Airguns verursachen besonders dramatische Verringerungen der Kommunikationsreichweite bei relativ geringem Umgebungslärm. Finnwale nutzen möglicherweise Fenster mit geringem Umgebungslärm für die Kommunikation über große Entfernungen. Die Modellergebnisse zeigen, dass selbst weit entfernte Airguns (in der Größenordnung von 500 km zwischen Empfängertier und Airgun) diese „Kommunikationsfenster mit großer Reichweite" vollständig blockieren können (durch Reduzierung der Kommunikationsreichweite auf weniger als 1 km).

Zusammenfassend lässt sich sagen, dass es erhebliche räumlich und zeitliche Überschneidungen zwischen seismischen Untersuchungen und dem Vorkommen des antarktischen Blauwals sowie des Finnwals gibt. In hohen Breitengraden sind sowohl die seismischen Untersuchungen, als auch die Blau- und Finnwalaktivität im australischen Sommer am höchsten. In niedrigen Breitengraden gibt es während des australischen Winters, wenn Blau- und Finnwale nach Norden migrieren, weiterhin seismische Vermessungsaktivitäten. Die Ergebnisse des Hörmodells zeigen, dass eine potentiell fitnessrelevante Maskierung von Blauwal-Z-Rufen auch in Entfernungen von mehr als 2000 km vom Airgun-Standort erfolgen kann. Die potentiell von einer einzigen seismischen Vermessung betroffenen Gebiete sind riesig (verglichen mit der Entfernung zwischen Australien und dem antarktischen Kontinent, die etwa 3000 km beträgt). Für die 20-Hz-Rufe der Finnwale legt das Hörmodell nahe, dass die Maskierung durch Airgunsignale hauptsächlich dann relevant ist, wenn die Umgebungslärmpegel moderat bis niedrig sind (bei hohen Umgebungslärmpegeln werden die Detektionsbereiche

hauptsächlich durch den Umgebungslärm begrenzt und die Airgunsignale verursachen nur eine geringe zusätzliche Reduzierung). Bei niedrigen Umgebungslärmpegeln können Airguns in einer Entfernung von 500 km eine potentiell fitnessrelevante Maskierung von Finnwal-Vokalisierungen verursachen. Bis heute ist kaum bekannt, wie sich das Migrationsverhalten von Blau- und Finnwalen zwischen den Geschlechtern und Altersgruppen, dem Fortpflanzungsstatus und zwischen den Populationen unterscheidet. Es ist wichtig, dass diese Wissenslücke geschlossen wird, da die Auswirkungen der Maskierung auf die individuellen Vitalraten wahrscheinlich von diesen Parametern abhängen (z.B. sind Jungtiere oder sich nicht-fortpflanzende Individuuen möglicherweise in ihrer Fitness anders betroffen, wenn ein Paarungsruf maskiert wird).

Schwertwal und Weddellrobbe werden im selben Unterkapitel behandelt, da diese Arten hochfrequente oder breitbandige Vokalisierungen erzeugen (Erbe et al. 2017). Nur einige ihrer Vokalisierungen überschneiden sich mit dem Frequenzbereich der Airgunsignale (< 500 Hz) und diese Vokalisierungen enthalten typischerweise auch erhebliche Energie in Frequenzbändern > 500 Hz. Die Hörmodelle haben bestätigt, dass Airgunsignale wenig Einfluss auf die Kommunikationsbereiche hat, falls die Tiere die Fähigkeit haben, sich durch Hochpassfilterung auf Frequenzen oberhalb von 500 Hz zu konzentrieren.

Für die breitbandigen Vokalisierungen von Schwertwalen und Weddellrobben haben tieffrequente Airgunsignale nur dann das Potential, die Fitness zu beeinträchtigen, wenn 1) das Gehör des Empfängertiers nicht in der Lage ist, tief- und hochfrequente Anteile der Vokalisierung getrennt zu analysieren oder 2) biologisch relevante Informationen (z.B. Informationen zur Individualerkennung) im tieffrequenten Teil der Vokalisierung kodiert sind. Im Fall 1) wird die Signalerkennung im hochfrequenten Teil durch tieffrequentes Rauschen behindert, während im Fall 2) die Tiere auf den tieffrequenten Teil der Vokalisierungen für die Kommunikation angewiesen sind (der tieffrequente Teil der Vokalisierungen kann besonders wichtig für die Kommunikation über große Entfernungen sein, über die hohe Frequenzen stark gedämpft werden).

Weddellrobben-Szenario 1: (Abbildung 5, links):

Parametereinstellungen: Weddellrobbe, Schallsequenz, Wassertiefe=500 m, Vokalisationstiefe=5 m, Empfängertiefe=50 m, Spektrogramm-Korrelator, 80 dB Umgebungslärm

Für die Weddellrobben-Schallsequenz (**Vokalisationstiefe von 5 m**) können bei geringem Umgebungslärm (80 dB) Detektionsreichweiten in der Größenordnung von 100 km bei Abwesenheit von Airgunsignalen erzielt werden. In Anwesenheit einer Airgun wird die Kommunikationsreichweite bereits bei einer Vollband-Analyse bis zu einer Entfernung von 2000 km von der Airgun stark beeinträchtigt und die Kommunikationsreichweite auf 40 km reduziert (was einem Verlust der Kommunikationsreichweite von 60% entspricht (im Verhältnis von verlorener Kommunikationsreichweite zu natürlicher Kommunikationsreichweite)). Mit abnehmendem Abstand zwischen Airgun und Empfänger verringert sich die geschätzte Kommunikationsreichweite stark auf 14 km (86% Verlust) für eine Airgun in 1000 km Entfernung. Für den tieffrequenten Übertragungsverlust bei großen Entfernungen ist der Pegel des sich aus 5 m Tiefe ausbreitenden Schalls stärker gedämpft als der aus 50 m Vokalisationstiefe stammende Schall.

Weddellrobben-Szenario 2: (Abbildung 5, rechts):

Parametereinstellungen: Weddellrobbe, Schallsequenz, Wassertiefe=500 m, Vokalisationstiefe=50 m, Empfängertiefe=50 m, Spektrogramm-Korrelator, 80 dB Umgebungslärm

Für die Weddellrobben-Schallsequenz (**Vokalisationstiefe von 50 m**) können bei geringem Umgebungslärm (80 dB) Detektionsreichweiten in der Größenordnung von 100 km ohne Airgunsignale erzielt werden. In Anwesenheit einer Airgun wird die Kommunikationsreichweite bereits bis zu einer Entfernung von 2000 km von der Airgun stark beeinträchtigt und die Kommunikationsreichweite auf 50 km reduziert (was einem Verlust der Kommunikationsreichweite von 50% entspricht (im Verhältnis

von verlorener Kommunikationsreichweite zu natürlicher Kommunikationsreichweite)). Mit abnehmender Airgun-Empfänger-Distanz sinkt die geschätzte Kommunikationsreichweite stark auf 14 km (86% Verlust) für eine Airgun in 500 km Entfernung. Das Maskierungspotential von Airguns ist also höher, wenn die kommunizierende Weddellrobbe in 5 m Tiefe vokalisiert, als in 50 m Tiefe.

Abbildung 5:   Übersichtsdarstellungen, die zeigen, wie der Pegel des sich aus 5 m Tiefe ausbreitenden Schalls stärker gedämpft wird als der aus **50 m Vokalisationstiefe** stammende Schall für den tieffrequenten Übertragungsverlust bei großen Entfernungen.
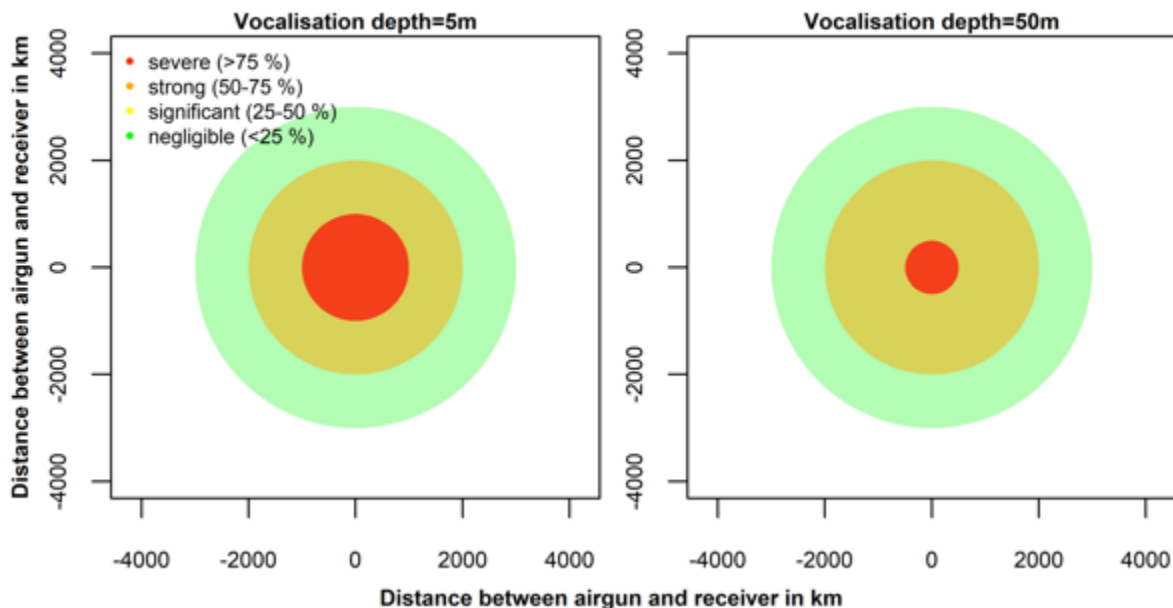
Die Maskierung der Kommunikation durch Airgunsignale betrifft nur den tieffrequenten Teil der Vokalisierungen von Schwertwalen und Weddellrobben. Wenn die Erkennung von Vokalisierungen allein ausreicht, ist es unwahrscheinlich, dass die Kommunikationsreichweite von Weddellrobben und Schwertwalen durch Airgunsignale beeinträchtigt wird. Wenn jedoch der tieffrequente Teil biologisch relevante Informationen enthält oder Individuen speziell auf den tieffrequenten Teil der Vokalisierungen angewiesen sind, um Informationen über entfernte Vokalisierer zu erhalten, können Airguns eine Maskierung der Kommunikation verursachen. Obwohl die Maskierung der Kommunikation durch Airgunsignale für Weddellrobben und Schwertwale weniger relevant sein dürfte als für die beiden oben genannten Bartenwalarten, bleibt es schwierig, das Risiko der Schallbelastung gegenüber der Maskierung der Kommunikation durch Airguns für diese Arten zu quantifizieren.

Es ist nicht bekannt, inwieweit **Weddellrobben** und **Schwertwale** auf den maskierten tieffrequenten Teil ihrer Vokalisierungen angewiesen sind, so dass das Ausmaß, in dem diese Arten unter der Maskierung der Kommunikation durch Airgunsignale leiden, unklar ist. Die Vokalisierungen der männlichen Weddellrobben werden während der Fortpflanzungszeit produziert und sind wahrscheinlich wichtig für die Etablierung von Unterwasserterritorien (Rouget et al. 2007) und für das Anlocken von Weibchen (Opzeeland et al. 2010). Rogers (2017) schlug einen Mechanismus vor, durch den Vokalisierungen als ehrliche Signale der männlichen Qualität dienen können: Die Produktion von sich wiederholenden Sequenzen von Unterwasservokalisierungen kann auf die Fähigkeit des Vokalisierers hinweisen, die Luft anzuhalten. Bei Seeleoparden waren nur große Männchen in der Lage, konsistente rhythmische Vokalisierungsmuster während der gesamten Fortpflanzungszeit beizubehalten, während die Anzahl der zwischen den Vokalisierungen liegenden Pausen bei kleinen Männchen im Laufe der Fortpflanzungszeit zunahm (Rogers 2017). Ähnliche Mechanismen könnten es

den Weddellrobbenweibchen ermöglichen, die Qualität der Männchen anhand der Vokalisierungen zu bewerten. Obwohl die Vokalisationsaktivität der Weddellrobben während der Fortpflanzungszeit ihr Maximum erreicht, sind die Vokalisierungen nicht auf diese Zeit des Jahres beschränkt. Weddellrobben produzieren eine Vielzahl unterschiedlicher Vokalisierungen (Erbe et al. 2017). Zu den Funktionen der Vokalisierungen an Luft gehört, dass die Bindung zwischen Mutter und Jungtier aufrechterhalten wird. Abhängig von der Bedeutung des tieffrequenten Teils der Vokalisierungen für die biologische Funktionalität können Airgunsignale die Aufrechterhaltung von Unterwasserterritorien, die Partnersuche, die Partnerwahl der Weibchen und noch unbekannte Funktionen des vielseitigen Weddellrobben-Vokalisationsrepertoires stören.

Die akustische Wahrnehmung ist typischerweise am wichtigsten, um Informationen über entfernte Objekte in Echtzeit zu erhalten. Die Evolution hochentwickelter auditorischer Systeme und des Biosonars (Au und Hastings 2008) ist ein überzeigender Beweis dafür, dass die natürliche Selektion auf das auditorische System bei Meeressäugern stark ist: Die Fähigkeit, detaillierte Informationen aus akustischen Signalen zu gewinnen, bietet einen Fitnessvorteil. Die Bedeutung der akustischen Wahrnehmung wurde in einer Vielzahl von Verhaltenskontexten dokumentiert. In diesem Bericht werden Verhaltenskontexte aufgelistet und Beispiele angeführt, mit Schwerpunkt auf Meeressäugetierarten, die im Südlichen Ozean vorkommen.

Meeressäuger haben sich dahingehend entwickelt, Schall als primäre Sinneswahrnehmung zu nutzen. Jegliche Störung der akustischen Kommunikation kann schwerwiegende Auswirkungen sowohl auf das Sender- als auch das Empfängertier haben, was sich auf die Fitness auswirken kann, z.B. wenn die Maskierung die Signalerkennung verhindert (Branstetter et al. 2016). Verhaltensreaktionen können sehr variabel sein und sind mit einfachen akustischen Metriken, wie z.B. dem empfangenen Schallpegel, möglicherweise unzureichend vorhersagbar. Vielmehr scheinen Unterschiede zwischen Arten und Individuen zusammen mit kontextuellen Aspekten der Schallbelastung die Wahrscheinlichkeit für Verhaltensreaktionen zu beeinflussen (Southall et al. 2016).

Um die Ergebnisse zu validieren, sind experimentelle Studien zur Maskierung erforderlich. Während Störungsreaktionen auf Airgunsignale bereits untersucht wurden, ist eine Ermittlung von Maskierungseffekten eine viel größere Herausforderung. Dies liegt daran, dass Störungsreaktionen häufig mit abrupten Verhaltensänderungen verbunden sind, die im Feld beobachtet werden können. Die Untersuchung von Maskierung auf der Grundlage von Verhaltensbeobachtungen erfordert Kenntnisse darüber, wie sich das Tier in An- und Abwesenheit des biologisch relevanten Signals verhält. Dies konnte bisher nur bei Tieren in menschlicher Obhut gezeigt werden, die darauf trainiert sind, auf ein Signal zu reagieren, um eine Belohnung zu erhalten. Solche Experimente wurden mit Delfinen (Branstetter et al. 2016) und kürzlich auch mit Tümmlern (Sills et al. 2017) durchgeführt, sind aber bei Bartenwalen unmöglich. Sills et al. (2017) untersuchten, wie gut zwei Individuen zweier arktischer Robbenarten (eine männliche Fleckenrobbe und eine weibliche Ringelrobbe) in der Lage waren, Testsignale (lineare Upsweeps von 95 bis 105 Hz in 500 ms) in Gegenwart von Airgunsignalen zu erkennen, der in einer Entfernung von 1 und 30 km von einem Airgun-Array aufgezeichnet wurde. Da nur zwei Individuen untersucht wurden, ist nicht bekannt, wie gut die Ergebnisse auf andere Individuen derselben Art übertragbar sind und ob diese auch für andere Arten zutreffen. Solche experimentellen Studien bieten eine hervorragende Gelegenheit für die zukünftige Validierung des in diesem Bericht entwickelten psychophysischen Modells. Sobald mehrere solcher Studien verfügbar sind, sollte die Hörsituation der Versuchstiere simuliert und die Vorhersagen des psychophysischen Modells mit der Leistung der Versuchstiere verglichen werden.

Abschließend wird das verfügbare Wissen über die modellierten antarktischen Populationen für jeden der Hauptschritte eines PCoD-Modells (Population Consequences of Disturbance model) diskutiert. Das Grundprinzip des PCoD-Konzeptes lässt sich wie folgt zusammenfassen: Wenn ein Individuum einem Stressor ausgesetzt ist, ändert sich sein physiologischer Zustand und sein Verhalten. Physiologische und

Verhaltensänderungen können sich direkt („akute Effekte") oder indirekt („chronische Effekte") auf die Vitalraten des Individuums auswirken, indem sie beispielsweise die Überlebensrate oder die Fruchtbarkeit beeinflussen. Dieser Zusammenhang wird durch die Umweltbedingungen beeinflusst. Basierend auf der Modellierung des Schallbelastungsrisikos eines Individuums und grundlegenden Populationsparametern kann dann die Populationsdynamik modelliert werden. Das PCoD-Konzept wird dafür verwendet, um die Diskussion der Maskierungseffekte auf Populationsebene zu strukturieren und Wissenslücken zu identifizieren.

Eine Aufzählung der wichtigsten Schlussfolgerungen dieses Berichts findet sich in **Kapitel sieben**. Die in dieser Studie für den Südlichen Ozean entwickelten Modelle zeigen, dass Airgunsignale wahrscheinlich die Vokalisierungen von Meeressäugern maskieren - insbesondere die tieffrequenten Vokalisierungen von Bartenwalen: Lärm von Airguns in einer Entfernung von 1000 – 2000 km vom empfangenden Tier kann die Kommunikationsreichweite von Blau- und Finnwalen stark reduzieren. Bei Arten mit hochfrequenten oder breitbandigen Vokalisierungen ist der Maskierungseffekt begrenzt, wenn das bloße Erkennen einer Vokalisierung ausreicht. Reduzierungen der Betriebszeit und der Airgun-Quellschallpegel können die Bereiche, in denen Maskierung auftritt, reduzieren. Eine Reduktion des Airgun-Quellschallpegels um 10 dB reduziert den betroffenen Bereich ungefähr auf ein Zehntel seiner ursprünglichen Größe. Der Verhaltenskontext der Vokalisierungen zusammen mit der Zeit und Energie, die die Tiere in das Vokalisieren investieren, deutet darauf hin, dass die Z-Rufe der antarktischen Blauwale und die 20-Hz-Rufe der Finnwale wichtige Funktionen im Zusammenhang mit der Paarung und möglicherweise auch der Nahrungssuche haben. Rückgänge in den individuellen Vitalraten (die Auswirkungen auf die Populationsebene nachsichziehen) sind daher wahrscheinlich, wenn Vokalisierungen maskiert werden.

1 Introduction

1.1 Background

The German Federal Environmental Agency (UBA) issues permits for German activities in the Antarctic. These activities include marine seismic surveys which typically use sound sources consisting of arrays of airguns. Airguns produce a high-intensity impulsive sound by suddenly releasing high-pressure air into the water.

The scientific basis for evaluating the effects of airgun operations on marine mammals still has gaps. Existing studies show that airgun noise can induce permanent and temporary shifts of the hearing threshold in marine mammals (Gedamke et al. 2011, Kastelein et al. 2017) and can trigger disturbance or displacement reactions (Castellote et al. 2012, Nowacek et al. 2015). Moreover, airgun noise can mask biologically relevant acoustic cues. Since even individuals at distances as far as several thousand kilometres away from the airgun location may suffer from masking (Nieukirk et al. 2012, Siebert et al. 2014), masking may be the most pervasive effect of airgun noise. Most energy of airgun pulses is concentrated in the low frequency band. This frequency range overlaps with many marine mammal vocalizations, especially the songs and calls of baleen whales. While acoustic cues are not limited to vocalizations of conspecifics and include cues of predator presence (Cure et al. 2015) as well as cues important for orientation (Clark et al. 2009), masking of communication sounds may have particularly negative effects on baleen whales. Knowledge on the extent of communication masking caused by airgun noise and on the effects of communication masking at the level of the individual and the population is still limited. This study aims at assessing the extent of communication masking by airgun noise for selected Antarctic marine mammals and discusses effects at the level of the individual and the population.

1.2 Structure of the report

Marine mammals may respond to increased noise levels by increasing the amplitude, by altering the frequency content or by increasing the repetition rate of their vocalizations (Erbe et al. 2016). **Chapter two** presents a **pilot study** that assesses the occurrence of such antimasking strategies in blue whales in Iceland.

To gain insight into the spatial extent of masking, sound propagation in the focal environment has to be understood. In **chapter three** sound **propagation models** are developed for the Antarctic Ocean. Models are validated based on recordings of two seismic surveys conducted in the Southern Ocean. Signals change in level, frequency content and duration (or more specifically temporal structure) as they radiate from the sound source. The validated models provide insight into physical phenomena governing sound propagation in the Southern Ocean.

High levels of ambient noise can reduce the range of audibility of airgun noise and consequentially the range over which airgun noise is a relevant masker of communication signals. In **chapter four ambient noise** recordings from three sonar buoys in the Southern Ocean are analysed.

Based on the validated propagation models developed in chapter three, the airgun noise that a listener receives can be inferred for any distance between the listener and the airgun source location. Moreover, the propagation models can be used to infer the vocalization that a listener receives for any distance between the listener and the vocalizing conspecific. All in all, mixing of the received airgun noise, the received vocalization and the ambient noise allows inference of the sound arriving at the receiver animal's ear for any given distances to the airgun location and the location of the vocalizing conspecific. In **chapter five** a **psychophysical model** is developed that predicts if a receiver animal can detect a conspecific's vocalization in any such scenario. Due to the strongly time-varying and spectrally complex character of the airgun noise as well as the vocalizations, the listening situation deviates markedly from

the continuous flat-spectrum noise and narrow band signals used to measure critical ratios in the laboratory (Erbe et al. 2016, Sills et al. 2017). In experiments with Arctic pinnipeds conventional masking models building on the concept of critical ratios have been found to provide accurate predictions of detection success only as long as variation in noise amplitude was limited (Sills et al. 2017). Therefore, a psychophysical model based on spectrogram correlation is proposed in chapter five. Detection ranges predicted by the model are provided for the blue whale z-call, the fin whale 20 Hz call, a multiharmonic call of a killer whale and two vocalizations by Weddell seals. For each of the vocalizations a multitude of environmental scenarios are explored including variation of the sound propagation scenario as well as the depth of the sender animal, the receiver animal and the ocean.

In **chapter six** the effects of airgun noise at the individual and population level are discussed based on the predicted communication ranges obtained in chapter five.

A bullet point list of the main conclusions of this report can be found in **chapter seven**.

2 Pilot project blue whale investigations in Iceland in the summer 2015

2.1 Introduction

The pilot blue whale project was conducted in North-East Iceland. The reason for this choice of location was that it is both easier and much more cost efficient compared to any location near Antarctica. Iceland is a very suitable location for testing equipment and to get some empirical data on coastal blue whales. Similar water depths and similar species of marine mammals can be found in both Antarctic and Arctic waters. For example, noise has been suggested to have the potential to mask communication of blue whales (Clark et al. 2009). By recording blue whales off northern Iceland, we have a chance to test this hypothesis, as the background noise levels in these waters is rapidly changing due to ships and boats in this area.

The pilot project was conducted off Húsavík in June 2015, the month where the blue whales usually are found in Skjálfandi Bay. Húsavík is easy to reach and the logistic of blue whale studies is therefore very easy from there.

This work package includes the following:

▶ Base line data of ambient noise with noise loggers
▶ Recording and identifying blue whales based on individual characteristics using a large hydrophone array (previously used by (Mohl et al. 2000) and (Tervo et al. 2012)).
▶ Projection of sound for masking the communication of blue whales and record the acoustic and behavioural reaction of masking.

2.2 Methods

The project was conducted in Skjálfandi Bay, Iceland (Northeastern Iceland; Figure 6) from 18th of June to 4th of July 2015.

Four vessels were used as platforms for the acoustic recordings: three sailing vessels from Denmark (Roxy), Belgium (Thoe), and Iceland (Gogo), and a fast speed local boat (Asa). Each recording vessel had a calibrated hydrophone (either Brüel & Kjær 8101 or Reson 4032) connected to an Olympus LS-10 or LS-14 digital recorder (sampling rate 44.1 kHz, 16 bits). The underwater sounds were recorded in one channel and a frequency-shift-keyed GPS signal, including PPS pulse (an electrical signal that has a width of less than one second and a sharply rising or abruptly falling edge that accurately repeats once per second) for timing, was recorded in the other channel (see (Mohl et al. 2000) for details). The hydrophone was lowered to a depth of 30 meters from each recording vessel. See Figure 7 for a schematic drawing of the setup. An additional hydrophone (type: Reson 4032) was lowered to 100 m and a Soundtrap data logger was deployed to 200 m depth in some recording sessions from two of the boats. These loggers were used to assess any difference in received level of the blue whale sounds as a function of depth.

Figure 6   Map of Iceland to the left. The red frame encircles Skjálfandi Bay, which can be seen in detail to the right. The town on the western side of the bay is Húsavík.
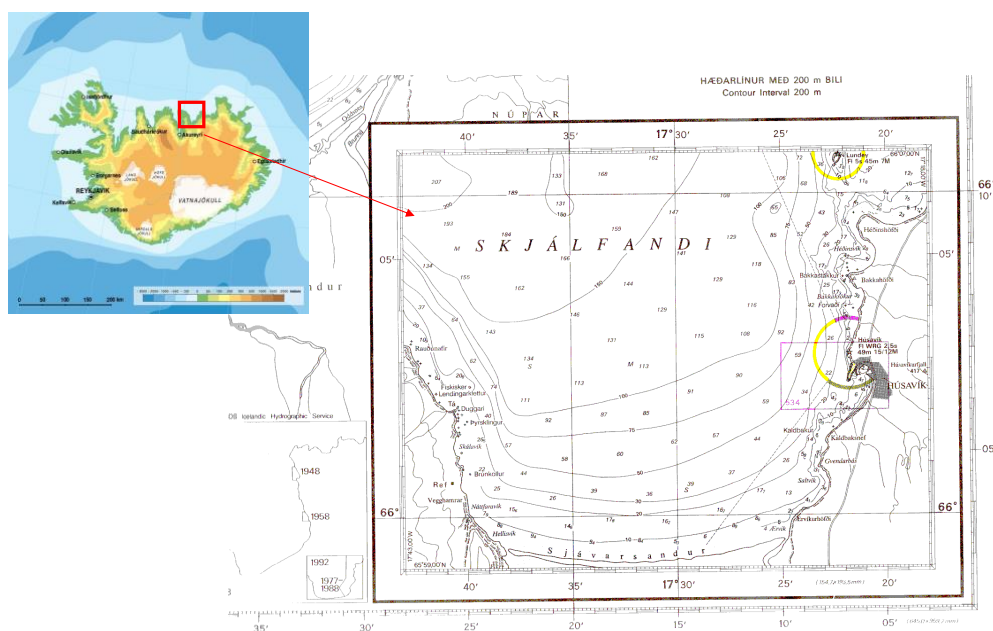
Figure 7   A schematic drawing of the recording setup using four vessels as a platform all equipped with a hydrophone and a recorder.
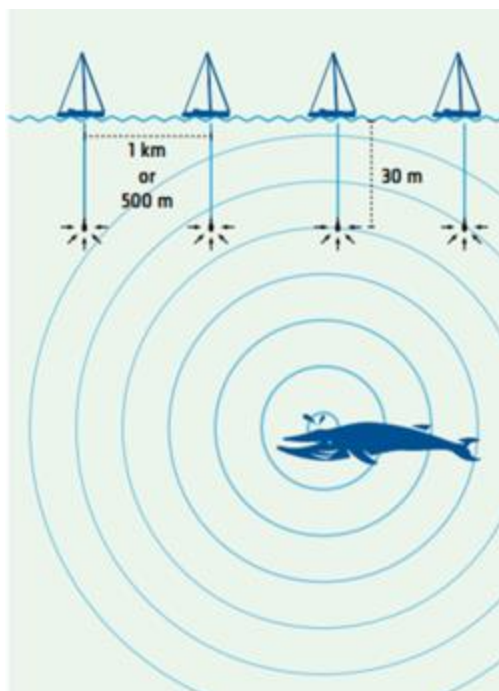
All recordings were made in Sea State 3 or less. During the recordings the boats were separated by either 500 meters or 1km either in North -South or East -West direction. Recordings were conducted both during night time and day time to include data both with and without high levels of boat traffic. Data were collected during ten different recording trips. The recordings were analysed both aurally and visually with a spectrogram viewer in BatSound Pro (Pettersson Electronik AB), Raven (Cornell Acoustic Lab) and Adobe Audition. The down-sweep blue whale calls usually gave well-defined time-of-arrival differences when the signals from the same call but recorded on different platforms were cross-

correlated. When the signals could be picked up on at least three platforms the acoustic localization of the call could be calculated using techniques described in (Wahlberg et al. 2001). These localizations were used to derive the transmission loss (assuming nearly spherical spreading) from whale to receiver, and this was used for source level estimates. Matlab was used for source localization and source level measurements. Information about larger ships present in the area was received from marinetraffic.com. Ambient noise levels were analysed from the platform recordings by selecting 10 min chunks with little or no self-noise, and thereafter using Welch spectral averaging method (Proakis and Manolaiks 2006) to derive average spectra with a filtering bandwidth of 2.7 Hz.

2.3   Results

Recordings were conducted on ten different recording days / nights. Blue whale down sweeps were used for localization and a total of 174 blue whale down-sweep calls were detected with good signal to noise ratio on six different days (21st of June, 22nd of June, 23rd of June, 24th of June, 3rd of July and 4th of July). Table 5 summaries the recording log for these days.

Unfortunately, due to equipment failure, relative few down sweeps were recorded on 3 channels and good localization was only possible for some down sweep calls (see Figure 8 for examples).

Table 2   Overview of recordings including: recording days, vessel ID, Start- and end time of recordings, duration of recordings in minutes, number of blue whales down sweeps and how many other boats were present (visual observations of for example whale watching vessels).

Recording date	Vessel	Start time	End time	Duration (min)	Number of down sweeps	Number of other boats
21062015	1	06:58:37	07:58:37	60	0	0
21062015	1	07:59:02	08:07:02	8	0	0
21062015	1	08:59:31	09:45:31	46	10	4
22062015	1	06:25:52	07:27:52	62	12	0
22062015	1	08:59:48	09:02:48	3	0	2
22062015	1	09:41:19	09:49:48	8	3	3
22062015	1	11:54:04	12:27:04	33	1	8
23062015	1	06:51:53	07:23:53	32	5	0
23062015	1	07:48:17	08:33:17	45	5	0
24062015	1	08:46:55	11:11:55	145	80	7
03072015	1	05:51:50	07:00:50	69	31	0
04072015	1	04:57:14	05:14:14	17	13	0
04072015	1	05:17:55	05:29:55	12	14	0
Total				**540**	**174**	

Figure 8   Spectrogram of two down sweep blue whale calls shown here in blue in this representation.
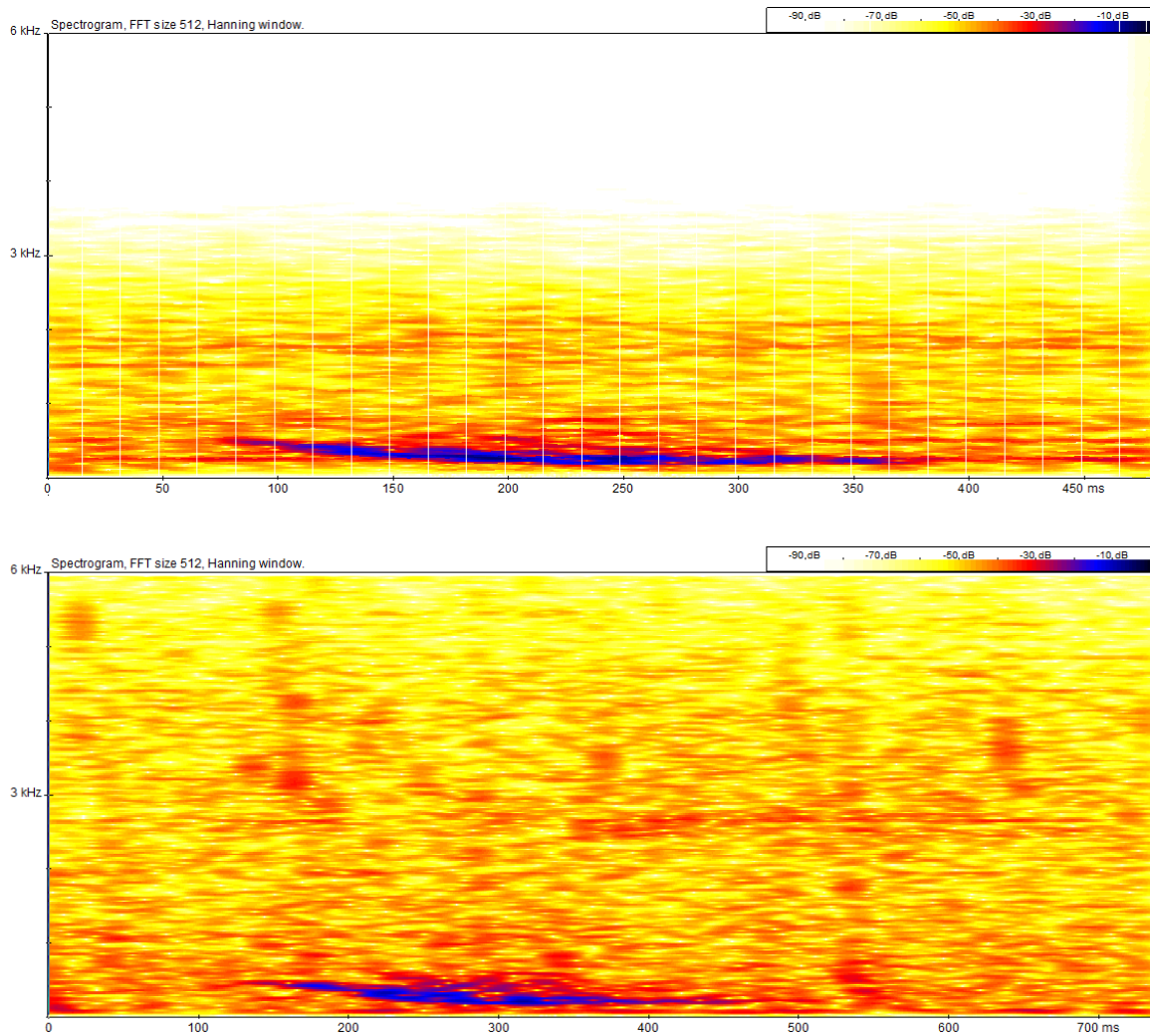
Results of cross-correlation can be seen on Figure 9 and Figure 10.

Figure 9   Two examples of acoustic localization of a blue whale down sweep. The red, black and blue signals to the left were recorded on three of the recording platforms (geometry given in the figure top right, where the platforms are indicated by circles with the same colour code as the signals to the left). The cross-correlation between the second and first signal is given in black to the right, and between the third and first signal in blue to the right. The peak of the cross-correlation signal gives the time lag between the three different signals, which is used as input for the acoustic localization algorithm. In the top right panel, the corresponding hyperbola curves are plotted, and the analytical source location is indicated with a star. See: (Wahlberg et al. 2001) for details.

Figure 10   Two examples of acoustic localization of a blue whale down sweep. The red, black and blue signals to the left were recorded on three of the recording platforms (geometry given in the figure top right, where the platforms are indicated by circles with the same colour code as the signals to the left). The cross-correlation between the second and first signal is given in black to the right, and between the third and first signal in blue to the right. The peak of the cross-correlation signal gives the time lag between the three different signals, which is used as input for the acoustic localization algorithm. In the top right panel, the corresponding hyperbola curves are plotted, and the analytical source location is indicated with a star. See: (Wahlberg et al. 2001) for details.

Source levels were estimated based on the distance between calling animal and recorders to be between 167 -192 dB re 1 µPa rms and the values are compared with other studies in Table 3. The distances to the recorded blue whale were between about 650 m to 1700 m. Duration of the signals were between 0.73-1.8s.

Table 3   Comparison of estimated source levels of down sweep calls from different populations of blue whales, recorded at different locations.

Population	Location	Vocalization type	Source level
North Atlantic	Skjálfandi Bay, NE Iceland	Down sweep	167 -192 dB re 1 uPa rms[a]
North Atlantic	Skjálfandi Bay, NE Iceland	Down sweep	159 to 169 dB re 1uPa rms [b]
Southern Hemisphere	off the Western Antarctic Peninsula	Southern Ocean blue whale song	189 ± 3 dB *re* 1 uPa at 1 m [c]

Population	Location	Vocalization type	Source level
Southern Hemisphere	off Chile	Down sweep	188 dB *re* 1 uPa at 1 m [d]
North Pacific	off California	Down sweep	186 dB *re* 1 uPa at 1 m [e]

[a] This study, b(Akamatsu et al. 2014), c (Sirovic et al. 2007), d (Cummings and Thompson 1971), e (McDonald et al. 2001)

Figure 11 shows the average boat noise during different recording conditions.

Figure 11   Spectral 10 min averages boat noise recordings off Húsavík during blue whale recordings. Based on Welch method for averaging spectra. Sampling rate 44.1 kHz, resolution 16 bits, FFT size 16384, Hann window.
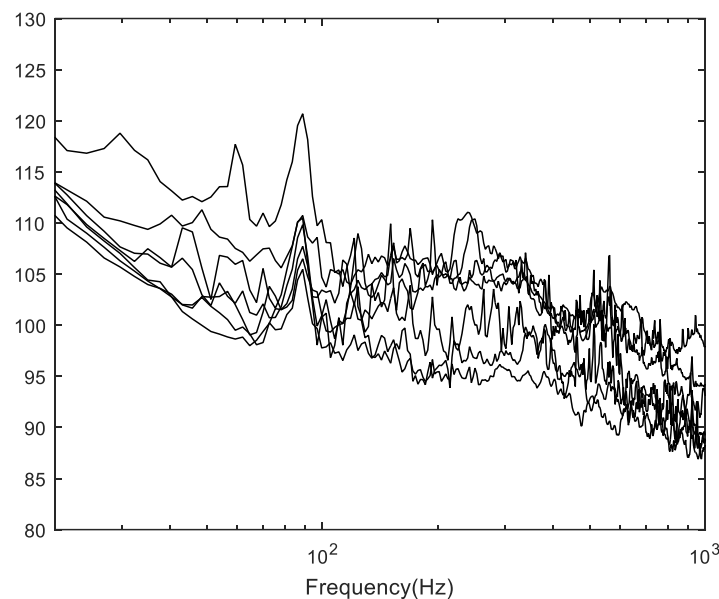
Figure 12 shows the number of detected blue whale calls per 10 min as a function of the background noise in the blue whale call frequency band according to (Iversen et al. 2011) (48-102 Hz; 4th order Butterworth filtering). Interestingly, it can be noticed that the number of blue whale calls are increasing, when the noise level is increasing.

Figure 12   Number of detected blue whale calls per 10 min as a function of the background noise in the blue whale call frequency band according to Iversen et al (2011) (48-102 Hz; 4th order Butterworth filtering;).
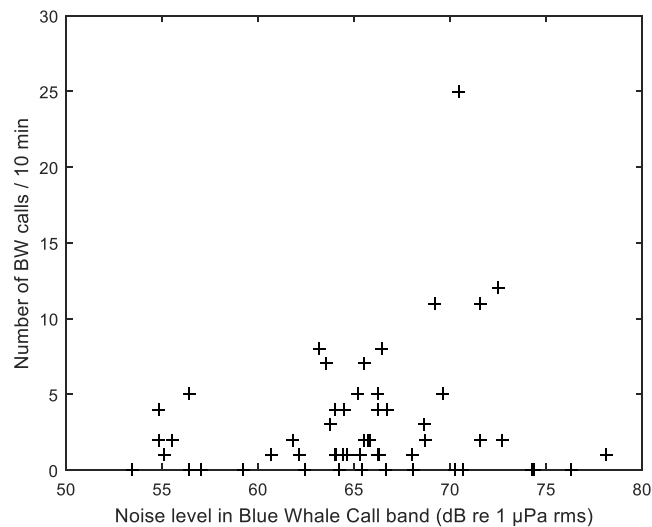
Figure 13 shows number of blue whale calls per 10 min at a higher frequency band (150 -500 Hz). Here it does not look like the number of blue whales is correlated with the noise level.

Figure 13   Blue whale calls per 10 min as a function of a higher frequency band (150-500 Hz).
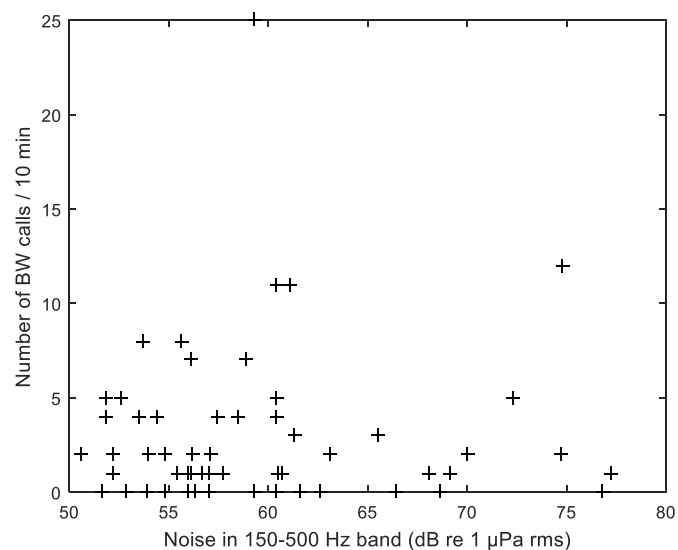
2.4   Discussion

We investigated the call rate and the relation with time of the day (day/night) or number of boats, but unfortunately no clear pattern was found. The calling rate was quite variable. For example, on 21st of June, we did not record any blue whale calls in 60 minutes from about 7 am to 8 am, but later between 9 and 9.45 am, we recorded 10 calls (Table 2). The maximum number of calls was recorded between 8:46:55 am to 11:11:55 on the 24th of June; we then recorded 80 down sweep call in 145 minutes (Table 2). In a previous study in the same area very few calls were recorded on tagged animals. Only three calls were recorded on one animal in 8 hours and 50 minutes (3 pm to 12 pm) and only one call on another animal in almost 13 hours (6 pm to 7 am) (Akamatsu et al. 2014).

The maximum source level estimated in this study of 192 dB re 1 μPa is more than 30 dB higher than the minimum source level of 159 dB re 1 μPa estimated from a previously study by (Akamatsu et al. 2014). However, the source levels in this study are on similar level to what is found at other locations such as between 186 -189 dB re 1 μPa from the Southern Oceans or from the North Pacific (Table 3). It is possible that the animals can turn up or down in volume when calling as adjustment to noise level or if many animals are present and they therefore call louder.

The noise level is influencing the blue whale calling rate. The blue whales are calling more, when it is more noisy (Figure 12). Similar was found by (Di Iorio and Clark 2010), they observed that blue whales emitted significantly more calls on seismic (noisy) than on no-seismic days. Noise level in other frequency bands (up to 500 Hz) than the blue whale frequency band (48 -102 Hz) seems not to have an influence on the blue whale calling rate (Figure 13).

3 Sound Propagation Modelling

Partial results of the present chapter have been published by Alexander Gavrilov (co-author of this report) in *Propagation of Underwater Noise from an Offshore Seismic Survey in Australia to Antarctica: Measurements and Modelling*, Acoustics Australia 46, 143–149 (2018).

Sound propagation models allow to derive the signal at the position of the listener (received signal) based on the signal at the source. Here, sound propagation models and the comparison of their predictions with recordings of propagated airgun-noise in the Antarctic Ocean serve two purposes:

1. Understanding the physical phenomena underlying the propagation of airgun signals and inference of the signal that arrives at a listener
2. Understanding the physical phenomena underlying the propagation of animal vocalizations (i.e. communication signals) and inference of the signal that arrives at a listener

Sound propagation models developed in this report are validated by a comparison of modelled signals with recordings of airgun noise. Two different datasets of recordings are compared to signals determined by the propagation models of this study. For each of the two datasets a corresponding modelling strategy was used. Table 4 gives a very short summary of the two different modelling approaches; a more detailed explanation is given in the corresponding chapters.

Table 4   Overview of modelling approaches

	Aragorn dataset	Araon dataset
Modelling approach	parabolic equation	parabolic equation
	normal mode	
	surface scattering	
Source Modell	(Duncan 1998) Bolt Gun	(Duncan 1998) G.Gun II

The first dataset (denoted as "**ARAGORN dataset**" from now on) was recorded in the Southern Ocean in 2006 using three autonomous underwater sound recorders (noise recorders) deployed at three different locations: southwest of Tasmania, within the Antarctic Convergence zone and near the Antarctic continental shelf. The devices were recording during the time period when an offshore seismic survey was conducted by PGS Geophysical over the continental shelf and slope in the western part of Bass Strait (chapter 3.1).

The second dataset (denoted as "**ARAON dataset**") was recorded in February 2015 during the Tangaroa 2015 Voyage at Ross Sea. HIDAR sonobuoys were deployed to track marine mammal presence. 28 sonobuoys were deployed while a nearby seismic survey was conducted from R/V Araon (chapter 3.2).

For modelling of the propagation of animal vocalisations the modelling approach for the Araon dataset is used, i.e. the input data for the masking model is derived using the same principle workflow as the airgun modelling. A detailed overview is given in chapter 3.4.

3.1 Modelling and Calibration of the ARAGORN dataset

3.1.1 Measurements

3.1.1.1 General information about measurements

From the 29th of March to the 30th of May 2006, a seismic survey (called Aragorn) was conducted at the edge of the continental shelf in the western part of Bass Strait. A total of 63 parallel seismic transects were made in the surveyed area, which are shown on the map in Figure 14.

Figure 14   Aragorn seismic transects (red lines) and location of the noise recorder in Bass Strait (yellow dot).
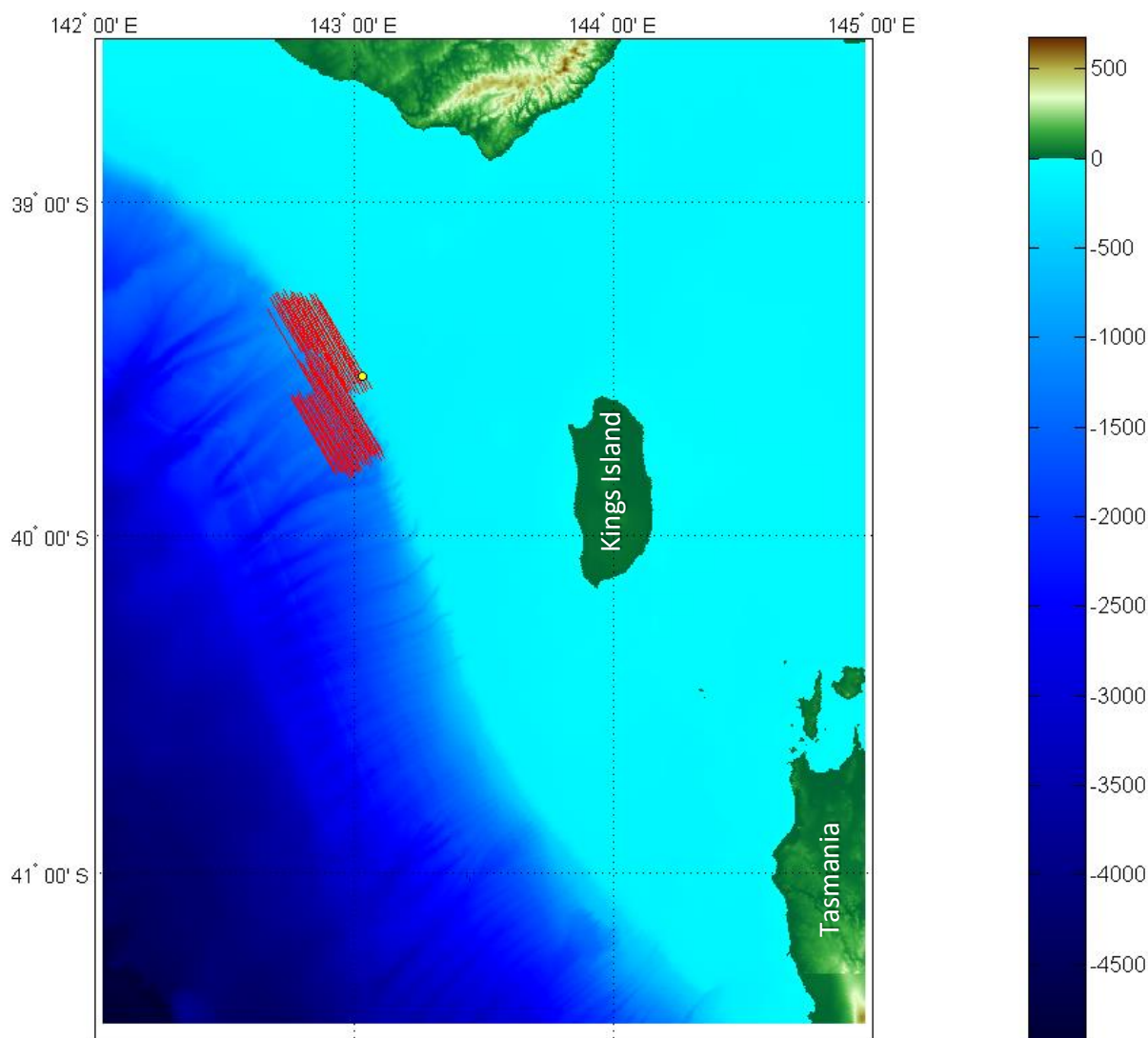
The positions and characteristics of individual guns in the Aragorn airgun array are given in Table 5 the total volume of guns was 3090 cubic inch.

Table 5   Positions and parameters of individual guns in the Aragorn airgun array.

GUN #	GUN TYPE	X (m)	Y (m)	Z (m)	VOLUME (in³)	PRESSURE (psi)	CLUSTER NUMBER
1	BOLT 1900 LLXT	0.00	12.90	6.00	150	2000	1
2	BOLT 1900 LLXT	0.00	12.10	6.00	150	2000	1
3	BOLT 1900 LLXT	3.00	12.90	6.00	60	2000	2
4	BOLT 1900 LLXT	3.00	12.10	6.00	60	2000	2
5	BOLT 1900 LLXT	5.00	12.50	6.00	20	2000	0
6	BOLT 1900 LLXT	7.00	12.50	6.00	40	2000	0
7	BOLT 1900 LLXT	9.00	12.50	6.00	60	2000	0
8	BOLT 1900 LLXT	11.00	12.90	6.00	100	2000	0
9	BOLT 1900 LLXT	11.00	12.10	6.00	100	SPARE	0
10	BOLT 1900 LLXT	14.00	12.90	6.00	250	2000	3
11	BOLT 1900 LLXT	14.00	12.10	6.00	250	2000	3
12	BOLT 1900 LLXT	0.00	0.40	6.00	100	2000	4
13	BOLT 1900 LLXT	0.00	-0.40	6.00	100	2000	4
14	BOLT 1900 LLXT	3.00	0.00	6.00	90	2000	0
15	BOLT 1900 LLXT	5.00	0.00	6.00	60	2000	0
16	BOLT 1900 LLXT	7.00	0.00	6.00	20	2000	0
17	BOLT 1900 LLXT	9.00	0.00	6.00	40	2000	0
18	BOLT 1900 LLXT	11.00	0.00	6.00	70	2000	0
19	BOLT 1900 LLXT	14.00	0.40	6.00	250	2000	0
20	BOLT 1900 LLXT	14.00	-0.40	6.00	250	SPARE	0
21	BOLT 1900 LLXT	0.00	-12.10	6.00	150	2000	5
22	BOLT 1900 LLXT	0.00	-12.90	6.00	150	2000	5
23	BOLT 1900 LLXT	3.00	-12.10	6.00	150	2000	0
24	BOLT 1900 LLXT	3.00	-12.90	6.00	150	SPARE	0
25	BOLT 1900 LLXT	5.00	-12.50	6.00	70	2000	0
26	BOLT 1900 LLXT	7.00	-12.50	6.00	40	2000	0
27	BOLT 1900 LLXT	9.00	-12.50	6.00	20	2000	0
28	BOLT 1900 LLXT	11.00	-12.10	6.00	70	2000	6
29	BOLT 1900 LLXT	11.00	-12.90	6.00	70	2000	6
30	BOLT 1900 LLXT	14.00	-12.10	6.00	250	2000	7
31	BOLT 1900 LLXT	14.00	-12.90	6.00	250	2000	7

In 2006, a research team from the Australian Antarctic Division (AAD) deployed three CMST sea noise recorders in the Southern Ocean as part of their marine mammal monitoring program. The locations of these three noise recorders are shown in Figure 15 and given in Table 6 along with the time of operation and setting of the recording regime.

Figure 15   Locations the sea noise recorders deployed in the Southern Ocean in 2006 (yellow triangles), location of the Aragorn seismic survey (yellow circle) and the sound propagation tracks (red lines): 1 -dataset 2731 (~500 km from Aragorn survey site), 2 - dataset 2716 (~1600 km) and 3 -dataset 2732 (~2900 km).
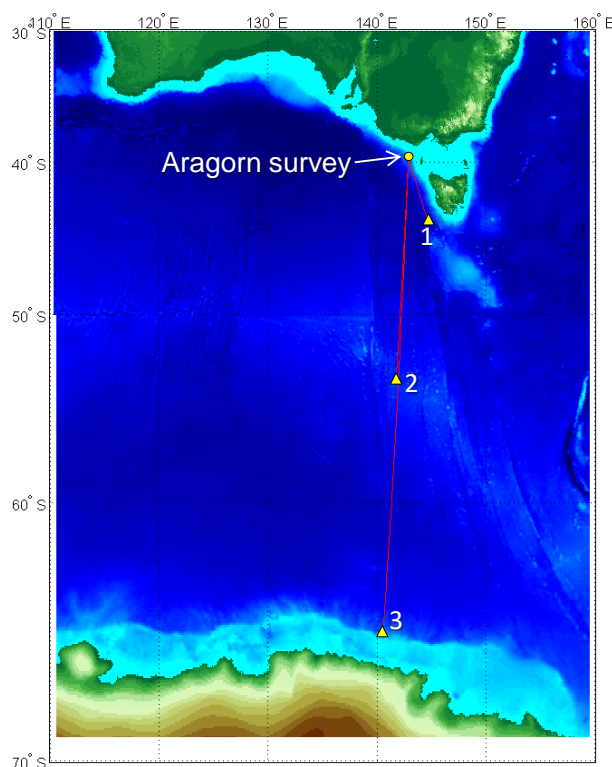
Table 6   Location, period of operation and settings of the sea noise recorders deployed in the Southern Ocean in 2006.

Recorder/Dataset No.	Latitude	Longitude	Start time	End time	Receiver depth (m)	Sampling frequency (Hz)	Recording length (s)	Recording repetition interval (min)
1 / 2731	44° 0.1'	144° 39.9'	12-Mar-2006 00:00	21-Feb-2007 05:06	1866	4000	780	60
2 / 2716	53° 44.4'	141° 46.2'	18-Dec-2005 00:00	04-Sep-2006 04:00	1600	4000	780	60
3 / 2732	65° 33.0'	140° 32.1'	21-Jan-2006 11:00	24-Jan-2007 22:00	1100	4000	780	60

The sea noise recorders used for these measurements were designed and built by CMST (http://cmst.curtin.edu.au/products). The recorders were attached to deep-water oceanographic moorings built and deployed by CSIRO. The gain of an impedance matching pre-amplifier in each noise recorder was set to be 20 dB. The underwater noise signal was digitized at a sampling rate of 4 kHz using a 16-bit analogue-to-digital converter. An anti-aliasing filter with a cut-off frequency at 1.8 kHz was applied to the analogue signal before conversion. All three recorders were programmed to make continuous 780 s long recordings with 1-hour intervals between the recording start times. All noise recorders were calibrated before deployment by using white noise of known level as an input signal of the recording system with the hydrophone connected in-series to the noise generator. The recorded sea noise signals and their spectra were corrected for the end-to-end frequency response of the recording

system, so that the sound pressure and power spectrum density were measured in absolute units (µPa and µPa^2/Hz respectively).

An example of long-time average spectrograms of sea noise recorded on these three noise recorders during the last eighteen days in May 2006 is shown in Figure 16. The spectrograms are compiled from the power spectral density of individual recordings. Periods of airgun noise from the Aragorn seismic survey can be easily distinguished in the middle and bottom spectrograms by vertical bands of higher noise intensity spanning frequencies from 5 Hz to about 50 Hz. The horizontal spectral lines at about 27 Hz and slightly below 20 Hz clearly seen in the middle and bottom panels are formed by a chorus of Z-shaped calls from many remote Antarctic blue whales (*Balaenoptera musculus intermedi*) (Gavrilov et al. 2011).

During this time period, the northernmost mooring system was affected by high underwater currents which resulted in noise artefacts of high intensity at low frequencies. These artefacts hid the airgun noise most of the time. Another reason why the airgun noise was not clearly seen in the recordings from Recorder #1 was that a significant part of the sound transmission path from the survey area to this recorder lay in shallower water over the continental slope, where sea depth was less than the depth of the sound channel axis of about 1000 m. The effect of bathymetry on the transmission loss of airgun signals propagated to the noise recorders in the Southern Ocean is considered in section 1.1.2 of the report using numerical modelling of sound propagation.

Figure 17 demonstrates an example of the sound pressure time series of sea noise recorded on Recorder #3 in Antarctica, which contains impulsive airgun noise from the Aragorn seismic survey.

Figure 16   Long-time average spectrograms of sea noise recorded by Recorders #1 (top panel), #2 (middle panel) and #3 (bottom panel) in May 2006.
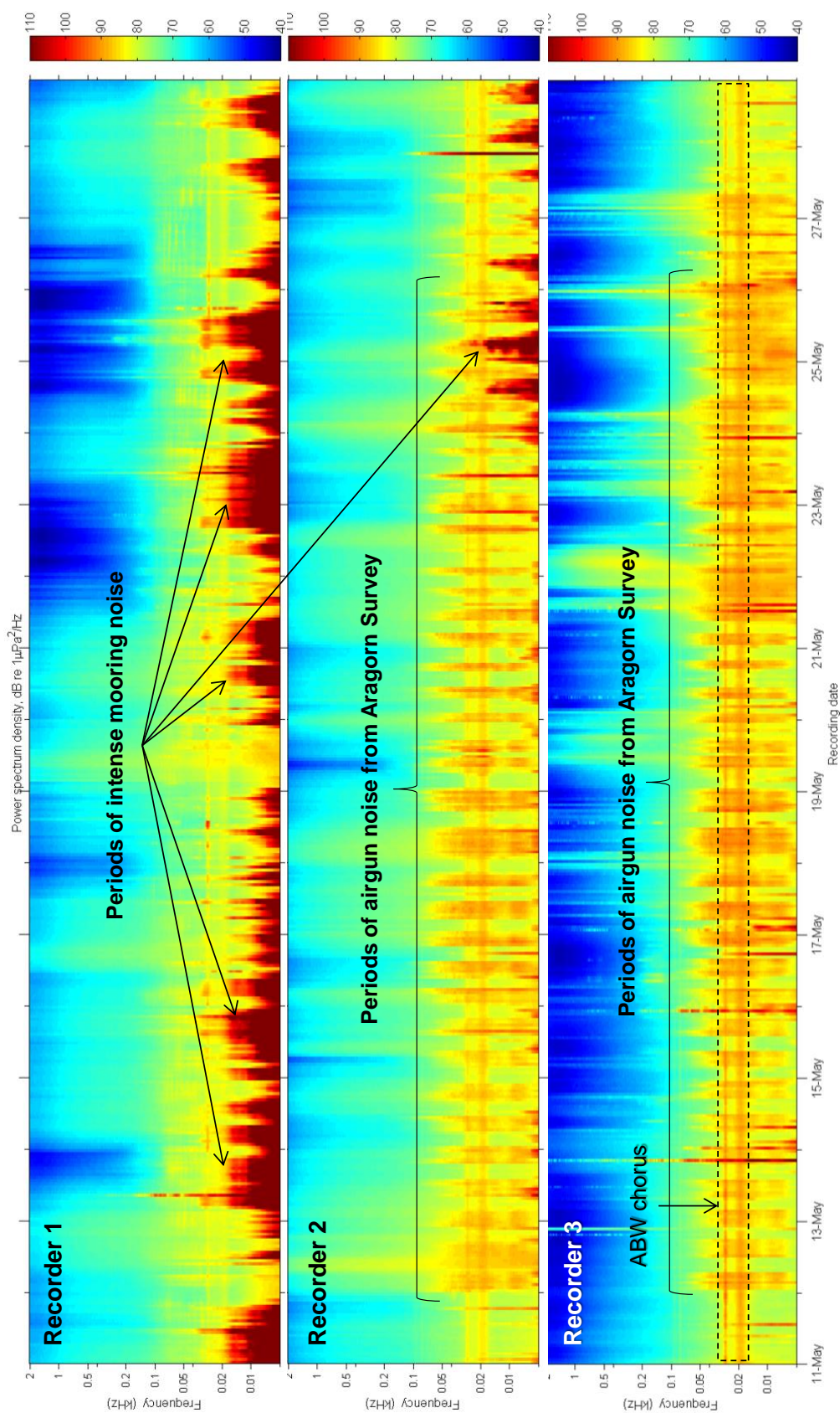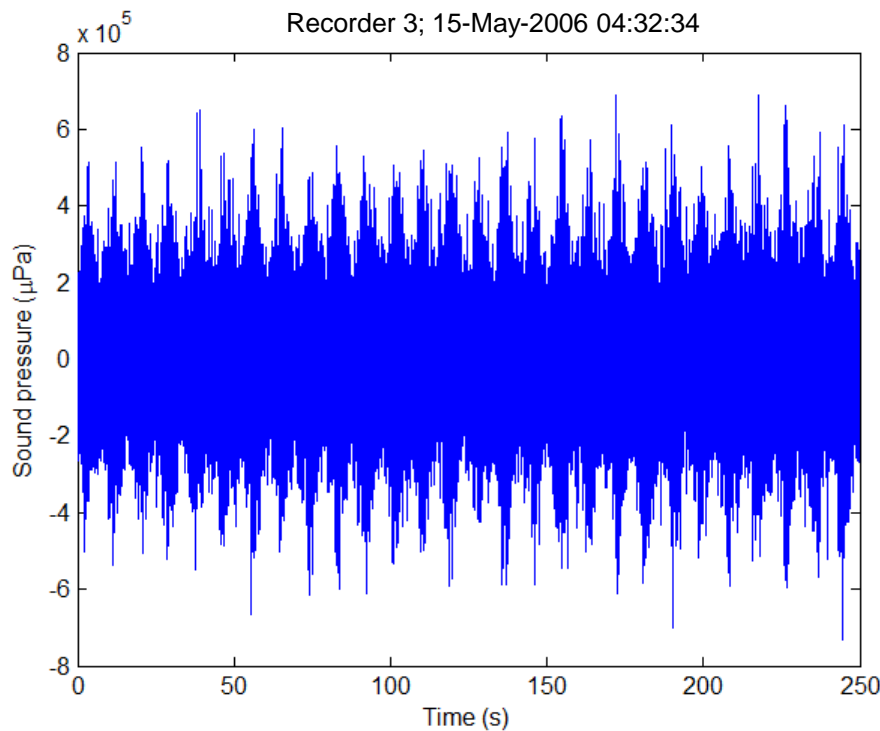
Impulsive airgun noise from the Aragorn seismic survey seen in the pressure time series of sea noise recorded by Recorder #3 in May 2006.

3.1.1.2   Description of data files

Twenty Aragorn seismic transects were selected for further analysis of the airgun noise recorded at the three noise recorders in the Southern Ocean. The transects were chosen such that various conditions of the environment at the sound source location would be represented, i.e. in relatively shallow water (~100 m) at the edge of the continental shelf, over the continental slope and in deep water (>3000 m) west of the continental slope. All sound recordings by each noise recorder that contained airgun signals from the selected transect were saved in a single Matlab data file.

3.1.2   Modelling

A numerical approach to model sound emission and propagation from the airgun array used in the Aragorn survey to the furthermost underwater sound recorder deployed on the continental slope in Antarctica at location 3 shown on the map in Figure 15 is presented below.

3.1.2.1   Modelling approach

3.1.2.1.1   Source signal

The sound signal emitted by the airgun array was modelled using a numerical model of sound emission from single guns and airgun arrays developed at CMST (Duncan 1998). The model calculates the signal waveform in the far field, i.e. at a distance much larger than the array dimensions. Then the waveform amplitude is back-extrapolated to a distance of 1 m from the array geometrical centre using the spherical spreading law for the transmission loss, so that the array is modelled by a directional point source. As the array is a directional source of sound signal, the source signal waveform is modelled for different azimuth and elevation angles. The azimuth angle is commonly measured clockwise relative to the vessel/array heading, and the elevation angle is measured relative to the downward vertical direction, so that it is 90° for the horizontal emission. The model has been verified by several experimental measurements (Duncan et al. 2013). The input parameters of the model are the array geometry and the volume and chamber pressure of each active gun in the array.

The heading direction of all seismic tracks of the survey was either about 30° or 330° relative to the direction of sound propagation to the recorder in Antarctica. Figure 18 shows the sound signal waveform emitted by the array at an azimuth angle of 330° and elevation angle of 90°.

Figure 18   Sound signal waveform at 1 m from the airgun array centre, modelled for an azimuth angle of 330° and elevation angle of 90°.
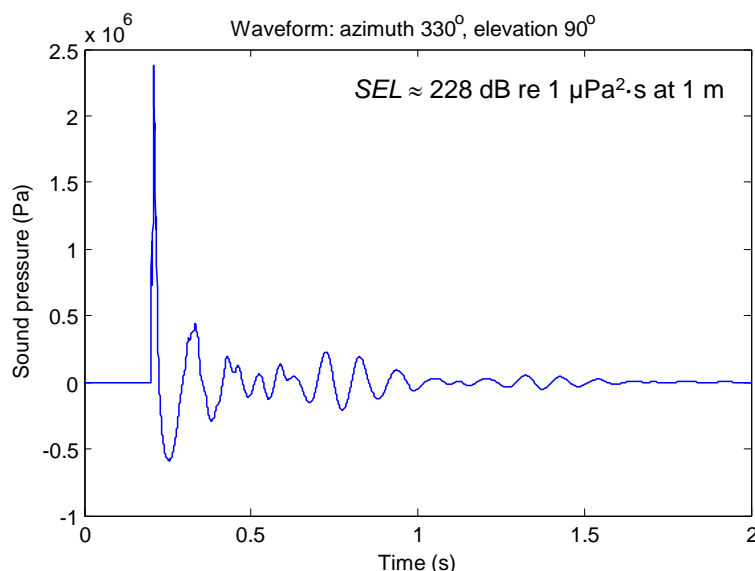
The Energy Spectral Density (ESD) level of the sound signal emitted by the array at 330° is shown in Figure 19. It is averaged over the elevation angles from 45° to 90° where most of the sound energy is coupled with the underwater sound channel. Averaging over the elevation angle is applied to simplify calculations of the sound transmission loss with range, as most of the common sound propagation models do not directly accept point sources with vertical directionality. The ESD level decays from about 10 Hz to nearly 100 Hz. The broad peak at around 10 Hz is formed by the energy of air bubble pulsations which have slightly different frequencies for airguns with different volumes in the array. The modelled ESD shown in Figure 19 was used to predict the ESD at the sound receiver in Antarctica.

Figure 19   Energy spectral density level of the sound signal at 1 m from the airgun array centre at an azimuth angle of 330°, averaged for elevation angles from 45° to 90°. SEL is 228 dB re 1 $\mu Pa^2 \cdot s$ at 1 m.
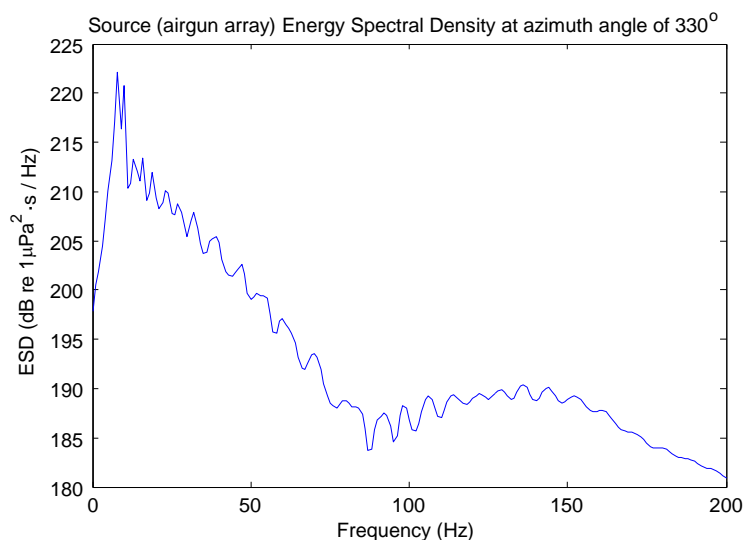
3.1.2.1.2   Sound transmission model

The underwater sound transmission channel from Bass Strait to Antarctica is highly range dependent. Firstly, it lies over a steep continental slope of Australia. Secondly, it crosses a sharp Polar front at the Antarctic convergence, where the axis of the underwater sound channel ascends rapidly from about 1100 m depth to the sea surface (Figure 20). The bathymetry along the sound transmission path was modelled using the Geoscience Australia bathymetry and topography grid of 250 m resolution (http://www.ga.gov.au/metadata-gateway/metadata/record/gcat_67703) for the initial path section of 350 km length over the Australian continental slope and the ETOPO2 (Earth TOPOgraphy of 2 min resolution)gridded   bathymetry/topography   data (https://www.ngdc.noaa.gov/mgg/fliers/01mgg04.html) for the following section of the path.

Figure 20   Bathymetry and sound speed profile along the sound transmission path from Bass Strait (on the left) to the sound recorder in Antarctica (on the right). Location of the sound recorder is shown by the red circle.
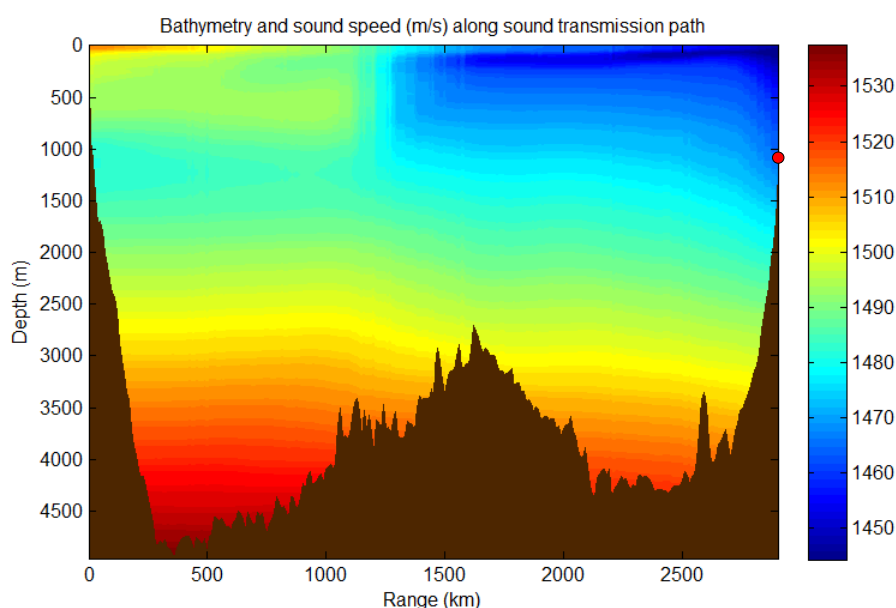
The sound speed profile along the transmission path was modelled using the World Ocean Atlas gridded climatology data of 0.25° spatial resolution (https://www.nodc.noaa.gov/OC5/woa13/). Water temperature and salinity data for austral autumn were used to calculate sound speed profiles.

As the geoacoustic properties of the seabed along the sound transmission path were generally unknown, the seabed was assumed to be covered with medium to coarse sand, based on a number of probes taken on the Australian continental slope at various locations. The sound speed in the seabed material was assumed in the model to be 1770 m/s, the density 1800 kg/m^3 and attenuation 0.47 dB/λ.

The airgun array was towed at 6 m below the sea surface. It was essential to accurately model the coupling of a near-surface sound source with the deep sound channel in the temperate ocean south of Australia. Therefore, a Parabolic Equation (PE) approximation method was chosen to model sound transmission from the airgun array over the initial 350 km section of the propagation path lying over the continental slope southwest of Bass Strait. The PE approximation is a computationally efficient method to numerically model sound wave propagation in range-dependent layered media (Jensen et al. 2011). However, the available PE computer models, including RAMGeo (http://cmst.curtin.edu.au/products/underwater/) used in this study, are not capable of accounting for the transmission loss due to scattering of sound waves by the surface wind waves, which is essential for the path section beyond the polar front. To include the scattering effect on the sound transmission loss, a normal mode approach was employed: the sound field predicted by the PE model at 350 km from the

source was expanded into a series of local normal modes, as described in (Wilkes et al. 2016). Then the modes were propagated over the rest of the transmission path from 350 km to about 2900 km to calculate the sound field and transmission loss at the sound receiver. The normal mode representation of the sound field in layered media, such as the ocean sound channel, is an efficient computational technique for predicting sound transmission in underwater environments with parameters varying gradually with range (Jensen et al. 2011). In this approximation, the sound field in the ocean channels is represented by a superposition of a set of local normal modes (channel eigenfunctions). This approximation also allows correction of the transmission loss for the effect of sound scattering at the boundaries of the sound channel. The normal modes were calculated using the computer normal mode model ORCA (Westwood et al. 1996).

Most of the underwater sound energy propagating in the temperate ocean north of the polar front is concentrated in the deep SOFAR channel. When crossing the polar front in the Antarctic convergence zone, the SOFAR channel is closer to the surface in polar waters. As the mode coupling effect across the polar front was not expected to be significant (Li and Gavrilov 2006), an adiabatic mode approximation (Jensen et al. 2011) was employed, which made calculations much more computationally efficient.

The surface scattering effect was modelled using the Kuperman-Ingenito boundary perturbation approximation (Kuperman and Ingentio 1977), where the imaginary part of the modal wavenumber is increased by the scattering component

$$\gamma_n^S = \frac{\sigma^2}{2\beta_n k_n} Z_n'(0)$$,

Where σ is the RMS height of surface waves, Z_n is the mode function (mode shape), k_n is the real part of mode wavenumber,

$$\beta_n = \sqrt{k^2 - k_n^2}$$

is the vertical component of the wavenumber

$$k = 2\pi f / c$$

The RMS height σ of surface roughness was assumed to be 2 m, which corresponds to a significant wave height of approximately 8 m typical for the Southern Ocean.

The transmission loss was calculated in the frequency band from 5 Hz to 100 Hz with a 1 Hz increment. The modelling band was limited by those frequencies because (1) the modelled source signal ESD drops steeply below 5 Hz and no airgun noise energy was observed below 5 Hz in the measurement data and (2) no energy of airgun signals was observed above approximately 70 Hz at Recorder #3 (see 0). The modelling band was extended to 100 Hz to assess the airgun noise spectrum at shallower receiver depths.

In the model, the sound source (airgun array) was placed at five different locations over the continental shelf and slope spanning the range of water depth variations in the area of the seismic survey. These locations are shown in Figure 21. Modelling results of sound transmission from locations 1 (water depth of ~160 m), 3 (~420 m) and 5 (~1160 m) are presented in the next section. No results are presented for locations 2 and 4. The receiver was placed at 1100 m below the sea surface which was the depth of sound recorder 3 in the measurements.

Figure 21   Five locations of the sound source assumed in the model.
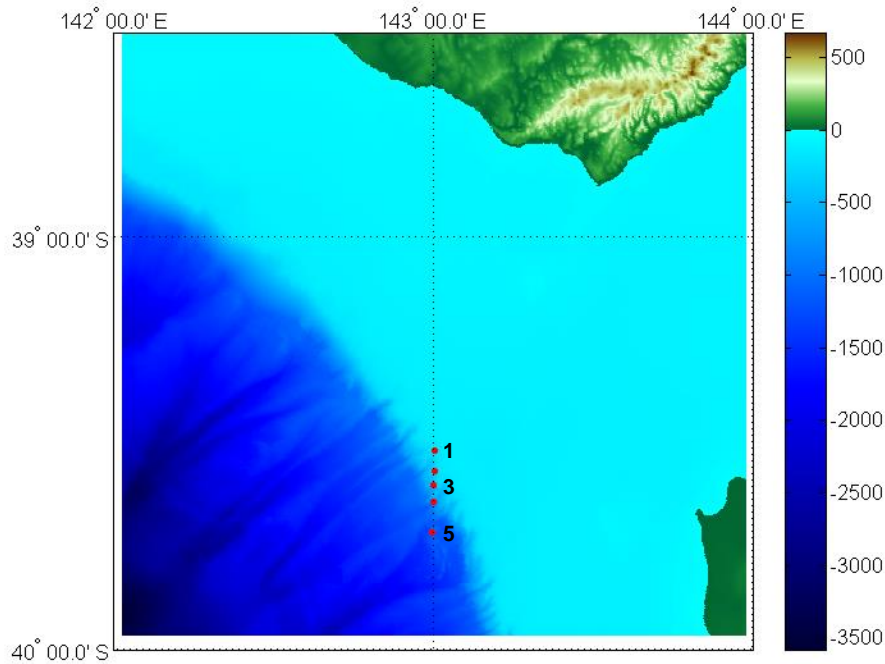
Modelling results and comparison with experimental data

The top panel of Figure 22 shows a long-time average spectrogram of sea noise recorded over the time period of the major part of the seismic survey in May 2006. Periods with airgun noise can be recognized in this spectrogram by broadband noise of higher intensity from approximately 7 Hz to nearly 50 Hz. The bottom panel shows the sea depth at the source location at the times of airgun discharge, which was taken from the p1/90 data record provided by Petroleum Geo-Services (PGS). P1/90 is the standard file format for seismic source positions. The airgun noise could not be distinguished in the background noise when the seismic vessel operated over the shelf in shallower water of less than 150 m sea depth. The figure suggests that the intensity of airgun noise received in Antarctica was slightly higher, when the sea depth at the source location varied within approximately 300-700 m, than that when the sea was deeper (800-1200 m).

Figure 23 shows the waveform (top) and spectrogram (bottom) of a 200-s section of the sea noise recording made on the 18th of May which contains the airgun noise of higher intensity. The sound exposure level (SEL) of the received airgun signals corrected for the intensity of background noise varied within 117.5-118 dB re 1 µPa²·s.

Figure 22   Long-time average spectrogram of sea noise recorded over the time period of the major part of the seismic survey in May 2006 (top panel) and sea depth at the source location (moving airgun array) at the airgun discharge times (bottom panel).
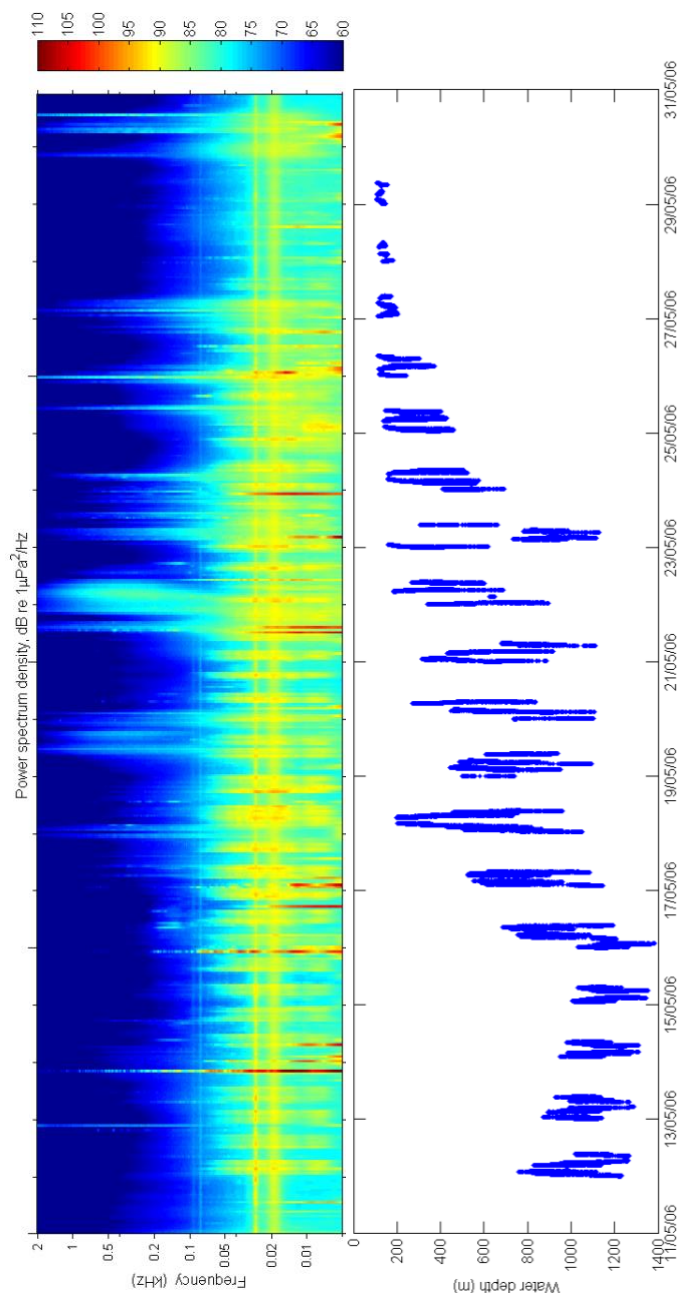
Figure 23   Impulsive airgun noise from the Aragorn seismic survey recorded on the 18th of May: waveform (top) and spectrogram (bottom). SEL of individual signals shown in this plot varied within 117.5-118 dB re 1 µPa^2·s, corrected for the contribution of background noise.
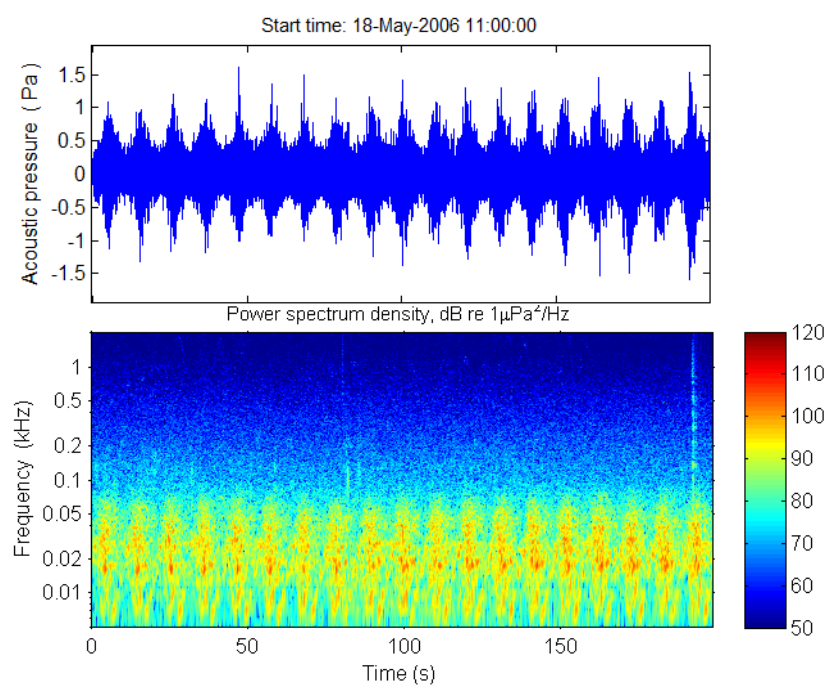
Figure 24   Transmission loss modelled at 10 Hz for source locations 1, 3 and 5. Bass Strait is on the left and Antarctica is on the right.
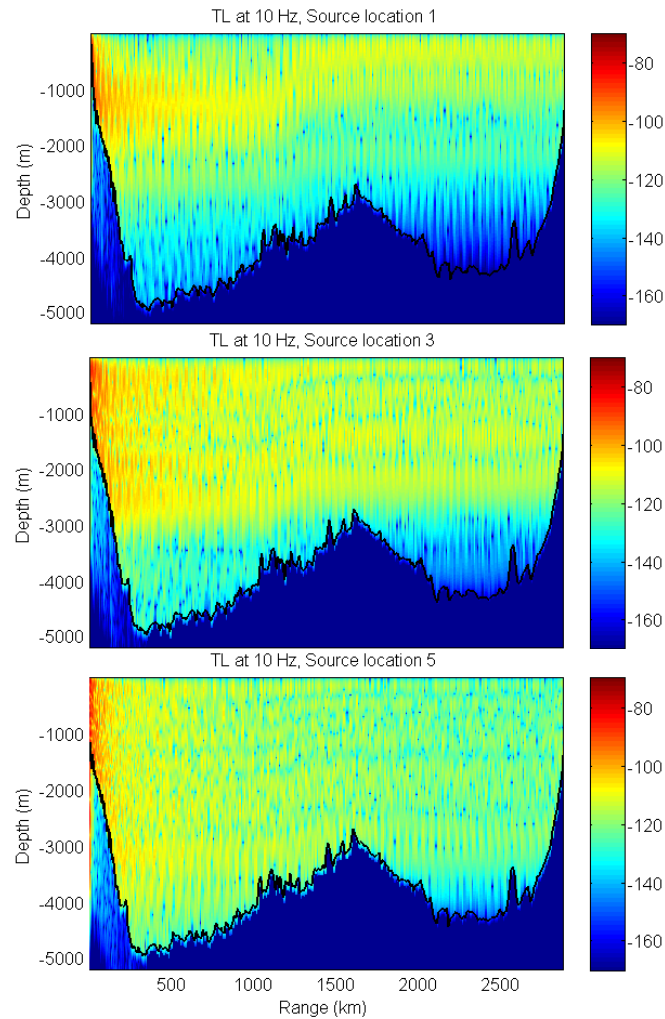

Figure 24, Figure 25 and Figure 26 show the transmission loss versus range and depth modelled at 10 Hz, 30 Hz and 100 Hz respectively. In these figures, the transmission loss is compared for source locations 1, 3 and 5, where the sea depth at the source location was about 160 m, 420 m and 1160 m respectively (Figure 15).

At 10 and 30 Hz, the effect of sound energy transmission from the deep SOFAR sound channel (at about 1000 m depth) to the near-surface channel in the polar environment is clearly seen at 1000 to 1200 km, from the sound source, when the source is located in shallower water (source location 1; top panel in Figure 25). This is not surprising as in shallow water low-order modes concentrated around the sound channel axis dominate in the sound field. For this reason, the sound level at the receiver placed near the bottom in Antarctica, i.e. far from the polar near-surface sound channel, is lower, when the sea depth at the source is shallower.

The role of the sound source and receiver depths compared to the sea depth at the source and receiver location is illustrated in Figure 27 where the shapes (vertical profiles) of normal modes 1, 3, 5 and 10 are shown as an example at the source (location 3) and receiver. At the source, the axis of the sound channel is near the bottom. Consequently, a sound source placed near the sea surface emits more energy into higher-order normal modes, as their amplitudes at the source depth are higher. Near Antarctica, the sound channel axis is near the sea surface and hence the higher-order modes contribute into the sound field near the bottom much more than the low-order ones.

The transmission loss at the receiver is generally lower in this frequency band, when the sea depth at the source is moderate but less than the depth of the SOFAR channel axis. The maximum transmission loss at all frequencies occurs when the sound source is located over the deep part of the continental slope at sea depth greater than 1000 m. In this case, a shallow source is not well coupled with the deep SOFAR channel through the interaction with the sloping seabed.

Figure 25   Transmission loss modelled at 30 Hz for source locations 1, 3 and 5. Bass Strait is on the left and Antarctica is on the right.
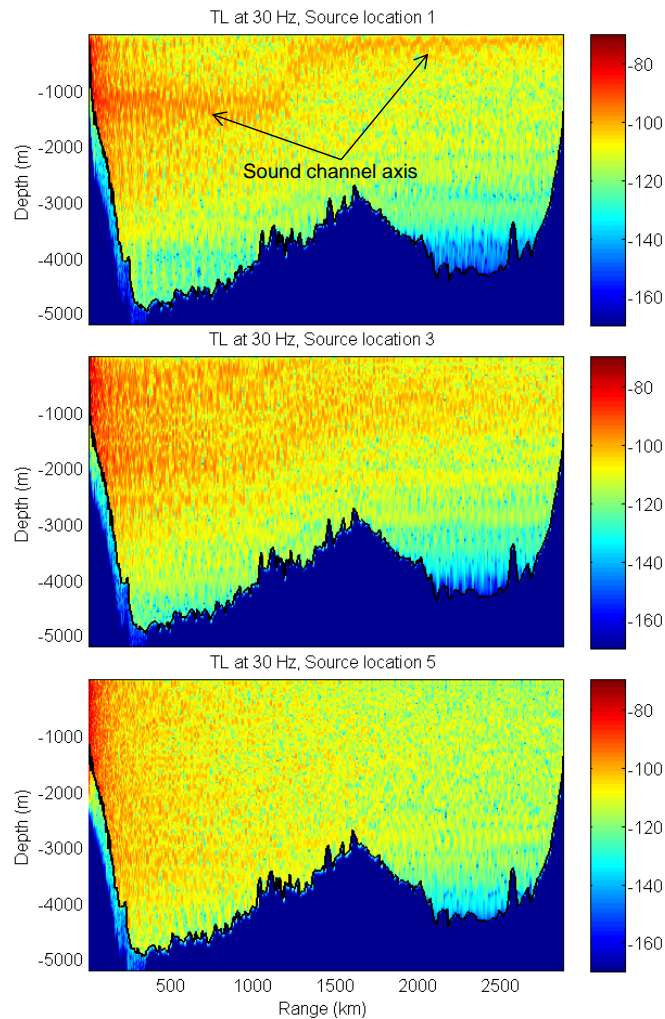
To illustrate the role of sea surface scattering in the sound transmission loss, Figure 28 shows the attenuation coefficient of mode 10 versus range and frequency. Mode 10 of medium order was chosen as an example because: (1) it contains more energy emitted into the underwater sound channel by a shallow source in the temperate ocean than the lowest order modes, (2) interacts significantly with the seabed over the shallower part of the continental slope, (3) interacts with the sea surface in the polar environment and (4) contributes more to the sound field at a deep (1100 m) receiver in Antarctica than modes of lower order. At low frequencies, attenuation of normal modes results primarily from sound absorption in the seabed, whereas at higher frequencies it is governed by the sea surface scattering effect, which is obvious beyond the polar front at about 1200 km where the sound channel is located close to the sea surface.

Figure 26   Transmission loss modelled at 100 Hz for source locations 1, 3 and 5. Bass Strait is on the left and Antarctica is on the right.
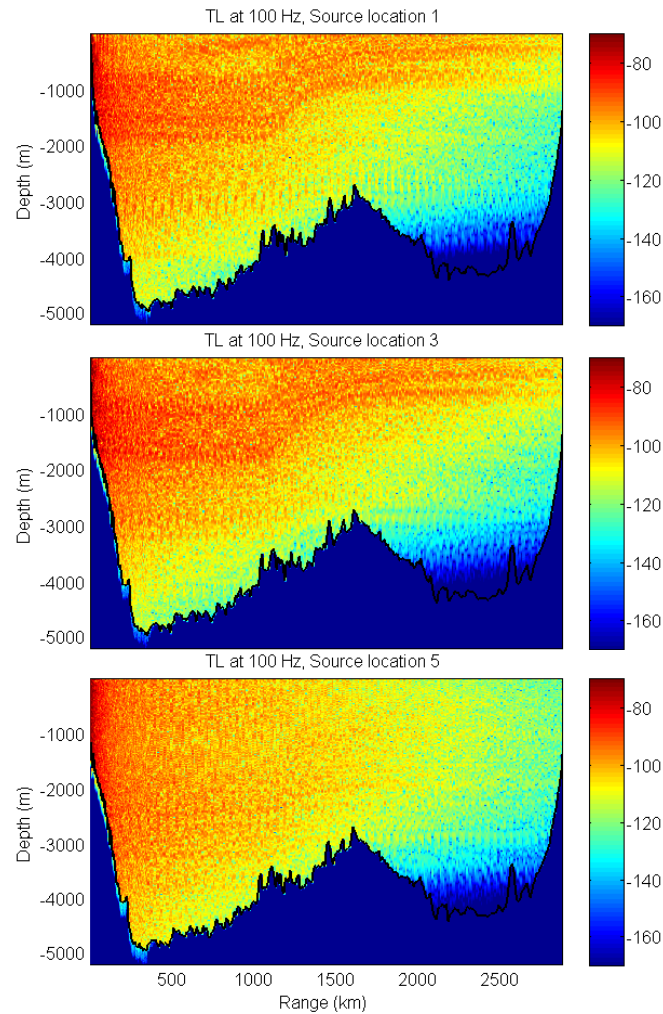

Figure 27   Vertical shapes of normal modes 1, 3, 5 and 10 at the source (location 3, sea depth 420 m) (left panel) and receiver (right panel). The dashed lines indicate the source and receiver depth.
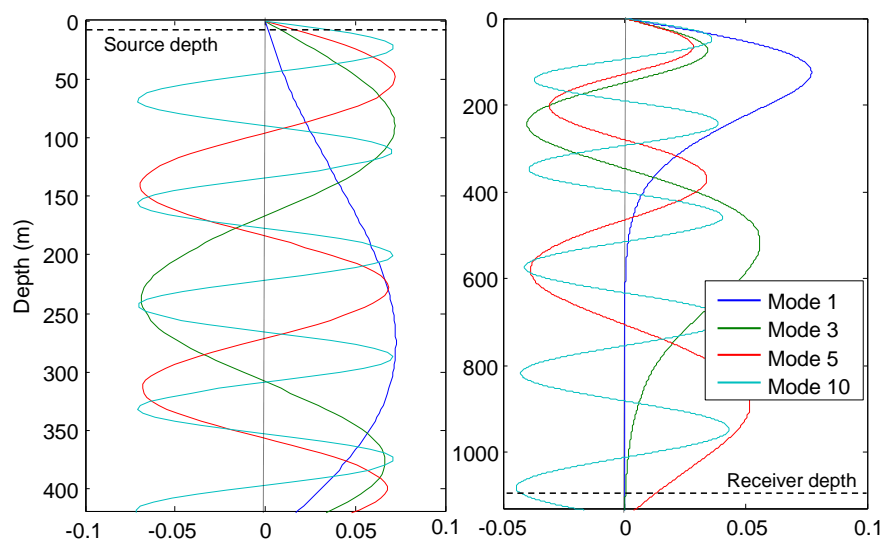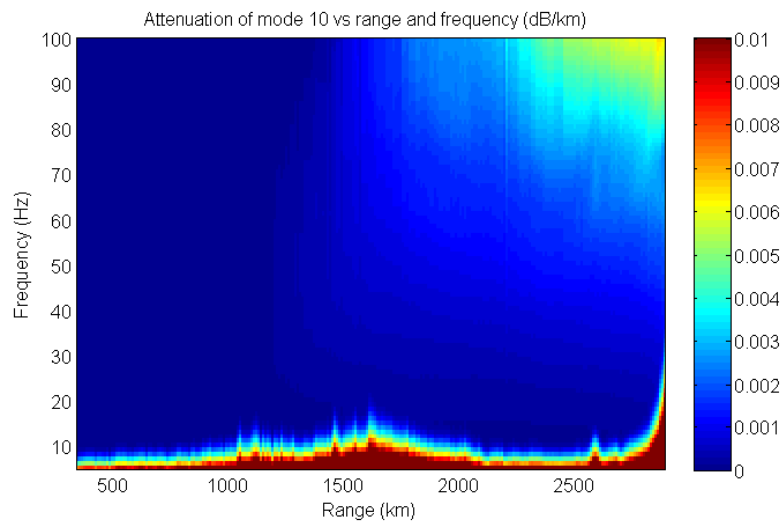
Figure 28   Attenuation coefficient of mode 10 vs range and frequency.

As airgun signals are impulsive, their acoustic energy is more relevant for characterising the noise environment than the power which rapidly changes within the signal duration. Moreover, it is important to know spectral characteristics of airgun noise to assess its potential effect on communication of marine mammal which takes place at various frequencies. For these reasons, the Energy Spectral Density (ESD) is commonly used to characterise impulsive noise of man-made origin.

The ESD level ESD_R of the received signal was calculated from the ESD level ESD_S of the source signal and the transmission loss TL, as $ESD_R = ESD_S - TL$. The ESD level of the airgun array signal recorded on the 18th of May, when it was near the maximum value, is compared in Figure 29 with that predicted by numerical modelling for three different locations of the sound source. The agreement between the modelling and measurement results is good, especially for the source location at sea depth of 420 m (source location 3).

Figure 29   Energy spectral density levels of airgun signals received at Recorder #3 (distance 2900 km, depth 1100 m) on 18th of May at the time, when the sea depth below the airgun array was between 400 and 600 m, and those modelled for three locations of the airgun array: 1 - sea depth at the array of 160 m; 2 - sea depth 420 m: and 3 -sea depth 1160 m.
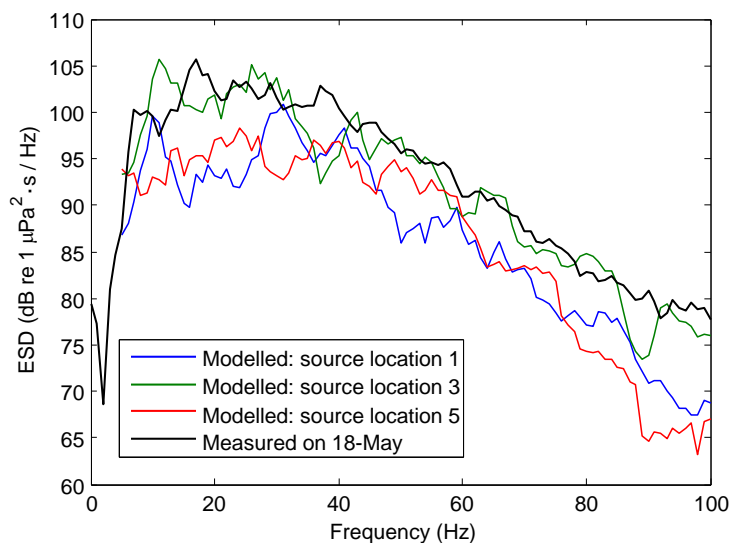
Finally, the SEL was calculated as a function of depth at the receiver location. Figure 30 shows the modelled SEL versus depth and the SEL value of the airgun signals measured on the 18th of May. The plot clearly demonstrates that the sound transmission from a shallow sound source (such as an airgun

array towed at 6 m below the sea surface) over the continental slope is more efficient when the sea at the source location is shallower than the SOFAR channel axis. When the sea depth at the source location is 150-200 m, the sound energy at the receiver location tends to concentrate in the top 200-m water layer. As the sea depth at the source location increases, the SEL becomes more evenly distributed across the water column.

Figure 30   SEL of the received signal vs receiver depth at the distance of sound recorder #3 (2900 km) modelled for three sound source locations. The horizontal error bar shows the range of SEL variations measured on the 18th of May.
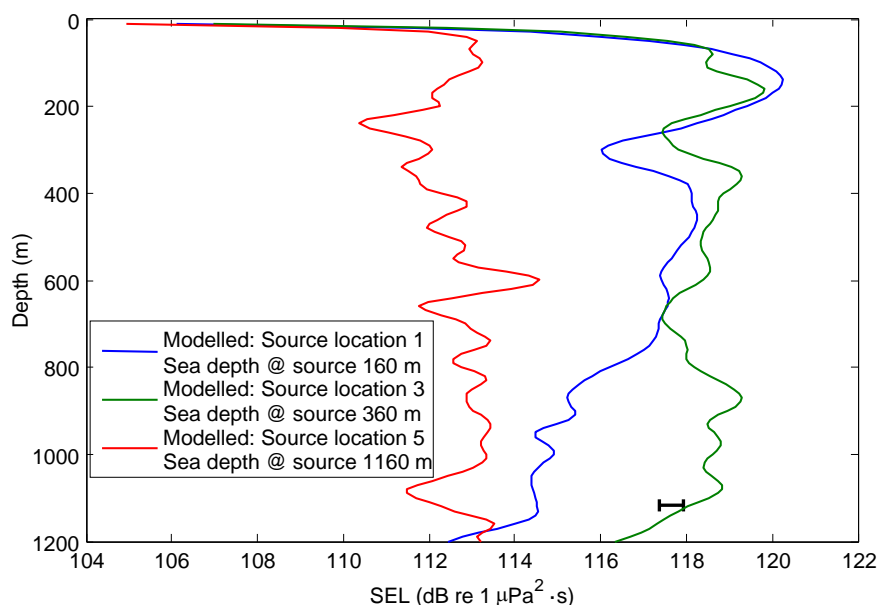
## 3.2 Modelling and Calibration of the ARAON dataset

3.2.1 Calibration data -Seismic Survey at Ross Sea (Recorded data)

3.2.1.1 General information on measured data: Audio data

The calibration data used for comparison were provided by the Australian Antarctic Division (AAD), an agency of the Australian Department of Environment and Energy.

During the Tangaroa 2015 Voyage in early 2015 High Dynamic Range DIFAR (HIDAR) sonobuoy were deployed at Ross Sea. By chance the sonobuoys recorded a nearby Korean seismic survey conducted from R/V Araon. The survey started on 13.02.2015 and was finished on 17.02.2015.

Figure 31   Tangaroa 2015 Voyage, geographic overview
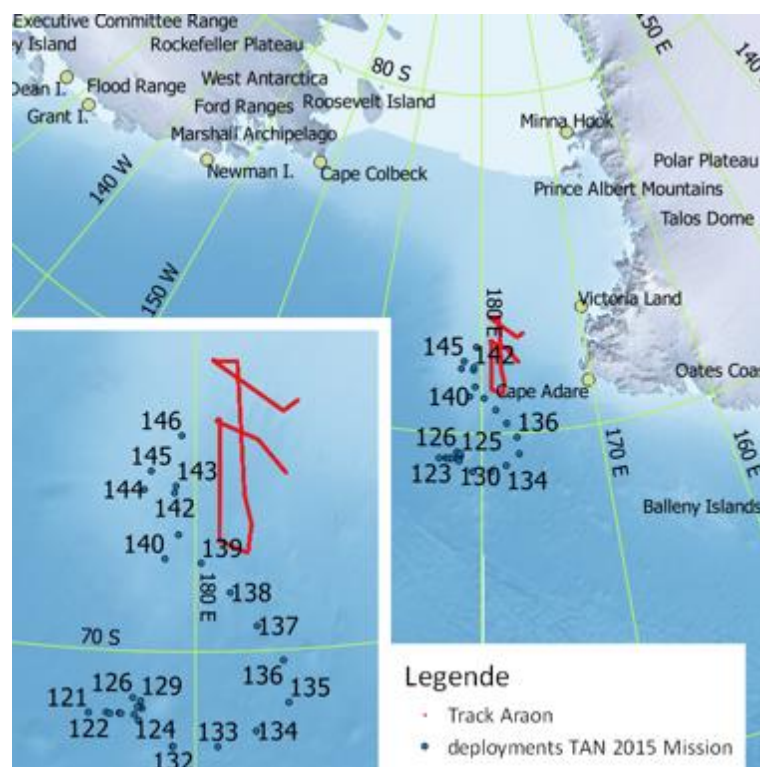
Deployed sonobuoys (blue circles) and ship track (red line) of R/V Araon during the Tangaroa 2015 Voyage

In total 28 buoys were deployed at a nominal depth of 140 m with 27 (of 28) buoy deployments providing audio data. Next to the seismic survey, the recorded data also included marine mammal vocalization and ice breaking noise.

The provided audio wav files had a sampling rate of 8 kHz covering 24 bits of dynamic range.

3.2.1.2   General information on measured data: Seismic survey

The seismic survey of R/V Araon was conducted using a parallel airgun cluster of 8 airguns, type Sercel G.Gun II. The total volume of the fully operational array is 1200 cubic inch (cu.in). The position (x, y, depth) for each individual airgun is given in meters. The data for the array layout was kindly provided by Joohan Lee from the Korea Polar Research Institute (KOPRI[3]).

---

[3] http://eng.kopri.re.kr

Figure 32   Principle sketch of the airgun array available on R/V Araon. Sketch based on data provided by Joohan Lee from KOPRI (joohan@kopri.re.kr).
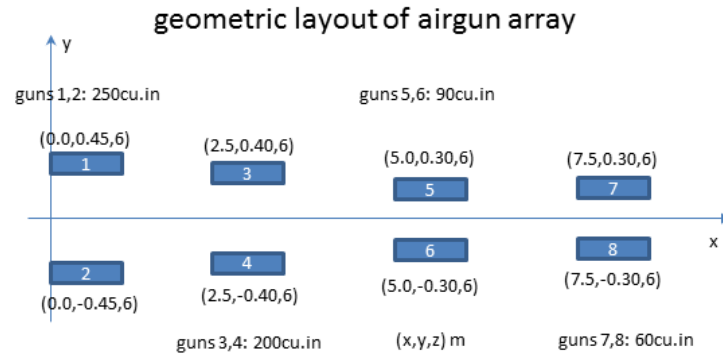
The airgun array was operated in various configurations, defined by the number of airguns that were operational 'on' or 'off'. According to the gun shot log the R/V Araon performed 15478 airgun shots within the recording period of all 28 sonobuoy deployments. During the recording time, in total 16 different airgun array configurations were conducted. Table 7 lists only the 8 airgun array configurations of highest energy.

Table 7   Listing of executed airgun configurations over all shots over all deployments

# of pattern	pattern (airgun on/off)	total volume	number of shots
1	1,1,1,1,1,1,1,1	1200	299
2	1,1,1,1,1,0,1,1	1110	2310
3	1,1,1,1,0,1,1,1	1110	3950
4	1,1,1,1,0,1,0,1	1050	5
5	1,1,1,1,0,0,1,1	1020	4
6	1,0,1,1,1,1,1,1	950	2
7	1,0,1,1,0,1,1,1	860	3753
8	1,0,1,0,0,1,1,1	660	1032

3.2.1.3   General information on measured data: Shot detection

The recorded data was analysed using an impulse detector to identify the airgun shots in the data.

The impulse detector uses a RMS time series derived from the original pressure time series for the shot identification. An integration time of 1 second was chosen. A chosen overlap factor of 0.8 resulted in a sample rate of 5 Hz for the RMS time series.

The onset of impulsive signals is characterized by showing a rapid increase of the pressure magnitude and consequently in the derived RMS time series. The RMS level at start of the impulsive signal was stored as reference level. The RMS time series was followed until it reached again the reference level within a small offset range (0.5 dB). These two distinct time stamps give the (impulsive) event duration.

Using the following parameters

1. RMS rate change
2. Minimum and Maximum event duration
3. RMS offset range

The airgun shots within the recorded data could be satisfyingly identified. For this project it was not intended to reach an optimized detection count for the airgun shots in the data. For the purposes within this working package an identification of distinct propagation scenarios was needed:

► which recorder (sonobuoy) did provide a good detection ratio
► what were the source-receiver distances/directions, i.e. how does the bathymetry along these directions change?
► are environmental data available along the propagation path, are they varying along the path

Table 8   Listing of airgun shot detections for the sonobuoy deployments

Sono-buoy	fired shots	detected shots	Sono-buoy	fired shots	detected shots	Sono-buoy	fired shots	detected shots
119	409	61	129	0	0	139	663	408
120	1121	233	130	0	0	140	961	602
121	783	288	131	0	0	141	946	366
122	186	53	132	339	122	142	125	28
123	1012	138	133	281	105	143	635	254
124	896	216	134	211	88	144	520	243
125	27	22	135	800	220	145	563	210
126	0	0	136	329	242	146	593	239
127	0	0	137	272	57			
128	0	0	138	361	162			

Table 8 shows the detection results of all deployments. The number of fired shots is derived intersecting the shot log protocol with the recording period of each individual deployment. The given detected shots are derived from initial impulse detection and a statistical post-processing of these results. For the measured inter shot interval, i.e. the temporal distance between two consecutive shots, the event duration estimates and standard variation are derived and non-matching detections are excluded.

Figure 33 shows the detection of airgun shots vs. range and the performance-target ratio per sonobuoy: Closer sonobuoys show generally better detection results. However, there are many deployments among the data set with very low detection ratio. This is explained by the high number of other ambient sounds in the recording such as ice noise, whale communication or heavy weather and a short recording slot for the seismic survey.

Figure 33   Detection results at the individual sonobuoys deployed during the Tangaora 2015 Voyage
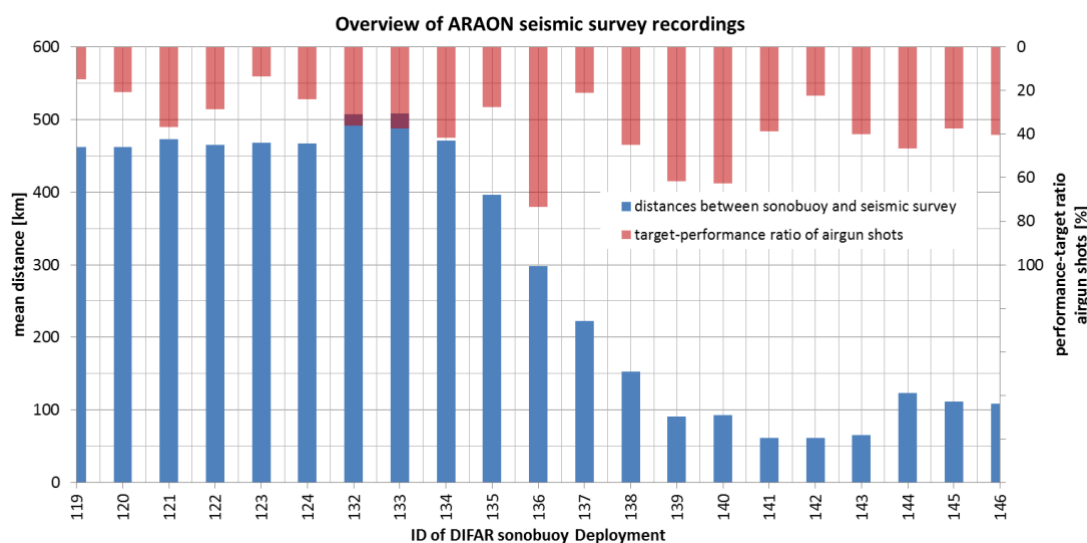
From the analysed data sonobuoy 136 and sonobuoy 140 were initially chosen to model a sound propagation along the source –receiver path. The airgun shot detection worked especially well for these stations and the individual source-receiver paths were considerably different. The individual distances between source and receiver differ by factor 3. While the mean distance for sonobuoy 136 is approx. 300 km the mean distance for sonobuoy 140 decreases down to approx. 93 km. The bathymetry for sonobuoys 136 can be characterized as a long downslope interspersed with sea mountains along the path. As for sonobuoys 140 the bathymetry can be summarized as upslope structure interspersed with minor, i.e. short plateaus. A comparison with respect to magnitude and signal stretching can be made for both selected sonobuoy. Due to the longer propagation distance for sonobuoy 136 the expected signal stretching is higher than for sonobuoy 140 with the consequence that conclusion from the frequency domain could only acceptably well be drawn for sonobuoys 136 so that sonobuoy 140 was eventually excluded from the modelling.

Sonobuoy 136 was tracking the seismic survey for approx. 90 min. The azimuth angle between ship course and recorder was approx. 7°.

3.2.2 Modelling

3.2.2.1 Modelling approach

In contrast to the presented modelling approach in chapter 3.1.2.1 for the ARAGON dataset the model for the ARAON dataset in this chapter outputs a received signal of a source signal (time domain representation). Modelling a received time signal brings the advantage to use the modelling results as input data for time domain-based post processing. In addition, time related propagation phenomena, e.g. signal stretching, of sound propagation can be assessed. Signal stretching is a result of frequency-dependent sound propagation. Even short pulses will experience pronounced stretching when traveling long distances (e.g. 1000 km +).

The source signal's attenuation (transmission loss (TL)) along the possible propagation paths to a specific location (range, depth) can be numerically modelled by abstracting the underlying physics and the numerical solving of the governing equations in so called propagation codes. These propagation codes have been validated over decades (Jensen et al. 2011) and appear reliable as long as they are correctly applied with respect to input parameters, i.e. the environmental conditions.

The source signal in question has its very own frequency spectra. Modelling a received signal at a requested location requires the following steps

1. Model transmission loss for each frequency of the source spectra
2. Transfer the source signal into the frequency domain
3. Correct each frequency by its corresponding modelled transmission loss
4. Transfer the received signal back into the time domain

The anticipated stretching of the signal indicates the frequency resolution which is required in the calculations of transmission loss. The stretching depends on environmental conditions, the spatial dimensions being the major component here. Greater depths and longer distances will lead to an increased signal stretching. An anticipated stretching of 10 seconds, i.e. a signal length of *T = 10 s* will lead to a required frequency resolution of *df = 0.1 Hz* (equation 1)

$$df = \frac{1}{T}$$

(1)

The propagation conditions are also subject to the (varying) environmental data. In general water depth, profiles (variation with depth) sound speed, density and attenuation coefficients will drive the propagation conditions and thus the transmission loss pattern in space (range over depth). Varying profiles over range will additionally impact the propagation conditions and increase the complexity/uncertainty of the modelling results. These (varying) propagation conditions should be known to model a realistic transmission loss. The environmental data are one big uncertainty to propagation modelling.

For example, the sound speed profiles are seasonally changing and bottom types as well as bathymetry are highly variable with location.

The challenges for a realistic modelling are given by numerical constraints of the propagation code in question to accurately map the transmission loss pattern and the availability and validity of environmental input data.

3.2.2.2 Source Signal

The far field representation of the source (waveform, time series) was needed for assembling a received modelled signal. The source waveforms for the Araon seismic array were derived using a model of the emission from single guns and airgun arrays developed at CMST (Duncan 1998). To consider the directionality of the sound source (the airgun array) the source signal is modelled for different azimuth

and elevation angles. The azimuth angle covers the horizontal angle towards the source and is measured clockwise relative to the vessel/array heading. The elevation angle is measured relative to the downward vertical direction, i.e. for horizontal emission the elevation angle is 90 °.

The source signal modelling of airguns or airgun arrays is fairly complicated. Recent CMST comparisons with measured data indicate that the CMST model is less accurate for the G. Gun II than it is for the more common Bolt guns. For more accurate results a sample waveform would have been useful but could not be provided by KOPRI.

The modelled source waveform for two different azimuth angles is presented in Figure 34 showing the directionality of the airgun array. 90 ° azimuth angle represents the transverse direction and has a 1.75 times higher signal amplitude around 0 secs than the 7 ° azimuth direction applicable for sonobuoy 136.

Figure 34   Waveform Source Signal, Azimuth angle 7° and 90 ° for Sonobuoy 136
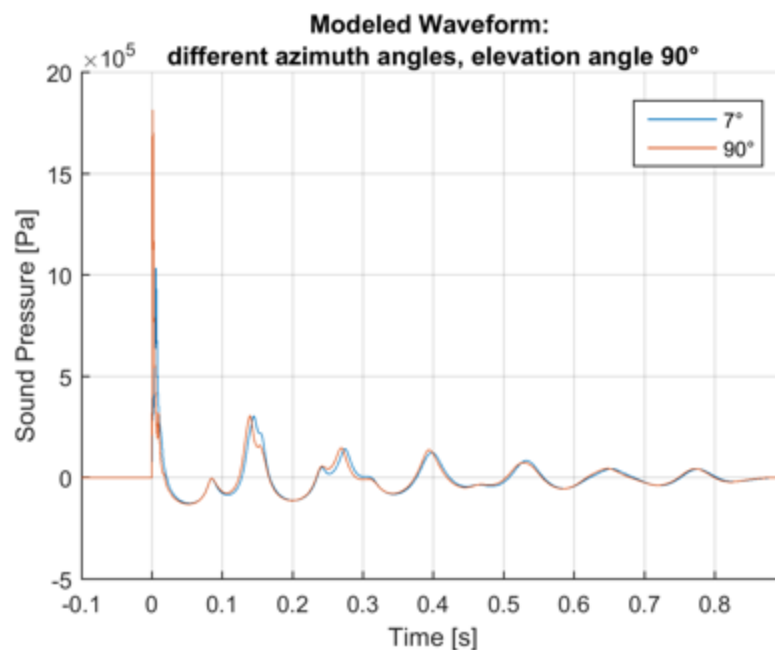
Figure 35   Energy Spectral Density of the Source Signal, Azimuth angle 7° for a low frequency range (up to 200Hz) and a broader frequency range (up to 1kHz)
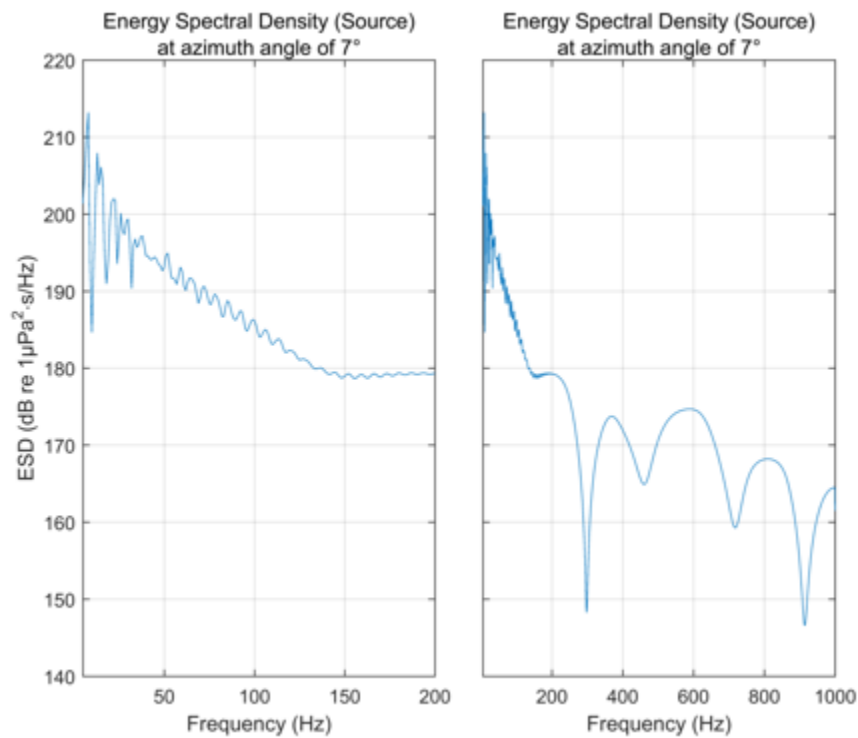
3.2.2.3   Measures for comparison

For comparison of recorded and modelled airgun shots 4 measures will be defined. Their quantities will be identified and the comparisons of these figures will verify or falsify the modelling method and assumptions (configuration).

Figure 35 shows modelled airgun shots from the Masking I project (Siebert et al. 2014). From the spectrogram in frequency and time domain representation the following measures could be defined:

1. Magnitude of time signal
2. Duration of continuous time signal (signal stretching)
3. Frequency range
4. Identification of upsweeps (modes) in frequency domain

Figure 36   Definition of measures for comparing recorded and modelled airgun shots. Frequency (left) and time (right) domain representation of modelled airgun shots from the Masking I project (Siebert et al. 2014).
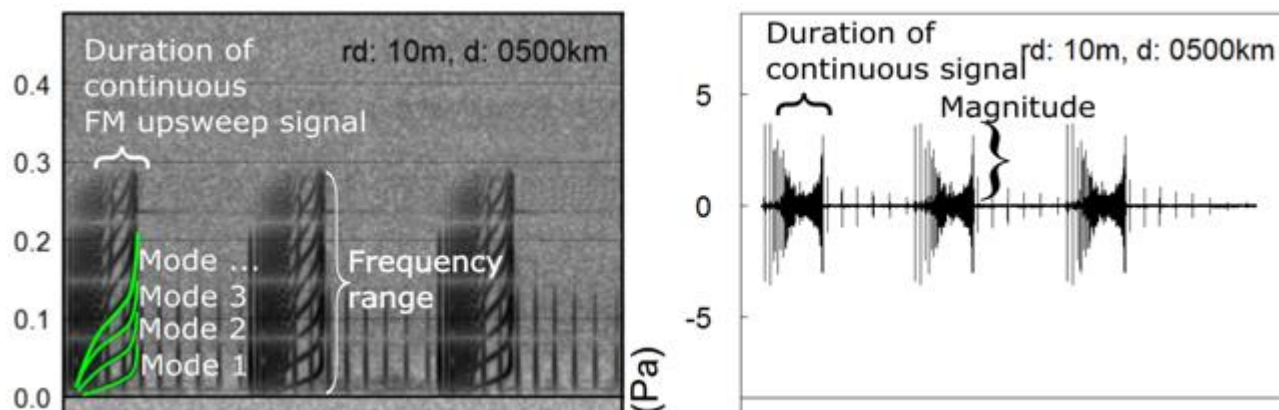
Magnitude and duration (signal stretching) of the time signal representation will be prioritized in the comparison.

Figure 36 shows the previously addressed upsweeps in the frequency domain of recorded airgun shots. The possibility to derive/show this feature in recorded data depends highly on the overall quality of the recorded data, i.e. a clean recording with no other noise contribution (ships, marine mammals, ice breaking), a high signal-to-noise ratio, a sufficiently high sampling rate, and the source-receiver distance, i.e. the signal stretching.

Figure 37   Frequency representation of recorded airgun shots
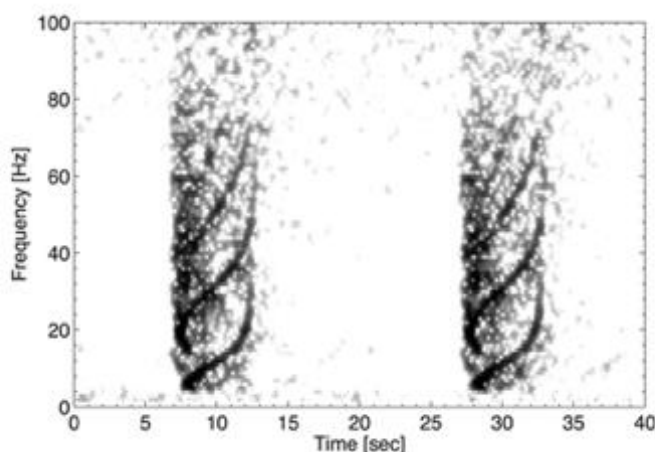
Figure 37 is taken from (Roth et al. 2012)

3.2.2.4   Sound transmission model

Sound propagation modelling was conducted for airgun shots received at sonobuoys 136 using RAMGeo (Collins 1993) as numerical solver (see chapter 3.4.2). As for density (Figure 37) and sound speed profile (Figure 38), the assumption of constant conditions along the propagation path can be made. The distances to be considered for the chosen scenarios are relatively small (approx. 300 km), compared to the ARAGORN (3000 km) scenario, and the physical properties, i.e. temperature, salinity, to derive the sound speed profile with depth, and the density of the water, are only varying on a minor scale.

The physical properties are taken from the World Ocean Atlas gridded climatology[4] data of 0.25 ° spatial resolution. The gridded data was interpolated along the propagation path. Water temperature and salinity data for winter period were used to calculate the sound speed profiles (Figure 38). The bathymetry data are taken from the ETOPO2[5] gridded data set (2" resolution) and mapped on the propagation path. The bathymetry indicates deep sea condition at the source location, i.e. the water depth at the source is approx. 2000 m. The original bathymetry features are simplified to constant down and up slopes if applicable.

Figure 38   Sonobuoy 136, Density Distribution along the Propagation Path

Density Distribution along Propagation Path
Sonobuoy 136

---

[4] https://www.nodc.noaa.gov/OC5/woa13/
[5] https://www.ngdc.noaa.gov/mgg/fliers/01mgg04.html
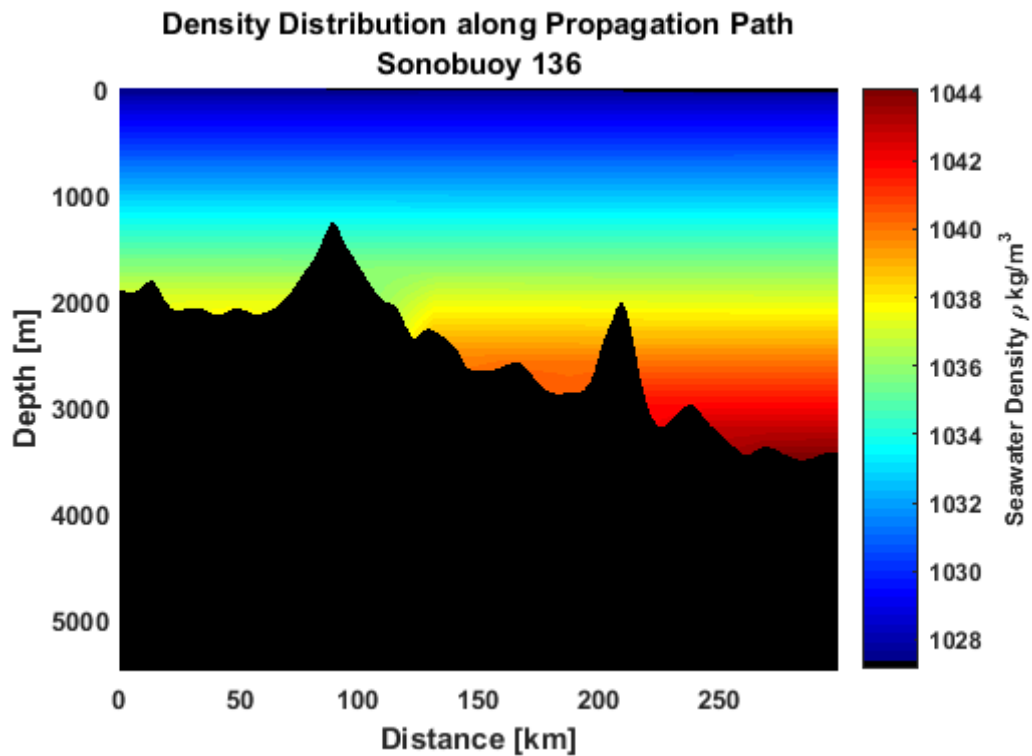
Figure 39   Sonobuoy 136, Sound Speed Distribution along the Propagation Path

Sound Speed Distribution along Propagation Path
Sonobuoy 136
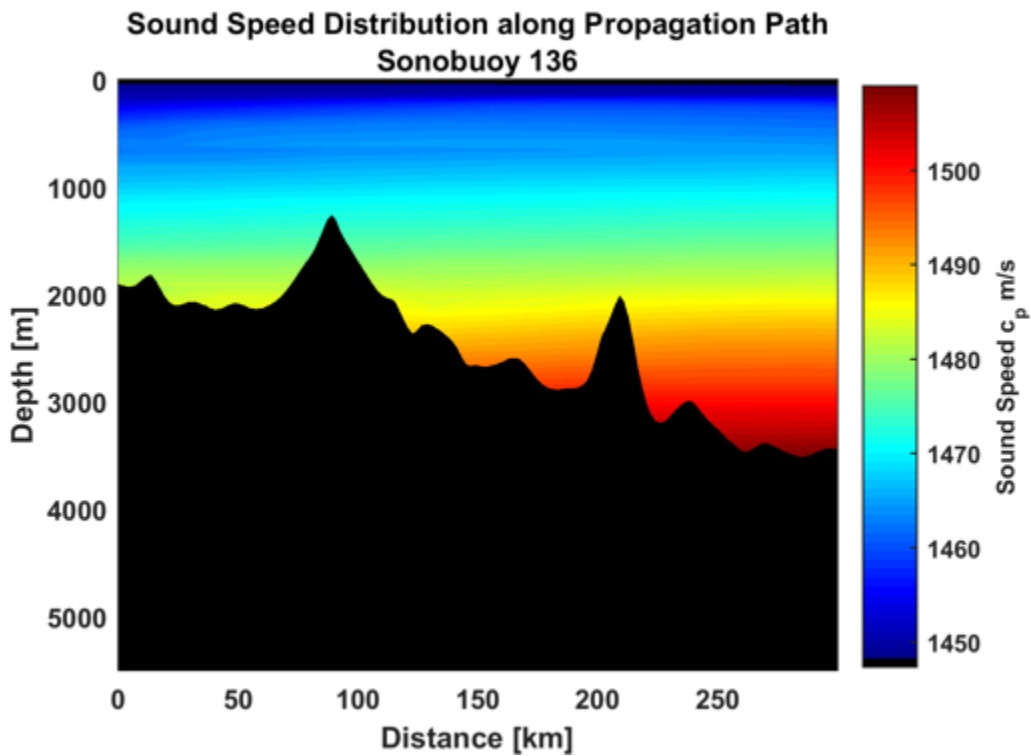
The final modelling parameters are shown in Figure 39 (geo-acoustic properties) and Figure 40 (simplified bathymetry).

Figure 40   SB136 Modelling, modelled environmental parameters, Sound speed (left) and density profile over depth

UBAG3: Modeling Propagation (R/VAraon to SB136)
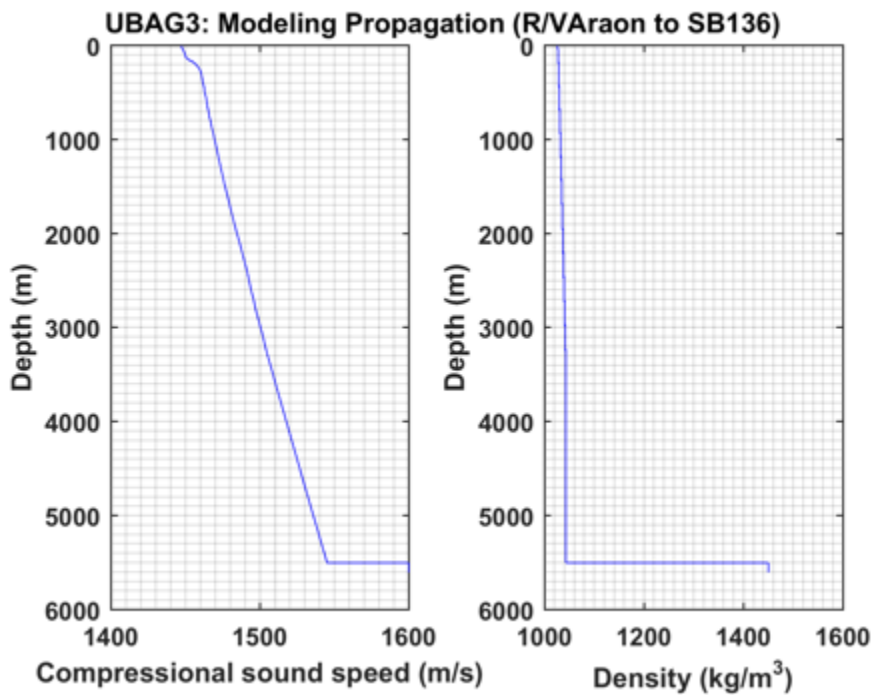
Figure 41   SB136 Modelling, modelled bathymetry (simplified)

Range (km)

3.2.2.5 Comparison of modelled and recorded data

The detected shots on sonobuoys 136 were analysed with respect to signal duration, i.e. signal stretching, sound exposure level (SPL_{RMS}) and peak-to peak sound pressure level (SPL_{pk-pk}). Table 9 holds a statistical summary of 243 processed shots.

Table 9   Statistical evaluation of 243 detected shots a sonobuoy 136

	signal duration t [s]	sound exposure level SEL [dB re 1 µPa²s]	peak sound pressure level SPLpk-pk [dB re 1 µPa]
mean	4.0504	120.79	131.72
median	4.1841	120.71	131.68
min	3.0400	118.60	130.04
max	5.1194	124.60	135.96

Figure 42 presents a recorded airgun shot at sonobuoy 136 to illustrate the statistical data in Table 9. The single shot was analysed using SpectroPlotter (Jasco Inc.) software. The signal was visually selected. The signal duration was determined to 3.75 s. SEL and SPL_{pk-pk} was determined to 120.4 dB re 1 µPa²s and 130.5 dB re 1 µPa respectively.

Figure 42   Time series (upper part) and frequency spectrum (lower part) representation of a recorded airgun shot (red box) at sonobuoy 136, timestamp 05:38:32.
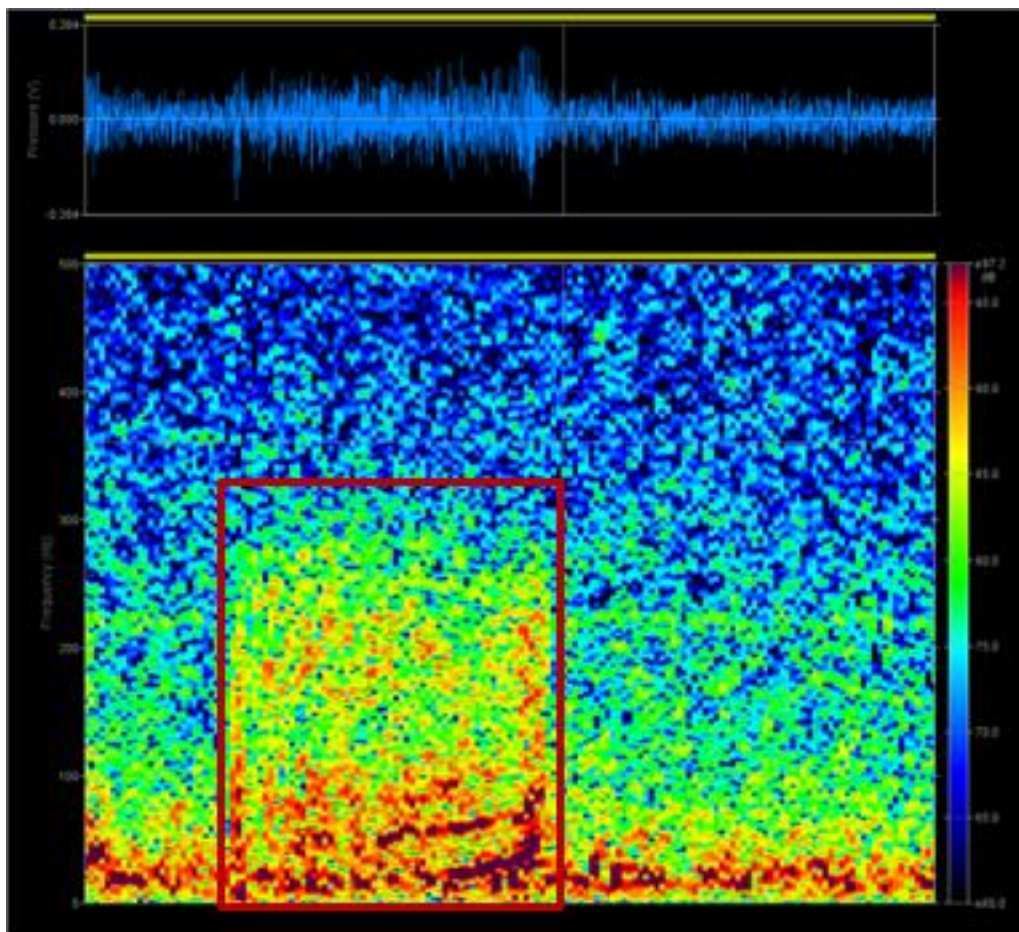
In chapter 3.2.2.3 four quantities were introduced to compare recorded and modelled received airgunshots. After 300 km propagation the initially short duration pulse has been stretched to approx. 3.75 seconds. The energy is concentrated within the frequency range below 100 Hz, even below 75 Hz. Upsweeps can be identified, but only in the low frequencies. In addition, higher levels especially above 100 Hz are seen during the shot time slot and the neighbouring background noise periods. No characteristic pattern can be found within this frequency range.

In Figure 44 and Figure 44 the modelled shots at range 300 km for the depths 140 m and 160 m are presented. The general spectrogram patterns at the two depths are highly similar. However, the energy distribution over frequencies varies at the right edge (arrival of the high energy part of the signal). The upsweeps in front of the right edge are present in both figures, but vary slightly in frequency for the two depths. Overall the amplitude of the individual signals is consistent for the two depths. The signal length is approx. 2.4 seconds.

Figure 43   SB136: modelled received shot at 300 km range and 140 m depth
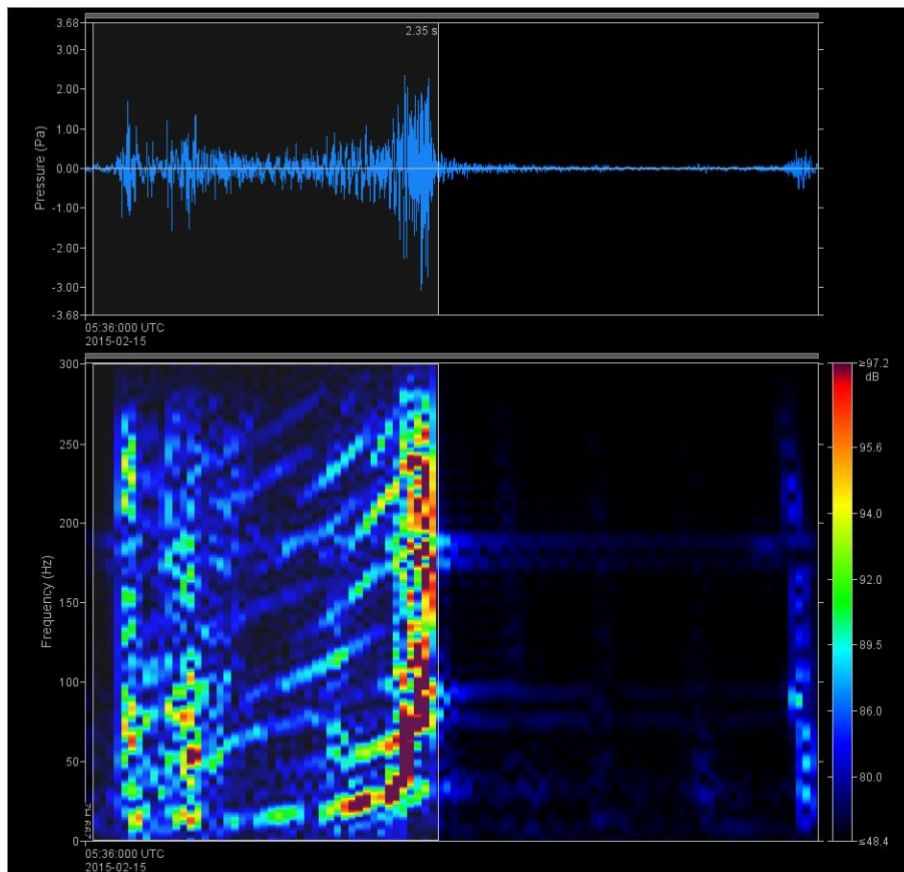
Figure 44   SB136: modelled received shot at 300 km range and 160 m depth
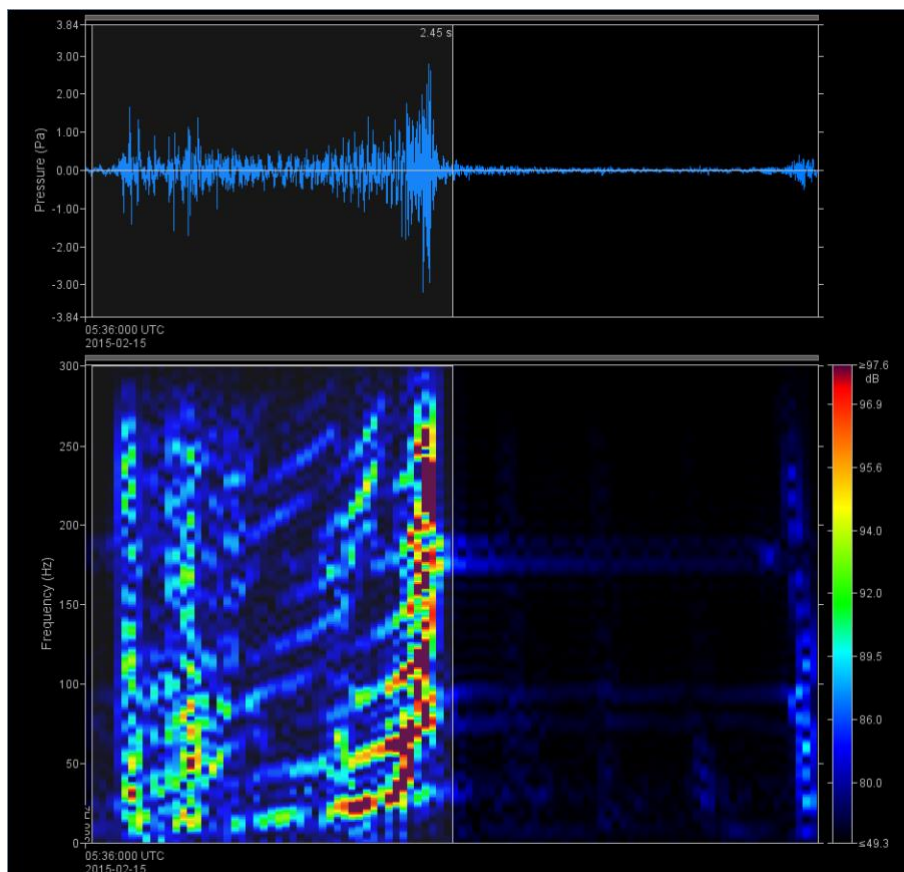
In comparison the recorded and the modelled airgun shots differ in all four measures. The modelled signal stretching reaches only 2/3 of the recorded stretching. For the recorded shots high energy levels are limited to frequencies below 100 Hz. The modelled shots contain high energy contributions up to 250 Hz. Due to the lower signal stretching the peak pressure level SPL_{pk-pk} holds higher values of approx. 3 dB for the modelled shots. The sound exposure levels differ as well. The recorded shots show raised levels up to approx. 4 dB compared to the modelled shots (120 and 116 dB re 1 µPa²s respectively).

Figure 45 and Figure 46 present the energy spectral density level (ESD) for comparison. The presented ESD cover the whole airgun shot period, as to been seen in Figure 42. In comparison with the source signal (Figure 35) most characteristics of the source signal can be found within the ESD (Figure 45) of the modelled shot, though on much lower levels. The low frequencies up to 50 Hz are subject to interference effects (Lloyd-Mirror's effect) and show expected much lower levels. There's a good agreement for the frequency range from 50 Hz up to 300 Hz. From 50 to 150 Hz a small decline is found. From 150 to 250 Hz the more or less constant levels of the source can be recognized as well as the sharp collapse towards 300 Hz.

Figure 45   SB136: ESD of modelled shot at 300 km range and 140 m depth
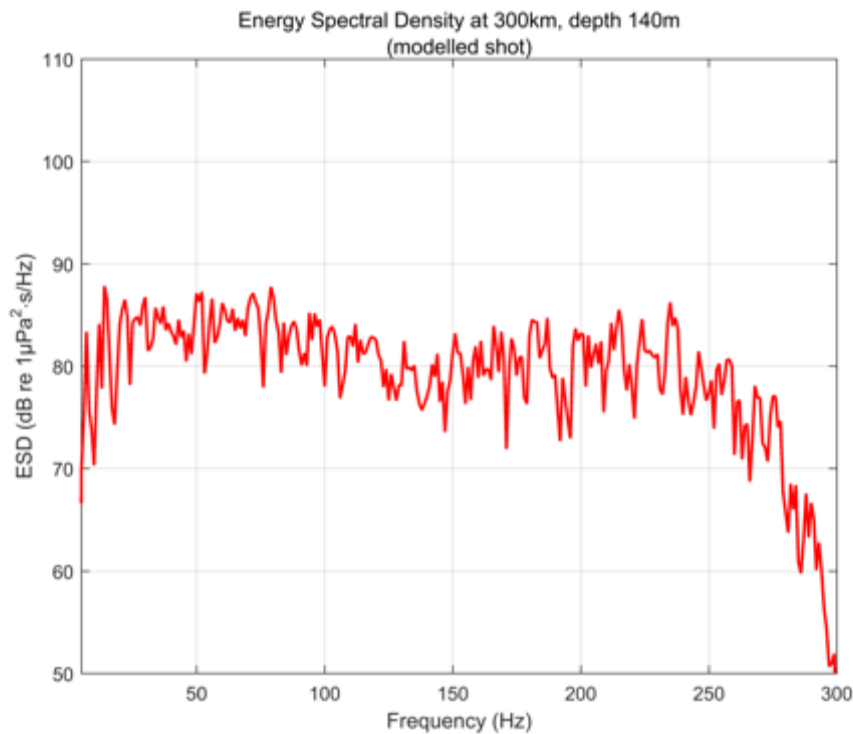
The comparison of recorded and modelled data in terms of ESD levels is given in Figure 46. There's a good overall agreement between the modelling and the recorded data. Frequencies below 50 Hz and above 275 Hz are masked by the high background noise levels (Figure 47). Frequencies up to 75 Hz might be partially influenced by the background noise. The frequencies from 30 Hz up to 125 Hz are underestimated by the modelling.

Figure 46   SB136: Comparison of ESD levels for recorded and modelled data at 300 km range and 140 m depth
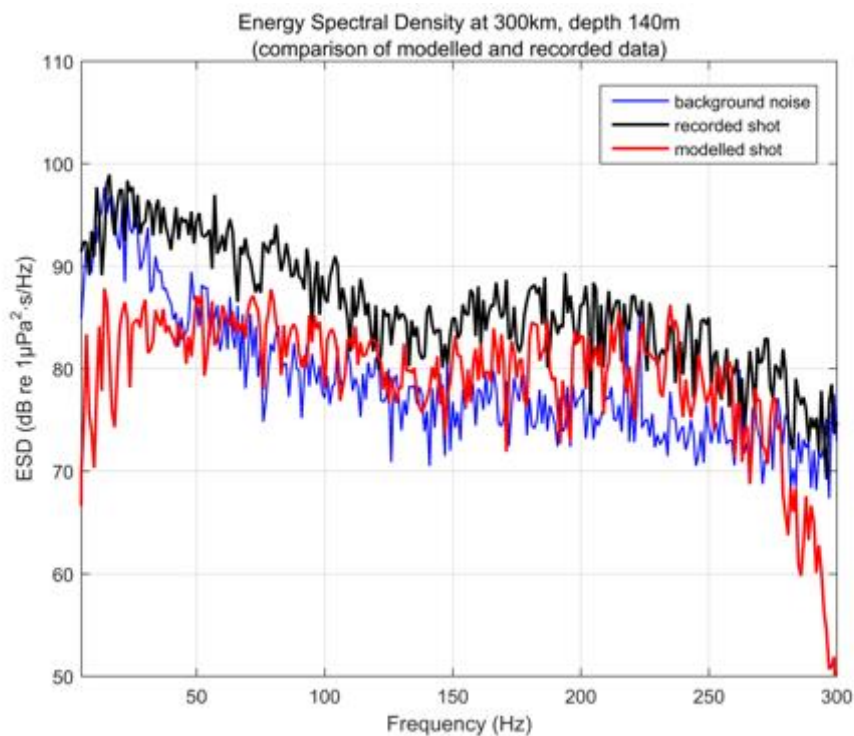
Figure 47   SB136: General noise levels within the recordings at 300 km range and 140 m dept. Recorded airgun shot framed by sequences of background noise.
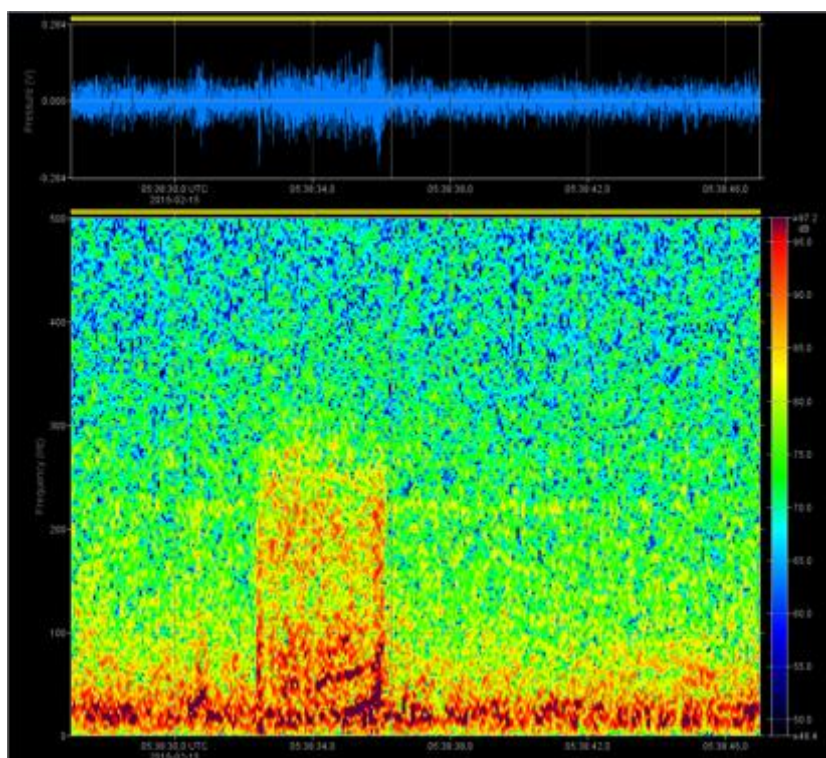
3.3 Conclusions for Sound Propagation Modelling

Sound propagation models for the Southern Ocean were generated and their prediction accuracy was evaluated by comparison with two experimental datasets.

For the Aragorn dataset a CMST numerical model of underwater sound emission by airgun arrays and a combined *PE-normal mode model* of sound propagation from the Aragorn offshore seismic survey in Bass Strait to Antarctica were employed. In addition to acoustic properties of the water column (sound speed profiles), the bathymetry and geoacoustic properties of the seabed, the normal mode model can account for the transmission loss due to sound scattering by surface wind waves (this sets the normal mode approach apart from the PE approximation). Sound scattering by surface wind waves was found to be an important cause of the transmission loss at high frequencies in the region south of the polar front where the sound channel is located close to the sea surface. The fact that the modelling predictions match the measurement data to within a few dBs with respect to both sound exposure and energy spectral density levels of the received airgun signals indicates that the model aptly captured all major effects on sound propagation in the Southern Ocean. Both modelling and measurement results demonstrate that the best transmission of underwater sound from a shallow source over the Australian continental shelf and slopes to Antarctica takes place when the water depth at the source location is about half the SOFAR channel axis depth (i.e. when the water depth at the source location is in the range of 300 -700 m). This is because in deep water (> 700m) a shallow source is not well coupled with the SOFAR channel through the interaction with the sloping seabed. In shallow water (<100-150) over the continental shelf in Bass Strait, low-frequency underwater sound interacts greatly with a calcarenite (soft limestone) seabed and hence attenuate rapidly with range and cannot reach the Antarctic waters.

For the ARAON dataset, a *PE-only* modelling approach was used to model the time series of the received airgun signal. Looking at the sound exposure levels only, modelled and recorded values differ by approx. 4 dB. The differences can be explained by a less accurate source model for the G.Gun II compared to the more commonly used Bolt Gun. Looking at the energy spectral density there's a good agreement for the frequency range between 75 Hz and 275 Hz. At the edges of the considered overall frequency range of 5 Hz and 300 Hz the recorded levels are dominated by the background noise. The signal spreading is underestimated in the modelling results showing only 2/3 of the recorded signal spreading.

It is important to notice that the modelling results were verified by measurements only for one receiver depth of 1100 m at the Aragorn surveys site and 140 m at the Araon site. The comparison of modelling and measurement results would be much more comprehensive if measurements were made at other receiver depths as well.

In austral winter, an extensive area of the Southern Ocean south of the East Antarctic coast is covered by sea ice, which affects the surface scattering mechanism and should be taken into consideration in the sound transmission modelling.

3.4 Input data for masking model

3.4.1 Method

The communication range of marine mammals is limited by the level of ambient noise in the respective frequency band, e.g. baleen whales use low-frequency vocalization to communicate. Noise from seismic airgun surveys covers a similar frequency range as this vocalization and may therefore interfere with these communication signals.

To infer the degree of masking an auditory model is developed in chapter 5. It takes all noise and sound signals hitting a receiving individual as input. In particular these signals are vocalisations by a conspecific, airgun-signals and ambient noise. Airgun-signals and vocalisation signals hitting the receiving individual have to be inferred from source signals based on a sound propagation model. This process of inferring received from source signals is described in this section.

The received signals have undergone sea water propagation and individual frequencies will show different attenuation, i.e. transmission loss. The transmission loss itself is a linear factor (0 … 1) expressing the attenuation for an individual frequency. It can be estimated based on the propagation conditions in the waterbody, the distance between source and receiver and the depth of the source and receiver. In consequence the transmission loss can be called transfer function since it relates output and input values for amplitude and phase information. Any source signal in question has its very own characteristic frequency spectrum, but each individual frequency in the source signals will undergo the same transmission loss when identical propagation conditions apply. This fact makes it possible to model propagation of sound signals (e.g. marine mammal vocalizations or airgun signals) in a two-step process. First the transmission loss for all individual frequencies in the considered frequency range is calculated ("sound propagation model", discussed in the focal chapter). Later the obtained transfer functions are applied to the source signals of interest in order to generate propagated signals as perceived by the receiving animal (this is discussed in chapter 5). The advantage of this workflow is that transmission loss has to be modelled only once even if different source signals (e.g. vocalisations of different marine mammal species) are to be evaluated in the masking model.

As described above the sound propagation model aims at evaluating the transmission loss for all individual frequencies in the considered frequency range. Technically this is achieved by modelling the transmission loss of a source signal in which all frequencies are equally represented (i.e. all frequencies have the same amplitude). Such a signal is termed Dirac Pulse. The modelled Dirac time series (for different depths and ranges) holds the transmission loss information for amplitude and phase.

The application of the masking model to marine mammal vocalization in general, i.e. not only the frequency range for airgun signals, broadens the frequency range to be considered. For the broadband vocalization of marine mammals, e.g. Weddell seal (*Leptonychotes weddellii*) or killer whale (*Orcinus orca*), frequencies up to several kilohertz are of interest. This increase in frequency range strongly affects the overall processing time for individual modelling scenarios.

In consideration of computational demands the maximum frequency was initially set to 2000 Hz, but was lowered to 1500 Hz after initial runs of RAMGeo (see 3.4.2).

Addressing the frequency dependent transmission loss due to the absorption in seawater, low frequencies up to 100 Hz will not suffer any substantial additional transmission loss (additional to geometric spreading) while propagating, even for long distances. Table 10 gives an impression on how much different frequencies are subject to TL due to water absorption. Following that low frequencies will propagate far distances, up to several thousand kilometres standing above background noise levels. The numbers in Table 10 are derived after Thorp's formula (Thorp 1967), equations 4 and 5, in a coarse manner for exemplary reasons.

Table 10   Exemplary transmission loss values due to water absorption using Thorp's formula

Frequency [Hz]	Relative attenuation dB/km	Transmission loss after 100km	Transmission loss after 1000km
100	0.0042	0.42	4.2
300	0.0131	1.30	13
500	0.0278	2.80	28
1000	0.0690	6.90	69
1500	0.1040	10.40	100
2000	0.1351	13.50	135

In consequence the modelling of low frequency propagation has to be extended to longer distances, while for higher frequencies modelling of shorter distances might be sufficient. The maximum modelling range has to reflect the (spectral) source level to assure that the received level is below the background noise level.

A transfer from time into frequency domain will result in a frequency resolution of

$$\Delta f = \frac{1}{T}$$

$$(2)$$

for a time signal of period T in seconds. The longer a signal of interest is (e.g. due to signal stretching), the finer the sampling rate in the frequency domain has to be chosen. This will considerably increase the modelling processing time since for each frequency step within the frequency range of interest a transmission loss calculation has to be performed.

Examining intermediate results within the current project the received time signal of the Dirac pulse reaches a signal stretching of 10 s already at distances below 1000 km. Covering distances up to 5000 km, stretched signals of 40 s and thus a frequency resolution of $\Delta f = 0.025$ s will have to be considered.

3.4.2   Numerical modelling

RAMGeo (Collins 1993) is chosen based on its features

1. Handling of low/lowest frequencies (long range propagation)
2. Handling of range-dependent problems to numerically solve the governing fundamental equations.

The masking model will be evaluated for only some few points (distance, depth) of the modelling space. To cover marine mammal communication an initial maximum frequency of 2000 Hz was chosen: High frequencies go along with small wavelengths leading to fine numerical grids. For a space marching solver, as RAMGeo, all points along the numerical grid have to be exploited. An increasing number of points will not linearly increase the processing time. The computational requirements for RAMGeo increase with frequency

$$f \cdot \log(f)$$

$$(3)$$

Due to the computational requirements (equation 3) it is used **for frequencies less than 1 kHz.**

In contrast to other propagation codes (e.g. Bellhop (raytracing code)) RAMGeo does not take water absorption into account. Therefore, an approximation accounting for the absorption is provided for the masking model. Many formulas have been promoted to calculate the absorption in sea water reflecting the latest scientific research. The more recent publications increase the demand for detailed data

reflecting the water individual composition (contribution of Boric acid, Magnesium & Sulphate)[6]. However, for this project the more simplified **Thorp formula** is used to calculate the absorption loss because specific parameters for more accurate calculation fluctuate seasonally and are unknown for the locations of interest (equation 4 and 5). Absorption loss $TL_{Absorption}$ is given by

$$TL_{Absorption} = r \cdot 10 \log_{10} a\,(f)$$ (4)

where r is the range in kilometres and a(f) is the frequency-dependent absorption coefficient. Frequency dependence of the $10 \log_{10} a(f)$ -term is given by

$$10 \cdot \log_{10} a(f) = 0.11 \frac{f^2}{1+f^2} + 44 \frac{f^2}{4100+f} + 2.75 \cdot 10^{-4} f^2 + 0.003$$ [dB/km] (5)

where f is frequency. To cover the frequency range up to 2 kHz accurately well and within justifiable time span a split workflow was proposed. Two different sets for transfer function were calculated:

1. **long distance low frequency** transfer functions covering frequencies from *5 Hz up to 375 Hz* and distances *up to 5000 km*
2. **broad band vocalization** transfer functions covering frequencies from *5 Hz up to 1500 Hz* and distances *up to 500 km*

Initial runs showed artefacts for frequencies above 1500 Hz. Re-runs on re-fined numerical grids and an adapted framework could not resolve this problem. The re-calculated transfer functions do still show the artefacts for frequencies above 1500 Hz (Figure 48 and Figure 49). However, a better alignment in the low frequency range is observed. In consequence the frequency range *above 1500 Hz was excluded* from the final results. The increased computational efforts due to the re-fined grid the maximum range was *limited to 100 km for the broad band* transfer function set.

Figure 48   Numerical artefacts in RAMGeo results
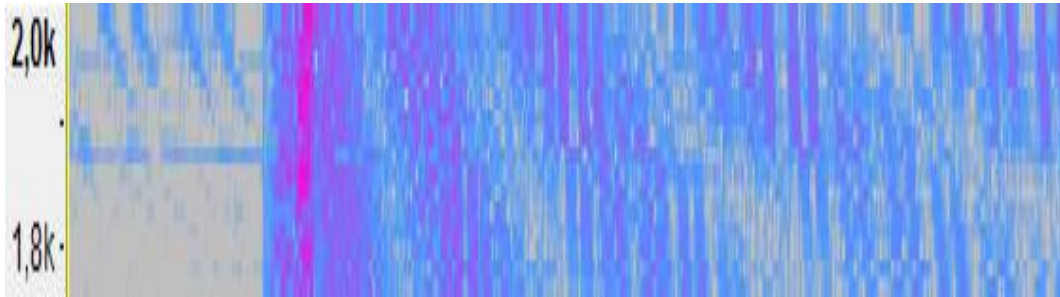
Figure 49   Numerical artefacts in RAMGeo results (re-fined grid)

---
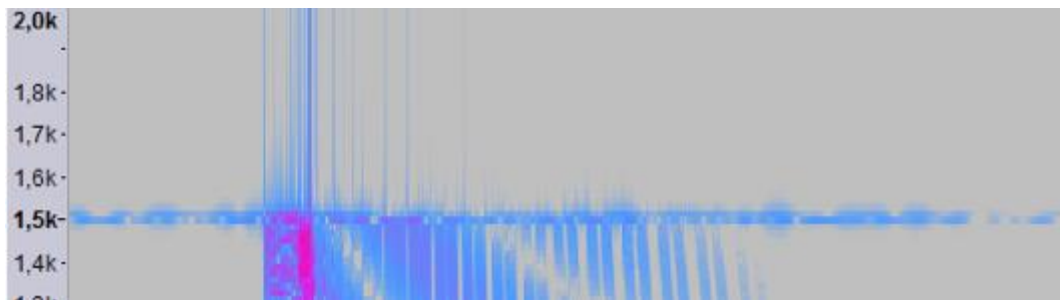
[6] For an introduction to approximations for sea water absorption, please see the website from the National Physical Laboratory (Middlesex, UK) http://resource.npl.co.uk/acoustics/techguides/seaabsorption/

Figure 48 shows unexpected results in the frequency range above 1500 Hz most probably attributed to interpolation errors on mal-adjusted grid settings. After refining the calculation grid and the output grid to spacing less than 1/4wavelengths artefacts still remain. In Figure 49, the re-fined grid was calculated only up to frequencies of 1510 Hz.

Up to 1500 Hz no artefacts are visible and the found spectrograms are in accordance with theoretical expectations and observed data. Due to the remaining artefacts the frequencies over 1500 Hz were excluded. An explanation for the artefacts could be the implemented (computational) type precession for variables in RAMGeo. To lower the processing time many propagation codes uses single precession for its variables. The used version of RAMGeo uses single precision variable types. Increasing the precision from single to double would result in a doubling of the processing time. The addressed frequency limit of 1500 Hz might interfere with the reference sound speed (being mandatory input) chosen for the modelling. Going above 1500 Hz, i.e the wavelength is dropping below 1.0 m, there is a numerical grid refining from 0.25 m to 0.20 m due to the reference sound speed and a chosen wavelength-dependent grid sampling criterion. The refined grid size or other expressions incorporating the wavelength could lead to unstable/faulty results on the single precision evaluation.

3.4.3   Modelling assumptions

The transmission loss modelling depends on environmental input data. This input data reflects

1. bathymetry
2. sound speed profile (referencing sea water properties like salinity, temperature, density)
3. geo-acoustic properties and
4. depth of the source signal

In (Boebel et al. 2009b) several hydrographic stations are presented, probed during Antarctic voyages conducted by the Alfred-Wegener-Institute. These stations are located at the Weddell Sea and the Amundsen/Bellinghausen Sea, typical regions for AWI's seismic operations. (Boebel et al. 2009b) consider the Amundsen/Bellinghausen Sea sound velocity profiles to be representative independent of the region for the austral summer situation, i.e. the time of the highest seismic research activity. Comparing these hydrographic stations, the thickest shallow sound channel was observed in the Amundsen/Bellingshausen Seas at S715. Due to its pronounced sound channel (sound channel axis at approx. 80 m) and its attributed sound guidance, S715 was chosen as input parameter for modelling, especially with regard to long range propagation. Station 715 lies at approx. 109°W and 67.5°S at the Amundsen Sea. At first a second hydrographic station, i.e. station 25 (S25) located at Weddell Sea, was considered as second modelling scenario representing a region-independent sound speed profile for the austral spring and fall time. Due to the high computational demand S25 could not be considered within the project time. S715 and S25 represent deep sea scenarios of water depths of approx. 4000 m. Below 300 m both sound speed profiles are almost identical.

For the modelling of transfer function for the masking model simplified assumptions were made for input data. The influence of variations to these simplified assumptions is considered in WP3.

1. All modelling assumes
2. flat bathymetry (no topographic features)
3. no range-dependent features, i.e. constant properties over range (but depth dependent)
4. source depth 5 m
5. sound speed profile for station 715 (Amundsen/Bellingshausen sea S715) with a shallow sound channel
6. Bottom properties set to: sound speed (1600 m/s), density (1450kg/m^3)

Two different water depths are modelled. Reflecting a shallow water environment is water depth is set to 500 m, for a deep-water scenario the depth is set to 4000 m.

The bottom in the Antarctic is described in (Breitzke and Bohlen 2010). This is converted to the properties of mud, a comparatively soft material with impedance and speed of sound close to water. As for the geo-acoustic bottom properties bottom half space with constant sound speed (1600 m/s) and constant density (1450kg/m^3) is modelled. The absorption for compressional waves is set to 0.3 dB/wavelength.

Figure 50   Environmental Properties for Station S715
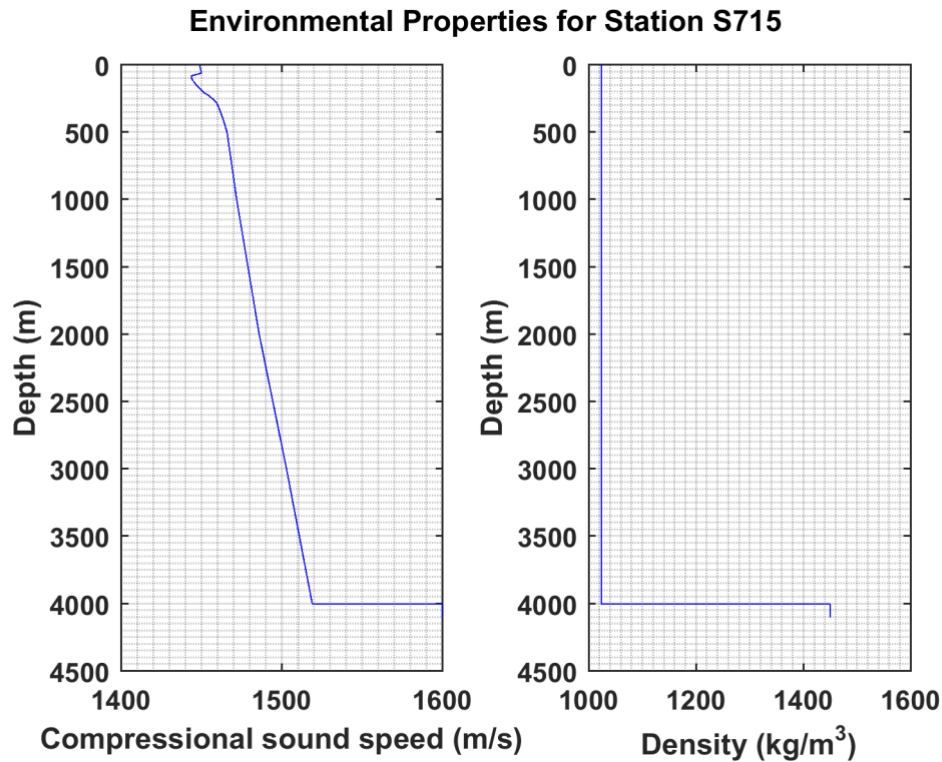
Sound speed profile (left chart) and density profile (right chart) for station 715 reflecting austral summer conditions for the Weddell Sea and the Amundsen/Bellinghausen Sea.

3.4.4 Data description for the provided input data for the masking model

A summary of the input parameter for the propagation modelling is given in Table 11 - Table 13.

The data for the masking model is examined on 25 distances per decade covering the individual modelling range for 3 receiving depths. Two parameters will decide on the maximum range coverage of the modelled data. The model is configured for a maximum range, e.g. 100 km (shallow water scenario) and 5000 km (deep water) respectively. Up to these ranges RAMGeo outputs result data. Transfer functions for these ranges depends on the completed calculations for all frequencies of a frequency step, i.e. does a certain frequency step provides a sufficiently long-time window for the anticipated signal stretching. In Table 12 and Table 13 the last column depicts the maximum range that can be covered with the masking model.

For each examined point (range, depth) two results are provided. The transfer function is provided as 24-bit wav-file with a sampling rate of 4 kHz. The filename holds all necessary information with respect to range (m), depth (m) and scaling. The transfer function is obtained by scaling, i.e. multiplying the loaded waveform (-1 ... +1) with

$$scl = 10^{-\frac{X}{20}}$$

(6).

The Thorp attenuation is provided as frequency domain representation for each frequency involved during the processing of the transfer function.

Table 11   Input parameter for the propagation modelling

Parameter	Realisation
Depths (m)	10, 50, 200 m
Bathymetry	shallow water: flat, 500 m deep water: flat, 4000 m
Sound Speed Profiles	S715, please see Figure 50
Source Depth	5 m

Table 12   Result summary for the shallow water modelling scenario

shallow water	Δf covered frequency step	$r_{max,\Delta f}$ max range covered by Δf setting	r_{max} max. modelled range
broad band set (5 Hz - 1500 Hz)	0.1 Hz	500 km	**100 km**
low frequency set (5 Hz - 375 Hz)	0.05 Hz	2000 to 3000 km	**2000 to 3000 km**

Table 13   Result summary for the deep-water modelling scenario

deep water	Δf covered frequency step	$r_{max,\Delta f}$ max range covered by Δf setting	r_{max} max. modelled range
broad band set (5 Hz - 1500 Hz)	n.a.	n.a.	**n.a.**
low frequency set (5 Hz - 300 Hz)	0.025 Hz	5000 km	**5000 km**

The high frequency range resulted in high computational demands and re-runs of calculations due to numerical troubleshooting. The range coverage for the broad band transfer function comprises a set of the shallow water case and additional environmental modelling scenarios However, the broad band set for the deep-water scenario could not be compiled within the project time. Necessary adaptions to RAMGeo's source code to get the modelling workable for the high frequency were numerical unstable. Further considerations addressing numerical precision of the source code and compiler issues would be necessary.

However, three out of four cases (see Table 12 and Table 13) could be provided as input data for the masking modelling.

4 Analysis of Ambient Noise Recordings

4.1 Spectral Characteristics of Ocean Ambient Noise in the Eastern Part of the Southern Ocean

4.1.1 Methodology

Ambient ocean noise data were recorded at three different locations in the eastern part of the Southern Ocean in 2006, as shown in Figure 31 and described in Gavrilov et al. (2016). A significant percentage of the sea noise recordings made at these locations contained low-frequency noise artefacts resulting from mooring vibrations under strong currents (for example see Figure 51). Sporadic events of broadband impulsive noise due to mechanical banging of mooring parts were also observed in some noise recordings, especially in dataset 2716. Sea noise recordings made during the operation periods of the Aragorn seismic survey(Geophysical 2006) contained impulsive noise from the airgun array. Time periods containing noise artefacts and airgun noise were excluded from the analysis of ambient noise spectra.

The length of continuous recordings made in all three sound recorders was 780 s. Each recording was divided into 100-s sections to calculate the Power Spectral Density (PSD) on a 1-Hz frequency grid from 1 Hz to 2 kHz. If an event of high-intensity impulsive noise artefact was found in any section, this section was removed from further spectral analysis, rather than the entire recording. The presence of noise artefacts was examined by comparing the mean intensity level of noise in the low-frequency band from 5 Hz to F_{trans} (Sp1) with that at higher frequencies from F_{trans} to 2 kHz (Sp2), where the transition frequency F_{trans} was chosen different for different datasets based on the bandwidth of noise artefacts. Once the recording sections with artefacts were localized and removed, 1/3-octave and 1/12-octave PSDs were calculated for each section without artefacts. The finer frequency resolution of 1/12-octave was used in addition to standard 1/3-octave to distinguish the contribution of narrowband sound sources in the ambient noise spectra. Then PSD levels were calculated against different percentile values for both spectral resolutions. These percentile levels were plotted (see Section 3) and saved in MS Excel spreadsheets for each of the three deployment locations. Percentile values indicate the percentage of time the spectral level of noise stays below the corresponding PSD level.

4.1.2 Results

4.1.2.1 Dataset 2731 (Site 1)

The bandwidth of noise artefacts due to mooring vibrations was about 20 Hz, as can be seen in Figure 51. So, the transition frequency F_{trans} for this dataset (site 1) was chosen to be 20 Hz. Figure 52 shows a 2-D histogram of the number of 100-s recording sections versus two parameters: *Sp1-Sp2* and *Sp1+Sp2* (i.e. mean intensity level in the entire band of recording). The sections with noise artefacts can be recognised in the long tail toward higher values of *Sp1-Sp2*. The boundary separating recording with and without artefact is shown by the dotted line. Its position (offset and slope) was empirically derived to keep real events of low-frequency impulsive sound (e.g. from earthquakes) but, at the same time, remove most of the sections with artefacts. As a result, about 60% of all recordings section were selected for spectral analysis of ocean ambient noise.

Figure 51   An example of long-time average spectrogram of sea noise recorded at site 1 (Figure 1.1) over 30 days in May (top panel). The bottom panels show the waveform (left) and spectrogram (right) of a 20-s section with low-frequency noise due to mooring vibrations.
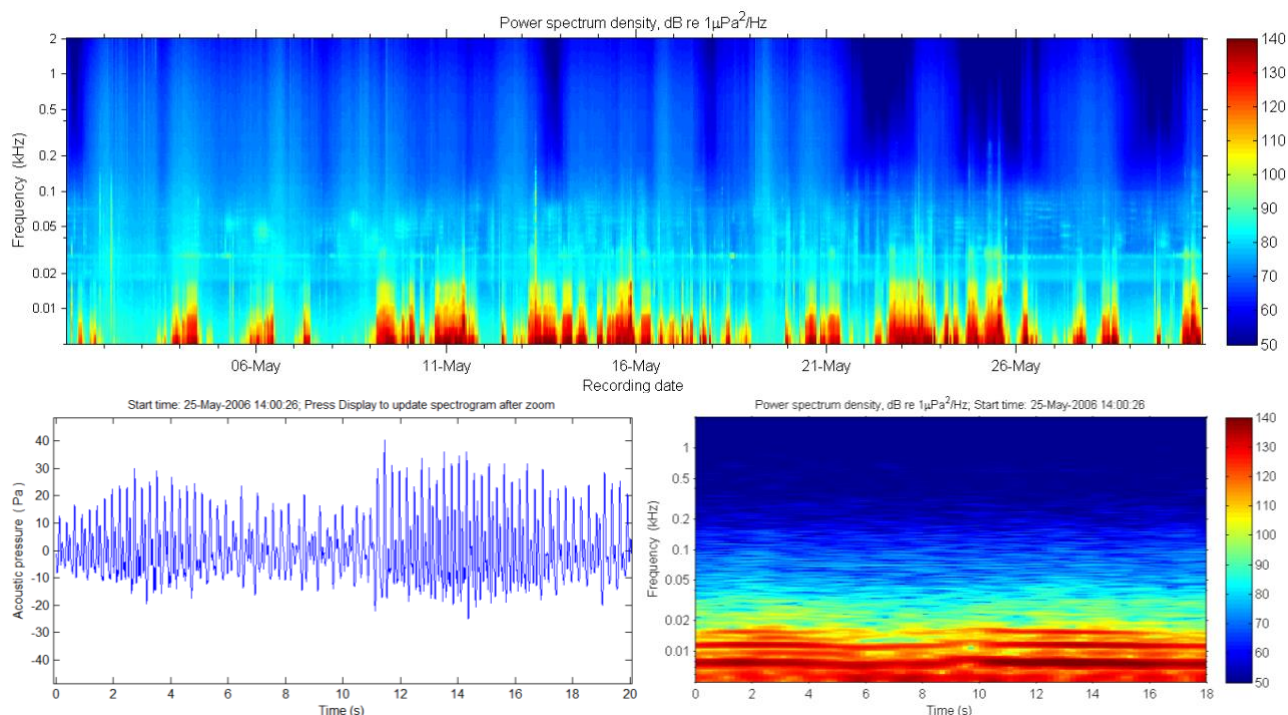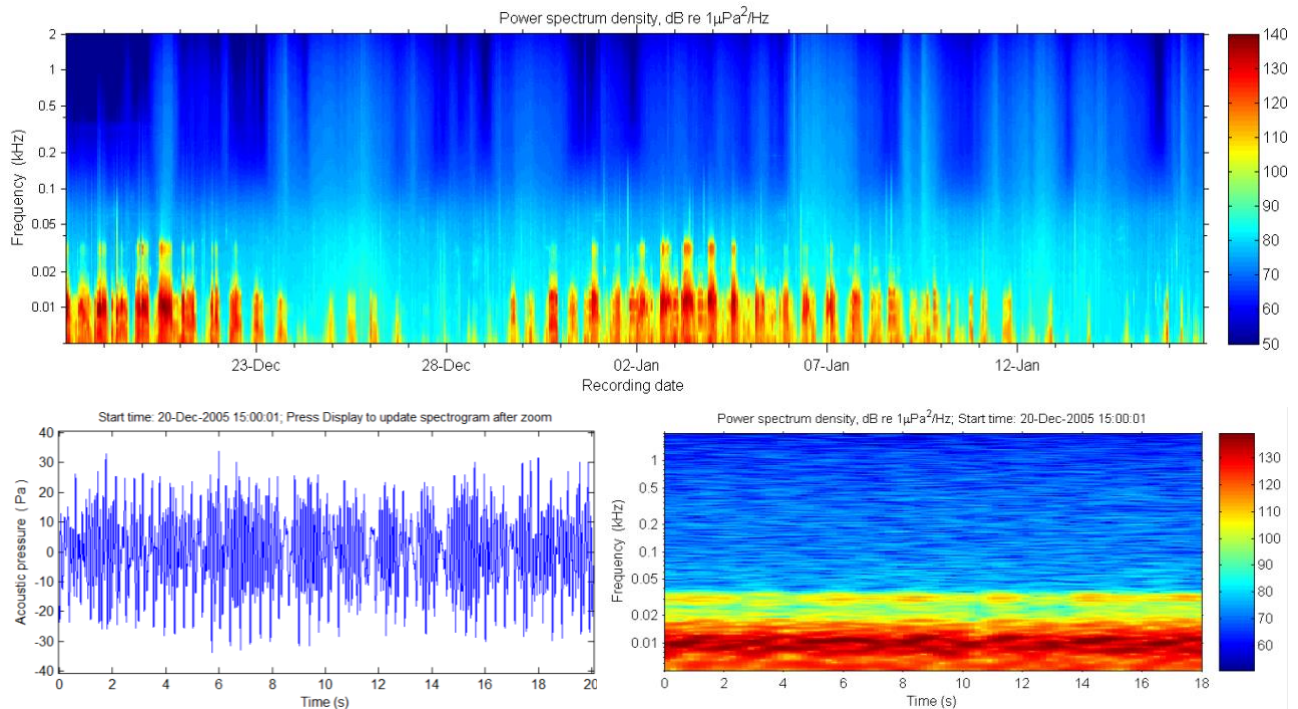

Figure 52   2-D histogram of the number of recording sections in dataset 2731 (site 1) versus two parameters: Sp1-Sp2 and Sp1+Sp2. The dotted line shows an empirically derived boundary between section classes with and without artefacts.
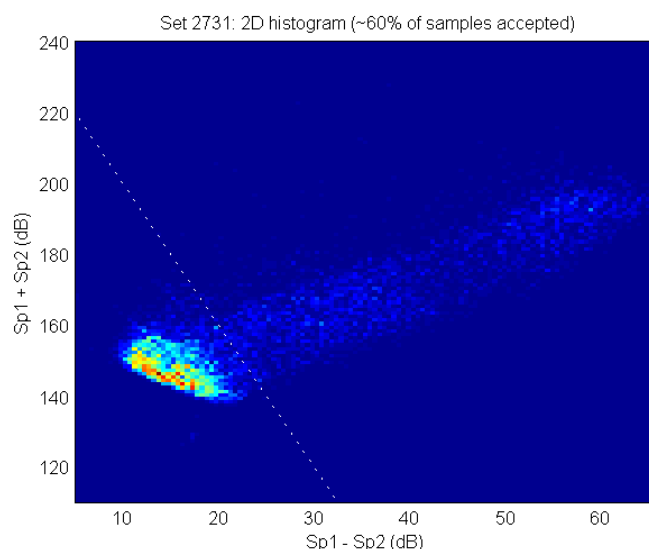
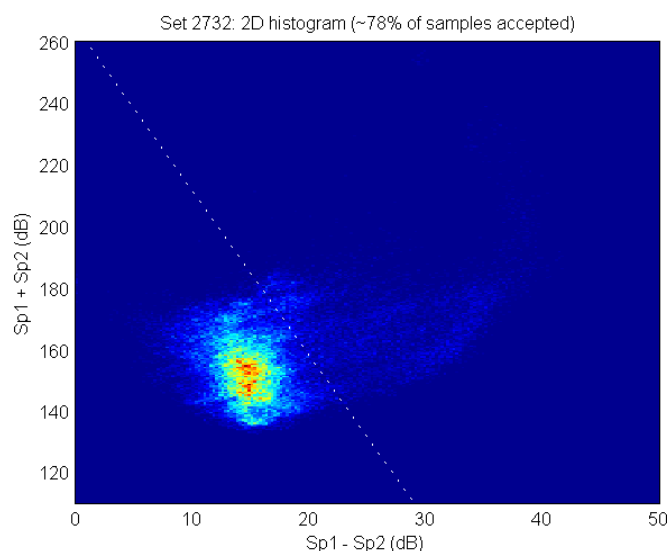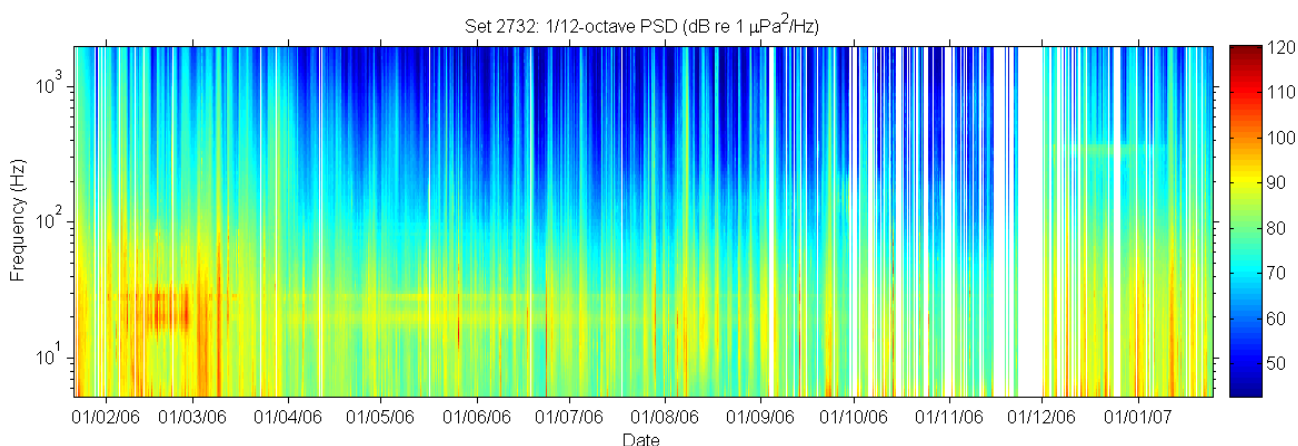Figure 53 shows the long-time average spectrogram of sea noise compiled from the 1/12-octave PSD of all recordings accepted for spectral analysis. The time periods containing noise artefacts are indicated by vertical white bands. Narrowband noise at slightly below 30 Hz is visible almost over the entire period of observation, with some short-term amplifications that can be seen from April to November as red spots in the spectrogram. This noise is formed by the so-called "spot-call" sounds from baleen whales which have not been identified yet (Gavrilov et al. 2015). Another, less prominent band of more intense noise is seen at about 20 Hz. This noise is formed by the third unit of the so-called Z-shaped calls

produced by many remote Antarctic blue whales (Gavrilov et al. 2012). Also slightly higher levels of noise can be seen at frequencies from about 20 Hz to 70 Hz from March to May. This noise is most likely formed be the songs sung by pygmy blue whales (*B. m. brevicauda)* of the south-eastern Indian Ocean population, in which the third harmonic of the most intense second unit is about 70 Hz (Gavrilov et al. 2011). The fundamental frequency of this unit, as well as frequency components of the other two units are not prominent in the spectrogram as they all are masked by background noise from other sources.

Figure 53   Long-time average spectrogram of sea noise calculated in 1/12-octaved bands for the entire period of measurements at location 1. The time periods containing noise artefacts are indicated by vertical white bands.
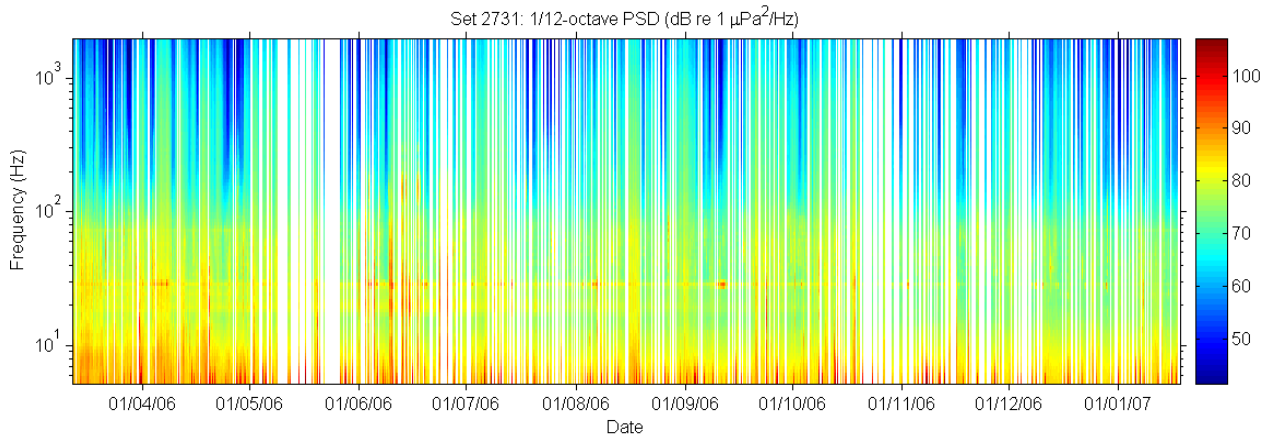

The 1/3 and 1/12-ocatve spectra of sea noise at different percentile values are shown in the left and right panels of Figure 54 respectively. The noise formed by the spot calls is the only spectral component clearly seen at all percentile levels. The contribution from Antarctic blue whale calls at about 20 Hz is noticeable only at lower percentile levels, as is that of the pygmy blue whale sounds making the noise spectrum nearly flat from 30 Hz to 70 Hz.

Figure 54   1/3-octave (left) and 1/12-octave (right) percentiles of spectral levels of ambient ocean noise measured at site 1 (shown in Figure 17).
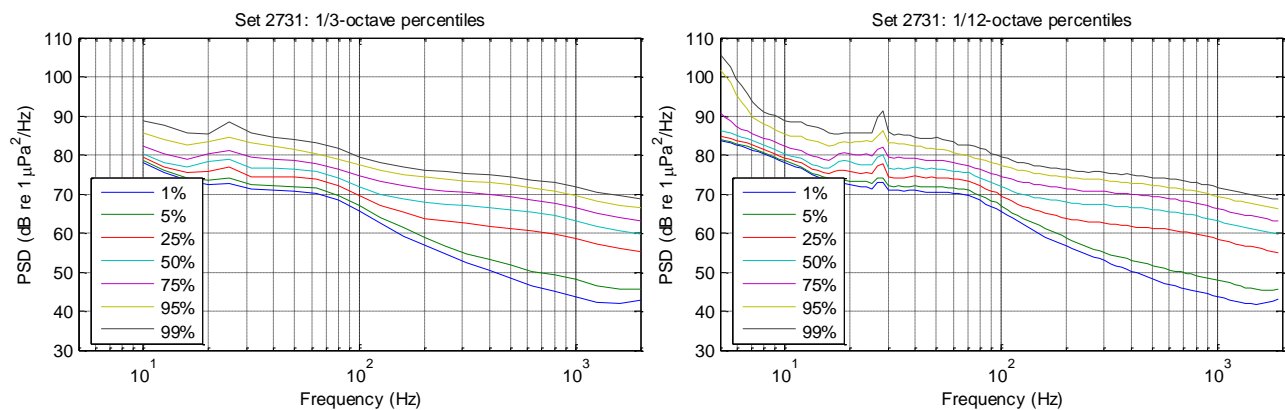
4.1.2.2   Dataset 2716 (Site 2)

The intensity and frequency of occurrence of low-frequency noise artefacts caused by mooring vibrations at site 2 were higher than those at the other two sites. This is most likely due to stronger underwater currents in the Antarctic Convergence zone. Moreover, the spectrum of this noise was broader than that at site 1 -in addition to more or less uniformly distributed noise from 5 to 20 Hz, mooring vibrations induced quasi-harmonic oscillations of sound pressure at about 30 Hz (Figure 55). For this reason, the transition frequency F_{trans} for this dataset (site 2) was changed to 40 Hz in the

artefact filtering algorithm. As in dataset 2731, the sections with noise artefacts can be distinguished by the tail toward higher values of Sp1-Sp2 in the 2-D histogram shown in Figure 56.

Figure 55   An example of long-time average spectrogram of sea noise recorded at site 2 (Figure 14) over 30 days in December-January (top panel). The bottom panels show the waveform (left) and spectrogram (right) of a 20-s section with low-frequency noise due to mooring vibrations.

Figure 56   2-D histogram of the number of recording sections in dataset 2716 (site 2) versus two parameters: Sp1-Sp2 and Sp1+Sp2 (F_{trans} = 40 Hz). The dotted line shows an empirically derived boundary between classes of sections with and without artefacts.
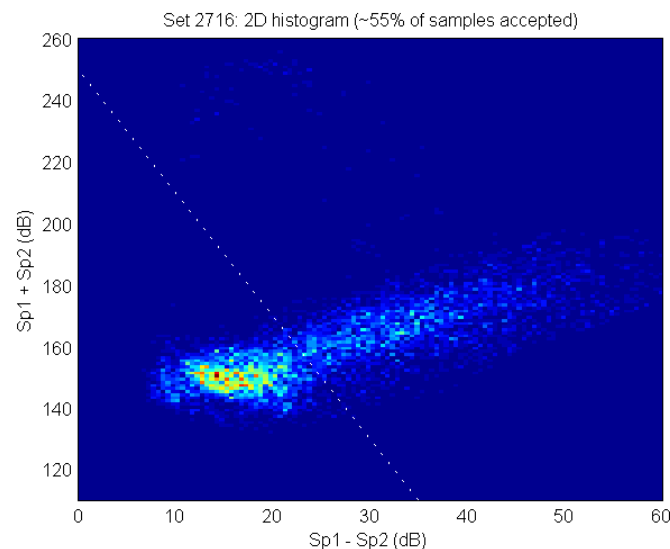
Moreover, relatively rare events of high-intensity broadband impulsive noise from the mooring banging can also be recognised in the 2-D histogram in Figure 56 by high levels of *Sp1+Sp2* (>200 dB) at relatively low levels of *Sp1- Sp2.*

The long-time average spectrogram of sea noise shown in Figure 57 demonstrates that there were several relatively long time periods when the level of artefact noise was too high to measure spectral levels of ambient noise at low frequencies. Despite these gaps in the PSD measurements, the noise from the chorus of Z-shaped calls from Antarctic blue whales at about 20 Hz and slightly below 30 Hz can be recognised in the long-term spectrogram from March to late October.

Figure 57   Long-time average spectrogram of sea noise calculated in 1/12-octaved bands for the entire period of measurements at site 2. The time periods containing noise artefacts are indicated by vertical white bands.
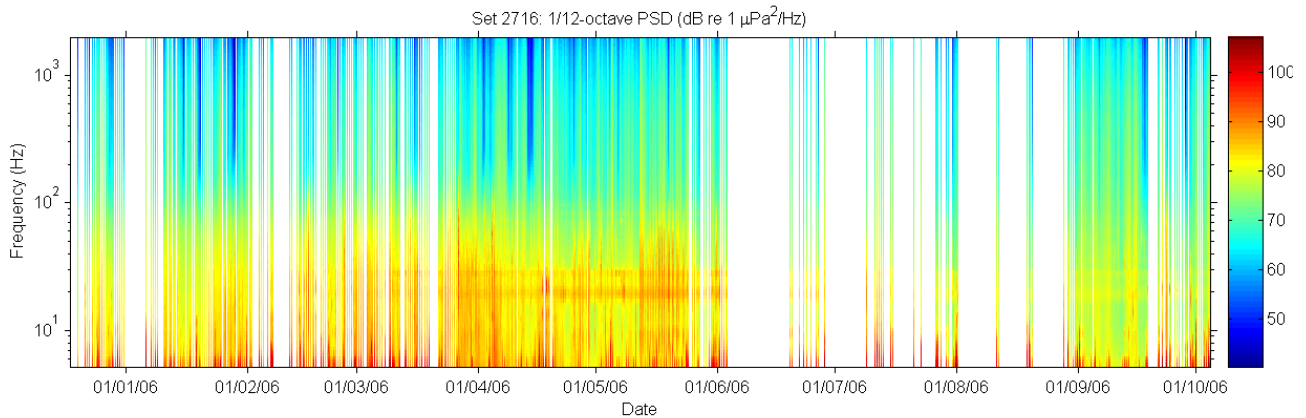
The contribution of this chorus to the ambient noise is also evident from the percentile plots of the spectral levels (Figure 58), especially in those of higher frequency resolution.

Figure 58   1/3-octave (left) and 1/12-octave (right) percentiles of spectral levels of ambient ocean noise measured at site 2 (shown in Figure 14).
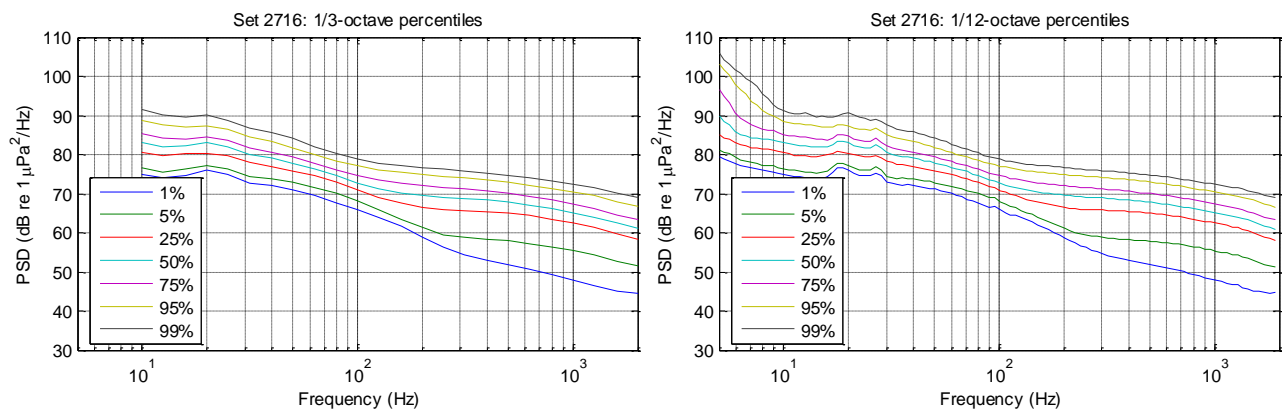
It is also important to notice that the noise levels increasing with the frequency decrease below 10 Hz at higher percentile values are partly caused by the noise artefacts of lower intensity which still remained in the data used for the spectral analysis after artefact filtering.

4.1.2.3   Dataset 2732 (Site 3)

The mooring system with the sound recorder deployed in Antarctica was least subject to vibrations, and the frequency band of the noise artefacts due to the mooring vibration was noticeably narrower than that at the other measurement sites. For this reason, the transition frequency F_{trans} for this dataset (site 3) was set to 10 Hz in the artefact filtering algorithm. However, the events of high-intensity broadband impulsive noise, which was most likely due to banging of mooring parts, were more frequent in this dataset. These impulsive noise artefacts can be recognised in a barely visible tail towards high values of $Sp1+Sp2$ at $Sp1-Sp2$ values of 30-40 dB in the 2-D histogram shown in Figure 59.

As a result of noise artefact filtering, nearly 80% of all 100-s recording sections were used to calculate the spectral levels of ocean ambient noise. The noise from mooring vibration was dominant for relatively long time periods only from mid to late November, as can be seen in Figure 60.

Figure 59   2-D histogram of the number of recording sections in dataset 2732 versus two parameters: Sp1-Sp2 and Sp1+Sp2 (F_{trans} = 10 Hz). The dotted line shows an empirically derived boundary between section classes with and without artefacts.

Figure 60   Long-time average spectrogram of sea noise calculated in 1/12-octaved bands for the entire period of measurements at site 3. The time periods containing noise artefacts are indicated by vertical white bands.

Three characteristic features can be distinguished in the long-time average spectrogram in Figure 60:

1. Intense broadband noise at about 15 to 30 Hz noticeable in February. This noise is formed by multiple calls from fin whales (*Balaenoptera physalus)*.
2. Chorus of Z-shaped calls from Antarctic blue whales visible at about 20 Hz and slightly below 30 Hz from February to July.
3. Relatively narrowband noise at 300-350 Hz visible from mid-December to early January. A detailed audio analysis of the noise recordings made during this time period revealed that this noise was most likely formed by multiple sounds from Antarctic seals. The particular seal species that made these sounds has not been identified yet, as different species of seals found in Antarctica produce similar sounds.

As the noise from the whale chorus was present only during the first half of the measurement time period and the seal sound was detected only during two months towards the end of observation, the spectral levels of ocean ambient noise at different percentile values were calculated separately for two time periods: from February to July and from August to January. The percentile plots of spectral levels are shown in Figure 61. The contribution of the above-mentioned biological sources of underwater sound to the ocean ambient noise spectra can be easily recognised in these plots, especially in those of higher frequency resolution.

Figure 61   1/3-octave (left panels) and 1/12-octave (right panels) percentiles of spectral levels of ambient ocean noise measured at site 3 (shown in Figure 17) in February-July (top panels) and August-January (bottom panels).
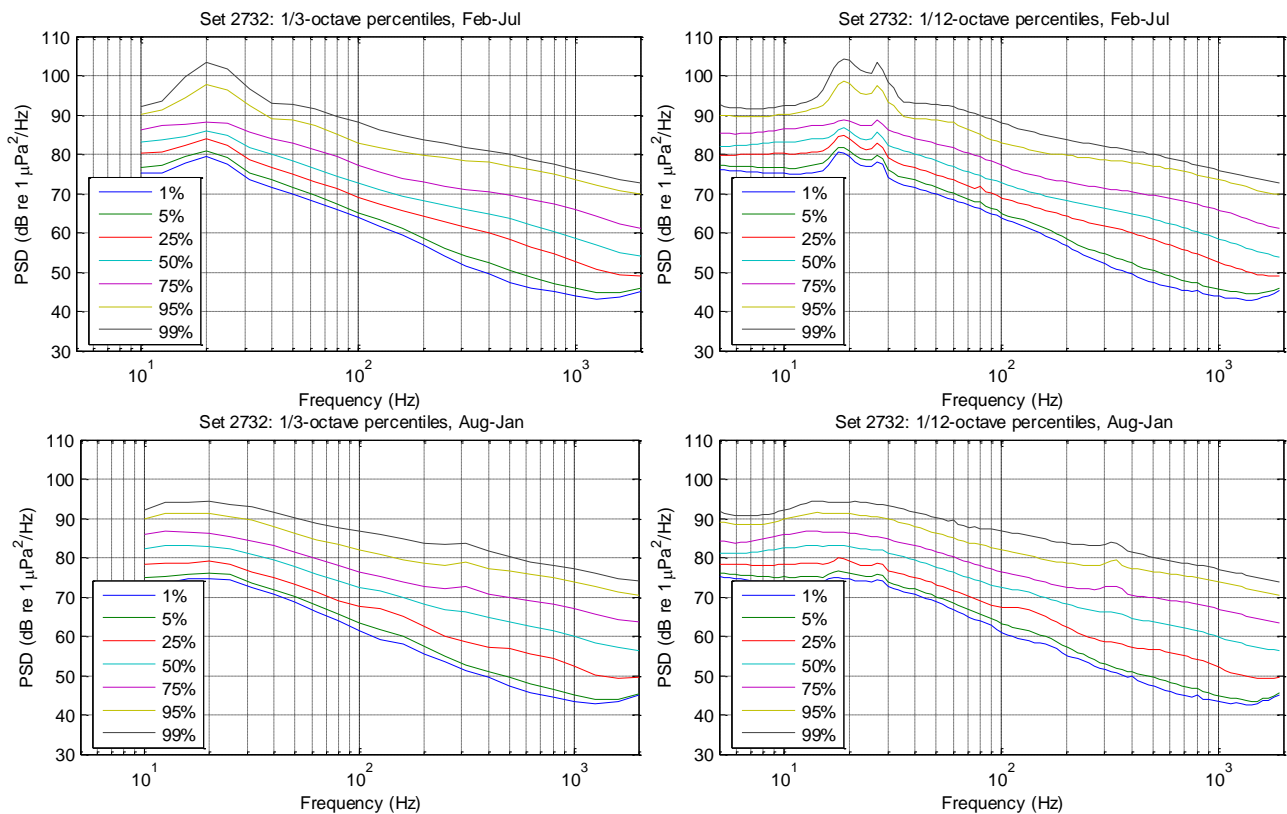
5 Assessment of the masking of animal vocalizations by airgun noise

5.1 Development of a psychophysical model

5.1.1 Signal detection by the auditory system

The ability of an animal to detect a signal in the presence of noise depends on the absolute sensitivity of its auditory system (summarized in an audiogram giving detection thresholds for narrowband signals across a range of sound frequencies), the frequency tuning characteristics of the system (to what resolution the auditory system can separate a sound into its individual frequency components) and the temporal processing characteristics of the system (auditory integration times) (Erbe et al. 2016).

For signals with a characteristic frequency and intensity pattern over time, a hearing system that searches for these patterns and thus make use of the combined time-frequency-intensity structure of a signal will be much more sensitive than a hearing system that only analyses the total energy accumulating within a time interval and frequency band. Terrestrial mammals and birds have been demonstrated to be capable of perceiving these combined frequency and intensity patterns over time (Feng and Ratnam, 2000). This has also been demonstrated for dolphins (Branstetter et al. 2016). The mere fact that Antarctic pinnipeds and baleen whales allocate considerable energy to the production of vocalizations with complex patterns and rely on the acoustic sense even more than most terrestrial mammals do, strongly suggests that Antarctic marine mammals can perceive frequency and intensity patterns over time as has been demonstrated for dolphins and terrestrial mammals (Edds-Walton, 1997).

The spectral and temporal characteristics of the masking noise affect the potential for and the degree of masking. E.g. time-varying noise can allow animals to detect signals during quieter parts of the noise. This phenomenon termed "dip listening" has been demonstrated in beluga whales (Erbe, 2008). Airgun noise is impulsive close to the source. Even at greater distances (> 1000 km) from the source, where pulses merge due to signal stretching caused by sound propagation, airgun noise is time-varying.

5.1.2 Discussion of existing receiver models

5.1.2.1 Leaky-integrator model developed in the preceding project (Siebert et al. 2014)

5.1.2.1.1 Description of the leaky integrator model developed in the preceding project (Siebert et al. 2014)

The receiver model of the earlier airgun project (Siebert et al. 2014) consisted of a leaky integrator model which integrated the received energy within the frequency band of the focal vocalization in a temporally lossy manner. The output of leaky integration is a measure for the energy in the focal frequency band over a sliding temporal window.

To decide whether detection of a focal vocalization is possible, the maximum output values of this integrator for background noise mixed with the vocalization were compared to the maximum output values of the same integrator for background noise in the presence of an airgun. It was postulated that detection is possible when the maximum output for the vocalization mixed with background noise is higher than the maximum output for airgun signals with background noise.

5.1.2.1.2 Fundamental shortcomings of the leaky integrator model developed in the preceding project (Siebert et al. 2014)

The leaky integrator model of the preceding project exclusively integrates the total energy accumulating within a certain time interval and frequency band without making use of characteristic frequency and intensity patterns over time. This is a shortcoming since marine mammals are likely to use these

patterns for signal detection as outlined above (section 5.1.1). Signal properties like characteristic frequency and intensity patterns over time are of high value for signal detection in the presence of interfering noise. As these signal properties are not taken into consideration by the leaky integrator model of the preceding project, it systematically underestimates detection performance and communication ranges while it overestimates masking for species that make use of characteristic frequency and intensity patterns and not just total accumulated energy in a frequency band.

The detection criterion postulates that for a detection the maximum output of the leaky integrator for vocalization and background noise needs to exceed the maximum output for background noise and airgun. This constitutes a very demanding criterion that results in very low communication ranges.

5.1.2.2 Power spectrum model (as reviewed in Erbe et al. 2016)

In contrast to the leaky integrator model developed in the earlier project (Siebert et al. 2014), the power spectrum model (Erbe et al. 2016) does not use leaky integration. Similar to the leaky integrator model of Siebert et al. (2014), the power spectrum model does not use the time structure for signal recognition, but, compares the level of an incoming vocalization (in dB re 1 μPa) within a certain frequency-band with the level of masking noise (in dB re 1 μPa^2 / Hz) within the same frequency band.

In the case of the power spectrum model, this comparison is achieved by assigning a narrowband received level to a received tonal narrow-band vocalization-signal. This level is then compared with the level of the assumed steady-state broadband masking noise while accounting for the integration within the auditory-filter-bandwidth through adding a corresponding critical-ratio-level to the noise.

However, this procedure implies 3 limitations, because of which it is not suited for the present study:

1. While a narrowband sound level aptly expresses the relevant power within the auditory filter band for a narrowband tonal signal, this is not the case for broadband or rapidly changing signals, where power or spectrum are non-constant or the power is distributed over a wider frequency-band. Only one of the vocalizations investigated in the present study (the blue whale z-call) can be considered narrow band. The spectrum of the Weddell seal long sound, the Weddell seal sound sequence and the killer whale multiharmonic sound are clearly broadband and extend over several filter bandwidths at every point in time. The spectrum of the vocalization of the fin whale call, rather short in comparison to the frequency, is also already somewhat broadened by this. Only segments of the extremely long vocalization of the blue whale z-call could be considered narrow-band.
2. The model depends on detailed knowledge of the specific auditory filterbank characteristics, i.e. knowledge on the auditory filter bandwidths of all filters that mimic the frequency resolution of the focal hearing system. For extending the critical ratio model to cases in which the masker is not broadband with a flat spectrum, the auditory filter bandwidth would have to be known. For studying non-constant signals or noise also auditory integration times would be necessary. This knowledge is not available for the studied species.

The model only applies to tonal signals and steady-state constant noise. It does not address masking of highly variable vocalization-signals by rapidly changing background-noise and does not address, how intermittent noise within the frequency-band of the vocalization could be differentiated from the vocalization. Since airgun noise is impulsive close to the source and still strongly time-varying at greater distances (> 1000 km) from the source, the central model assumption of a steady-state white noise masker does not hold for our study.

Note that the fundamental idea of the power spectrum model - the comparison of sound power of signal and noise within the same auditory filter band - is, however, also similarly implemented by the "band-pass leaky integrator" model for broadband signals and time-variant noise and unknown auditory filter bandwidth in a simpler manner. In band-pass leaky integrator models (such as Siebert et al. 2014), the sound power of the minimal frequency band comprising the vocalization is also calculated and

compared. The individual bandwidths of the individual auditory filter bands are unknown and are not included in this model. As a first approximation, the total frequency bandwidth of the vocalisation is used. This approach can be challenged, since most vocalizations are not extremely narrowband signals, but span several auditory filter bands. An advantage of the use of a leaky integrator for the detection of vocalizations against time-variable airgun interference signals is that time-variable aspects of signal and noise can be incorporated by the (lossy) integration of the sound power according to the time constant. This allows for the consideration of the extremely variable signal conditions in the case of complex vocalizations and airgun-noise, which is not possible with the "power spectrum" model.

5.1.2.3 Algorithms of signal detectors that make use of the time-frequency structure of the signal

Algorithms for receivers that make use of the time-frequency structure of the signal can be classified into phase sensitive or phase-insensitive receiver algorithms. A **phase-sensitive** fully-coherent cross-correlation-receiver that has detailed knowledge of the hidden signal compares the phase-accurate microstructure of a received signal with the pattern signal and integrates their match over time. The detection performance of this receiver decreases rapidly if the signal is altered (e.g. stretched) along the transmission path. The degree to which a phase perception of the sound is possible is uncertain in most hearing systems. Moreover, the variability of the emitted vocalizations examined leaves a phase-sensitive full-coherent cross-correlation-receiver unsuited for their detection in this study.

A spectrogram correlator is a **phase-insensitive** receiver which matches a spectral representation of the signal over time with a temporally limited pattern of the searched signal and evaluates their similarity over time. This principle can be implemented in various ways (different possible transformations and representations of the acoustic signal into the temporal-spectral plane, as well as different settings for the similarity evaluation and weighting).

In conclusion, the spectral intensity of a sound over time is similar to the sound in the mammalian cochlea at the beginning of the auditory pathway (which correspondingly permits a comparison of the spectral sequence of a signal over time with a search pattern in subsequent higher centres). Consequently, a spectrogram correlation receiver model should be well suited for simulating acoustic pattern recognition in mammals.

5.1.3 Development of a detection model on the basis of psychophysically plausible assumptions with subsequent standardized analysis on the basis of classic classification and detection theory

5.1.3.1 Psychophysical model

The psychophysics of the examined species (blue whale, fin whale, killer whale, Weddell seal) with respect to the exact mechanism of detection and recognition of conspecific vocalizations is mostly unknown. In order to achieve plausible estimates of detection and masking, assumptions thus have to be derived from knowledge on the psychophysics of other species.

<u>Assumptions of the model</u> (based on physics and general psychophysics in vertebrates, especially mammals and humans) are:

1. Mammals with complex social vocalizations exhibit characteristic sequences of frequency and intensity over time. They can therefore recognize spectral and intensity patterns over time for detection of conspecific vocalizations and, for this purpose, compare acoustic stimuli with a pattern of the expected spectral and intensity responses over time and thus evaluate their similarity.

   This is modelled with a phase-<u>in</u>sensitive spectrogram correlator, which functionally corresponds to the comparison of the stimulation pattern of the cochlear output over time with a comparison

pattern and thus is physiologically plausible. An evaluation of the similarity of an acoustic stimulus with the comparison pattern does not occur in the inner ear but subsequently in the brain. Thus, the evaluation of similarity is not only possible within the temporal integration time of an individual neuron but also over longer melody courses, such as is possible for humans, birds and other vertebrates, as for example for the recognition of bird songs (e.g. Marler, 1997).

The emphasis in this investigation was placed on the results of a receiver model on the basis of a phase-insensitive spectrogram correlator for the reasons outlined above. However, a receiver model on the basis of a band-pass signal leaky integrator was implemented additionally, to facilitate comparison of results.

2. The relation between the physical intensity Φ of an external acoustic stimulus and the intensity of its perception Ψ can be psychophysically approximated through a power function with an exponent E typical for the sense modality: $\Psi \sim \Phi^E$ (Schmidt et al. 2000). The exponent for the sense modality of hearing determined in extensive experiments (similar to the one of vision due to the extremely wide input intensity spectrum to be represented) is ~0.6 for sound amplitude A, and ~0.3 for sound intensity Φ ($\Phi \sim A^2$) (Schmidt et al. 2000).

$$\Psi \sim A^{0.6} \text{ or } \Psi \sim \Phi^{0.3}$$

To approximate psychophysical intensity perception, the spectrograms used in the spectrogram correlator (both input signals and search patterns) were scaled by this power function (and not logarithmically). Similarly, the leaky integrator takes the focal frequency band of the power density scaled spectrogram as input (for details on the implementation of the leaky integrator see section below and appendix 3).

3. Infinitesimally small stimulus differences, and corresponding arithmetic perception differences, are not sufficient for a reliable differentiation of two stimuli due to the measuring inaccuracy of a sensory system. In psychophysics, a stimulus difference threshold of approximately 1 dB is frequently assumed as a minimum criterion.

In our model, a perception difference is postulated for reliable differentiation of two cues that differ in intensity, which corresponds at least to a stimulus difference of 1 dB intensity difference (headroom). The exact magnitude of the headroom required physiologically or psychophysically, however, is not known. If a headroom of 1 dB should not be necessary for detection, it can be considered, alternatively, as a small amount of signal excess necessary for comfortable communication (compare Erbe et al. 2016). For comparison we additionally evaluated the psychophysical model when setting the headroom to 0 dB.

5.1.3.2 Estimation of communication ranges based on a statistical evaluation of the output of the psychophysical model

We aim at estimating communication ranges (i.e. maximal distances between conspecifics at which signal detection is possible with sufficient precision) for different environmental scenarios and different distances between the airgun and the receiving animal. A comparison of the communication ranges in the presence of airgun noise versus the ranges estimated with the same method in the absence of airgun sound then serves as a measure for the masking strength of airgun noise in the focal environmental scenario.

For each examined environmental scenario and distance of the receiving animal from an airgun, the noise and vocalization signals arriving at the receiver animal's ear were generated and fed into the psychophysical model (Figure 62). The communication range was then determined through an iterative procedure as follows. Nested intervals were used to determine the maximal vocalization transmission distance between the vocalizing animal and the receiving animal in which signal detection is possible with sufficient precision. Broadly speaking, the receiver model is challenged with sound samples in

which the propagated vocalization signal is either present or not. The precision of signal detection can then be evaluated as the proportion of correct classifications by a receiving animal as to whether or not a vocalization is present in a sound sample.

Both for the spectrogram correlator and the leaky integrator model, the evaluation of whether a sufficiently successful classification was possible in the focal scenario was performed according to standardized classification theory based on the statistics of correct classification of the receiver model within a limited decision-time-window. A sufficiently successful correct classification was defined as possible, if the area under the receiver operating characteristic curve (ROC AUC) exceeded 0.9. Thus, in this situation, it is possible to find a classification cut-off value for the output values of the receiver model (the maximum values of the matching function within the decision-window) for multiple phase shift combinations, which allows a decision with sufficient precision, if a vocalization is present or absent.

Figure 62   Schematic representation of the general setup of the psychophysical model. For every scenario the signal arriving at the animal's ear is modelled first (by mixing the propagated airgun and/or vocalization with ocean noise). Next the auditory system is modelled by a signal detector, that decides based on an adjustable threshold if a vocalization is present or not. For details on the signal detector see next chapter.
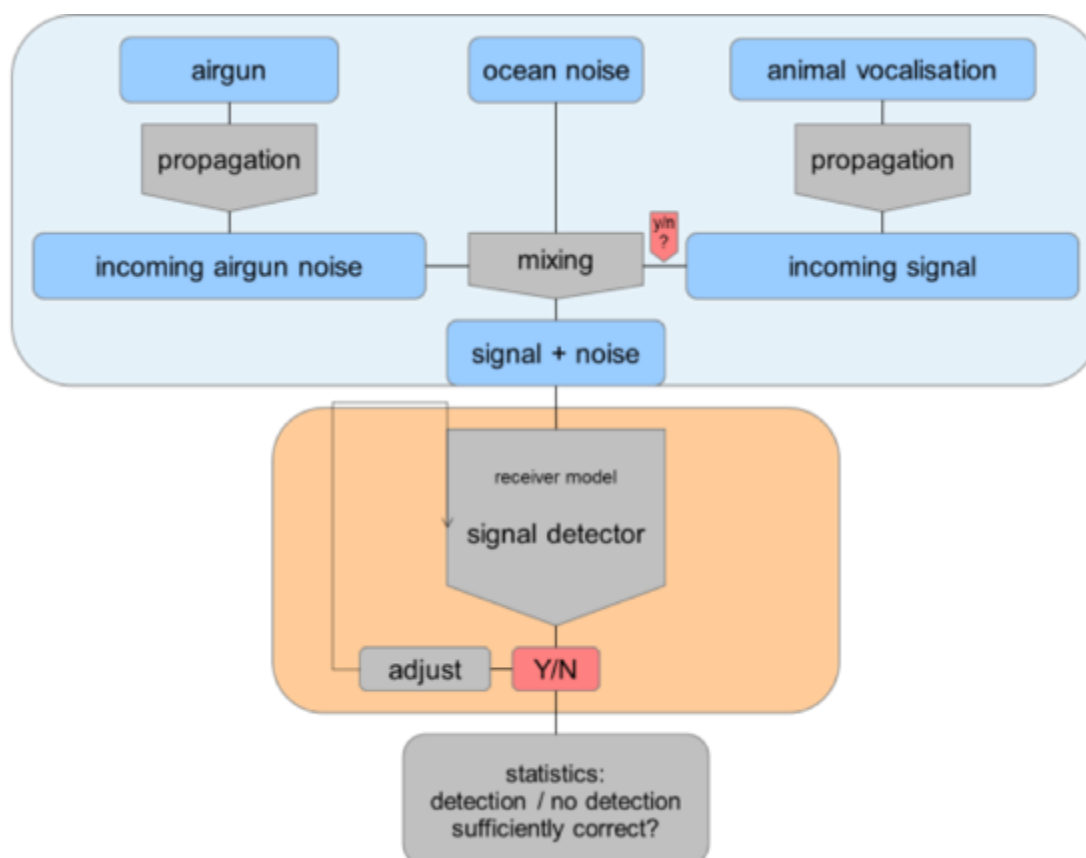
5.1.3.3   Details on the implementation of the spectrogram correlator receiver model

In detail, implementation of the spectrogram correlator receiver model (Figure 63) involved the following steps (a list of the numerical values of the model parameters can be found in appendix 3):

c)   The sampling rate of all input signals (noise, vocalization, airgun) was standardized to 200 Hz for blue whale as well as fin whale and 4,000 Hz for other vocalizations.

Figure 63   Details of the implementation of the spectrogram correlator receiver model. The bandpass filtered and rescaled (to mimic psychophysical intensity perception) spectrogram of the incoming signal is correlated with the corresponding vocalization search pattern. The output of the spectrogram correlation is fed into a leaky integrator and the peak value in the decision window is determined. The rational is that an animal decides if a vocalization is present or not by comparing the peak value to a detection threshold, that allows optimal classification. The statistical evaluation based on the ROC-AUC is the basis for the decision if classification of whether or not a vocalization is present is sufficiently successful to allow communication.
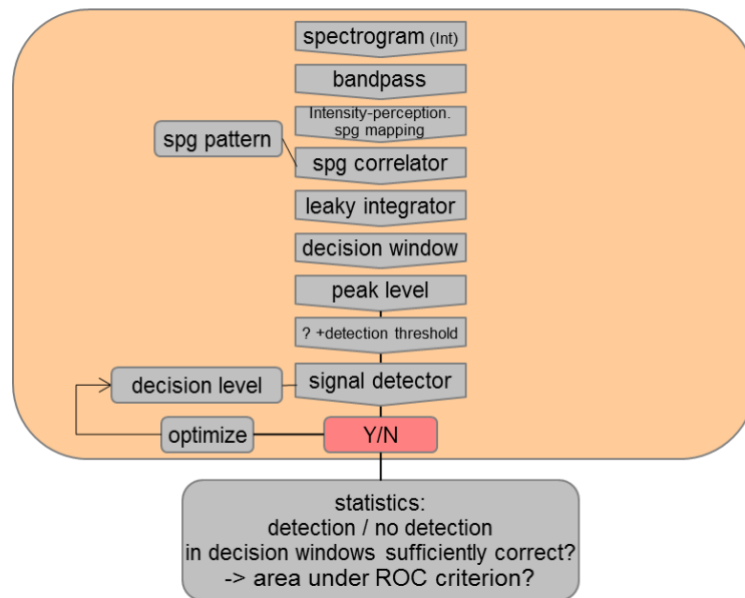
d) The vocalization spectrogram search patterns were generated. Depending on availability, one to fifty mutually corresponding vocalizations of a vocalization type of a species were brought to an optimal temporal synchronization through cross-correlation, and their power density spectrograms were compiled. They were subsequently convoluted in two dimensions with a vocalization-specific smoothing function to make the matching less specific thereby accounting for a certain variability of the vocalizations. These spectrograms were attenuated according to a vocalization-adjusted bandpass filter with 12 dB / octave from the filter limits. Then, the power density spectrograms were rescaled according to the psychophysical perception function $\Psi = c * \Phi^{0.3}$ for representation of the spectral intensity perception. Finally, the spectrograms of the available number of sample vocalizations were averaged.

The synchronized, smoothed, bandpass-filtered, intensity perception-approximated, scaled and averaged spectrograms were saved as correlation patterns for the similarly generated (see next step) perception spectrograms of the signals arriving at the receiver animal.

e) Next, the input signals were prepared. This involved

- the generation of the transmitted airgun signals according to the transmission scenario and the repetition rate of one airgun signal per 15 seconds,
- the generation of the transmitted vocalization at the test distance according to the transmission scenario and the repetition rate of the vocalization (if available), or using the airgun repetition rate for shorter individual vocalizations (this results in modelling the detection of a single vocalization) and

- selection of recordings of incoming background noise of the ocean (for low recording artefacts such as anchor chain noise).

f) Power density scaled spectrograms were generated over the cycle length of the airgun signals and vocalization signals. (For exclusion of boundary effects of the spectrograms, adjacent cycles were included in calculation and later cut of.) Additionally, a long-term spectrogram of ocean noise of at least the ten-fold length of the longer cycle of airgun and/or vocalization was generated.

g) Spectrograms of the signal that arrives at the listener's ear were calculated by overlaying up to three components (airgun, ocean noise and vocalization). For each scenario, a representative sample of spectrograms was calculated using different phase shifts between the components. In particular: **Overlay and summation** in a time window of over the double length of the detection time window for the investigated vocalization of subsequent cycles of each of the three overlaid cyclic component spectrograms of airgun, ocean noise and vocalization in three-dimensionally varied phase shifts of the three components. The numbers (l, m, n) of the respective phase shifts (airgun phase, ocean noise phase and vocalization phase) of the three components are chosen prime to each other (such as e.g. 5, 4 and 7), so that l*m*n actually different phase overlays of the three components falling equidistantly in the corresponding cycles are overlayed in the second detection time window. The total length of the overlay time window is chosen as extended by the length of the correlation sample spectrogram, so that a completely valid correlation is possible with a correlation function of the mixed spectrogram with the pattern spectrogram during the second detection window over its entire length.

h) The mixed power density spectrograms obtained in e) were treated in the same way as the search pattern in b). This involved the application of the bandpass corresponding to the vocalization and intensity scaling of the power density spectrogram according to the psychophysical perception function $\Psi = c \cdot \Phi^{0.3}$ (see step b).

We used the power function $\Psi = c \cdot \Phi^{0.3}$ for rescaling the physical intensity Φ to a perception intensity Ψ in order to approximate intensity perception. Other common intensity scalings of spectrograms (namely logarithmic scaling and linear power density scaling) would produce artefacts when correlating the search pattern with the spectrogram of the incoming signal to obtain a so-called similarity function (see step g).

With *logarithmic scaling* of the spectrograms small changes at low intensities result in huge amplitudes or even large negative values of the logarithmically scaled function. Infinitesimally small (not at all perceivable) intensity differences at low intensities will therefore have a pronounced influence on the correlation function applied to the logarithmic values. In the high intensity range only very large intensity differences would have an impact of a similar magnitude on the correlation function. Thus, a logarithmic scaling is unsuitable for evaluating similarity between the search pattern and the spectrogram of the incoming signal using a correlation function.

A *linear power density scaling* does not correspond in any manner to the relative intensity perception of different intensities over a perceived total intensity range of many decimal powers. Through such scaling only the highest intensities would be relevant and have significance for a calculated similarity function, while all low intensities would have almost no effect. This does not correspond to the intensity perception, which, in wide areas can be better approximated through a logarithmic function, or in still wider areas even better through a power function (Schmidt et al. 2000).

In summary the scaling of spectrograms according to the psychophysical power function $\Psi = c \cdot \Phi^{0.3}$ provides a sound approximation of the intensity perception, while also circumventing the otherwise almost insolvable problems of other scalings.

i) The two-dimensional correlation of the psychophysically scaled spectrograms of the incoming mixed signal in the time window and of the search pattern (as generated in step b) was calculated. This resulted in a similarity function over the duration of the incoming signal in the time window with the search pattern.

j) A leaky integrator was applied to the similarity function (obtained in step g). The resulting smoothed detection function closely resembles the primary similarity function. It is, however, somewhat more tolerant in cases in which the similarity function does not cumulate in a distinct point in time but distributes the pattern match a little longer over time. An example in which this can occur is when the transmitted signal is altered and stretched along the transmission path.

In the psychophysical model presented here, this detection function measures the similarity of the vocalization pattern with the presently incoming acoustic signal, or how probable the current presence of a vocalization over the time of the incoming signal is.

k) Extraction of the maximum value of the detection function within the detection window within the total time window, i.e. a length of the detection window beginning at a duration of the detection window after the start of the total time window. The integration time of the leaky integrator corresponds at most to the vocalization duration. The detection window, on the other hand, in each case is noticeably longer than the vocalization. Thus, the preparation of the detection window ensures that the function generated by a leaky integrator is continuously valid within the detection window and corresponds to a function which would result from a continuous signal analysis. Sound events which occurred before the total time window are negligible for the detection function and leaky integrator within the detection window.

l) The maximum values of the respective detection function are determined in the detection window for all tested phase combinations of possible overlays of the input components.

Furthermore, all maximum values of the detection functions are determined in the corresponding manner for comparison, in which ocean noise and airgun signals are mixed with corresponding phase shifting, but the vocalization signal is absent.

The result is a set of maximum detection values for multiple different possible overlays within the detection window of attenuated airgun signal, ocean noise and attenuated vocalization, as well as a set of maximum detection values of possible overlays in absence of the airgun.

m) In the case that a stimulus difference threshold of 1 dB is postulated for a successful detection, the maximum values of the detection functions, in absence of the vocalization, are increased in this step by the factor that corresponds to a stimulus increase of 1 dB.

For a psychophysical exponent of the stimulus intensity of 0.3 this corresponds to a factor of $(10^{(1 \text{ dB} / 10 \text{ dB})})^{0.3} = 1.0715$. This corresponds to the increase of the amplitude of the entire incoming signal without vocalization by 1 dB.

In the event that no stimulus difference threshold was postulated, no modification of the values is done.

The resulting sets of maximum detection function values for different overlay possibilities with presence or absence of a vocalization now serve as a basis for the subsequent classification analysis that determines if the receiver animals' decisions on whether or not a vocalization is present can be made with sufficient precision.

5.1.3.4 Details on the statistical evaluation of the output of the psychophysical model

Standardized classification analysis was used to determine if decisions on whether or not a vocalization is present can be made with sufficient precision. It takes the maximum values of the detection functions in the absence and presence of vocalizations as input.

On the basis of the maximum values of the detection functions in the presence or absence of vocalizations, a standardized receiver operating characteristic curve is created, which indicates for all possible choices of a classifier (cut-off values of the maximum values for the decision on whether or not the presence of a vocalization is assumed) the ratio of the correct and incorrect decisions for the cases with presence and absence of a vocalization.

Based on Branstetter et al. (2016) we assumed that detection of vocalizations was sufficiently precise to allow communication if the area under the ROC (in short: ROC AUC) exceeded 0.9.

5.1.3.5 Iterative determination of the maximal possible communication distance in an environmental scenario

For a given distance between sender and receiver animal standard classification theory allowed us to infer if communication is possible (see 5.1.3.3). In order to determine the maximum distance between sender and receiver animal up to which communication is possible (i.e. the upper limit of the communication range) a nested interval approach was used.

The iteration was performed over the distances in the range of 10 m to 5,000 km on a logarithmic scale. The distance steps used in each decade were [1, 1.2, 1.4, 1.6, ..., 4.8, 5, 6, 7, 8, 9]. In total, a maximum of 150 test transmission distances were thus available for each scenario. These were searched according to the method of interval bisection at the distances on a logarithmic scale to determine the maximum successful communication distance. This method assumes that the communication success diminishes (for the most part) monotonically with increasing communication distance between the animals. This assumption proved later to not always be correct within the provided complex transfer functions for the vocalizations.

5.1.3.6 Details on the implementation of the leaky integrator receiver model

For comparison of the results with the communication ranges resulting on the basis of a simpler receiver model on the basis of a bandpass leaky integrator, the communication ranges were additionally calculated on the same data basis with a simplified model of a leaky integrator.

Figure 64   Details of the implementation of the leaky integrator receiver model. Here the bandpass-filtered signal power over time is fed into a leaky integrator. Downstream steps are analogous to the spectrogram correlation receiver model.
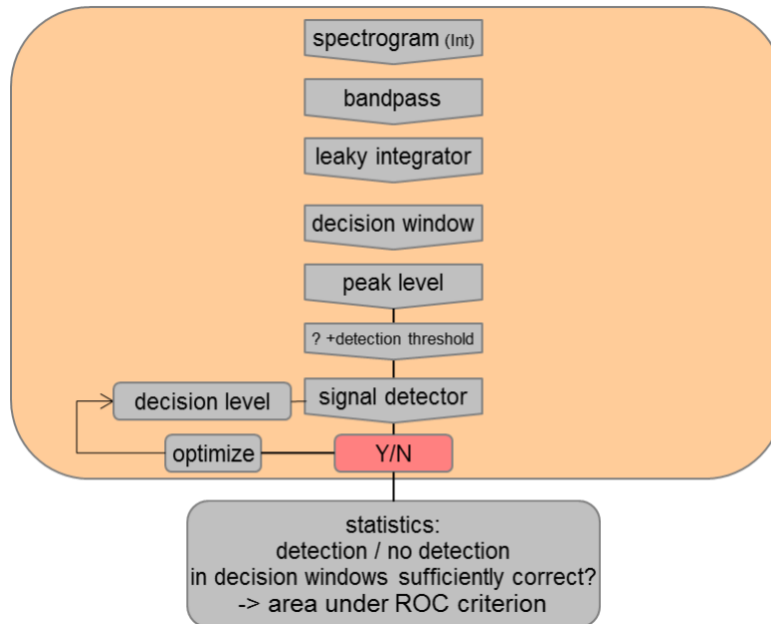
Most steps in the implementation of the bandpass leaky integrator (Figure 64) corresponded exactly to the described implementation of the spectrogram correlator. Solely the steps f) and g) of the above description of the spectrogram correlator, which comprise the application of the psychophysical spectrogram scaling and the spectrogram correlation, were replaced by simpler steps, so that the respective bandpass-filtered signal power over time (determined from the vocalization-corresponding frequency band of the spectrogram) is the similarity function over time that serves as input into the leaky integrator in step h).

In detail the steps f) + g) of the above description of the spectrogram correlator for implementation of the simpler bandpass leaky integrator are replaced by:

f) + g*) The summarized power density spectrogram of the phase-overlaid components (attenuated airgun, attenuated vocalization and ocean noise) is integrated over the frequencies within a frequency band adjusted to the vocalization (with a slope of -12 dB/octave beyond the limiting frequencies), which results in the complete energy content within a time slice of the spectrogram which corresponds to the total power of the signal in said frequency band at the sampling points of the spectrogram. Because the sampling points of the spectrogram, in any case, are located more closely by magnitudes than the time constant of the leaky integrator in the subsequent step h), its output is not significantly influenced by the somewhat coarser time sampling of the spectrogram in comparison to the power determination for the integration from the primary signal.

The total power within the vocalization-corresponding frequency band determined from the spectrogram is passed on as a similarity function to a leaky integrator that can be configured differently with different time constants, as needed, in step h).

5.1.3.7   Comparison of the leaky integrator model implemented in this project with that of the preceding project (Siebert et al. 2014)

The receiver model of the preceding project corresponds largely to the simplified leaky integrator also used here, except for the fact that signal power in the previous project was inferred directly from the primary signal instead of from the spectrograms. Due to the additivity of the spectral energy of a Fourier transformation, as well as due to the much longer time constants of the leaky integrator compared to

the sampling rates of the spectrograms, the fact that signal power was directly inferred from the primary signal in Siebert et al. (2014) whereas it is inferred from the spectrograms in the current project should have no influence on model predictions.

The determination of the detection success and ranges, however, is fundamentally different. In the leaky integrator model of Siebert et al. (2014) the maximum levels of the leaky integrator output of vocalization and interference noise were analysed and compared (in the alternative analysis, only over a certain time slice), and it is postulated on the basis of this comparison whether communication is possible or not. The current project ("spectrogram correlator" model as well as the leaky integrator model implemented in this project) uses a standardized classification analysis on the basis of the statistical success rate of decisions which are based on time-limited decision time windows on similarity functions with a search pattern simulating psychophysics. In the case of the leaky integrator implemented in this project, the search pattern corresponds to the energy content, within a time and frequency window corresponding to the vocalization. In the case of the spectrogram correlator, the search pattern is an averaged and smoothed psychophysically scaled spectrogram.

5.1.4 Input data and examined scenarios

5.1.4.1 Overview over the examined scenarios

For each of the considered scenarios (defined by the vocalization type, the distance of the receiver animal from the airgun, the sound transmission models for vocalization and airgun transmission, the sender and receiver depths and the ocean noise situation) the communication range between two animals was determined.

The scenarios differed from one another regarding the following characteristics:

1. Vocalization types:

    ► Blue whale: Z-call;
    ► Fin whale call;
    ► Killer whale: multi-harmonic call;
    ► Weddell seal: long sound;
    ► Weddell seal: sound sequence

2. Transmission scenarios of the airgun

    a) Transmission by geometric propagation (spherical spreading); ocean water absorption according to Ainslie & McColm (1998)
    b) Transmission by convolution with transfer functions, absorption according to Thorp (1965).

    Transfer function scenarios for airgun:
    ► Sender depth: 5 m
    ► Receiver depths: 10 m, 50 m, or 200 m
    ► Water depths: 500 m, 4,000 m.

3. Transmission scenario of the vocalization

    a) Transmission by geometric propagation (spherical spreading); ocean water absorption according to Ainslie & McColm (1998)
    b) Transmission by convolution with transfer functions, absorption according to Thorp (1965).

    Transfer function scenarios for blue whale and fin whale (low-frequency vocalizations):
    Identical transfer functions as for airgun with

- ► Sender depths: 5 m, 50 m
- ► Receiver depths: 10 m, 50 m, or 200 m
- ► Water depths: 500 m, 4,000 m.

Transfer function scenarios for killer whale and Weddell seal (broadband vocalizations):

Broadband transfer functions with

- ► Sender depths: 5 m, 50 m
- ► Receiver depths: 10 m, 50 m, or 200 m
- ► Water depth: 500 m.

4. Broadband analysis and, additionally for broadband vocalizations, high-pass analysis: For the three broadband vocalizations, in addition to the range determination from using the entire vocalization frequency band, additionally the range was determined using only the high-frequency band above the airgun frequencies (high pass 500 Hz)
5. Receiver model: spectrogram correlator or leaky integrator
6. Perception difference threshold and/or postulated headroom: 1 dB perception difference threshold (for comparison also models with 0 dB headroom were implemented)

5.1.4.2 Sound transmission models

For sound transmission of airgun noise and vocalizations, two different transmission principles were tested.

1. Transmission of the source signal according to an attenuation through geometric spreading and sound attenuation by ocean water according to a numerical attenuation model (Ainslie, McColm). In this sound transmission model, only the propagation geometry of **spherical propagation** was considered. (Transmission distances: 10 m - 10,000 km)
2. Transmission of the sound events according to the numerical propagation model developed in chapter 3, which each generates a modelled transfer function of a Dirac pulse for different environmental scenarios (sender depth, receiver depth, water depth, transmission distance), which is used to calculate the signal received by the receiver after transmission, by convolution with the sent signal. As outlined in chapter 3 frequency-dependent absorption of sound in sea water was calculated according to Thorp (1965).

The following transmission scenarios were considered:

Transfer function were calculated for two sender depths (5 m and 50 m) and three receiver depths (10 m, 50 m, 200 m) for each of the following **environmental settings**.

a) Water depth 500 m, transmission distances 100 m - 3,600 km, frequencies up to a maximum of 375 Hz
b) Water depth 500 m, transmission distances 10 m -100 km, frequencies up to a maximum of 1,500 Hz
c) Water depth 4,000 m, transmission distances 10 m - 2,600 km, frequencies up to a maximum of 375 Hz

In total, 19 transmission scenarios were used:

- ► spherical propagation
- ►   two vocalization depths, each with three receiver depths and for each of the three scenarios a), b), and c) as described above.

In each distance decade distance increments of [0.10, 0.12, ... 0.48, 0.5, 0.6, 0.7, 0.8, 0.9] were calculated and used for inferring received vocalization signals in the iterations.

As to distances from the airgun source, the distance increments [1, 2, 5] were tested from 100 m to 2,000 km in each decade. Additionally, the absence of airgun noise (~ infinite airgun distance) was examined for comparison.

The **distances of the transfer functions** calculated in chapter 3 indicate **horizontal distances along the water surface**. For consideration of the diagonal direct-transmission distance, the sender depth and the receiver depths must still additionally be considered. This has to be taken into account in particular for very short transmission distances if sender and receiver depth differ considerably.

The distances of the spherical propagation calculated for comparison indicate the direct transmission distance.

5.1.4.3   Source signal of the airgun

The airgun signal used was provided by DW-SC and corresponds to the configuration 8G+B (8 Gun + Bolt). This source pulse yields (arithmetically) a source level of approximately 250 dB @ 1m (peak) (chapter 3.4).

5.1.4.4   Ocean background noise

Six scenarios of different background ocean noise were tested:

1. No noise: comparison of the situation in absence of any background noise
2. 80 dB noise: 80 dB RMS. The noise scenario used in the preceding report (Siebert et al. 2014) for comparison
3. Medium noise -> 90 dB: 90 dB RMS. Medium noise (5.) attenuated by 12 dB for comparison (moderate low-frequency noise)
4. Low noise: 94 dB RMS. Observe, however, that recordings have a very intensive low-frequency component ~20 Hz, that make this recording very similar to the medium noise scenario in the frequency range around 20 Hz.
5. Medium noise: 102 dB RMS.
6. High noise: 112 dB RMS.

Noise recordings representing situations 4.) - 6.) were collected in the Antarctic Ocean and were provided by C. Erbe, Curtin University. For our study, dominant vocalizations in the recordings were removed manually, since they would invalidate our detection analysis of artificially superpositioned vocalizations (detection of superpositioned vocalizations which are weaker than the vocalizations already contained in the recordings would be impossible).

Noise situation 3 was artificially generated arithmetically from situation 5 by attenuation by 12 dB, so that results for a noise scenario with a weaker low-frequency component could be obtained.

Noise situation 2 corresponds to the noise recording and the assumed noise level used in the preceding project ("leaky integrator" model).

In noise situation 1, the noise corresponds to a constant zero signal, thus absence of any background noise.

5.1.4.5   Examined vocalizations

1. Blue whale: Z call (Samaran et al. 2010), SL: 180 dB

Figure 65   Spectrogram of the blue whale z-call.
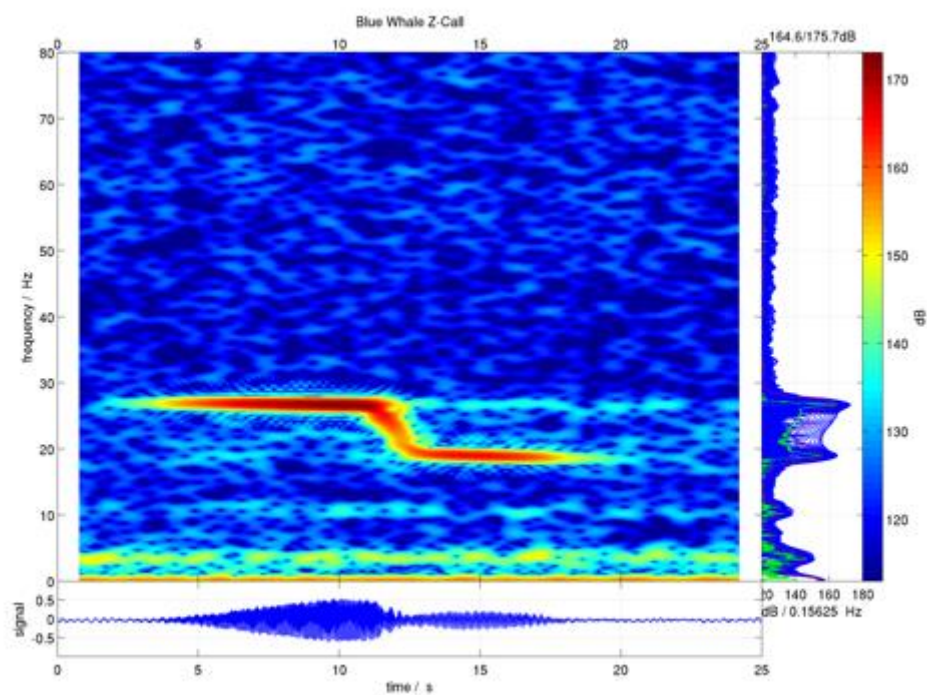
2. Fin whale (Sirovic et al. 2007), SL: 189 dB

Figure 66   Spectrogram of the fin whale 20 Hz call.
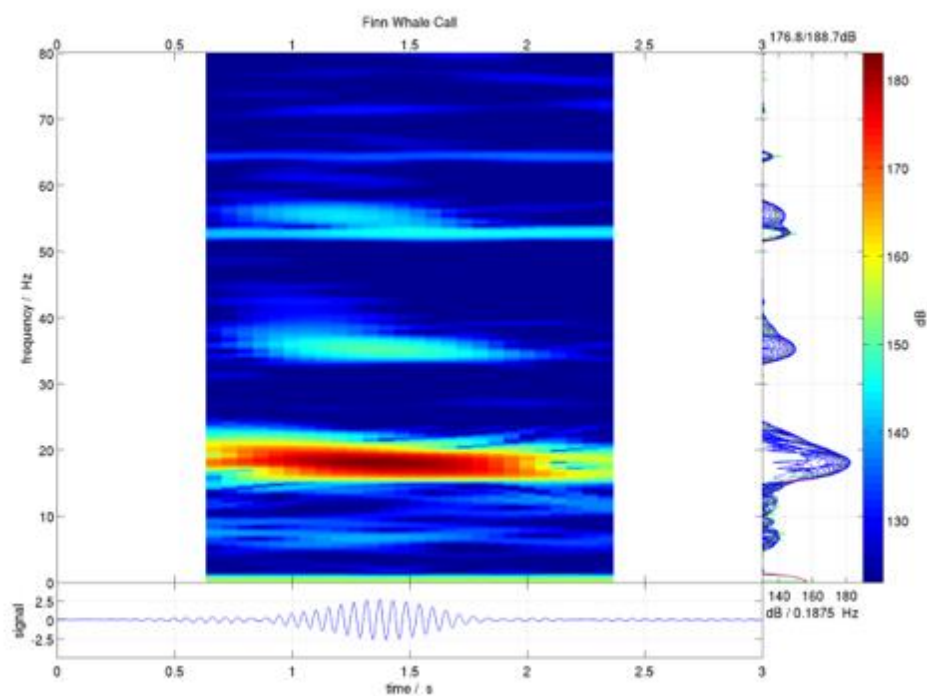
3. Killer whale: multiharmonic call

Figure 67   Spectrogram of the killer whale multiharmonic call.
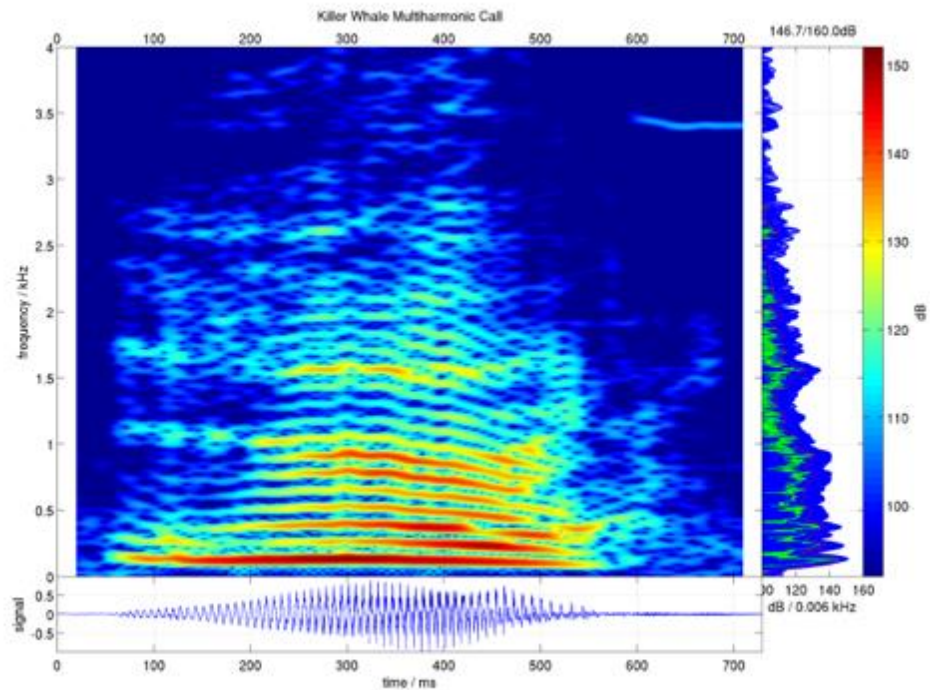
4. Killer whale: click with phase duration of the main oscillation of approximately 40 μsec
    (corresponds to 25 kHz)

Figure 68   Spectrogram of the killer whale click
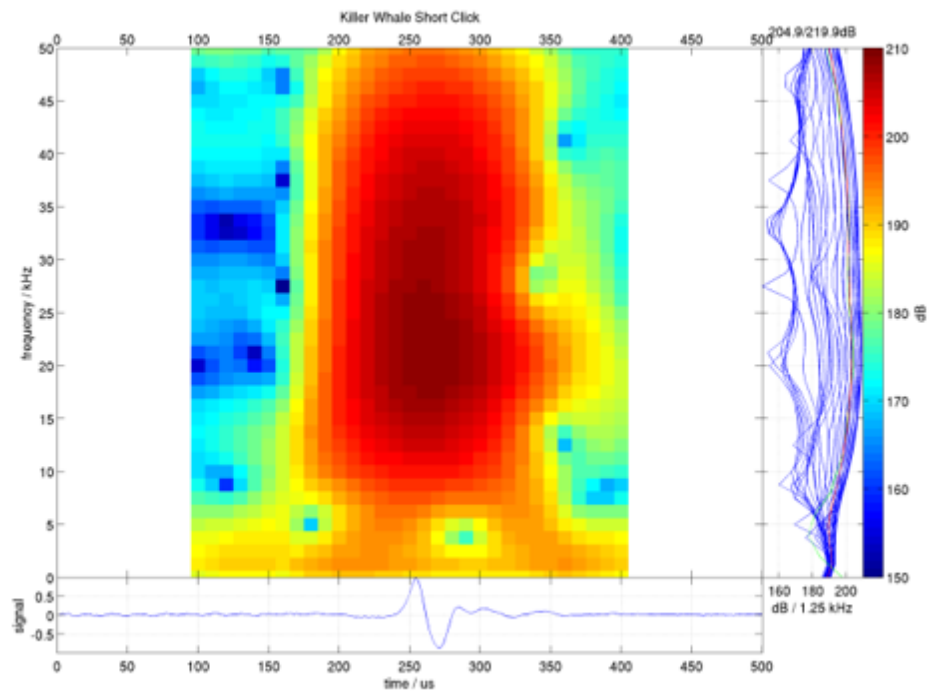
Longest time window of all sound events which could be associated with the vocalization (including possible transmission artefacts) was approximately 100 μsec (phase duration corresponds to approximately 10 kHz)

Minimum frequency that can be attributed to this vocalization from the existing recordings: >5,000 Hz

The energy spectral density of airgun source signals is maximal at low frequencies (approx. 10 Hz). Since energy is concentrated in the low frequency part of the airgun source signal and absorption by sea water increases with frequency, the energy spectral density of airgun signals rapidly decays for frequencies exceeding approx. 500 Hz.

Maximum frequency of the ocean noise recordings (sample rate 4 kHz) (and thus upper limit of these examinations): 2,000 Hz

Maximum frequency treatable by the transfer functions: 1,500 Hz.

All relevant frequencies of this vocalization type are far above the maximum frequencies of the airgun and above the maximum frequencies of the available ocean noise recordings. An analysis is neither possible nor meaningful because there is no overlap of the frequency ranges.

In psychophysical models that assume an independence of the sound perception above 5 kHz from sound events below 500 Hz, no masking by airguns can occur.

5. Weddell seal: low-frequency downward-sloped sound with a duration of approximately 4.5 s (Thomas et al. 1983), SL: 179 dB

Figure 69   Spectrogram of the Weddell seal long call.
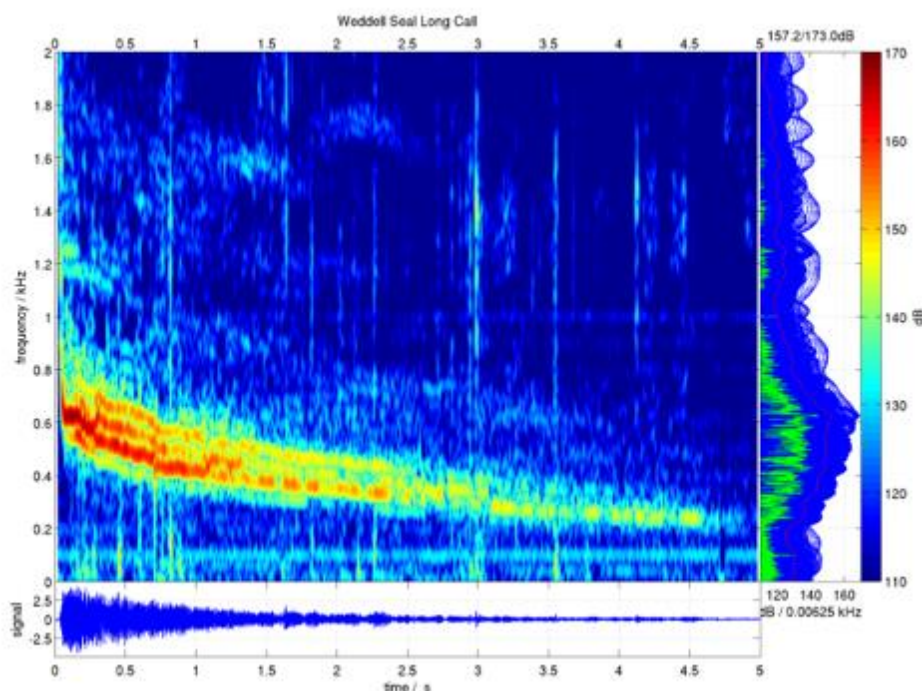
6. Weddell seal: low-frequency downward-sloped sound sequence (call train) with a duration of approximately 5 s (Thomas et al. 1983), SL: 179 dB

Figure 70   Spectrogram of the Weddell seal call train.
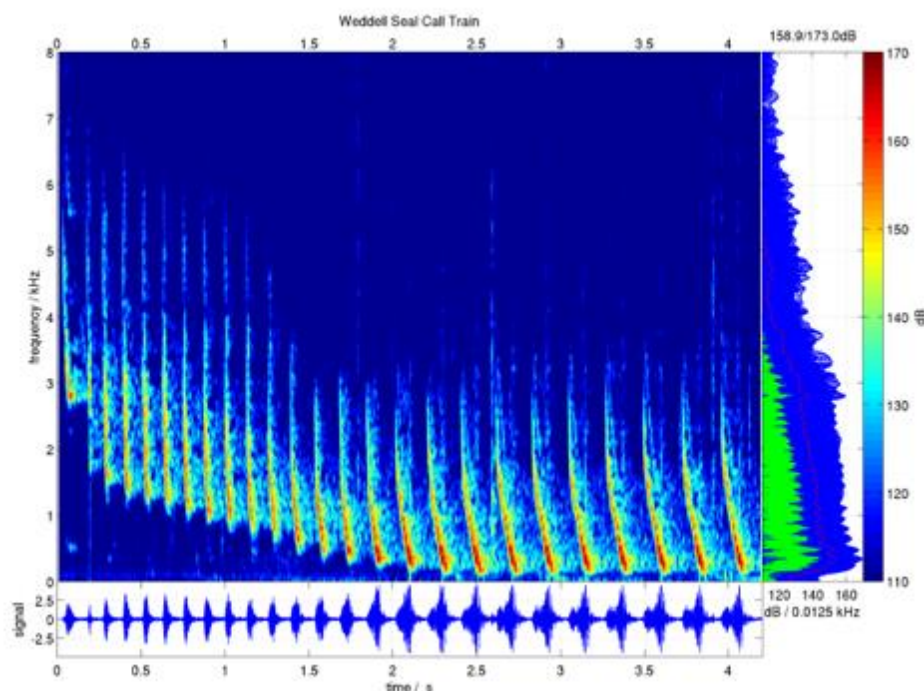
5.2   Presentation and discussion of the estimated communication ranges

Quantitative predictions of communication ranges depend on the vocalisation, environmental conditions (natural background noise and sound propagation conditions / assumptions) and the psychophysical model (spectrogram correlator model or bandpass leaky integrator model). This chapter closes (see chapter 5.2.11) with quantitative predictions for the different vocalizations in the most relevant models (i.e. most relevant water depths, sender and receiver depths; sound propagation according to the numerical model developed and verified by measurements in chapter 3; a headroom of 1 dB in the psychophysical models). Moreover, quantitative results for all modelled scenarios are available in appendix 9.1. We start our presentation of the predicted communication ranges by a qualitative description of the general phenomena we observe as the receiver animal moves away from the airgun location (5.2.1). We then discuss the effects of different sound propagation models (the numerical propagation model developed in chapter 3 versus spherical spreading) and of different sender and receiver animal depths as well as of different water depths. Next we compare the output of different psychophysical models (spectrogram correlator model versus bandpass leaky integrator model) and discuss predictions for communication ranges of broadband vocalizations, whose frequency range only partially overlaps with the airgun frequency range. As described above we close with the quantitative predictions for the different vocalizations in the most relevant models.

5.2.1   Qualitative description of general phenomena

Estimated communication ranges were plotted against the distance of the receiver animal from the airgun (up to an infinite distance between receiver animal and airgun, i.e. absence of airgun noise) for different ocean noise levels (represented by different colours in the diagrams). Broadly speaking three areas of different behaviour of the functions can frequently be recognized. This is especially clear in the scenarios in which airgun and vocalization were spherically attenuated (Figure 71).

1. For **small distances** between receiver animal and airgun, the interference and limitation of the communication distances through the <u>airgun is by far dominant</u> in comparison to the limitation

through ocean noise. The communication distances are thus almost exclusively dependent on the distance to the airgun but mostly independent of ocean noise. The curves for the different ocean noises are very close together and increase with the distance from the airgun.

2. For **intermediate distances** between receiver animal and airgun the communication ranges are dependent on <u>both, ocean noise</u> (the curves run at different heights) <u>and the distance to the airgun</u> (they increase with increasing distance from the airgun).

Figure 71   Communication ranges of blue whales as estimated based on the <u>spectrogram correlation receiver model (**a**)</u> and the <u>leaky integrator receiver model (**b**)</u> are plotted against the distance between the receiving animal and the airgun. Colours denote different ocean noise scenarios. Propagation of airgun noise and the vocalization was modelled by spherical spreading.
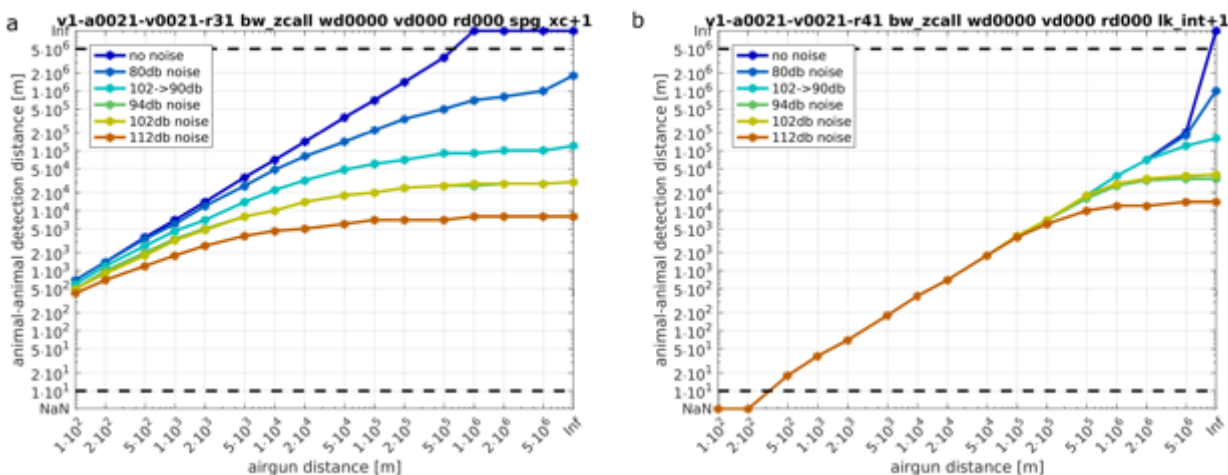
3. For **large distances** between receiver animal and airgun the <u>communication range is practically</u> <u>**constant**</u> and <u>independent of the airgun distance</u>. According to the model results, airgun noise has no effect on communication ranges for these large distances between receiver animal and airgun and the **communication ranges are exclusively dependent on the level of ocean noise.**

For very small and very large distances between airgun and receiver animal, communication ranges may fall outside of the distance range for which transfer functions were available (the distance range for which transfer functions were available is indicated by horizontal dashed lines in the figures).

The masking by airguns exerts an influence on the communication ranges for small and intermediate airgun distances (cases 1) and 2) above). For large airgun distances (case 3) above) the communication ranges are independent of the distance to the airgun and correspond to the range in absence of the airgun (Figure 62).

As expected, the distance range in which an airgun causes interference is generally larger in low ocean noise scenarios than in higher ocean noise scenarios (Figure 62).

When interference from an airgun is present, two general distance ranges can often be differentiated: 1.) the distance range in which the interference by the airgun is so dominant that communication ranges are exclusively determined by the airgun and are mostly independent of ocean noise, and 2.) the area in which both ocean noise and distance from the airgun determine the communication range.

Both the determined communication ranges and the extent of the three zones around the airgun location, in which communication ranges are limited by airgun noise, ocean noise or a combination of both, are different for the different receiver models (spectrogram correlator and leaky integrator).

Most often the **leaky integrator** predicted noticeably shorter communication ranges than the spectrogram correlator, particularly with intensely interfering airgun noise and consequently

noticeably reduced communication ranges (Figure 62). Moreover, the three interference zones around the airgun location tended to extend to larger distances from the airgun.

5.2.2 Comparison of the propagation models (spherical propagation versus numerical propagation model)

If spherical sound propagation is assumed, the attenuation of airgun and vocalization signals increases continuously and monotonically with distance.

This results in a continuous increase of communication range with increasing distance to airgun (Figure 71 a). Because no time dilatation of the vocalizations occurs as compared to the search pattern, high communication ranges are obtained, particularly for the spectrogram correlation receiver. Because the attenuation both for the airgun and the vocalization was somewhat lower than in the numerical propagation models, the net effect on communication ranges differs depending on whether the distance is larger from the airgun or from the vocalization. Because both incoming signals are somewhat stronger, the influence of the background noise is somewhat smaller than in the models based on numerical sound propagation.

Figure 72   Estimated communication ranges for blue whales (z-calls) are plotted against the distance between the receiving animal and the airgun under the assumption of **spherical sound propagation** for the vocalization and the airgun (**a**) and based on a **numerical propagation model** (for a water depth of 4000 m, a vocalization source depth of 50 m and a receiver depth of 50 m)(**b**). Colours denote different ocean noise scenarios. Dashed lines indicate the distance range for which transfer functions were available.
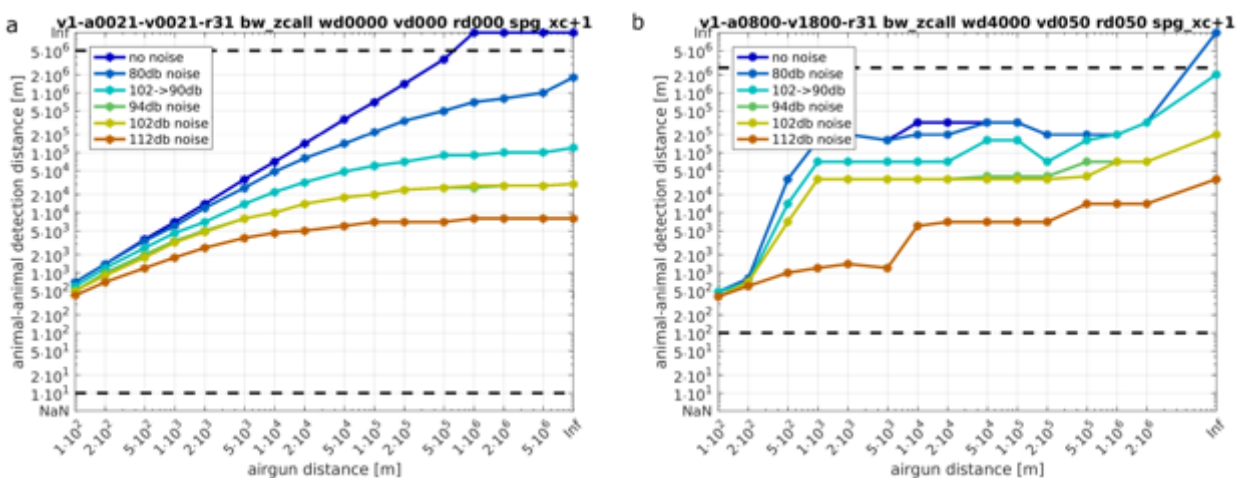
When **sound propagation is modelled numerically**, the attenuation of vocalization and airgun does not increase monotonically with distance in many scenarios. While there is a general increase in communication ranges with increasing distance from the airgun, local behaviour can be complex and non-monotonous (Figure 71 b). In particular, bifurcally different results can occur in the non-monotonic areas due to the non-monotonic behaviour of the vocalization attenuation with the iterative approach of determination of the maximum communication ranges depending on the position of the iteration steps of the verified vocalization distances (partly visible leaps / back-leaps of the determined vocalization distances for adjacent airgun distances or noise scenarios in the diagrams).

The transfer functions model the time dilatation in the vocalizations with large vocalization distances. This leads to a worse matching with the search patterns of the spectrogram correlator as vocalization distances increase. This leads to a decreasing advantage of the spectrogram correlator as compared to

the leaky integrator with increasing vocalization distances. **Generally overall attenuation is somewhat higher than with spherical propagation**.

The difference between the assumed ocean water attenuation as per calculation according to Ainslie / McColm and/or the corresponding Thorp information of DW-SC was shown to be generally comparatively small and thus had negligible influence on the results.

5.2.3 Comparison of the transfer functions of the numerical propagation model

18 sets of transmission distance-dependent transfer functions (corresponding to two source depths, three receiver depths and three environmental scenarios) were used. The source depth of the airgun was always 5 m when using transfer functions for sound transmission. For 2 vocalization source depths (5 m and 50 m), each for 3 receiver depths (10 m, 50 m, and 200 m) the following 3 transmission scenarios were calculated:

1. Water depth 500 m, maximum frequency 375 Hz, transmission distances 100 m - 3,600 km
2. Water depth 500 m, maximum frequency 1,500 Hz, transmission distances 10 m -100 km
3. Water depth 4000 m, maximum frequency 375 Hz, transmission distances 100 m - 2,600 km

Figure 73   Loss of transmitted total energy of a dirac pulse and reduction of its peak amplitude is plotted against the distance from the sound source. The red line denotes energy loss when spherical spreading is assumed and the green line denotes energy loss when cylindrical spreading holds. Results for the loss of total transmitted energy and reduction of peak amplitude in the numerical model are depicted in blue and black. The sound source is located 5 m (scenario a on the left) or 50 m (scenario b on the right) below the water surface. The upper frequency limit is 375 Hz, the water depth is 4000 m and the receiver is located 50 m below the water surface in both scenarios.
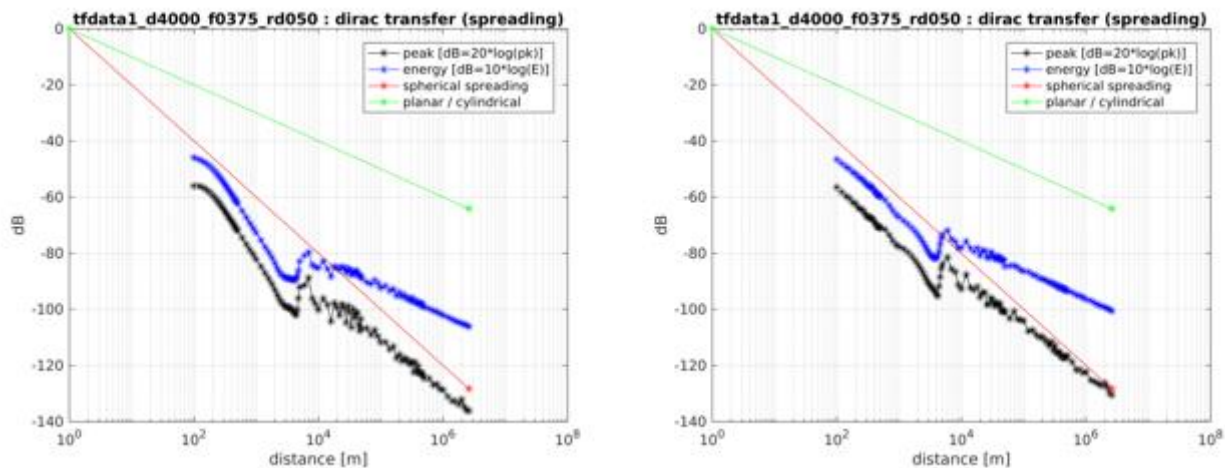
All transfer functions behave distinctly non-monotonically down-ward sloping over the distance regarding the transmitted total energy and the maximum amplitude (Figure 73 for an example and appendix 2 for all scenarios). This causes partly non-intuitive behaviour of the resulting communication ranges. With increasing distance from the airgun communication ranges can locally increase. In particular, reversals distinctly above 20 dB result partly in the deep-water transfer functions occur over a distance area of more than two magnitudes (approximately 300 m -100 km). Depending on the position of the iteration steps of the vocalization distances in this range, estimates of communication ranges vary.

5.2.4 Non-monotonic propagation behaviour of the transfer functions

As described in 3.2 and 3.3 the sound propagation model revealed that signal energy and amplitude do not decrease monotonically with distance (Figure 73). The non-monotonic transfer functions were used to model the propagation of both airgun and vocalization and lead to two types of reversions:

1. For a given airgun distance communication may be impossible at a given animal-animal distance, yet become possible again at an even greater animal-animal distance.
2. Masking does not increase monotonically with distance from the airgun.

While phenomenon 2) does not interfere with our modelling approach, phenomenon 1) implies that **the concept of a communication range strictly speaking does not hold for all scenarios**. While the concept of a communication range implies that communication is always possible up to a certain threshold distance and impossible for all distances beyond, non-monotonic transfer functions can give rise to a sequence of communication windows along the distance axis which are interspersed by regions where communication is impossible. In a graph with airgun distance on the x-axis and animal-animal distance on the y-axis a patchwork of areas where communication is possible would arise. This causes considerable problems when determining the communication range via an iteration approach: The outcome of the iteration may depend on the initial value and the precise rules that determine which value to test in the subsequent iteration step. Extensive detailed sampling of the two-dimensional distance field (spanned up by the airgun distance axis and the animal-animal distance axis) to test where communication is possible represents an obvious way to avoid iteration. However, extensive detailed sampling would have increased the computational effort by a factor of approximately 100. Given that computational time was already a limiting factor when using the iteration approach, carrying out the extensive detailed sampling was clearly impossible.

The Iteration problem with the non-monotonic behaving transfer-functions does not exist if vocalization transmission is performed by geometric spreading, which was tested as an alternative in this project, and which was the only vocalization transfer method used in Siebert et al. (2014). For the numerical transfer functions the range and amplitude of the reversals differs between the transfer-functions for the different scenarios (appendix 2). When used for the iteration of vocalization transfer distances, this has implications on how deterministic the resulting communication distance is achieved. Below we discuss in which scenarios the iteration approach is expected to produce robust results and in which scenarios results should be interpreted with care.

For the transmission of the low-frequency vocalizations of blue and fin whale in shallow water (500 m), the transfer functions 1 - 3 and 11 - 13 were used for receiver depths of 10 m, 50 m and 200 m with sender depths of 5 m and 50 m respectively. Of these functions, the worst reversals appeared in the transfer functions for the scenario of a sender depth of 5 m and a receiver depth of 10 m. Intermediate reversals appeared for a sender depth of 5 m with a receiver depth of 50 m, and for a sender depth of 50 m with a receiver depth of 10 m. For the remaining 3 transmission scenarios (sender depth 5 m with receiver depth 200 m, sender depth 50 m with receiver depth 50 m, and sender depth 50 m with receiver depth 200 m) reversals are moderate, which suggests, that the iteration approach should yield very robust estimates of communication ranges.

For the transmission of the wide-band vocalizations in shallow water, the transfer functions 4 - 6 and 14 - 16 were used. All these transfer functions have conspicuous reversals. The reversals over the longest distance-ranges (causing the largest uncertainties in range estimates) occur in the transfer function for a sender depth of 5 m with a receiver depth of 10 m or 200 m, as well as the transfer function for a sender depth of 50 m and a receiver depth of 200 m. The functions for a receiver depth of 50 m with a sender depth of each 5 m or 50 m have reversals over an intermediate range. For the transfer function for a sender depth of 50 m and a receiver depth of 5 m, the range of reversals is rather limited, which causes the results for broadband vocalizations in this scenario to be most robust.

For the transmission scenarios of low-frequency-vocalizations in deep ocean (4000 m), all scenarios have obvious reversals. For the scenario of 5 m sender depth and 10 m receiver depth, reversals are pronounced in range as well as in amplitude. Within the range of approximately 500 m -100 km the communication distances can be affected by iteration artefacts. The scenarios of 5 m sender depth and 50 m receiver depth, as well as 50 m sender depth with 10 m receiver depth still have very distinct reversals. Reversals in the cases of 5 m sender depth with 200 m receiver depth, and the case of 50 m sender depth and 50 m receiver depth are less distinct. The least reversals in these scenarios appeared in the case of 50 m sender depth and 200 m receiver depth, making this scenario the most reliable for the iterations for estimating the communication ranges of low-frequency vocalizations in deep ocean.

5.2.5   Comparison of sender depths of 5 m and 50 m

Airgun signals were transmitted using transfer functions from a sender depth of 5 m in all scenarios. For vocalizations, however, two different sender depths, 5 m and 50 m, were studied. (Geometric signal spreading was also used as an alternative both for airgun and vocalization transmission.) The fine structure of all transfer functions is highly complex, and its details depend in a complex manner on multiple aspects of the transfer scenario. Generally, the following similarities and differences in overall parameters of the transfer functions of respective sender depth can be seen in the plots of loss of transmitted total energy and reduction in amplitude against the distance to the source (appendix 2).

► In almost all cases at least minor reversions of the monotonic decay of transmitted amplitude and energy occur.

► In short ranges, where the receiver is close to the sender, the transfer loss depends also on the vertical depth difference of sender and receiver. If they are not approximately equal in depth, the transmission loss is increased through the non-negligible increased diagonal at short distances (note that the presented diagrams all plot horizontal distances).

► In short distances, the inclination of the amplitude reduction resembles the inclination of spherical spreading very well, most strikingly for 50 m sender depth. In long distances, the inclination of the maximum amplitudes resembles the order of spherical spreading, while overall energy is distributed in long ranges cylindrically.

► Due to surfaces effects and complex interaction of sound with the water surface and the ocean floor, the worst deviations from a monotonous decay of transmission with distance occur from the source depth of 5 m at ranges close to the sender. Amplitudes and ranges of deviation from monotonic behaviour are somewhat less at a source depth of 50 m (though still present). Thus, the transmission functions from a source depth of 50 m yield more robust results when using an iteration approach for maximum communication range estimation.

► Regarding overall attenuation, there is no striking general difference in the levels of signal attenuation from 5 m and 50 m source depth for the wideband transfer up to the maximum distances. Thus, not profoundly different communication ranges should result here.

► For the low-frequency transfer functions however, at long ranges, the levels of the transfer functions originating from 5 m, are distinctly lower (more attenuated) than the transfer functions originating from 50 m vocalization depth for receiver depths of 50 m and 200 m. This holds for both ocean depths (500 m as well as 4000 m). Thus, an increase in communication ranges is expected for blue and fin whale when these species vocalize at greater depths (50 m versus 5 m sender depth). This increase in communication ranges for vocalizations from 50 m source depth can be very clearly seen for both, blue whale and fin whale in all diagrams illustrating the communication ranges under various conditions.

► For the remaining species using wideband vocalizations (with fullband analysis) no such unambiguous difference can be seen between 5 m and 50 m source depth in the range diagrams.

5.2.6   Comparison of receiver depths of 10 m, 50 m and 200 m

Regarding the diagrams of the overall parameters of the transfer functions (appendix 2), the most striking differences between the respective transfer functions for different receiver depths are:

► the larger irregularities of the functions from monotonic behaviour close to the source at shallow receiver depths (10 m) caused by more dominant influence of surface effects

► at very short ranges different inclinations of the transfer functions depending on depth difference of sender and receiver and diagonal length.

► at short ranges, and 500 m ocean depth, and wideband transfer, the transfer function levels for 200 m receiver depth are very low.

At longer ranges, the differences between different receiver depths are not substantial.

Thus, in the range diagrams (appendix 1), for the blue whale, having long communication ranges, no clear systematic difference between different receiver depths is obvious. Also, for the fin whale, no striking systematic difference is obvious.

For the wideband-vocalizations at very close distances to the airgun causing short communication ranges, the communication ranges for 200 m receiver depth are distinctly shorter than for 10 m or 50 m receiver depth, corresponding to the low transfer functions for 200 m receiver depth, at short ranges.

5.2.7   Comparison of ocean depths of 500 m and 4000 m for the low-frequency vocalizations

For 4000 m ocean depth, transfer functions were only available for low-frequency vocalizations. In the intermediate distance range, where superpositions of different reflections from sea floor, water surface and direct transmission path cause conspicuous irregularities from monotonic decreasing behaviour of the transfer functions, the levels of the transfer functions in shallow ocean are distinctly higher than the levels of the transfer functions in deep ocean. Consequently, where communication distances of blue whale and fin whale are in the intermediate distance range, the communication ranges in the shallow ocean scenarios are generally distinctly higher than communication ranges in deep ocean (appendix 1). However, since these irregularities cause non-deterministic behaviour of the iterations, the resulting communication ranges in distances of the airgun, where intermediate animal communication ranges result, are not very robust and display huge jitter in the diagrams in these communication ranges.

5.2.8   Comparison of the spectrogram correlator and leaky integrator receiver models

The spectrogram correlator detects vocalizations with higher precision than the leaky integrator, particularly if vocalizations have a characteristic spectral / frequency / intensity structure over the signal course, provided that the incoming signals are not distorted strongly and were not temporally stretched. For narrow-band signals, without a strong temporal signature (e.g. fin whale), the advantage can be only minor (Figure 74).

Figure 74   Communication ranges for **fin whales** as estimated by the spectrogram correlation model (**a**) and the leaky integrator model (**b**) are plotted against the distance between the receiving animal and the airgun. Sound propagation of the vocalization as well as airgun noise was based on numerical propagation models for a scenario of a water depth of 4000 m, a vocalization source depth of 50 m and a receiver depth of 50 m. Colours denote different ocean noise scenarios. Dashed lines indicate the distance range for which transfer functions were available.
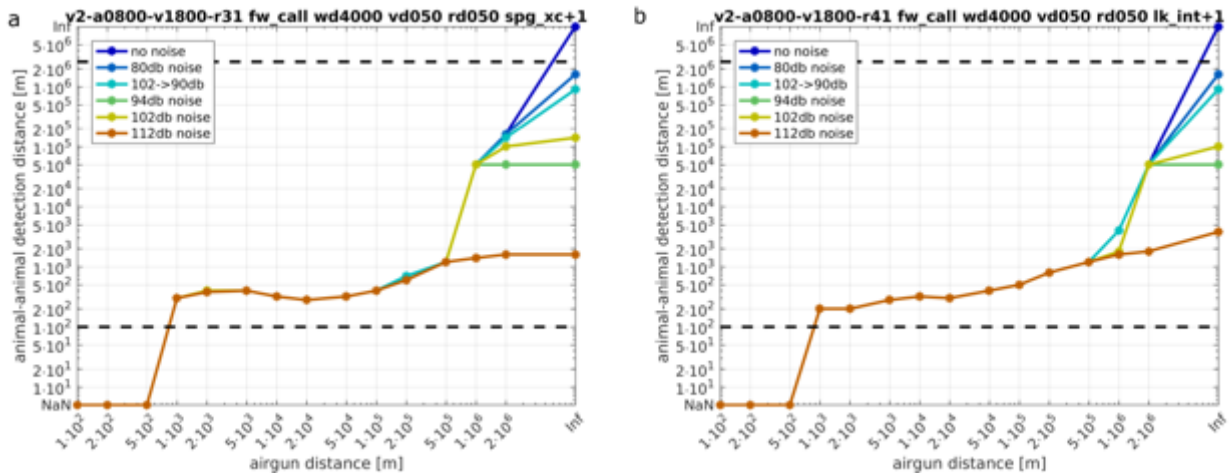
In the same manner, this advantage disappears with very large vocalization distances when the transmitted signal was temporally stretched (as an effect of sound propagation) so that the temporal frequency structure is no longer recognizable. This effect starts at different distances depending on vocalization duration and length of its temporal structure (for the 25-second blue whale Z call only at much larger distances than for the <1-second killer whale sound; Figure 75 and Figure 76).

Figure 75   Communication ranges for **blue whales** (z-call) as estimated by the spectrogram correlation model (**a**) and the leaky integrator model (**b**) are plotted against the distance between the receiving animal and the airgun. Sound propagation of the vocalization as well as airgun noise was based on numerical propagation models for a scenario of a water depth of 4000 m, a vocalization source depth of 50 m and a receiver depth of 50 m. Colours denote different ocean noise scenarios. Dashed lines indicate the distance range for which transfer functions were available.
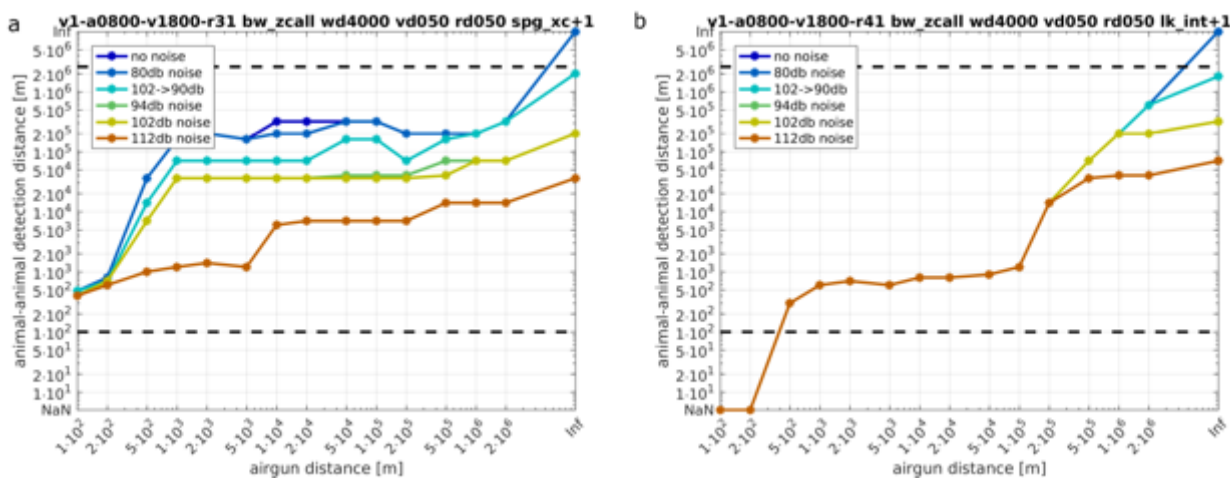
When communication ranges were short, i.e. when the interfering masking by ocean noise and airgun is strong), the ability to evaluate patterns allows the spectrogram correlator to achieve distinctly larger communication distances than the leaky integrator in almost all cases.

Figure 76   Communication ranges for **killer whale** (multiharmonic call) as estimated by the spectrogram correlation model (**a**) and the leaky integrator model (**b**) are plotted against the distance between the receiving animal and the airgun. Sound propagation of the vocalization as well as airgun noise was based on numerical propagation models for a scenario of a water depth of 500 m, a vocalization source depth of 50 m and a receiver depth of 50 m. Colours denote different ocean noise scenarios. Dashed lines indicate the distance range for which transfer functions were available
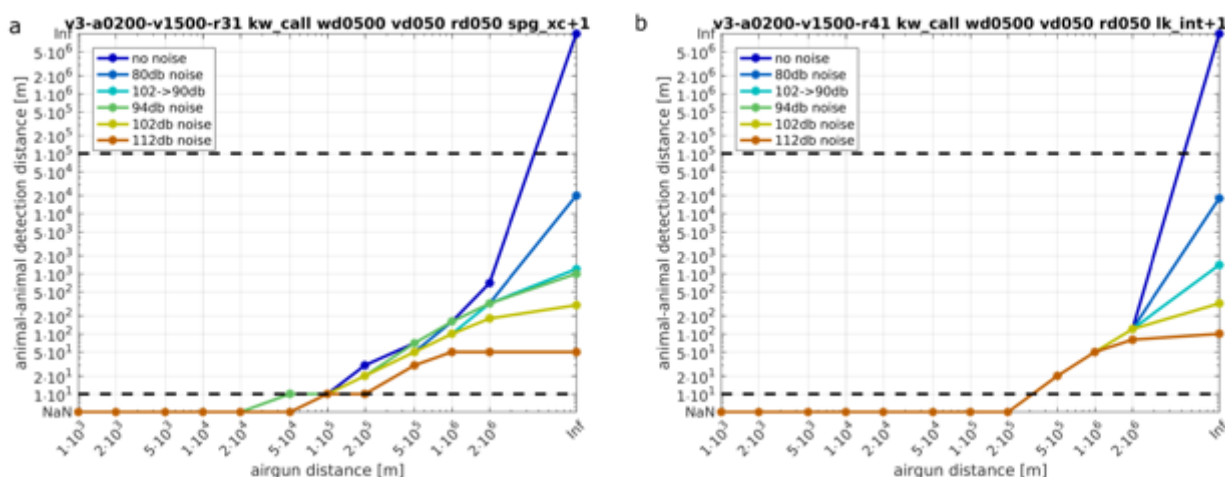
In situations when communication was possible over very large distances (i.e. when the distance to the airgun was larger) the leaky integrator often yielded larger communication distances than the spectrogram correlator (e.g. Figure 70). The exact cause for this could not be examined (in the available time) and is possibly connected to the temporal and spectral blurriness (smoothing) of the search patterns, which was purposely created to expand the signal matching somewhat for "similar" signals. Furthermore, an additional leaky integrator was inserted after the spectrogram correlator, which was intended to increase the receiver tolerance for vocalizations that are temporally stretched by the transmission. An optimization of the parameters used here was not performed due to time constraints. With an optimal adjustment of the spectrogram correlator and its subsequent leaky integrator, the advantage of the leaky integrator model in some cases, compared to the spectrogram correlator model, could possibly be reduced at long airgun distances.

5.2.9   Analysis of broadband vocalizations: fullband and with bandpass above 500 Hz

Animals listening for broadband vocalizations may be able to focus exclusively on higher frequencies, when the low frequency parts of the vocalization are masked by noise. To test which communication ranges could be achieved when the frequency band below 500 Hz (the upper limit of the frequency band possibly masked by the airgun) was completely neglected in broadband vocalization analysis, comparative analyses for the three broadband vocalizations (the killer whale multi-harmonic call, the Weddell seal long call and the Weddell seal call train) were conducted with a bandpass above 500 Hz.

In the absence of airgun noise communication ranges were somewhat reduced in the bandpass-filtered analysis as compared to the fullband analysis. This can be explained by the somewhat reduced total energy of the vocalization in this frequency sub-band in comparison to the use of the total band. Importantly, however, the presence of airgun noise causes almost no reduction in communication ranges in the bandpass-filtered analysis (Figure 77), because the frequency band of the airgun and the frequency of the bandpass-filtered vocalization due not overlap. The net effect is that communication ranges in the bandpass-filtered analysis are often larger than communication ranges in the fullband analysis when airgun noise is present.

Figure 77   Communication ranges for **Weddell seals** (call train) as estimated by **the spectrogram correlation model**. (<u>**a**</u>) <u>shows results for a fullband-analysis</u>, while results for a <u>high pass analysis (threshold 500 Hz) are shown in (**b**)</u>. Sound propagation of the vocalization as well as airgun noise was based on numerical propagation models for a scenario of a water depth of 500 m, a vocalization source depth of 50 m and a receiver depth of 50 m. Colours denote different ocean noise scenarios. Dashed lines indicate the distance range for which transfer functions were available.
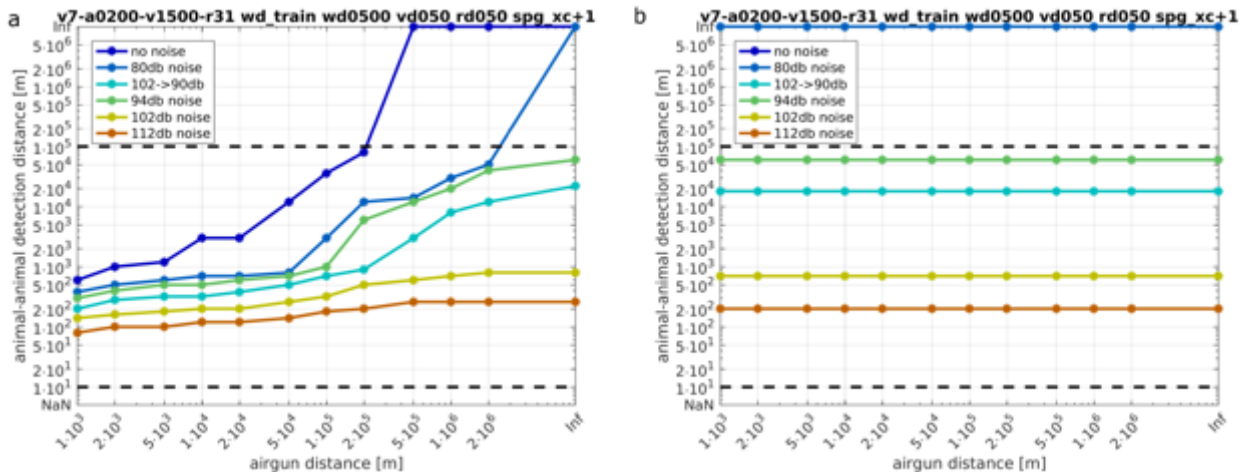
Thus, it would be optimal for broadband vocalizations to neglect the cluttered low frequency-band for vocalization recognition in the absence of loud, strongly time-variable interference signals in the low-frequency range, but to use the full frequency band for vocalization recognition with broadband continuous ocean noise.

The extent to which the animals are capable of selectively using specific frequency bands for vocalization recognition, depending on interference situation, is unknown. However, this does not appear to be impossible.

5.2.10   Communication ranges for the different vocalizations

For each vocalization estimated communication ranges differ extremely between the different scenarios. While we observed a reduction of the communication ranges in the presence of airgun noise in almost all cases in which the frequency band of the airgun was included in the analysis, further generalizations are difficult.

In <u>almost all examined cases,</u> in which the frequency band of the airgun was included in the analysis, a **reduction of communication ranges was present even at distances of more than 200 km from the airgun** (appendix).

Very frequently (in all scenarios with <u>ocean noise levels of up to 90 dB</u>), such a reduction occurred **even up to a minimum distance of 1,000 km from the airgun**.

The following species-specific observations refer to the assumed 1 dB detection threshold criterion and propagation of the airgun as well as the vocalization according to the numerical sound propagation model developed and verified by measurements in chapter 3 (for fin whale fig 74b shows results for spherical spreading in addition to 74a which shows results based on the numerical propagation model).

5.2.10.1   Blue whale (z-call):

In comparison to other species (e.g. fin whale) the models predict large communication ranges for blue whales. Airgun noise generally leads to marked reductions in the communication ranges even if the distance between the airgun and the receiving animal is as large as 500 km. Close to the airgun (below 100 km distance) the spectrogram correlator predicts markedly larger communication distances than

the leaky integrator (Figure 78). In deep water communication ranges are smaller than in shallow water (appendix 1). In spectrogram correlator models ocean noise has a strong influence on communication ranges for a wide range of airgun -receiver animal distances. With use of the leaky integrator, by contrast, airgun noise markedly reduces communication ranges for small airgun -receiver animal distances. Here, ocean noise has little effect and the interference by the airgun is dominant, so that the communication ranges exclusively depend on the distance from the airgun.

Figure 78   Communication ranges for blue whales (z-call) as estimated by the spectrogram correlation model (a) and the leaky integrator model (b) are plotted against the distance between the receiving animal and the airgun. Sound propagation of the vocalization as well as airgun noise was based on numerical propagation models for a scenario of a water depth of 4000 m, a vocalization source depth of 50 m and a receiver depth of 50 m. Colours denote different ocean noise scenarios. Dashed lines indicate the distance range for which transfer functions were available.
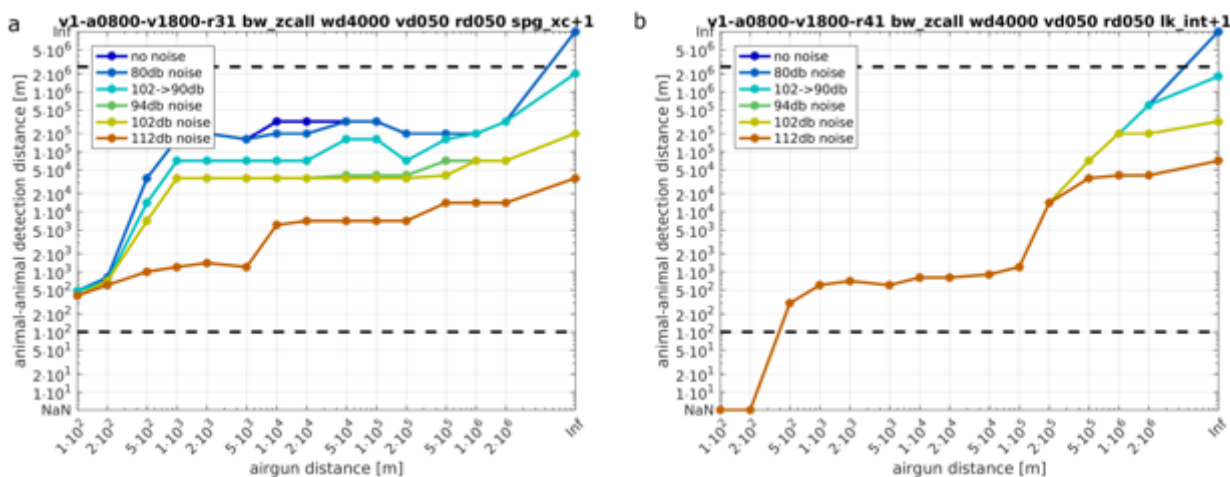
5.2.10.2   Fin whale:

The estimated communication ranges for fin whales are surprisingly short, particularly when sound propagation was modelled by the numerical transfer functions (Figure 79a). If vocalization transmission is modelled as geometric spreading, by contrast, much longer communication ranges are obtained (Figure 79b).

The transfer functions attenuate particularly strongly in the small distance range, which would result from spherical spreading as the possible communication distance, thus the ranges here are once more particularly reduced when using transfer functions.

Compared to the blue whale z-call, relatively little energy is contained in the very short fin whale vocalization in spite of its high level.

Additionally, the short duration of the vocalization entails that signal stretching causes it to be markedly weakened. The fine structure of the transfer functions partly also causes a weak transmission of short signals in this frequency range through interferences.

The limitation of the communication ranges by airgun noise is dominant in most cases, while the significance of the ocean noise in presence of an airgun almost always plays a subordinate role.

The comparatively short and not very characteristic fin whale signal, which contains quite limited energy at a single low frequency, is strongly masked by the airgun whose spectral power reaches a maximum in this frequency range.

Figure 79   Communication ranges for **fin whales** as estimated by the spectrogram correlation model are plotted against the distance between the receiving animal and the airgun. Sound propagation of the vocalization as well as airgun noise was based on **numerical propagation models** for a scenario of a water depth of 4000 m, a vocalization source depth of 50 m and a receiver depth of 50 m in **figure a**. In **figure b** sound propagation of the vocalization was assumed to follow **spherical spreading**. Colours denote different ocean noise scenarios. Dashed lines indicate the distance range for which transfer functions were available.
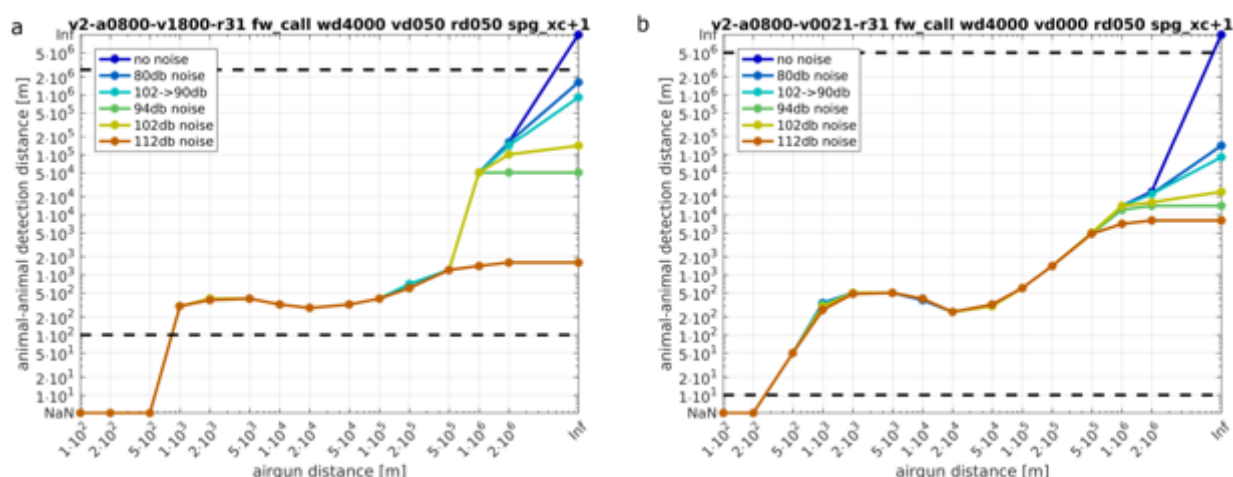
5.2.10.3   Killer whale (multi-harmonic call):

In the presence of airgun noise communication ranges of killer whales are predicted to be approximately 1/10 of the communication ranges obtained for fin whales. While communication ranges of fin whales increase considerably in the absence of airgun noise (depending on ocean noise), only limited effects of airgun noise on killer whale communication ranges are observed (Figure 80, especially in the high pass model Figure 80b). This is due to the fact that the short low-frequency, far-ranging fin whale signal is very strongly masked by the airgun, while the killer whale has a wide frequency range above the centre of the airgun frequency band, through which it can communicate at close distances and which is not masked by the airgun.

Due to the moderate energy content of the short and not very loud killer whale vocalization and due to the fact that the lowest frequencies are much higher than in the fin whale, the communication ranges are also comparatively small in the absence of the airgun.

With use of the highpass, airgun noise has no effect on estimated killer whale communication ranges. Compared to using the full bandwidth of the signal, the maximum communication ranges in the absence of airgun noise are somewhat reduced.

Figure 80   Communication ranges for killer whales (multiharmonic call) as estimated by the spectrogram correlation model. (a) shows results for a fullband-analysis, while results for a high pass analysis (threshold 500 Hz) are shown in (b). Sound propagation of the vocalization as well as airgun noise was based on numerical propagation models for a scenario of a water depth of 500 m, a vocalization source depth of 50 m and a receiver depth of 50 m. Colours denote different ocean noise scenarios. Dashed lines indicate the distance range for which transfer functions were available.
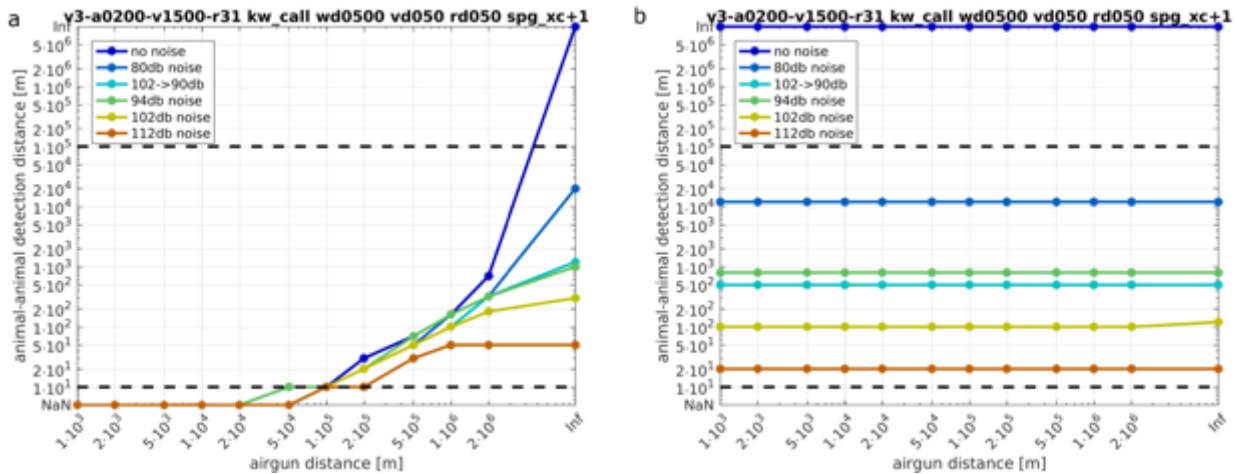
5.2.10.4   Weddell seal: long vocalization

In the spectrogram correlator model airgun noise only causes a moderate reduction of Weddell seal communication ranges and ocean noise remains the dominant factor determining communication ranges. This is due to the fact that the spectral focus of the Weddell seal vocalization is located above the frequency band of the airgun.

In the leaky integrator (over the total frequency band) the presence of an airgun in the vicinity of the receiving animal causes a pronounced range reduction.

With use of the high pass, airgun noise has no effect on communication ranges.

Figure 81   Communication ranges for Weddell seals (long call) as estimated by the spectrogram correlation model. (a) shows results for a fullband-analysis, while results for a high pass analysis (threshold 500 Hz) are shown in (b). Sound propagation of the vocalization as well as airgun noise was based on numerical propagation models for a scenario of a water depth of 500 m, a vocalization source depth of 50 m and a receiver depth of 50 m. Colours denote different ocean noise scenarios. Dashed lines indicate the distance range for which transfer functions were available.

137
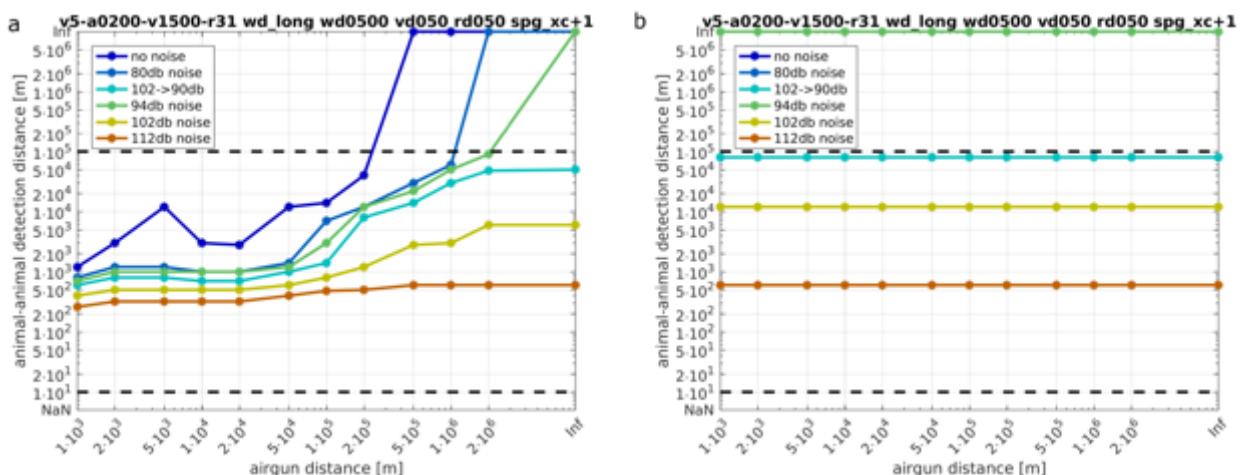
5.2.10.5   Weddell seal: vocalization sequence

For the Weddell seal vocalization sequence, the maximum communication distances in absence of the airgun are similar to the ones of the long Weddell seal signal (appendix 1). However, reduction of communication ranges is slightly stronger for the vocalization sequence than for the long vocalization, especially for the leaky integrator model. This is due to the greater overlap of this vocalization band with the frequency band of the airgun.

With use of the high pass, airgun noise has no effect on communication ranges.

6 Discussion of the effects of airgun noise at the individual and population level

6.1 Importance of the acoustic sense for marine mammals

6.1.1 Sound as the primary sensory modality in marine mammals

Acoustic energy propagates in water more efficiently than almost any form of energy. Light, electromagnetic and thermal energy are severely attenuated in water. In order to gather information on conspecifics, obstacles, predators or prey outside of the immediate vicinity of the individual and in order to navigate in the vast ocean environment, marine organisms have to rely on the acoustic sense, the olfactory system and on senses of the magnetic field. Odors spread slowly and are subject to drift in ocean currents, so that their use is mainly limited to either short ranges or relatively stationary sources. The acoustic sense is typically the only sense that provides information on distant (i.e. distances exceeding a few meters to a few tens of meters) objects in real time. The evolution of sophisticated auditory systems and biosonar (Au and Hastings 2008) constitutes a powerful proof that natural selection on the auditory system is strong in marine mammals: The ability to gather detailed information from acoustic signals provides a fitness advantage. In turn, individuals that cannot use acoustic information efficiently have reduced vital rates.

6.1.2 Biological functions of vocalizations of Antarctic species

The importance of the acoustic sense has been documented in a wide variety of behavioural contexts. Here we list behavioural contexts and provide examples with a focus on marine mammal species that occur in the Antarctic Ocean.

Vocalizations play a role in finding and competing for mating partners. Fin whale songs (sequences of 20 Hz calls) recorded in a fin whale breeding ground were found to be exclusively produced by males (Croll et al. 2002). The behavioural context strongly suggests that these displays serve to attract females from great distances (Croll et al. 2002). Song sequences of Antarctic blue whale z-calls have also been proposed to be male reproductive display signals (Thomisch et al. 2016, Croll et al. 2002). Male Weddell seal calls during the breeding season are likely important for the establishment of underwater territories (Rouget et al. 2007) and for attracting females (Opzeeland et al. 2010) and may serve as honest signals of male fitness as studied for leopard seals (Rogers et al. 2017).

Moreover, calls can advertise feeding opportunities. The fin whale songs discussed above have e.g. been suggested to serve two functions: Males call to attract females, while females move towards the callers to take advantage of good feeding opportunities (Croll et al. 2002).

Another important function of vocalizations is that they facilitate the reunion of mothers with their young. In Weddell seals airborne calls of mothers and pups that facilitate successful reunions after foraging excursions of the mother have been studied in detail (Collins et al. 2005, Collins et al. 2011, Opzeeland et al. 2012). These studies have shown that there is substantial inter-individual variation between the calls of mothers as well as pups. Despite this variation in vocalizations between individuals, playback experiments suggest that acoustic cues alone are not sufficient for individual recognition between a pup and its mother (Collins et al. 2005, Opzeeland et al. 2012). In baleen whales contact calls are likely important to maintain or re-establish the mother-calf bond (e.g. after deep dives of the mother).

Similar to the function of maintaining the union between a mother and its young, acoustic cues can serve to maintain cohesion between members of larger groups that forage or migrate together.

In summary marine mammals have evolved to use sound as their primary sensory modality. If sound is used for the purpose of communication both sender and receiver animal can suffer a fitness cost, if e.g. masking impedes signal detection or recognition (Branstetter et al. 2016).

6.2 Assessment of the effects of airgun noise at the individual level

6.2.1 Behavioural responses to noise

Apart from having the potential to induce permanent or temporary shifts of the hearing threshold in the vicinity of the airgun (Finneran 2015), airgun noise can trigger disturbance reactions, i.e. behavioural changes. While some behavioural responses can be interpreted as antimasking strategies, many behavioural responses can best be interpreted as stress responses to a disturbance. Behavioural responses can have a negative impact on vital rates (i.e. survival, fecundity and growth), because they are energetically costly (e.g. flight reactions), disrupt normal behaviour (e.g. cessation of resting, feeding or mating activity), disrupt mother-young bonds, or lead to avoidance of otherwise attractive habitats. The use of antimasking strategies in response to anthropogenic noise is yet another indication that biologically-relevant signals are masked: the animal invests additional time or energy to mitigate fitness costs inflicted by the masking noise.

The animals can respond in different ways to disturbance or to noise pollution. For example, it has been reported that killer whales respond by increasing call duration in respond to increased numbers of whale watching boats (Foote et al 2004). Animals can also respond by increasing call amplitude (Holt et al. 2009). Such vocal compensation is often interpreted as an antimasking strategy for high background noise levels. Blue whales have been reported to lower their call frequencies in response to increased ocean background noise (McDonald et al. 2009). Blue whales have also been reported to increase their call rate during seismic activities (Di Iorio and Clark, 2009). Fin whales moved away from the airgun array source and this displacement persisted for a time period well beyond the 10-day duration of seismic airgun activity (Castellote et al. 2012). In addition, fin whales shortened 20 Hz note duration, decreased bandwidth, centre frequency and peak frequency in high noise conditions (Castellote et al. 2012).

Another response to seismic activity has been reported for humpback whales. The number of humpback whale singers significantly decreased with increasing received level of seismic survey pulses (Cerchio et al. 2014). Humpback whales increased the source level of their songs proportionately to increases in wind-dependent ambient noise (Dunlop et al. 2014). Humpback whales have also been shown to increase the length of their songs in response to low frequency sonar (Miller et al. 2000). Dunlop et al. (2013) found that humpback whales responded differently to two stimuli (social sound or tone stimuli), measured by changes in course travelled and dive behaviour.

The animals can also produce non-acoustic behavioural responses to noise. For example, minke whales changed swimming pattern and swimming directions in response to whale watching boats compared to a control site with no whale watching boat (Christiansen et al. 2013).

Animal tags such as D-TAGS or other acoustic tags have been deployed during different exposure experiments to investigate the short-term behavioural reactions such as changes in dive pattern and horizontal swimming speeds in minke whales (Kvadsheim et al. 2017). Miller et al. (2012) reported a strong change in behaviour in response to sonar. The killer whales changed their behavioural state, in this case from feeding to travelling, which appears to represent a complex behavioural reaction to the sonar exposure. The killer whales also showed a change in dive behaviour (Sivle et al. 2012). Kuningas et al. (2013) and left an area to avoid sonar activity. Whale numbers sighted in Vestfjord gradually declined after the start of the 2006 naval fleet FLOTEX Silver exercise in Vestfjorden.

The severity and duration of a behavioural response depends upon the exposure duration. Some animals may choose to leave an area as has been observed for bottlenose dolphins in Australia (Bejder et al.

2006). However, if the area is an important feeding area, this may not be an option for animals all the time. Southall et al. (2007) defined duration on a time scale relative to exposure duration. A moderate change in behaviour had duration similar to the duration of the exposure, and minor or brief responses were considered to be progressively shorter than the exposure; whereas a prolonged response was significantly longer than the exposure, considering the behavioural and diving patterns of the whale species. Sivle et al. (2015) summarized behavioural reactions of marine mammals in their Table 15(see Table 14 below).

Responses can be highly variable and may not be fully predictable with simple acoustic exposure metrics (e.g. received sound level). Rather, differences among species and individuals along with contextual aspects of exposure (e.g. behavioural state) appear to affect response probability (Southall et al. 2016).

Table 14   Behavioural responses of a marine mammal to a disturbance (after Sivle et al. 2015).

Score	Behavioural responses
0	No observable response
1	Brief orientation response
2	Moderate or multiple orientation responses Brief or minor changes in respiration rates Brief cessation/modification of vocal behaviour **Brief change in dive profile**
3	Prolonged orientation behaviour Minor change in locomotion (speed/direction) and or dive profile but no avoidance of sound source Minor cessation/modification of vocal behaviour Individual alert behaviour Moderate change of respiration rate
4	Extended change in locomotion (speed/direction) and or dive profile but no avoidance of sound source **Brief avoidance of sound source** Minor shift in group distribution Moderate cessation/modification of vocal behaviour ***Brief cessation of feeding***
5	Extended change in locomotion (speed/direction) and or dive profile but no avoidance of sound source **Minor avoidance of sound source** Moderate shift in group distribution Change in inter-animal distance and/or group size Prolonged cessation or modification of vocal behaviour ***Minor cessation of feeding***
6	Moderate avoidance of sound source Extended cessation or modification of vocal behaviour Visible startle response **Moderate cessation of feeding** Prolonged shift in group distribution Brief or minor separation of female and dependent offspring Aggressive behaviour related to noise exposure Brief cessation of reproductive behaviour Moderate cessation of resting behaviour

Score	Behavioural responses
7	**Prolonged cessation of feeding** Moderate separation of female and dependent offspring Severe and or sustained avoidance of sound source Extensive or prolonged aggressive behaviour Clear anti-predator response Moderate cessation of reproductive behaviour ***Prolonged avoidance***
8	Obvious aversion and/or progressive sensitization Long-term avoidance of area Prolonged or significant separation of female and dependent offspring with disruption of acoustic reunion mechanisms Prolonged cessation of reproductive behaviour
9	Outright panic, flight, stampede, or attack Avoidance related to predator detection

6.2.2 Frequency ranges of vocalizations of Antarctic species

Communication of marine mammals can be masked by noise, especially if the frequency range of the noise and that of the vocalizations overlap. In order to evaluate if a marine mammal is affected by noise, it is important to know the spectral, temporal, and amplitude characteristics of the species vocalizations. The tables below summarize the best available knowledge for the different species of marine mammals commonly found in Antarctic waters. Detailed information about each species is compiled in the final report of the first masking project (Siebert et al. 2014). Species hearing ranges were calculated from composite audiograms for different functional hearing groups, defined by Finneran (2016). Composite audiograms were calculated from the best available behavioural or evoked potential audiogram data. For mysticetes, the audiograms were derived from anatomical-based model predictions (Finneran 2016). The lower and upper frequency cut offs are defined as the values where the lower and upper frequency parts of the audiograms cross the 100 dB values.

Table 15   Overview of pinnipeds around Antarctica including vocalization type, frequency range, source levels and hearing (based on Finneran et al. 2016 and Erbe et al. 2017)

Species	Vocalization type	Vocalization range (Hz)	Source level (dB *re* 1 μPa at 1 m)	Hearing (kHz)
Southern Elephant Seal / Male		178-1617	NA	.016 - 68
Southern Elephant Seal / Female		50-3,00	NA	.016 - 68
Antarctic Fur Seal	Bark	100-8000	NA	.194 - 36
Antarctic Fur Seal	Full threat call	100-3000	NA	.194 - 36
Crabeater Seal	groan	100-8000	NA	.016 - 68
Crabeater Seal	low moan call	250-2600	NA	.016 - 68
Crabeater Seal	high moan call	990-4900	NA	.016 - 68

Species	Vocalization type	Vocalization range (Hz)	Source level (dB *re* 1 µPa at 1 m)	Hearing (kHz)
Leopard Seal	hoot	130-320	NA	.016 - 68
Ross Seal	pulses	250-1000	NA	.016 - 68
Ross Seal	high sirene call	800-4300	NA	.016 - 68
Weddell Seal	34+ call types	100-12800	153-193	.016 - 68

Table 16   Overview of Cetacean species around Antarctica including the time present, vocalization type, frequency range, source levels and hearing (based on Finneran et al. 2016 and Erbe et al. 2017)

Species	Season	Peak Season	Vocalization type	Vocalization range (Hz)	Source level (dB *re* 1 mPa at 1 m)	Hearing (kHz)
Baleen whales						
Blue whale	Nov - March	Jan - Feb	Southern Ocean blue whale song	16-28	189±3	.002 - 31
Blue whale	Nov - March	Jan - Feb	Down sweep	16-100	188	.002 - 31
Fin whale	Nov - March	Jan -Feb	pulse	20	189	.002 - 31
Sei Whale	Nov - March	Feb	tonal and up-sweep calls	200-600	156	.002 - 31
Antarctic Minke Whale	Nov - March	Jan - Feb	sweeps, moans	60-140	151-175	.002 - 31
Dwarf Minke Whale						.002 - 31
Humpback Whale	Nov - March	Jan - Feb	Song	100-4000	144-186 144-174	.002 - 31
Southern Right Whale			tonal, mainly moans	30-1500	NA	.002 - 31
Tooth whales						
Sperm Whale	Nov - March	Jan	clicks	100-30000	220	.815 -144
Beaked Whales	Dec - Feb	Dec - Feb				
Arnoux Beaked Whale	Dec - Feb	Dec - Feb	amplitude-modulated calls	1000-8500	NA	.815 -144
Strap-Toothed Whale	Dec - Feb	Dec - Feb	NA	NA	NA	.815 -144

Species	Season	Peak Season	Vocalization type	Vocalization range (Hz)	Source level (dB *re* 1 mPa at 1 m)	Hearing (kHz)
Southern Bottlenose Whale	Dec - Feb	Dec - Feb	clicks in short bursts	18000	NA	.815 -144
Sei Whale	Nov - March	Feb	tonal and up-sweep calls	200-600	156	.002 - 31
Antarctic Minke Whale	Nov - March	Jan - Feb	sweeps, moans	60-140	151-175	.002 - 31
Dwarf Minke Whale						.002 - 31
Humpback Whale	Nov - March	Jan - Feb	Song	100-4000	144-186 144-174	.002 - 31
Southern Right Whale			tonal, mainly moans	30-1500	NA	.002 - 31
Tooth whales						
Sperm Whale	Nov - March	Jan	clicks	100-30000	220	.815 -144
Beaked Whales	Dec - Feb	Dec - Feb				
Arnoux Beaked Whale	Dec - Feb	Dec - Feb	amplitude-modulated calls	1000-8500	NA	.815 -144
Strap-**Toothed Whale**	Dec - Feb	Dec - Feb	NA	NA	NA	.815 -144
Southern Bottlenose Whale	Dec - Feb	Dec - Feb	clicks in short bursts	18000	NA	.815 -144
Gray's beaked whale	Dec - Feb	Dec - Feb	NA	NA	NA	.815 -144
Dolphins	Dec -Feb	Feb				
Hourglass Dolphin	Dec -Feb	Feb	clicks	122.000-131.000	190-203	.815 -144
Killer Whale	Nov - March	Jan - Feb	pulsed calls	500-25,000	160	.815 -144
Killer Whale	Nov - March	Jan - Feb	clicks	20000 -60000	200	.815 -144
Long-finned Pilot Whale	Dec -Feb	Jan	whistles	1000-8000	178	.815 -144

6.2.3 Probability of exposure to communication masking airgun noise

6.2.3.1 Spatiotemporal distribution of airgun noise

Seismic surveys in the Antarctic Ocean are typically conducted during the austral summer with an activity peak in the months of January to March (e.g. Boebel et al. 2009), while seismic explorations at lower latitudes are also undertaken in winter (e.g. the Aragorn survey analysed in chapter 3). Our analysis of recordings of seismic surveys as well as the sound propagation models (chapter 3) illustrate that low-frequency airgun noise can be detected at distances exceeding 2 000 km from the source location. For seismic surveys conducted at the northern edges of the Southern Ocean, the best coupling of the airgun sound source with the SOFAR underwater sound channel and thus the highest potential for masking in Antarctic waters occurs when the airgun is located over the continental slope (chapter 3). Such seismic surveys may not only lead to masking in lower latitudes but also to masking in high latitudes. As expected, masking generally decreases (and communication ranges generally increase) with distance from the airgun source (all models in chapter 5). However, as the transmitted total (airgun) energy does not decline monotonously with distance to the source, our models indicate local deviations from the general trend: E.g., a fin whale individual at a distance of 20 - 50 km from the airgun has a shorter detection range than a fin whale at a distance of 2 - 5 km from the airgun (Figure 79).

6.2.3.2 Antarctic blue whale (*Balaenopetera musculus intermedia*) and fin whale (*Balaenoptera physalus quoyi*)

Antarctic blue whales generally feed at higher latitudes during austral summer and migrate to breed at lower latitudes during winter. Acoustic recordings of Antarctic blue whale calls document that Antarctic blue whales are present in low latitudes of the Indian Ocean, the eastern Pacific Ocean and the South Atlantic Ocean during the austral winter but are missing during the austral summer (Stafford et al. 2004, Samaran et al. 2013, Shabangu et al. 2019). In the high latitudes Antarctic blue whale calls are detected year-round with a peak in call detections between January and April (Thomisch et al. 2016). This pattern is in accordance with the occurrence pattern of z-calls at the Antarctic recording station analysed in this report (Figure 60) and suggests a non-obligatory migratory behaviour of Antarctic blue whales. To date it can only be speculated how age, sex and reproductive state influence migratory behaviour. Krill distribution changes within and between seasons as well as between years. It likely influences the specific locations of Antarctic blue whale feeding grounds, breeding grounds and possibly also impacts on migratory decisions (Attard et al. 2016, Thomisch et al. 2016).

The auditory model for the **Antarctic blue whale z-call** finds that noise from an airgun in a distance of 2000 km (the maximal distance analysed) from the blue whale reduces its detection range for a conspecific's call to half of the range achieved in the absence of airgun noise (Figure 78). The absolute detection ranges for blue whale z-calls in the absence of airgun noise have been estimated to 40 km for a scenario with 4 000 m water depth and high background noise (112 dB) which is typical of the Southern Ocean (Figure 78a). It seems plausible that a reduction of the detection range from 40 km to below 20 km (by an airgun in 2000 km distance) will affect an individual's vital rates as we discuss in the next section. Note that the estimated communication ranges depend on model assumptions as outlined in chapter 5. We estimate detection ranges -if the receiving animal needs to decipher more from the signal than just the mere presence or absence of a vocalization (e.g. transmitted information as to the state of the sender or its individual identity) communication ranges are expected to be shorter than the detection ranges (in dolphins recognition thresholds have been found to be 4dB above detection thresholds by Branstetter et al. 2016). We report estimates of the absolute detection ranges to give the reader an idea of the order of magnitude, but emphasize that model results always hinge on the underlying assumptions. This holds for all reports of model estimates below and the cautionary note will not be repeated each time. For Antarctic blue whales the more conservative statement is that our model results indicate that masking of z-calls even occurs in distances from the airgun in the order of thousand kilometres.

Similar to Antarctic blue whales, the Southern hemisphere **fin whale** subspecies *Balaenoptera physalus quoyi* has a circumpolar distribution during the austral summer months. In comparison to blue whales, fin whales are less closely associated with the ice edge and mostly occur in more northerly latitudes. Their distribution in the summer feeding grounds is likely driven by the distribution of specific krill species (Herr et al. 2016). In winter fin whales migrate to lower latitudes where they breed (Aguilar et al. 2009, Leroy et al. 2018, Shabangu et al. 2019). Fin whales have been reported to vocalize more during the winter months and less in summer (Sirovic et al. 2009, Thomisch et al. 2016). It has been observed that only male fin whales produce stereotypic repetitions of the **20 Hz call** (Croll et al. 2002).

The most prominent and loudest fin whale vocalization is the 20 Hz call. Our model results suggest that detection ranges for this call strongly depend on natural ambient and airgun noise levels (Figure 79). When ambient noise levels are low detection ranges can be in the order of 1000 km in the absence of airgun noise, while detection ranges only amount to a few kilometres under higher ambient noise levels (112 dB in Figure 79) typical of the Southern Ocean. Under high ambient noise levels detection ranges are already limited by ambient noise and airgun noise causes little additional reduction of detection ranges (except when distances to the airgun fall below 1 km). By contrast, detection ranges under low ambient noise levels are estimated to diminish from 1000 km in the absence of airgun noise to approximately 1 km when an airgun is operated within a distance of 500 km from the receiving animal. Airgun noise thus has the strongest impact on fin whale communication ranges under relatively quiet ambient noise conditions.

In summary there is substantial spatiotemporal overlap between seismic surveys and Antarctic blue whale as well as fin whale distributions. In high latitudes seismic survey as well as blue and fin whale activity peak during the austral summer. In low latitudes there is continued seismic survey activity during the austral winter when blue and fin whales migrate northward. Based on the result of the auditory model that potentially fitness-relevant masking of blue whale z-calls occurs even in distances exceeding 2 000 km from the airgun location, the areas potentially affected by a single survey are huge (compare to the distance between Australia and the Antarctic continent which is approximately 3 000 km). For fin whale 20 Hz calls the auditory model suggests that masking by airgun noise is mainly relevant when ambient noise levels are moderate to low (under high ambient noise levels detection ranges are mainly ambient noise limited and airgun noise causes little additional reduction). When ambient noise levels are low, airguns in a distance of 500 km can cause potentially fitness-relevant masking of fin whale calls. For blue and fin whales little is known as to how migratory behaviour differs between sex and age groups, reproductive state and between populations. Closing this knowledge gap is important since effects of masking on individual vital rates likely depend on these parameters as we discuss in the next section (e.g. an immature or non-breeding individual may not suffer a reduction in vital rates when a mating call is masked).

6.2.3.3   Killer whale and Weddell seal

Killer whale and Weddell seal are discussed in the same subchapter, because these species produce high frequency or broadband vocalizations (Erbe et al. 2017). Only some of their vocalizations overlap with the frequency range of airgun noise (< 500 Hz) and these vocalizations typically contain substantial energy in frequency bands > 500 Hz. The auditory models have confirmed that airgun noise has no effect on communication ranges if animals can use a highpass filter to focus on frequencies above 500 Hz (Figure 80, Figure 81). In absence of airgun noise detection ranges tend to be slightly smaller if only the high frequency part (i.e. > 500 Hz) and not the full bandwidth is used (Figure 80).

For killer whale and Weddell seal broadband calls, low frequency airgun noise only has potential fitness effects if either

► the auditory system of the receiving animal cannot analyse low and high frequency parts of the vocalization separately, so that signal recognition in the high frequency part is hampered by low frequency noise, or

► biologically relevant information (e.g. information for individual recognition) is coded in the low frequency part of the vocalization that is not redundantly encoded in the high frequency part, or

► animals rely on the low-frequency part of the calls for long distance communication (over which high frequencies are severely attenuated).

Given the importance of acoustic cues and the auditory capabilities of marine mammals, it seems unlikely that signal recognition in the high frequency part is severely hampered by low frequency noise (a). Weddell seals have a very diverse vocal repertoire (Opzeeland et al. 2010, Erbe et al. 2017) and in-air calls of mothers have been reported to be so diverse that they may facilitate mother-pup recognition (Collins et al. 2005) and contain information on motivational state (Collins et al. 2011). It can therefore not be excluded that a Weddell seal that focuses exclusively on higher frequencies misses out on information encoded in the low frequency part (b). If animals rely on the low-frequency part of the calls for long distance communication is unknown (c).

In summary communication masking by airgun noise only applies to the low frequency part of killer whale and Weddell seal calls. If it suffices to detect the mere presence of a call, airgun noise likely has very limited effects on communication ranges in Weddell seals and killer whales. However, if the low frequency part contains biologically relevant information or if individuals listen specifically for the low frequency part of the vocalizations to obtain information on distant callers, airguns can cause communication masking. While communication masking by airgun noise is predicted to be less relevant for Weddell seals and killer whales than for the two baleen whale species discussed above, it remains difficult to quantify the risk of exposure to communication masking by airguns for these species.

6.2.4 Effects of communication masking at the individual level

Behavioural responses (including stress and antimasking responses) to anthropogenic noise have been discussed above (chapter 6.2.1). Here we discuss the effects of masking when it cannot be avoided by the animal, i.e. the effects of the inability of an animal to detect biologically relevant acoustic cues because they are masked by noise. Note that biologically relevant acoustic cues are not limited to vocalizations of conspecifics. Detection of sounds from predators is a key strategy to reduce predation risk in some species (Cure et al. 2015) and abiotic sounds from distant shorelines or the ice edge may be important cues for orientation (Clark et al. 2009). This study focused on the effects of communication masking by airgun noise and we discuss its effect on individual vital rates based on the modelling results in chapter 5.

Antarctic blue whales often repeat **z-calls** multiple times. This results in patterned sequences that can last for hours (Erbe et al. 2017). These songs are believed to be male display signals that serve to attract females and possibly advertise male quality and/or good foraging opportunities (Croll et al. 2002). Therefore, masking of z-calls may lead to missed foraging opportunities, may interfere with female mate choice and may even lead to missed mating opportunities for the calling male as well as a female receiving animal. Selection of a mate of high genetic quality whose genetic makeup is compatible with that of the choosing female should increase offspring fitness and can mediate adaptation to changing environmental conditions (Jones & Ratterman 2009). Since Antarctic blue whale abundance is still below 1% of the pre-exploitation levels (Branch et al. 2004), communication over extended distances may be necessary for a male to attract females and for a female to find and compare males.

Under relatively quiet ambient noise conditions (e.g. 90 dB scenario Figure 78) and in the absence of airgun noise, the auditory model predicts communication ranges exceeding 1 000 km. It is unknown if communication over such vast ranges is biologically relevant. Moreover, it is likely that these distant calls get masked by more proximal calls. Note that predicted communication ranges rapidly shrink as **ambient noise** increases to levels **typical of the Southern Ocean**: For the **112 dB scenario** we obtain an estimate of roughly 40 km in the absence of airgun noise and of roughly 15 km for an airgun in a distance of 2 000 km (Figure 78). As the airgun -receiver animal distance decreases, the estimated

communication range decreases to below 1 km. It seems very likely that a female looking for and comparing males will profit from any increase in communication range for communication ranges in this order of magnitude. Observe that the stereotypic repetition of calls may increase detection ranges, whereas e.g. the need to extract more information from the call then just its mere presence will reduce communication ranges.

We conclude that it is likely that blue whale z-calls get masked by airguns even if the distance between receiver animal and airgun is large and that this has an impact on individual vital rates. Quantifying the effects of communication masking on individual vital rates is still challenging, since we have only limited knowledge on the biological functions of the calls, have only rough estimates of communication ranges that need to be validated by experimental data and have no knowledge as to the importance of mate choice in blue whales or to the extent an individual can compensate a missed mating or foraging opportunity.

The **fin whale 20 Hz call** is believed to serve similar biological functions to the z-call in blue whales (finding and comparing mates, advertising good foraging opportunities) with only males producing stereotypic repetitions of the call (Croll et al. 2002). The call only has a short duration in comparison to the blue whale z-call and lacks a very characteristic pattern, so that it is strongly masked by airgun noise but also by ambient noise. Airguns cause particularly dramatic reductions in communication range under relatively quiet ambient noise conditions (Figure 79). *Fin whales may use windows of quiet ambient noise conditions for long range communication.* Our model results indicate that even distant airguns (in the order of 500 km between receiving animal and airgun) can totally block these "long range communication windows" (by reducing communication ranges to less than 1 km; Figure 79). Since fin whale 20 Hz calls and blue whale z-calls are assumed to serve the same biological functions, the discussion of biological effects of masking for blue whale z-calls also applies to fin whale 20 Hz calls.

As discussed in chapter 6.2.3.3 we do not know to what extent **Weddell seals** and **killer whales** depend on the masked low frequency part of their vocalizations, so that the extent to which these species suffer from communication masking by airgun noise is unclear. Male Weddell seal calls during the breeding season are likely important for the establishment of *underwater territories* (Rouget et al. 2007) and for *attracting females* (Opzeeland et al. 2010). Rogers (2017) suggested a mechanism by which calls can serve as *honest signals of male quality*: The production of repetitive sequences of underwater calls may indicate the breath-holding ability of the caller. In leopard seals only large males were able to maintain consistent rhythmic calling patterns throughout the breeding season, whereas the number of inter-vocalizing rests increased over the breeding season in small males (Rogers 2017). Similar mechanisms may allow Weddell seal females to evaluate male quality based on vocalizations. Although Weddell seal vocalization activity peaks during the breeding season, vocalizations are not restricted to this time of the year and Weddell seals produce a wide variety of different calls (Erbe et al. 2017). Functions of in-air calls include mother-pup contact calls. Depending on the importance of the low frequency part of the vocalizations for biological functionality, airgun noise may interfere with maintenance of underwater territories, mate finding, female mate choice and still unknown functions of the rich Weddell seal vocal repertoire.

6.2.5 Notes on the interpretation of the results of the psychophysical model

The **spectrogram correlation receiver model** is a very sensitive receiver, because it makes use of the full time-frequency information in the signal and the masker. Animals are expected to perform slightly worse than this receiver model that is designed to be a perfect detector using physical principles. Moreover, they are generally faced with a more challenging detection task, than the one presented to our simulated animals. In nature there is often substantial variation between instances of the same vocalization type whereas our simulated animals were faced with only a subset of this variation (indeed sometimes only a single recording of a vocalization was available). The spectrogram correlation model therefore generally tends to overestimate communication ranges and to underestimate masking. The

leaky integrator model, by contrast, only makes use of the energy in a focal frequency band. Animals are likely to perform better than this receiver, because they are expected to make at least some use of the time-frequency structure of the signal. All in all, we generally expect that the **spectrogram correlation receiver overestimates detection ranges and underestimates masking**, while the **leaky integrator** tends to underestimate detection ranges and overestimates masking.

An important aspect of communication to consider, is that for communication to occur, an animal must not only **detect a signal** in the presence of noise (energetic masking), the animal must also **recognize the signal** in the presence of noise (informational masking). Recognition requires that the animal can distinguish the temporal-spectral pattern of the received signal with enough fidelity to match the received signal with one stored in memory. Theoretically, the signal stored in memory is associated with objects and events such as *what* produces the sound and under what contexts the sound is produced. For example, it is not enough that an animal detects the signal of a conspecific, the animal must be able to recognize if the pattern of the signal has in the past, been associated with a threat, sexual advertisement, or some other context. The extra cognitive demands associated with recognition result in **increased "recognition thresholds"** relative to "detection thresholds." In bottlenose dolphins, recognition thresholds are 4 dB greater than detections thresholds (Branstetter et al. 2016). In the psychophysical model discussed in this report a headroom of 1 dB was assumed. If the actual headroom is larger (as has been found in bottlenose dolphins), our model overestimates communication ranges and underestimates masking. A low headroom was assumed in order to provide conservative estimates of masking (i.e. actual masking should be at least as strong as the model output indicates).

Masking release mechanisms such as *directional hearing* (Erbe et al. 2016) may allow animals to achieve greater communication distances than predicted by the model. There is no data as to the extent of directional hearing in baleen whales, let alone the amount of masking release that it might facilitate. Note, however, that *directional hearing abilities are generally poor at low frequencies* and that the frequencies of the vocalizations of fin and blue whales (approximately 20 Hz) have to be regarded as extremely low.

To validate our results, experimental studies on masking are needed. While disturbance responses have been studied in the field, this is much more challenging with masking. This is because disturbance responses are often associated with somewhat abrupt changes in behaviour, which can be observed in the field (such as e.g. swimming away from the noise source at high speed). Studying masking based on behavioural observations requires knowledge on how the animal behaves in the presence and absence of the biological cue. This is typically only available for captive animals that are trained to respond to a cue in order to receive a reward. Such experiments have been conducted with dolphins (Branstetter et al. 2016) and recently also pinnipeds (Sills et al. 2017), but are impossible to conduct with baleen whales. The study by Sills et al. (2017) studied how well two individuals of two Arctic seal species (one male spotted seal and one female ringed seal) were able to detect test signals (linear upsweeps from 95 to 105 Hz in 500 ms) in the presence of airgun noise recorded 1 and 30 km from an airgun array. Since only two individuals have been studied it is unknown how well the results generalize to other individuals of the same species and whether or not they apply to other species. Nevertheless, such experimental studies provide an excellent opportunity to validate the psychophysical model developed in this report. As more such studies become available, the listening situation of the experimental animals should be simulated and the predictions of the psychophysical model should be compared to the performance of the experimental animals.

6.3 Framework for understanding the consequences of disturbance at the population level

6.3.1 Introduction to strategies to evaluate population level consequences

Groups established by the National Research Council of the US National Academies and the US Office of Naval Research have developed a conceptual framework of how to study responses of individuals to a disturbance and then scale up these individual responses to demographic effects in order to study consequences of disturbance at the population level (Pirotta et al. 2018). This framework was termed "Population Consequences of Disturbance" (PCoD) and can be implemented as a quantitative model that predicts population dynamics (e.g. population growth) if sufficient data on the focal population, species and responses to disturbances are available. To date knowledge gaps exist even for the best studied marine mammal populations, so that no PCoD model has been fully parameterized with empirical data yet (Pirotta et al. 2018). However, PCoD models for well-studied populations and exposures have been implemented by drawing on knowledge from related species, using expert judgements and making informed assumptions where data on the target population and responses to exposure were incomplete. The benefits of a quantitative model are manifold:

1. Model predictions provide a robust basis for conservation and management decisions provided that sufficient data is available and predictions are robust (see next point).
2. Robustness of predictions to uncertainties in input parameters can be tested quantitatively (e.g. by evaluating worst- and best-case scenarios and by evaluating distributions of outcome variables).
3. The modelling process forces researchers to think clearly about the system and state clearly any assumptions they are making. This way knowledge gaps can be identified and their effect on the model predictions can be evaluated.

In this study we use the PCoD framework to structure our discussion of the masking effects at the population level and to identify knowledge gaps. The rational of the PCoD framework (Figure 82) can be summarized as follows: When an individual is exposed to a stressor, its physiological state and its behaviour change. Physiological and behavioural changes can in turn directly ("acute effects") or indirectly ("chronic effects") affect the individual's vital rates (i.e. survival and fecundity). This relationship is modulated by environmental conditions. Based on modelling the exposure risk of an individual and based on basic population parameters, the population dynamics can then be modelled. In the following we discuss the available knowledge on the modelled Antarctic populations for each of the main steps of a PCoD-model.

Figure 82   : Conceptual framework of the PCoD-model (reproduced from Pirotta et al. 2018). Exposure to a stressor and effects of exposure on physiology, behaviour and ultimately vital rates are studied at an individual level (grey boxes). The effects on all individuals in the population (stacked grey boxes) are then integrated to model the population dynamics.
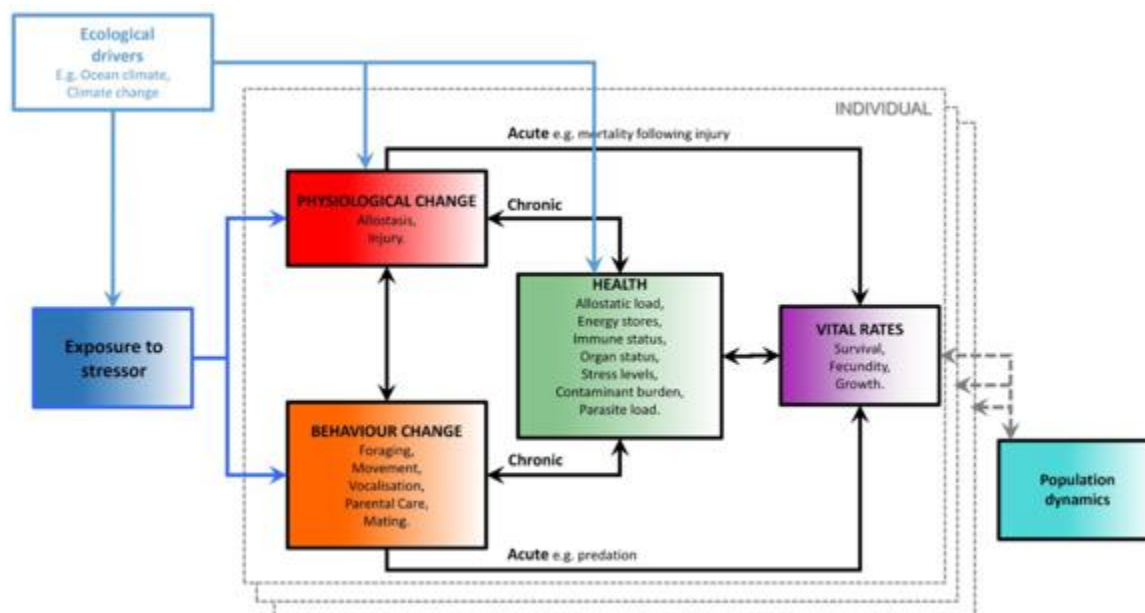
6.3.2 Identify populations and obtain basic demographic and population parameters

In order to preserve biodiversity and ecosystem functionality, conservation efforts should focus at the population level. Loss of populations entails loss of genetic diversity and can destabilize local ecosystem functionality (even if other populations of the same species thrive). Knowledge of population structure is therefore important to define optimal units for management and conservation purposes. When building a PCoD model the first logical step is to identify the target population and obtain estimates of the sex and age structure (i.e. how many individuals are in each sex and age class of the population) as well as the basic demographic rates (survival and fecundity of individuals in the different age and sex classes in the absence of disturbance).

For **Antarctic blue whales** (*Balaenoptera musculus intermedia*) it is e.g. known that they become sexually mature around the age of 10 years (Branch et al. 2009). An inter-calf interval of 2 -3 years is assumed for females, because gestation lasts for at least 10 months, weaning lasts for 7 months and simultaneous pregnancy and lactation is rare (Branch 2008). The number of Antarctic blue whales declined from 239 000 before the start of blue whale hunting in the austral summer of 1904/05 to only 360 individuals when hunting was ended in the summer of 1972/73 (Branch et al. 2004). Based on surveys conducted between 1992 and 2004 the number of Antarctic blue whales was estimated to be 2 280 individuals (Branch et al. 2007). Genetic studies of the population structure have found evidence of *three Antarctic blue whale populations* (Attard et al. 2016). The three populations are sympatric in the Antarctic feeding grounds but likely breed in separate geographic areas (Attard et al. 2016). To ensure that the breeding grounds of all populations remain occupied and to prevent further loss of genetic diversity in the Antarctic blue whale subspecies, which has experienced a severe bottleneck and whose numbers are still below 1% of the pre-exploitation abundance, conservation measures have to preserve all three populations. Observe that a single seismic survey may expose a substantial proportion of all individuals in a population to airgun noise, particularly if the survey coincides with aggregations of blue whales at e.g. breeding or feeding grounds. Precise data on the sex and age structure as well as the demographic rates of the individual populations are currently not available. This is a typical challenge

when developing PCoD models. Modelling studies have shown that while highly precise estimates of population structure and demographic parameters are always an asset, high precision in these parameters is not absolutely essential to develop models that give insight into effects of a disturbance at the population level (Pirotta et al. 2018).

All in all the data and studies cited above should suffice to make informed assumptions on the missing values of demographic rates with similar efforts having been done in the past (Taylor et al. 2007). For fin whales and Weddell seals informed assumptions can be made in a similar way.

6.3.3 Estimate exposure probabilities for individuals in the population

This step has already been discussed when evaluating the effects at the individual level (chapter 6.2.3).

6.3.4 Estimate effects of exposure first on behaviour or physiology and ultimately on vital rates of an individual

This step has already been discussed when evaluating the effects at the individual level (chapter 6.2.4).

6.3.5 Modelling the population dynamics

The final step of the PCoD framework scales up the effects on vital rates of individuals to predict the dynamics of the population over time. Typically, no additional input data is needed for this step. Depending on how exposure probability and exposure effect vary between individuals or are contingent on events in an individual's life history, different modelling techniques can be used. The extreme approaches are that either all individuals in a population are treated as identical or that each individual is explicitly followed from birth to death (Pirotta et al. 2018).

7 Conclusion and research needs

The sound propagation models for the Antarctic Ocean and the auditory models for different marine mammals indicate that airgun noise is likely to mask marine mammal calls - in particular low frequency calls of baleen whales (e.g. Antarctic blue whale and Southern fin whale). The behavioural context of call production together with the time and energy animals invest in calling indicates that Antarctic blue whale z-calls and fin whale 20 Hz calls have important functions in mating and possibly also foraging contexts. Declines in individual vital rates (that entail effects at the population level) are therefore likely when calls are masked. Main conclusions of the study are:

▶ The pilot study on blue whales in Iceland suggests that blue whale calling rates increase as ambient noise levels increase. This may be an antimasking strategy.

▶ The **numerical sound propagation models** based on a parabolic equation and a parabolic equation -normal mode approach have been found to predict transmission loss and signal stretching accurately. Model predictions have been verified based on recordings of airgun signals in the Southern Ocean (including recordings at a depth of 140 m which is a typical dive depth for blue and fin whales). Sound scattering by surface wind waves was found to be an important cause of transmission loss at higher frequencies in the region south of the polar front (where the sound channel is located close to the sea surface). For airguns at the northern edge of the Southern Ocean (over the Australian shelf) highest noise levels in Antarctica were predicted and observed when the airgun was located over the continental slope at water depths of 300 -700 m (at greater water depths the shallow airgun source is not well coupled with the SOFAR channel). If recordings in multiple receiver depths can be obtained, more comprehensive validation of the sound propagation models can be conducted in the future.

▶ **Low -frequency airgun noise (< 300 Hz**) could be detected in recordings at a distance of several thousand kilometres from the airgun source location despite the high ambient noise levels in the Southern Ocean. In line with this observation, the auditory model predicts that noise from airguns in a distance of 1000 - 2000 kilometres from the receiving animal can severely reduce communication ranges of blue and fin whales (Figure 73 and 74). In fin whales ambient noise can severely reduce communication ranges even in the absence of airgun noise. Airgun noise during periods of low ambient noise levels can block time windows of long range communication opportunities for fin whales.

▶ Reductions in operation time and airgun source levels can reduce the areas in which masking occurs. (A 10dB reduction of the airgun source level roughly reduces the affected area to a tenth of its original size.)

▶ Killer whales and Weddell seals have **high-frequency or broadband vocalizations**. Only the low frequency part of the calls is masked by airgun noise. If it suffices to detect the mere presence of a call, airgun noise likely has very limited effects on communication ranges in Weddell seals and killer whales. However, as discussed in 6.2.3, it is likely that the low frequency part contains biologically relevant information and that individuals listen specifically for the low frequency part of the vocalizations to obtain information on distant callers. If either is the case, airguns can cause communication masking in these species.

▶ The context in which blue whale z-calls and fin whale 20 Hz calls are produced indicates that these calls have important functions for mating and possibly also foraging. Masking may lead to missed foraging opportunities, may interfere with female mate choice and may even lead to missed mating opportunities for the calling male as well as a female receiving animal. This certainly has the potential to affect individual vital rates and population dynamics, albeit quantifying effects is still difficult. Studies on the behavioural context of calls (e.g. using tags and possibly additional data on the environmental and social context) can help to shed light on biological functions of calls (see e.g. Lewis et al. 2018). Playback experiments may be used to study behavioural responses of individuals to calls. Individual follows over longer time periods (accompanied by collections of as much data as

possible on the environmental and social context) may allow us to learn more about the extent to which an individual can compensate a missed mating or foraging opportunity. Moreover the rough estimates of communication ranges need to be verified by experimental data.

► The crucial knowledge gap that hampers development of models of population consequences is, that exposure effects on individual vital rates are still difficult to quantify (as discussed in the bullet point above). Data to make informed assumptions on population parameters are available, albeit models would profit from a better understanding of the population delineations and migration patterns.

8 References

Aguilar. 2009. Fin whale - Balaenoptera physalus.*in* W. Perrin, B. Würsig, and J. Thewissen, editors. Encyclopedia of marine mammals. Academic Press, Amsterdam.

Ainslie, M. A., and J. G. McColm. 1998. A simplified formula for viscous and chemical absorption in sea water. Journal of the Acoustical Society of America **103**:1671-1672.

Akamatsu, T., M. H. Rasmussen, and M. Iversen. 2014. Acoustically invisible feeding blue whales in Northern Icelandic waters. Journal of the Acoustical Society of America **136**:939-944.

Attard, C. R. M., L. B. Beheregaray, and L. M. Moller. 2016. Towards population-level conservation in the critically endangered Antarctic blue whale: the number and distribution of their populations. Scientific Reports **6**.

Au, W. W. L., and M. C. Hastings. 2008. Principles of Marine Bioacoustics.

Bejder, L., A. Samuels, H. Whitehead, and N. Gales. 2006. Interpreting short-term behavioural responses to disturbance within a longitudinal perspective. Animal Behaviour **72**:1149-1158.

Boebel, O., M. Breitzke, E. Burkhardt, and H. Bornemann. 2009a. Strategic assessment of the risk posed to marine mammals by the use of airguns in the Antarctic Treaty area. Alfred Wegener Institute for Polar and Marine Research.

Boebel, O., M. Breitzke, E. Burkhardt, and H. Bornemann. 2009b. Strategic assessment of the risk posed to marine mammals by the use of airguns in the Antarctic Treaty area. AWI.

Branch, T. A., K. Matsuoka, and T. Miyashita. 2004. Evidence for increases in Antarctic blue whales based on Bayesian modelling. Marine Mammal Science **20**:726-754.

Branch, T. A., and Y. A. Mikhalev. 2008. Regional differences in length at sexual maturity for female blue whales based on recovered Soviet whaling data. Marine Mammal Science **24**:690-703.

Branch, T. A., Y. A. Mikhalev, and H. Kato. 2009. Separating pygmy and Antarctic blue whales using long-forgotten ovarian data. Marine Mammal Science **25**:833-854.

Branch, T. A., K. M. Stafford, D. M. Palacios, C. Allison, J. L. Bannister, C. L. K. Burton, E. Cabrera, C. A. Carlson, B. G. Vernazzani, P. C. Gill, R. Hucke-Gaete, K. C. S. Jenner, M. N. M. Jenner, K. Matsuoka, Y. A. Mikhalev, T. Miyashita, M. G. Morrice, S. Nishiwaki, V. J. Sturrock, D. Tormosov, R. C. Anderson, A. N. Baker, P. B. Best, P. Borsa, R. L. Brownell, S. Childerhouse, K. P. Findlay, T. Gerrodette, A. D. Ilangakoon, M. Joergensen, B. Kahn, D. K. Ljungblad, B. Maughan, R. D. McCauley, S. McKay, T. F. Norris, O. Whale, S. Rankin, F. Samaran, D. Thiele, K. Van Waerebeek, R. M. Warneke, and G. Dolphin Res. 2007. Past and present distribution, densities and movements of blue whales Balaenoptera musculus in the Southern Hemisphere and northern Indian Ocean. Mammal Review **37**:116-175.

Branstetter, B. K., K. Bakhtiari, A. Black, J. S. Trickey, J. J. Finneran, and H. Aihara. 2016. Energetic and informational masking of complex sounds by a bottlenose dolphin (Tursiops truncatus). Journal of the Acoustical Society of America **140**:1904-1917.

Breitzke, M., and T. Bohlen. 2010. Modelling sound propagation in the Southern Ocean to estimate the acoustic impact of seismic research surveys on marine mammals. Pages 818-846 Geophysical Journal International.

Castellote, M., C. W. Clark, and M. O. Lammers. 2012. Acoustic and behavioural changes by fin whales (Balaenoptera physalus) in response to shipping and airgun noise. Biological Conservation **147**:115-122.

Cerchio, S., S. Strindberg, T. Collins, C. Bennett, and H. Rosenbaum. 2014. Seismic Surveys Negatively Affect Humpback Whale Singing Activity off Northern Angola. Plos One **9**.

Christiansen, F., C. G. Bertulli, M. H. Rasmussen, and D. Lusseau. 2015. Estimating Cumulative Exposure of Wildlife to Non-Lethal Disturbance Using Spatially Explicit Capture-Recapture Models. Journal of Wildlife Management **79**:311-324.

Christiansen, F., M. Rasmussen, and D. Lusseau. 2013. Whale watching disrupts feeding activities of minke whales on a feeding ground. Marine Ecology Progress Series **478**:239-+.

Clark, C. W., W. T. Ellison, B. L. Southall, L. Hatch, S. M. Van Parijs, A. Frankel, and D. Ponirakis. 2009. Acoustic masking in marine ecosystems: intuitions, analysis, and implication. Marine Ecology Progress Series **395**:201-222.

Collins, K. T., P. D. McGreevy, K. E. Wheatley, and R. G. Harcourt. 2011. The influence of behavioural context on Weddell seal (Leptonychotes weddellii) airborne mother-pup vocalisation. Behavioural Processes **87**:286-290.

Collins, K. T., T. L. Rogers, J. M. Terhune, P. D. McGreevy, K. E. Wheatley, and R. G. Harcourt. 2005. Individual variation of in-air female 'pup contact' calls in Weddell seals, Leptonychotes weddellii. Behaviour **142**:167-189.

Collins, M. D. 1993. A split-step Padé solution for the parabolic equation method. Pages 1736-1742 J. Acoust. Soc. Am.

Croll, D. A., C. W. Clark, A. Acevedo, B. Tershy, S. Flores, J. Gedamke, and J. Urban. 2002. Bioacoustics: Only male fin whales sing loud songs - These mammals need to call long-distance when it comes to attracting females. Nature **417**:809-809.

Cummings, W. C., and P. O. Thompson. 1971. UNDERWATER SOUNDS FROM BLUE WHALE, BALAENOPTERA-MUSCULUS. Journal of the Acoustical Society of America **50**:1193-&.

Cure, C., L. D. Sivle, F. Visser, P. J. Wensveen, S. Isojunno, C. M. Harris, P. H. Kvadsheim, F. P. A. Lam, and P. J. O. Miller. 2015. Predator sound playbacks reveal strong avoidance responses in a fight strategist baleen whale. Marine Ecology Progress Series **526**:267-282.

Di Iorio, L., and C. W. Clark. 2010. Exposure to seismic survey alters blue whale acoustic communication. Biology Letters **6**:334-335.

Duncan, A. 1998. Research into the Acoustic Charateristics of an Air Gun Sound Source. CMST Report C98-18 prepared for the Defence Science and Technology Organisation, Curtin University.

Duncan, A. J., A. N. Gavrilov, R. D. McCauley, I. M. Parnum, and J. M. Collis. 2013. Characteristics of sound propagation in shallow water over an elastic seabed with a thin cap-rock layer. Journal of the Acoustical Society of America **134**:207-215.

Dunlop, R. A., D. H. Cato, and M. J. Noad. 2014. Evidence of a Lombard response in migrating humpback whales (Megaptera novaeangliae). Journal of the Acoustical Society of America **136**:430-437.

Dunlop, R. A., M. J. Noad, D. H. Cato, E. Kniest, P. J. O. Miller, J. N. Smith, and M. D. Stokes. 2013. Multivariate analysis of behavioural response experiments in humpback whales (Megaptera novaeangliae). Journal of Experimental Biology **216**:759-770.

Edds-Walton. 1997. Acoustic communication signals of mysticete whales. Bioacoustics **8**:47-60.

Erbe, C. 2008. Critical ratios of beluga whales (Delphinapterus leucas) and masked signal duration. Journal of the Acoustical Society of America **124**:2216-2223.

Erbe, C., R. Dunlop, K. C. S. Jenner, M. N. M. Jenner, R. D. McCauley, I. Parnum, M. Parsons, T. Rogers, and C. Salgado-Kent. 2017. Review of Underwater and In-Air Sounds Emitted by Australian and Antarctic Marine Mammals. Acoustics Australia **45**:179-241.

Erbe, C., C. Reichmuth, K. Cunningham, K. Lucke, and R. Dooling. 2016. Communication masking in marine mammals: A review and research strategy. Marine Pollution Bulletin **103**:15-38.

Feng, A. S., and R. Ratnam. 2000. Neural basis of hearing in real-world situations. Annual Review of Psychology **51**:699-725.

Finneran, J. J. 2015. Noise-induced hearing loss in marine mammals: A review of temporary threshold shift studies from 1996 to 2015. Journal of the Acoustical Society of America **138**:1702-1726.

Finneran, J. J. 2016. Auditory weighting functions and TTS/PTS exposure functions for marine mammals exposed to underwater noise. SSC Pacific TR 3026, San Diego.

Foote, A. D., R. W. Osborne, and A. R. Hoelzel. 2004. Environment - Whale-call response to masking boat noise. Nature **428**:910-910.

Gavrilov, A. N., R. D. McCauley, C. Salgado-Kent, J. Tripovich, and C. Burton. 2011. Vocal characteristics of pygmy blue whales and their change over time. Journal of the Acoustical Society of America **130**:3651-3660.

Gavrilov, A. 2018. Propagation of Underwater Noise from an Offshore Seismic Survey in Australia to Antarctica: Measurements and Modelling. Acoust Aust **46**, 143–149.

Gedamke, J., N. Gales, and S. Frydman. 2011. Assessing risk of baleen whale hearing loss from seismic surveys: The effect of uncertainty and individual variation. Journal of the Acoustical Society of America **129**:496-506.

Geophysical, P. 2006. PGS Geophysical on Aragorn 3D survey in Bass Strait, Tasmania. prepared for Wooside Energy Ltd., Project No. 20598.

Herr, H., S. Viquerat, V. Siegel, K. H. Kock, B. Dorschel, W. G. C. Huneke, A. Bracher, M. Schroder, and J. Gutt. 2016. Horizontal niche partitioning of humpback and fin whales around the

West Antarctic Peninsula: evidence from a concurrent whale and krill survey. Polar Biology **39**:799-818.

Holt, M. M., D. P. Noren, V. Veirs, C. K. Emmons, and S. Veirs. 2009. Speaking up: Killer whales (Orcinus orca) increase their call amplitude in response to vessel noise. Journal of the Acoustical Society of America **125**:EL27-EL32.

Iversen, M., M. Rasmussen, E. E. Magnusdottir, and M. O. Lammers. 2011. Recordings of a blue whale sound with single hydrophone and ecological acoustical recorders (EARS). Poster at the 19-biannual conferences by Society of Marine Mammology, Tampa, Florida.

Jensen, F. B., W. A. Kuperman, M. B. Porter, and H. Schmidt. 2011. Computational Ocean Acoustics. Springer, New York.

Jones, A. G., and N. L. Ratterman. 2009. Mate choice and sexual selection: What have we learned since Darwin? Proceedings of the National Academy of Sciences of the United States of America **106**:10001-10008.

Kastelein, R. A., L. Helder-Hoek, S. V. Van de Voorde, A. M. von Benda-Beckmann, F. P. A. Lam, E. Jansen, C. A. F. de Jong, and M. A. Ainslie. 2017. Temporary hearing threshold shift in a harbor porpoise (Phocoena phocoena) after exposure to multiple airgun sounds. Journal of the Acoustical Society of America **142**:2430-2442.

Kuningas, S., P. H. Kvadsheim, F. P. A. Lam, and P. J. O. Miller. 2013. Killer whale presence in relation to naval sonar activity and prey abundance in northern Norway. Ices Journal of Marine Science **70**:1287-1293.

Kuperman, W. A., and F. Ingentio. 1977. Attenuation of coherent component of sound propagating in shallow water with rough boundaries. Pages 1178-1187 J. Acoust. Sco. Am.

Kvadsheim, P. H., S. DeRuiter, L. D. Sivle, J. Goldbogen, R. Roland-Hansen, P. J. O. Miller, F. P. A. Lam, J. Calarnbokidis, A. Friedlaender, F. Visser, P. L. Tyack, L. Kleivane, and B. Southall. 2017. Avoidance responses of minke whales to 1-4 kHz naval sonar. Marine Pollution Bulletin **121**:60-68.

Leroy, E. C., F. Samaran, K. M. Stafford, J. Bonnel, and J. Y. Royer. 2018. Broad-scale study of the seasonal and geographic occurrence of blue and fin whales in the Southern Indian Ocean. Endangered Species Research **37**:289-300.

Li, B., and A. N. Gavrilov. 2006. Hydroacoustic observation of Antarctic ice disintegration events in the Indian Ocean. First Australasian Acoustical Societies' Conference, Acoustics 2006: Noise of Progress.

Marler, P. 1997. Three models of song learning: Evidence from behavior. Journal of Neurobiology **33**:501-516.

McDonald, M. A., J. Calambokidis, A. M. Teranishi, and J. A. Hildebrand. 2001. The acoustic calls of blue whales off California with gender data. Journal of the Acoustical Society of America **109**:1728-1735.

McDonald, M. A., J. A. Hildebrand, and S. Mesnick. 2009. Worldwide decline in tonal frequencies of blue whale songs. Endangered Species Research **9**.

Miller, P. J. O., N. Biassoni, A. Samuels, and P. L. Tyack. 2000. Whale songs lengthen in response to sonar. Nature **405**:903-903.

Miller, P. J. O., P. H. Kvadsheim, F. P. A. Lam, P. J. Wensveen, R. Antunes, A. C. Alves, F. Visser, L. Kleivane, P. L. Tyack, and L. D. Sivle. 2012. The Severity of Behavioral Changes Observed During Experimental Exposures of Killer (Orcinus orca), Long-Finned Pilot (Globicephala melas), and Sperm (Physeter macrocephalus) Whales to Naval Sonar. Aquatic Mammals **38**:362-401.

Mohl, B., M. Wahlberg, P. T. Madsen, L. A. Miller, and A. Surlykke. 2000. Sperm whale clicks: Directionality and source level revisited. Journal of the Acoustical Society of America **107**:638-648.

Nieukirk, S. L., D. K. Mellinger, S. E. Moore, K. Klinck, R. P. Dziak, and J. Goslin. 2012. Sounds from airguns and fin whales recorded in the mid-Atlantic Ocean, 1999-2009. Journal of the Acoustical Society of America **131**:1102-1112.

Nowacek, D. P., C. W. Clark, D. Mann, P. J. O. Miller, H. C. Rosenbaum, J. S. Golden, M. Jasny, J. Kraska, and B. L. Southall. 2015. Marine seismic surveys and ocean noise: time for coordinated and prudent planning. Frontiers in Ecology and the Environment **13**:378-386.

Pirotta, E., C. G. Booth, D. P. Costa, E. Fleishman, S. D. Kraus, D. Lusseau, D. Moretti, L. F. New, R. S. Schick, L. K. Schwarz, S. E. Simmons, L. Thomas, P. L. Tyack, M. J. Weise, R. S. Wells,

and J. Harwood. 2018. Understanding the population consequences of disturbance. Ecology and Evolution **8**:9934-9946.

Proakis, J. G., and D. G. Manolaiks. 2006. Digital signal processing. 4th edition. Pearson, New York.

Reichmuth, C., Sills, J. M., Mulsow, J., & Ghoul, A. (2019). Long-term evidence of noise-induced permanent threshold shift in a harbor seal (Phoca vitulina). The Journal of the Acoustical Society of America, 146(4), 2552-2561.

Rogers, T. L. 2017. Calling underwater is a costly signal: size-related differences in the call rates of Antarctic leopard seals. Current Zoology **63**:433-443.

Roth, E. H., J. A. Hildebrand, S. M. Wiggins, and D. Ross. 2012. Underwater ambient noise on the Chukchi Sea continental slope from 2006-2009. Pages 103-114 J. Acoust. Soc. Am.

Rouget, P. A., J. M. Terhune, and H. R. Burton. 2007. Weddell seal underwater calling rates during the winter and spring near Mawson Station, Antarctica. Marine Mammal Science **23**:508-523.

Samaran, F., K. M. Stafford, T. A. Branch, J. Gedamke, J. Y. Royer, R. P. Dziak, and C. Guinet. 2013. Seasonal and Geographic Variation of Southern Blue Whale Subspecies in the Indian Ocean. Plos One **8**.

Schmidt, R. F., G. Thews, and F. Lang. 2000. Physiologie des Menschen. 28 edition. Springer.

Shabangu, F. W., K. P. Findlay, D. Yemane, K. M. Stafford, M. van den Berg, B. Blows, and R. K. Andrew. 2019. Seasonal occurrence and diel calling behaviour of Antarctic blue whales and fin whales in relation to environmental conditions off the west coast of Check for South Africa. Journal of Marine Systems **190**:25-39.

Siebert, U., M. Dähne, S. Danehl, O. Meyer-Klaeden, A. van Neer, D. Wittekind, M. Max Schuster, K. Lucke, C. W. Clark, P. Stilz, J. Tougaard, S. von Benda-Beckmann, and M. A. Ainslie. 2013. Assessment of potential for masking in marine mammals of the Antarctic exposed to underwater sound from airguns. Umweltbundesamt, FKZ 3711 19 121.

Sills, J. M., B. L. Southall, and C. Reichmuth. 2017. The influence of temporally varying noise from seismic air guns on the detection of underwater sounds by seals. Journal of the Acoustical Society of America **141**:996-1008.

Sills, J. M., Reichmuth, C., Southall, B. L., Whiting, A., & Goodwin, J. (2020). Auditory biology of bearded seals (Erignathus barbatus). Polar Biology, 43(11), 1681-1691.

Sirovic, A., J. A. Hildebrand, and S. M. Wiggins. 2007. Blue and fin whale call source levels and propagation range in the Southern Ocean. Journal of the Acoustical Society of America **122**:1208-1215.

Sirovic, A., J. A. Hildebrand, S. M. Wiggins, and D. Thiele. 2009. Blue and fin whale acoustic presence around Antarctica during 2003 and 2004. Marine Mammal Science **25**:125-136.

Sivle, L. D., P. H. Kvadsheim, C. Cure, S. Isojunno, P. J. Wensveen, F. P. A. Lam, F. Visser, L. Kleivane, P. L. Tyack, C. M. Harris, and P. J. O. Miller. 2015. Severity of Expert-Identified Behavioural Responses of Humpback Whale, Minke Whale, and Northern Bottlenose Whale to Naval Sonar. Aquatic Mammals **41**:469-502.

Sivle, L. D., P. H. Kvadsheim, A. Fahlman, F. P. A. Lam, P. L. Tyack, and P. J. O. Miller. 2012. Changes in dive behavior during naval sonar exposure in killer whales, long-finned pilot whales, and sperm whales. Frontiers in Physiology **3**.

Southall, B., A. E. Bowles, and W. T. Ellison. 2007. Marine mammal noise exposure criteria: Initial Scientific recommendations. Aquatic Mammals **33**.

Southall, B. L., D. P. Nowacek, P. J. O. Miller, and P. L. Tyack. 2016. Experimental field studies to measure behavioral responses of cetaceans to sonar. Endangered Species Research **31**:293-315.

Stafford, K. M., D. R. Bohnenstiehl, M. Tolstoy, E. Chapp, D. K. Mellinger, and S. E. Moore. 2004. Antarctic-type blue whale calls recorded at low latitudes in the Indian and eastern Pacific Oceans. Deep-Sea Research Part I-Oceanographic Research Papers **51**:1337-1346.

Taylor, B. L., M. Martinez, T. Gerrodette, J. Barlow, and Y. N. Hrovat. 2007. Lessons from monitoring trends in abundance of marine mammals. Marine Mammal Science **23**:157-175.

Tervo, O. M., M. F. Christoffersen, M. Simon, L. A. Miller, F. H. Jensen, S. E. Parks, and P. T. Madsen. 2012. High Source Levels and Small Active Space of High-Pitched Song in Bowhead Whales (Balaena mysticetus). Plos One **7**.

Thomas, J. A., K. C. Zinnel, and L. M. Ferm. 1983. ANALYSIS OF WEDDELL SEAL (LEPTONYCHOTES-WEDDELLI) VOCALIZATIONS USING UNDERWATER PLAYBACKS. Canadian Journal of Zoology-Revue Canadienne De Zoologie **61**:1448-1456.

Thomisch, K., O. Boebel, C. W. Clark, W. Hagen, S. Spiesecke, D. P. Zitterbart, and I. Van Opzeeland. 2016. Spatio-temporal patterns in acoustic presence and distribution of Antarctic blue whales Balaenoptera musculus intermedia in the Weddell Sea. Endangered Species Research **30**:239-253.

Thorp, W. H. 1965. DEEP-OCEAN SOUND ATTENUATION IN SUB- AND LOW-KILOCYCLE-PER-SECOND REGION. Journal of the Acoustical Society of America **38**:648-&.

Thorp, W. H. 1967. Analytic description of the low-frequency attenuation Coefficient. Page 270 The Journal of the Acoustical Society of America.

Van Opzeeland, I., S. Van Parijs, H. Bornemann, S. Frickenhaus, L. Kindermann, H. Klinck, J. Plotz, and O. Boebel. 2010. Acoustic ecology of Antarctic pinnipeds. Marine Ecology Progress Series **414**:267-291.

Van Opzeeland, I. C., S. M. Van Parijs, S. Frickenhaus, C. M. Kreiss, and O. Boebel. 2012. Individual variation in pup vocalizations and absence of behavioral signs of maternal vocal recognition in Weddell seals (Leptonychotes weddellii). Marine Mammal Science **28**:E158-E172.

Wahlberg, M., B. Mohl, and P. T. Madsen. 2001. Estimating source position accuracy of a large-aperture hydrophone array for bioacoustics. Journal of the Acoustical Society of America **109**:397-406.

Westwood, E. K., C. T. Tindle, and N. R. Chapman. 1996. A normal mode model for acousto-elastic ocean environments. Journal of the Acoustical Society of America **100**:3631-3645.

Wilkes, D. R., T. P. Gourlay, and A. N. Gavrilov. 2016. Numerical Modeling of Radiated Sound for Impact Pile Driving in Offshore Environments. Ieee Journal of Oceanic Engineering **41**:1072-1078.

9   Appendix

9.1   Appendix: Estimated communication ranges for the different environmental scenarios

9.1.1   Introduction

The diagrams show the calculated maximum communication range (ordinate) between two animals dependent on the distance of an airgun from the receiver animal (abscissa). Each colour represents a different ocean noise condition. Many different environmental scenarios were examined. The diagrams are ordered (from top level to lowest level) by species and call type, propagation model, vocalization depth, water depth, receiver depth and auditory model. Word users can quickly access the results diagram of a focal scenario using the navigation pane, which provides an overview over the nested headlines. Diagram titles also contain all information on the modelled scenario in abbreviated form -the coding is explained below. Thus, users can either access a focal scenario by following the verbal headlines or (alternatively) get all information on the modelled scenario based on the diagram title.

The distances of the receiver animal from the airgun (horizontal axis) and the sender animal (vertical axis) are scaled logarithmically. The distance "Inf" at the far right of the diagram indicates the condition without airgun ("infinite distance"). Results for the spectrogram correlator model are shown on the left; results for the leaky integrator model are shown on the right.

The dashed horizontal lines indicate the total interval sampled for determination of the maximum communication range. If the determined maximum communication range is above this testing interval, it will be indicated by the maximum value "Inf," if the range falls below, it will be indicated by the minimal "Nan."

Six ocean noise situations were examined:

1. "112 dB noise" = high levels of ocean noise
2. "102 dB noise" = medium levels of ocean noise
3. "94 dB noise" = moderate levels of ocean noise (high low-frequency proportion)
4. "102 -> 90 dB" = the 102 dB noise reduced by 12 dB
5. "80 dB noise" = the noise situation of the earlier report
6. "no noise" = absence of noise

The sequence of the line drawing is ordered from the lowest noise first to the highest noise last. If a line is partially covered, it is thus always covered by lines of higher noise.

The diagram titles contain all information on the modelled scenario in abbreviated form. The coding is as follows.

a)   Exact code block for exact specification: for example

"v1-a700-v0021-r31"

b) Readable block: for examples

"bw_zcall wd4000 vd000 rd010 spg_xc+1"

Code block:

"v1-a700-v0021-r31"

1. "v1-": vocalization number:

"v1" = blue whale Z call

"v2" = fin whale

"v3" = killer whale multi-harmonic

"v5" = Weddell seal long sound

"v7" = Weddell seal, sound sequence

2. "-a0700-": sound propagation model (= transfer scenario) of the airgun (four digits)

a) First three digits indicate the transfer function used

"a002_" = spherical geometrical attenuation (2D)

"a010_" = transfer scenario 1: sd:5 m, water depth 500 m, receiver depth 10 m, up to 375 Hz,

"a020_" = transfer scenario 2: sd:5 m, water depth 500 m, receiver depth 50 m, up to 375 Hz

"a030_" = transfer scenario 3: sd:5 m, water depth 500 m, receiver depth 200 m, up to 375 Hz

"a040_" = transfer scenario 4: sd:5 m, water depth 500 m, receiver depth 10 m, up to 1,500 Hz

"a050_" = transfer scenario 5: sd:5 m, water depth 500 m, receiver depth 50 m, up to 1,500 Hz

"a060_" = transfer scenario 6: sd:5 m, water depth 500 m, receiver depth 200 m, up to 1500 Hz

"a070_" = transfer scenario 7: sd:5 m, water depth 4,000 m, receiver depth 10 m, up to 375 Hz

"a080_" = transfer scenario 8: sd:5 m, water depth 4,000 m, receiver depth 50 m, up to 375 Hz

"a090_" = transfer scenario 9: sd:5 m, water depth 4,000 m, receiver depth 200 m, up to 375 Hz

"a110_" = transfer scenario 11: sd:50 m, water depth 500 m, receiver depth 10 m, up to 375 Hz,

"a120_" = transfer scenario 12: sd:50 m, water depth 500 m, receiver depth 50 m, up to 375 Hz

"a130_" = transfer scenario 13: sd:50 m, water depth 500 m, receiver depth 200 m, up to 375 Hz

"a140_" = transfer scenario 14: sd:50 m, water depth 500 m, receiver depth 10 m, up to 1,500 Hz

"a150_" = transfer scenario 15: sd:50 m, water depth 500 m, receiver depth 50 m, up to 1,500 Hz

"a160_" = transfer scenario 16: sd:50 m, water depth 500 m, receiver depth 200 m, up to 1500 Hz

"a170_" = transfer scenario 17: sd:50 m, water depth 4,000 m, receiver depth 10 m, up to 375 Hz

"a180_" = transfer scenario 18: sd:50 m, water depth 4,000 m, receiver depth 50 m, up to 375 Hz

"a190_" = transfer scenario 19: sd:50 m, water depth 4,000 m, receiver depth 200 m, up to 375 Hz

b)   Last digit: modelling attenuation

"a__0" = attenuation according to Thorp

"a__1" = attenuation numerically calculated (Ainslie, McColm)

3.   "-v0021-": transfer scenarios of the vocalization with identical designations as for airgun under 2.)

4.   "-r31": receiver model and stimulus difference limit

a)   First digit: receiver model:

"r3_" = spectrogram correlator

"r4_" = leaky integrator

b)   Second digit: difference limit:

"_0" = 0 dB

"_1" = 1 dB

Readable title block:

"bw_zcall wd4000 vd000 rd010 spg_xc+1"

1.   Designation vocalization:

"bw_zcall" = blue whale Z call

"fw_call"   = fin whale

"kw_call"   = killer whale multi-harmonic

"wd_long"   = Weddell seal long sound

"wd_train" = Weddell seal, sound sequence

2.   Water depth of the airgun propagation in meters

wd0500 = 500 m

wd4000 = 4,000 m

wd0000 = spherical modelling of the airgun and vocalization propagation

3. Vocalization depth

vd005 = 5 m

vd050 = 50 m

vd000 = spherical modelling of the vocalization propagation

4. Receiver depth

rd010 = 10 m

rd050 = 50 m

rd200 = 200 m

rd000 = spherical modelling of the airgun and vocalization propagation

5. Receiver model

spg_xc = spectrogram correlator

lk_int = leaky integrator

6. Stimulus difference threshold

+0 = 0 dB

+1 = 1 dB

9.1.2   Blue whale z-call

9.1.2.1   Propagation of both airgun and vocalization are modelled by numerical transfer functions

9.1.2.1.1   Vocalization depth is 5 m
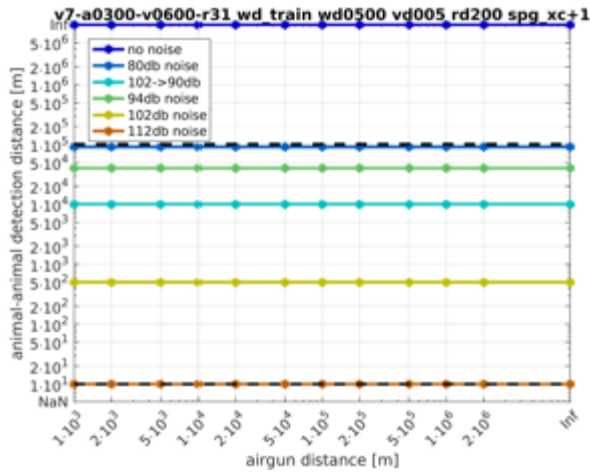
9.1.2.1.1.1   Water depth is 500 m

► Receiver depth is 10 m:
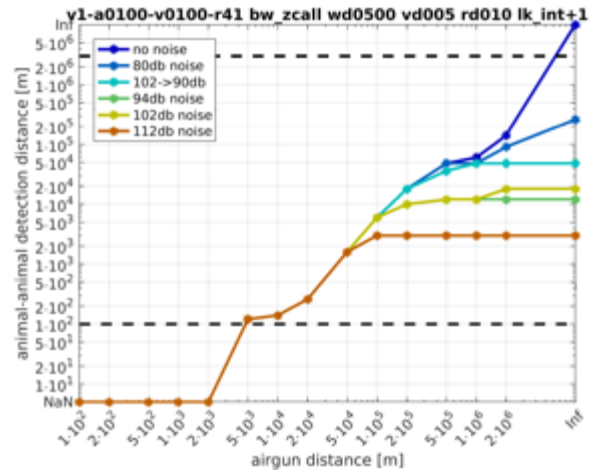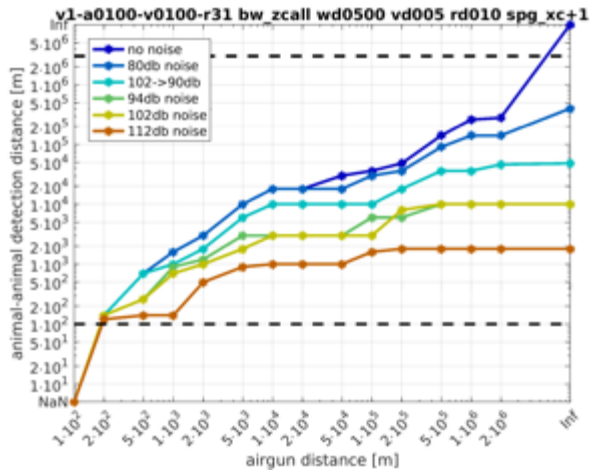
► Receiver depth is 50 m:
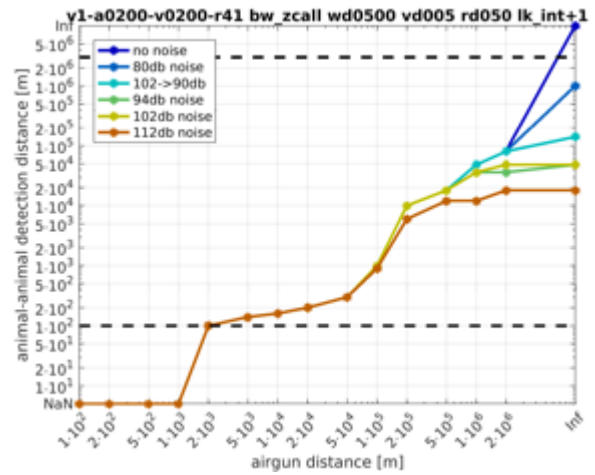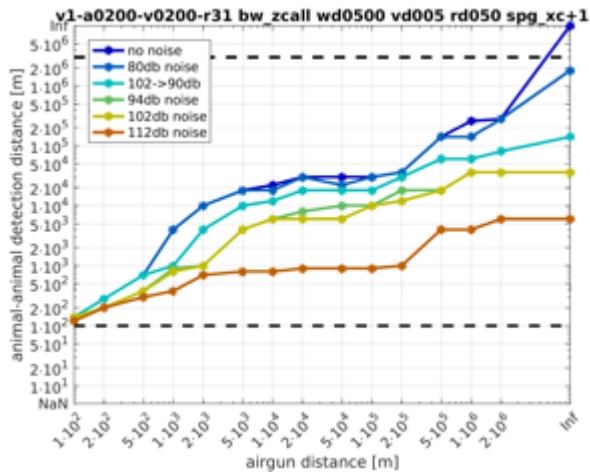
► Receiver depth is 200 m:
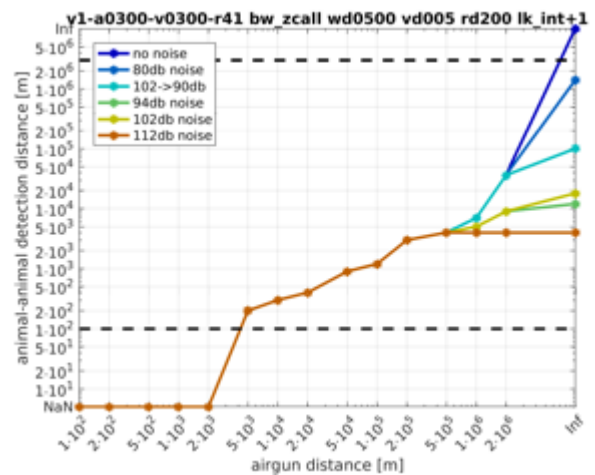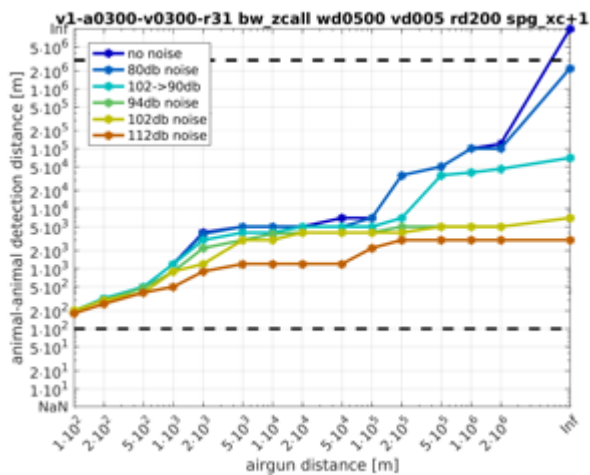
9.1.2.1.1.2 Water depth is 4000 m

► Receiver depth is 10 m:
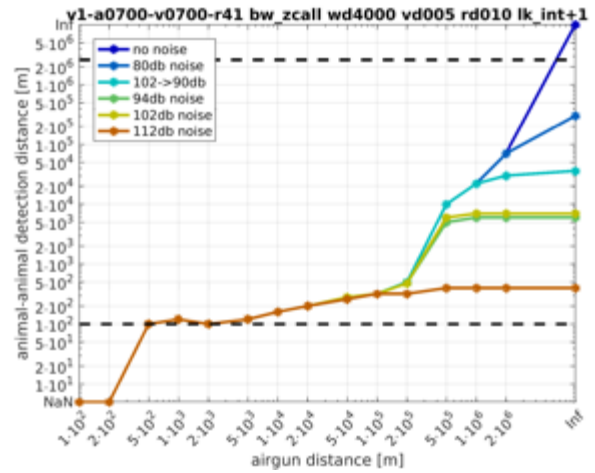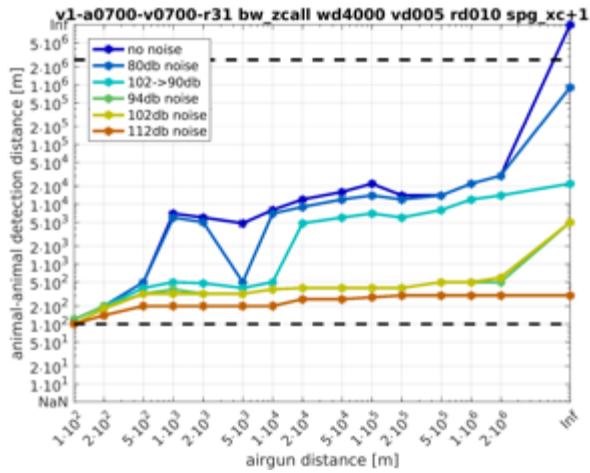
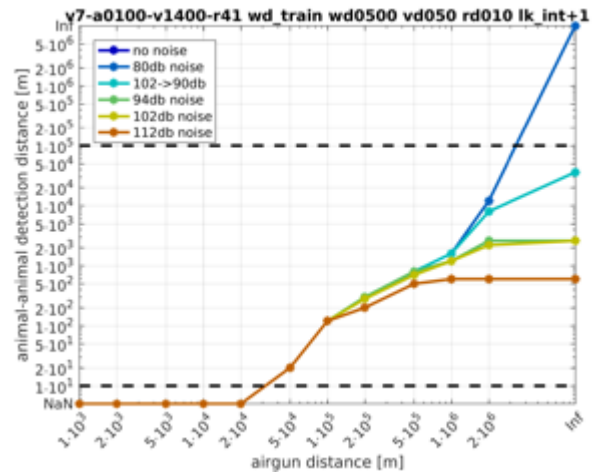▶ Receiver depth is 50 m:
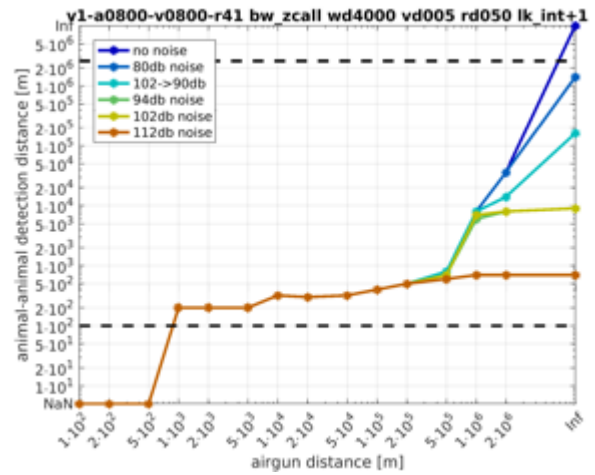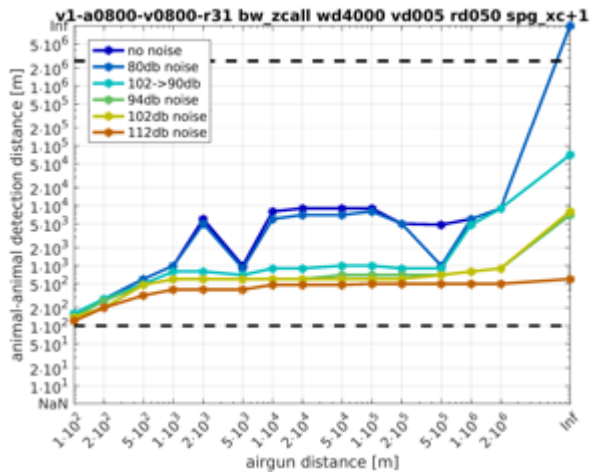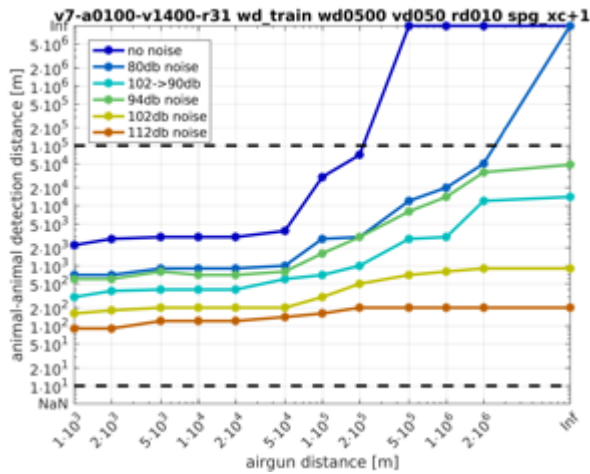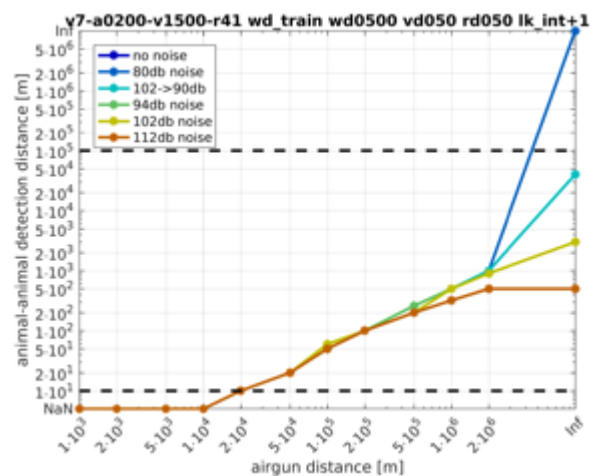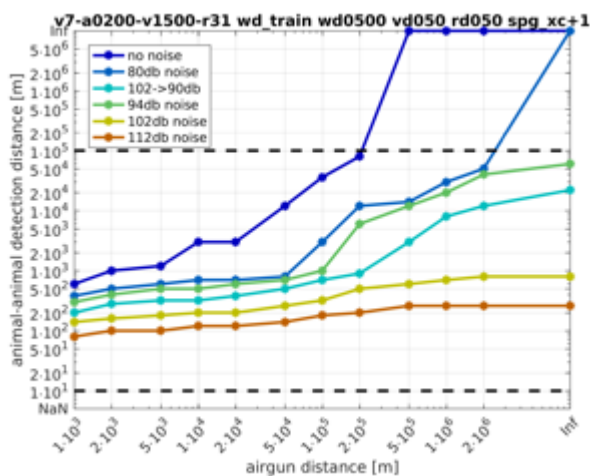

▶ Receiver depth is 200 m:
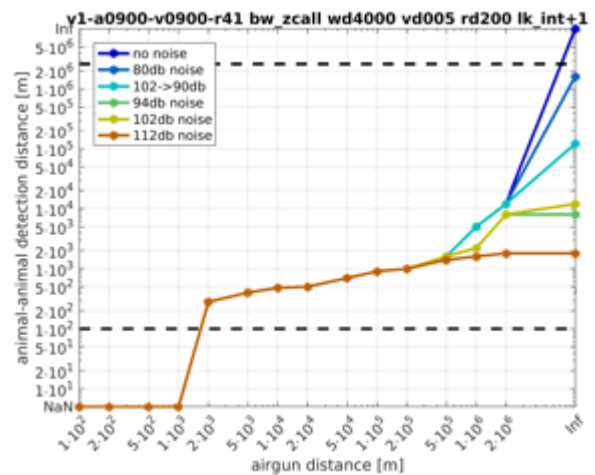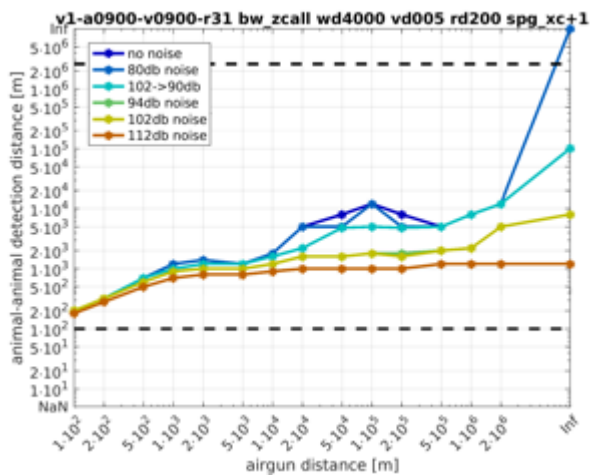
9.1.2.1.2 Vocalization depth is 50 m

9.1.2.1.2.1 Water depth is 500 m

▶ Receiver depth is 10 m:
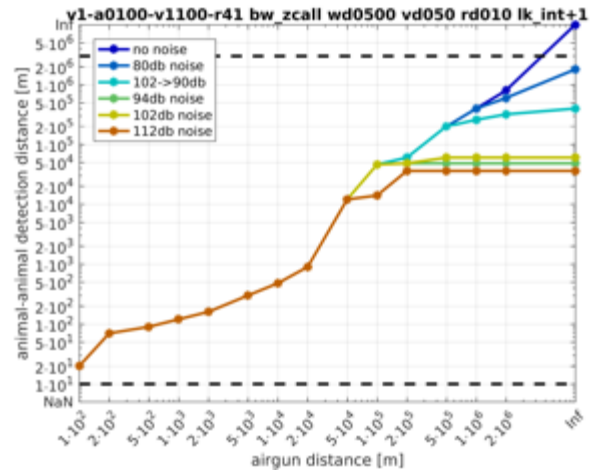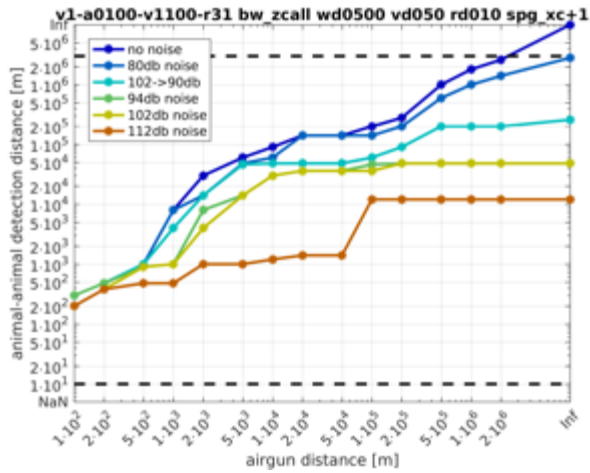
► Receiver depth is 50 m:
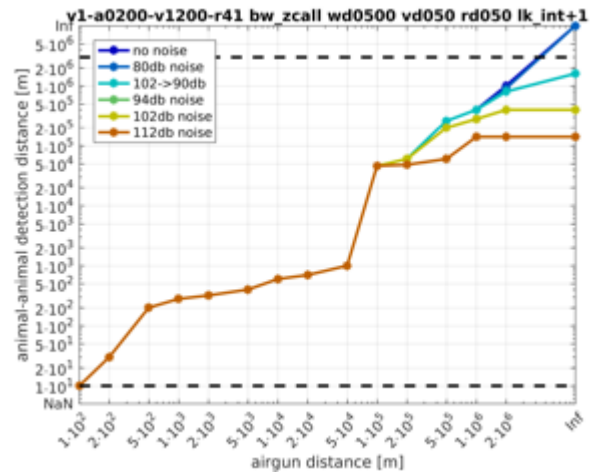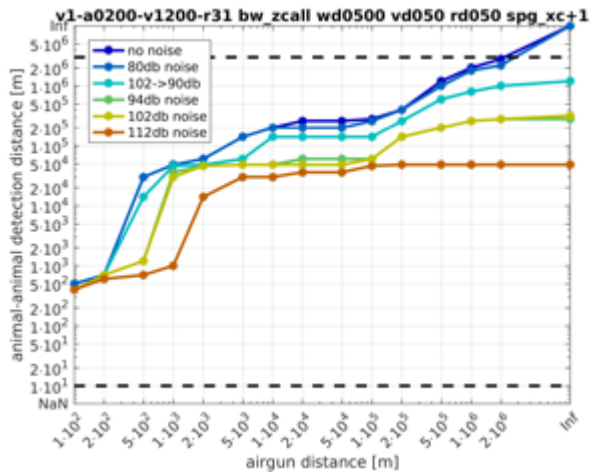
► Receiver depth is 200 m:
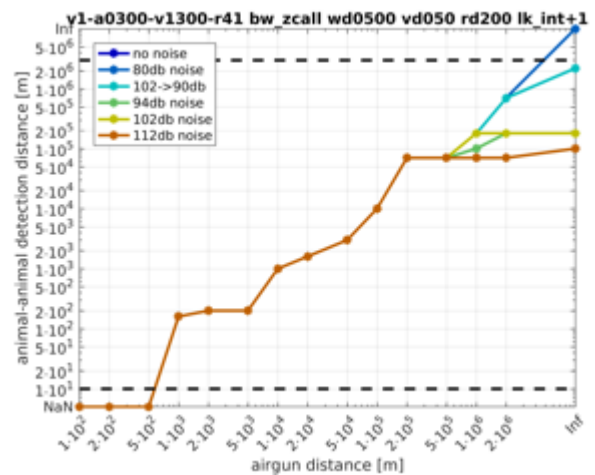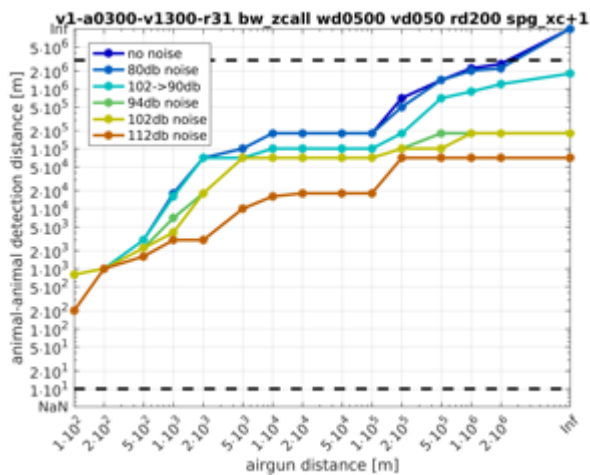
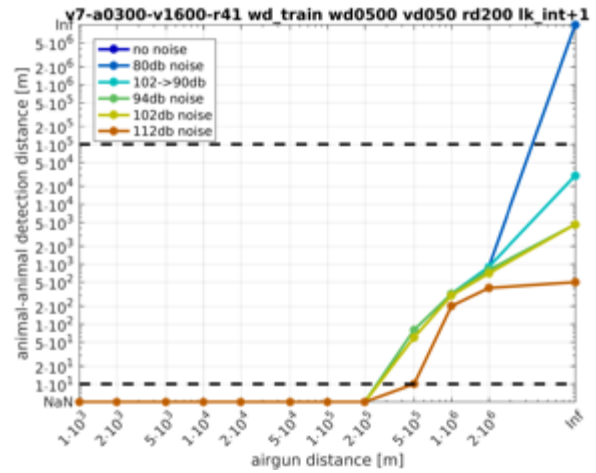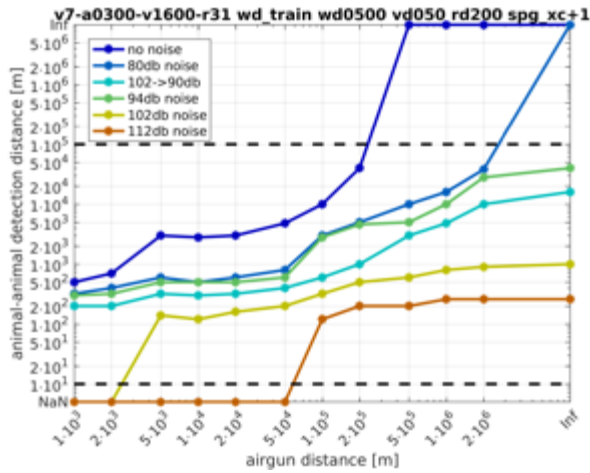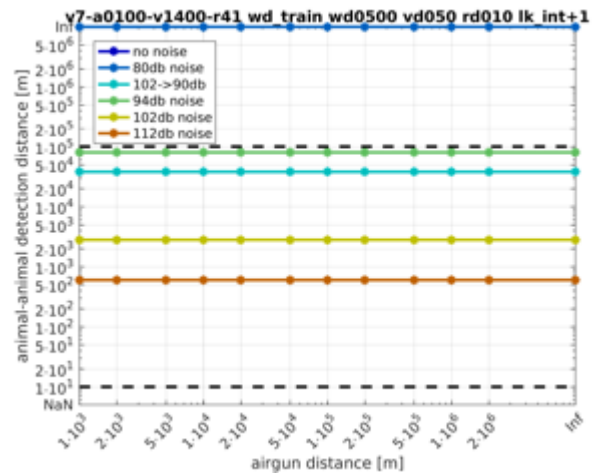### 9.1.2.1.2.2   Water depth is 4000 m

► Receiver depth is 10 m:
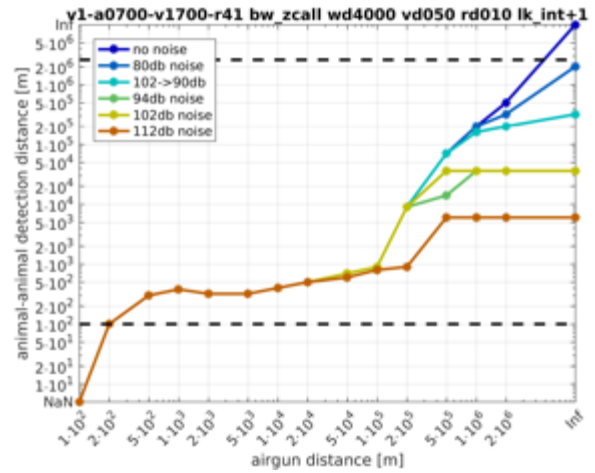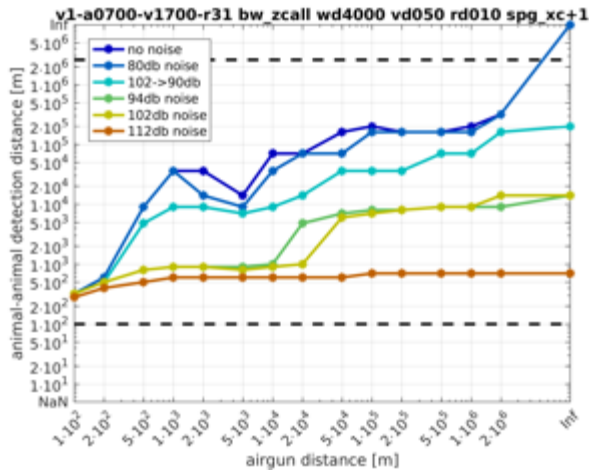
► Receiver depth is 50 m:
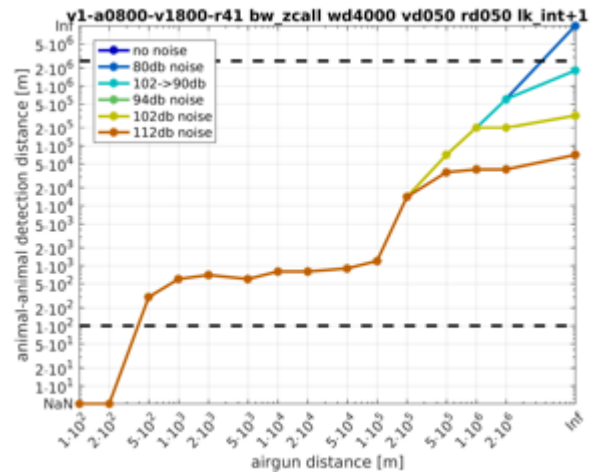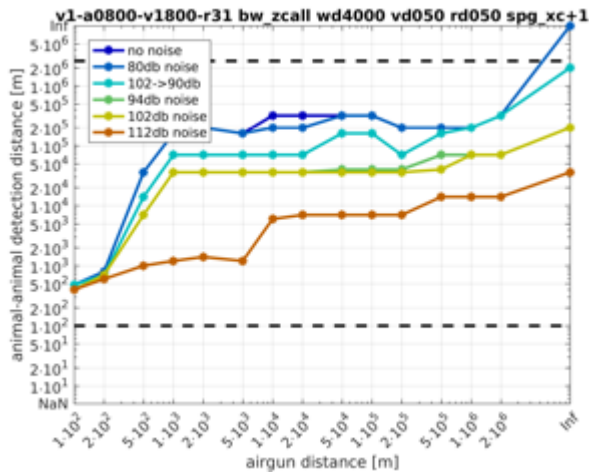
► Receiver depth is 200 m:
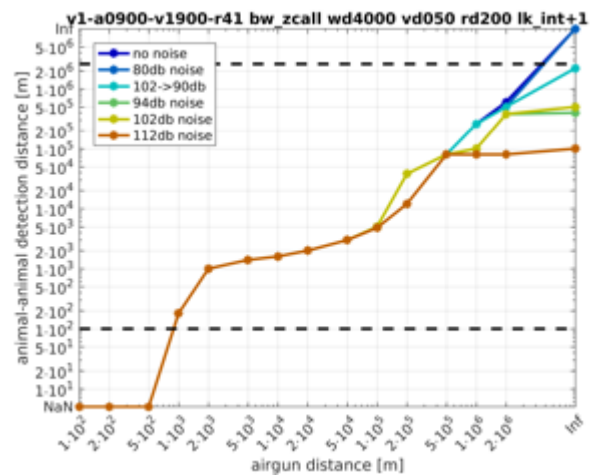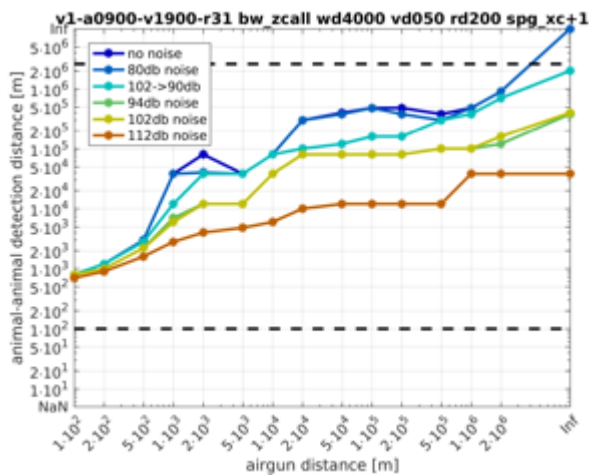
9.1.2.1.3 Propagation of airgun is modelled by numerical transfer functions, propagation of vocalization is modelled assuming spherical spreading

9.1.2.1.3.1 *Water depth is 500 m*
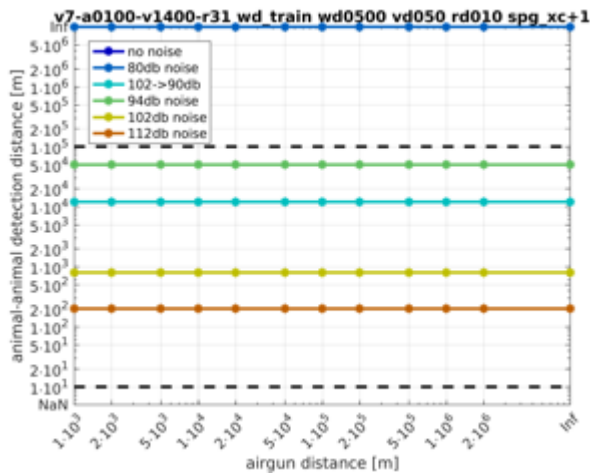
► Receiver depth is 10 m:
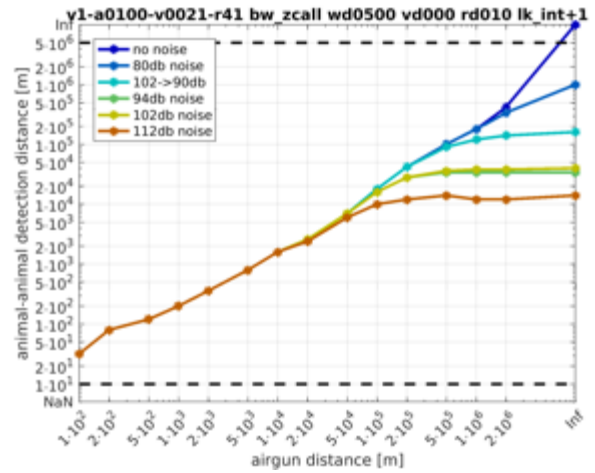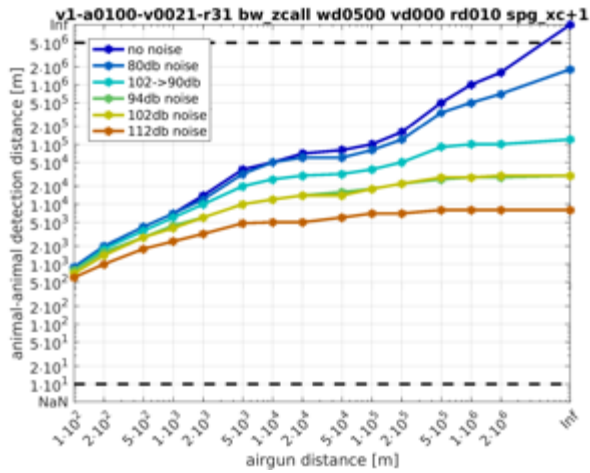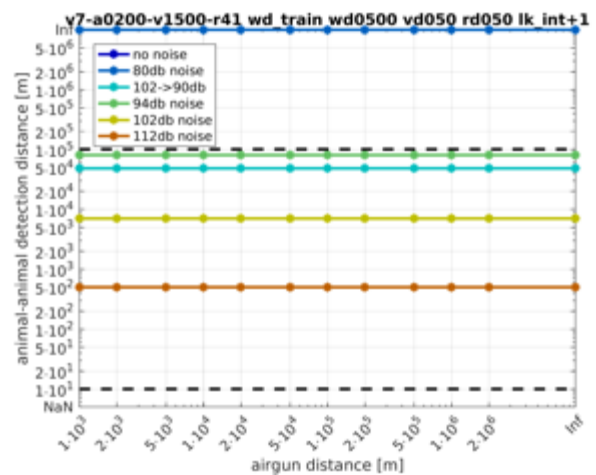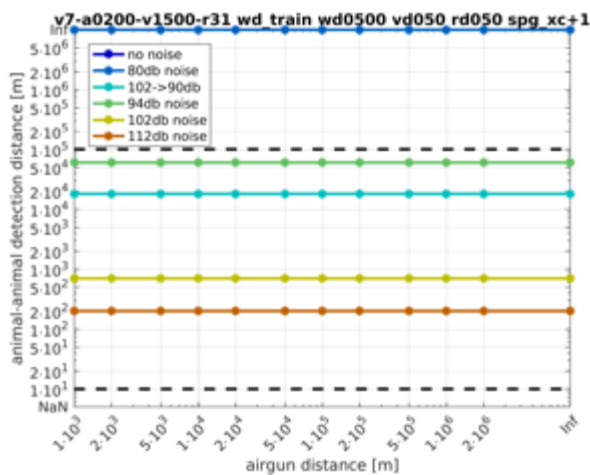
► Receiver depth is 50 m:
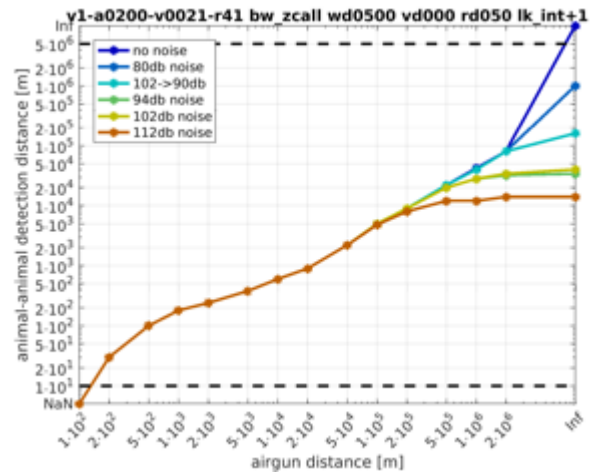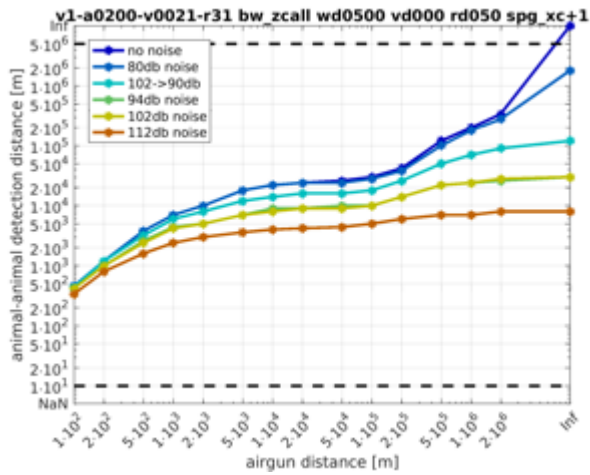
► Receiver depth is 200 m:
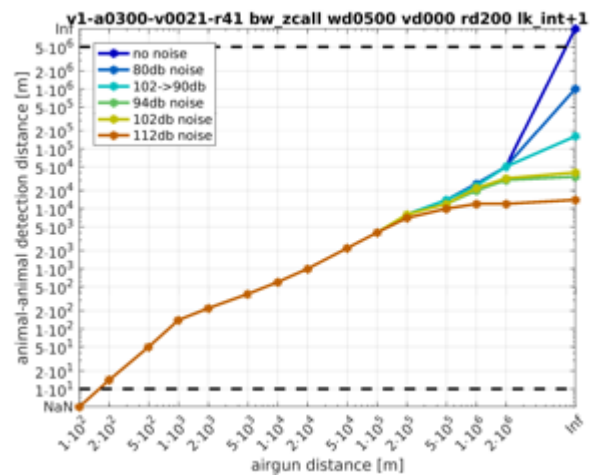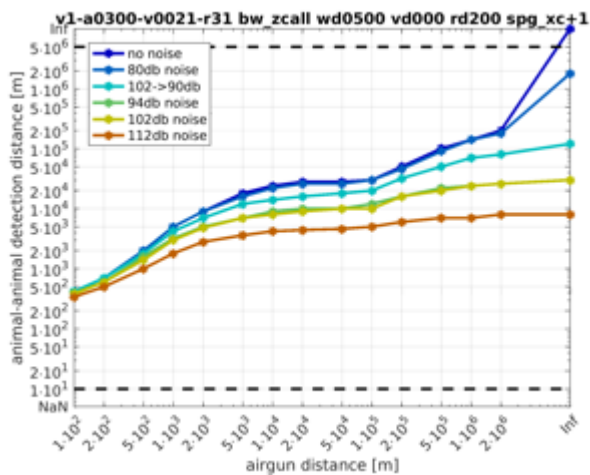
9.1.2.1.3.2 Water depth is 4000 m

► Receiver depth is 10 m:
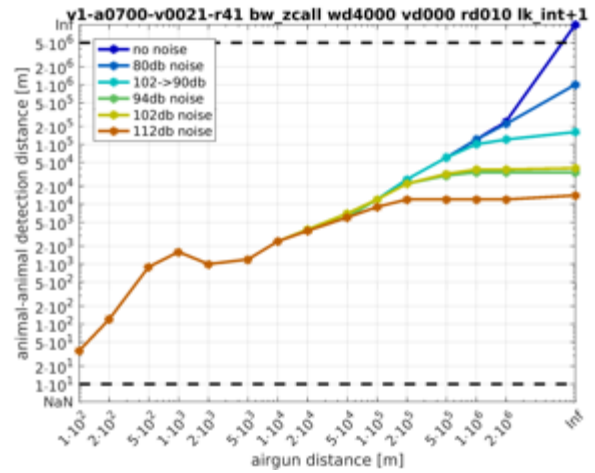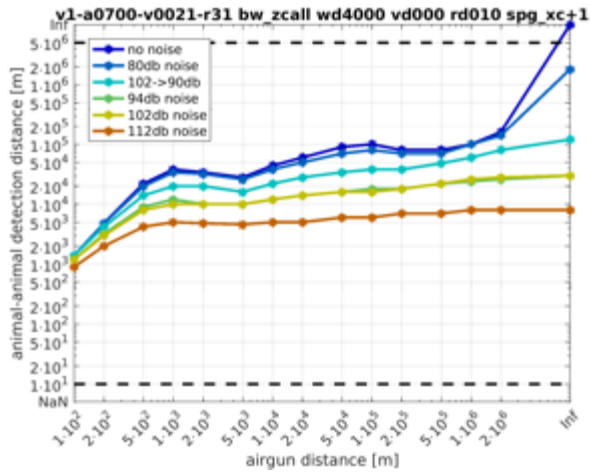
► Receiver depth is 50 m:
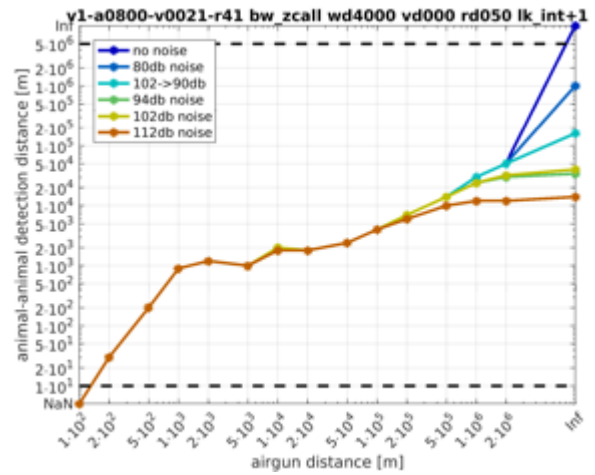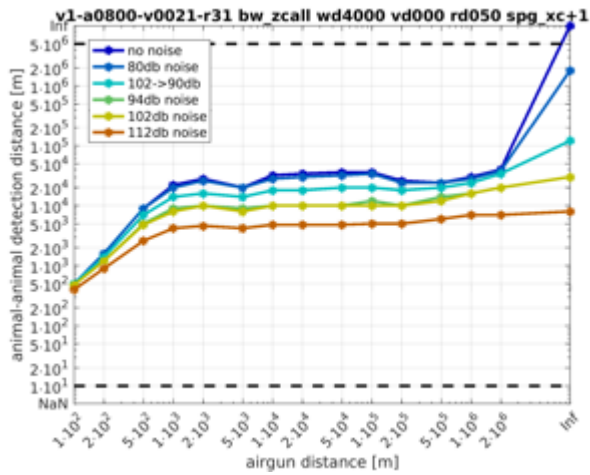
► Receiver depth is 200 m:
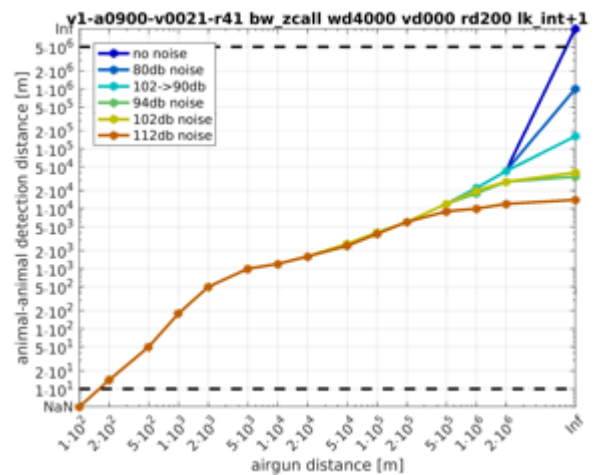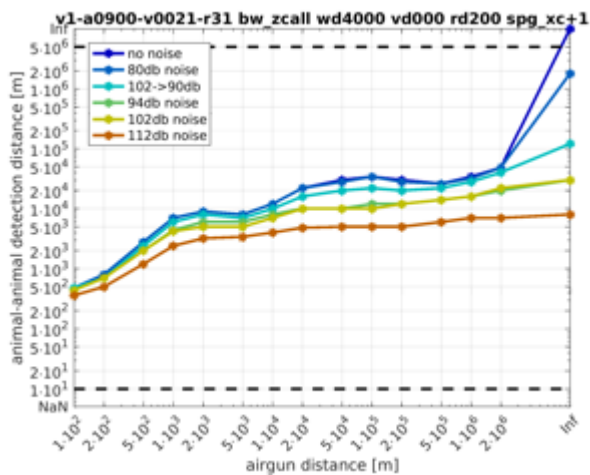
9.1.2.1.4 Propagation of airgun and vocalization is modelled assuming spherical spreading
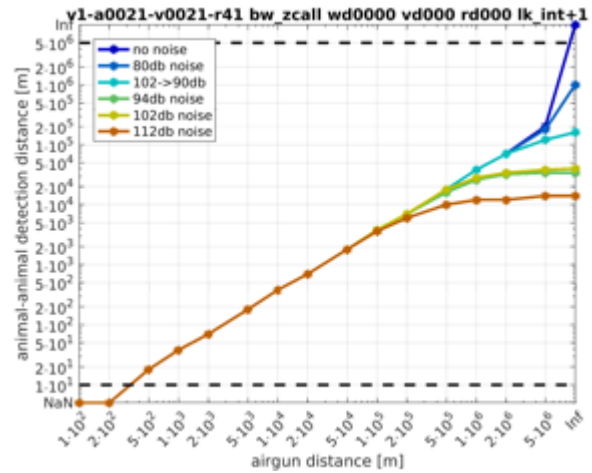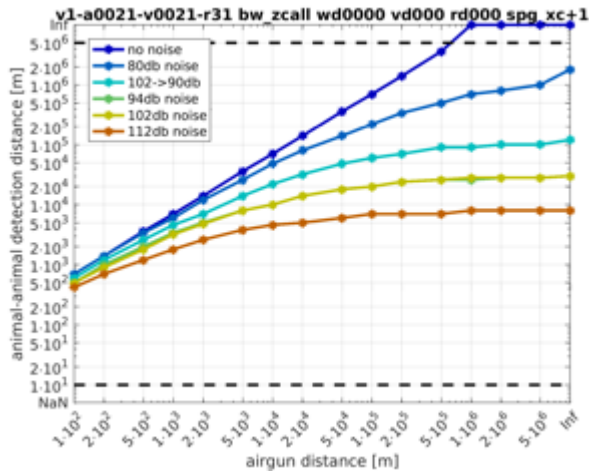
9.1.3 Fin whale 20 Hz call

9.1.3.1 Propagation of both airgun and vocalization are modelled by numerical transfer functions

9.1.3.1.1 Vocalization depth is 5 m

9.1.3.1.1.1 Water depth is 500 m

► Receiver depth is 10 m:
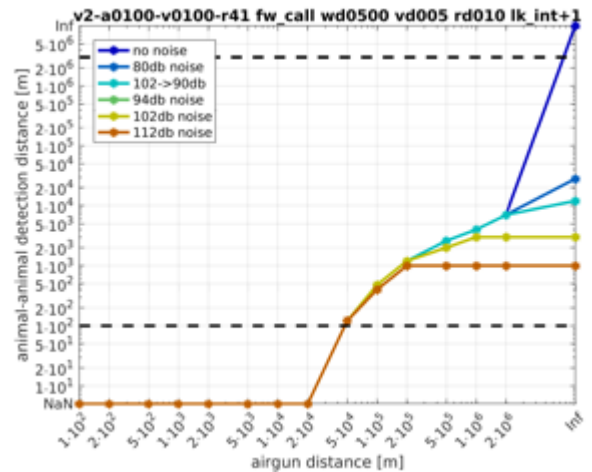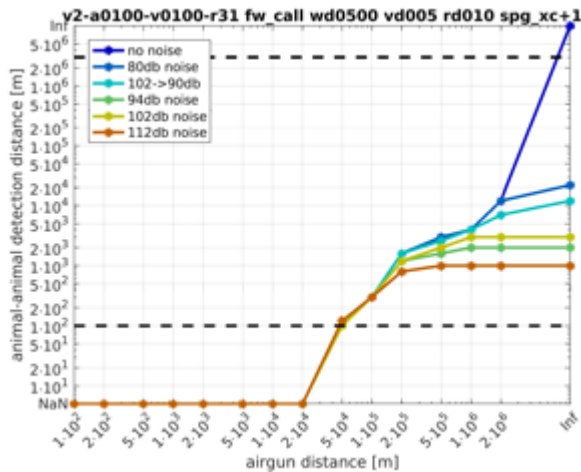
► Receiver depth is 50 m:
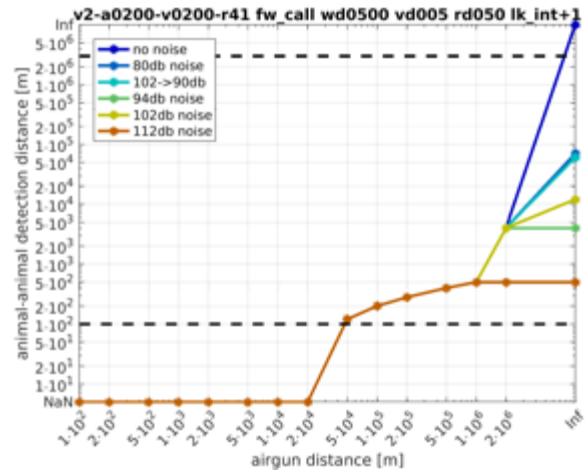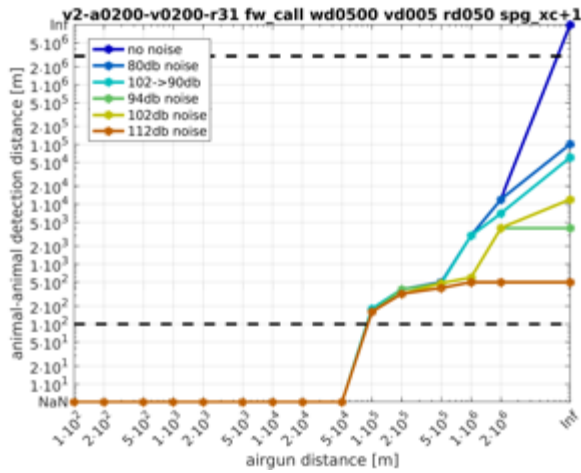
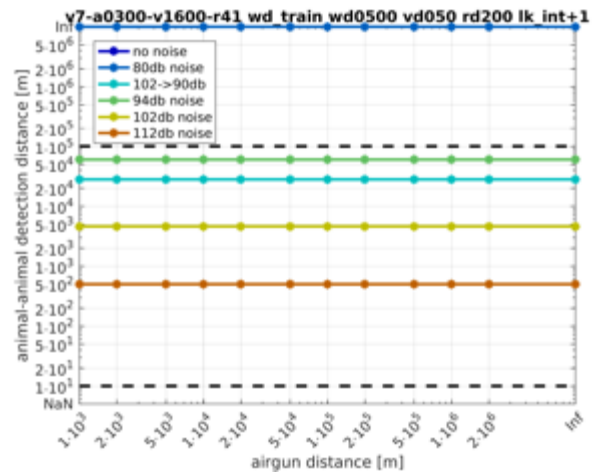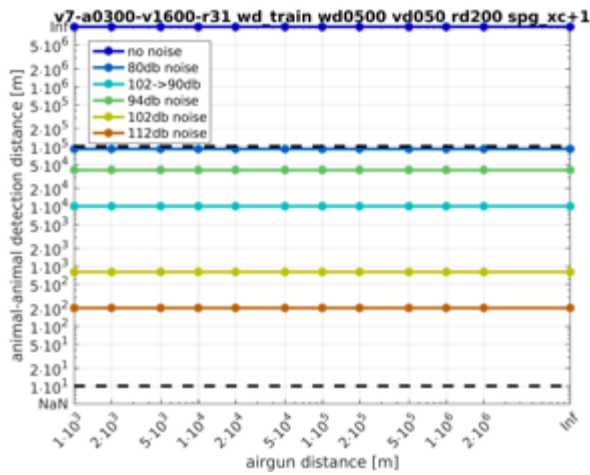► Receiver depth is 200 m:
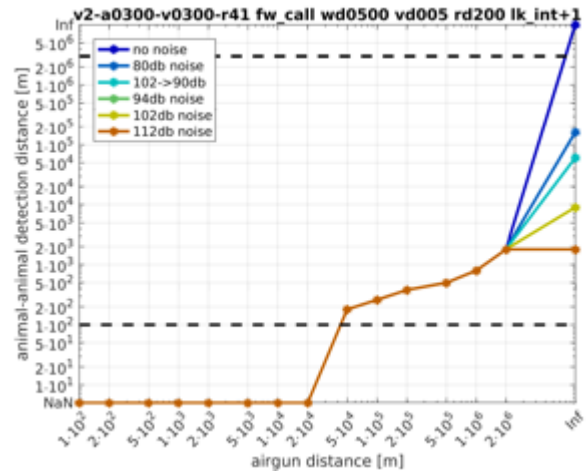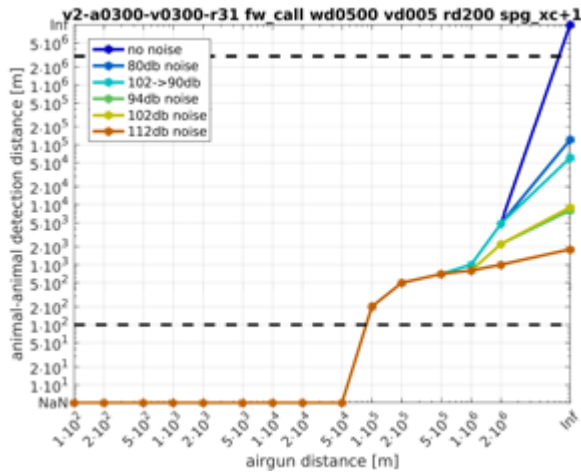
9.1.3.1.1.2 Water depth is 4000 m

► Receiver depth is 10 m:
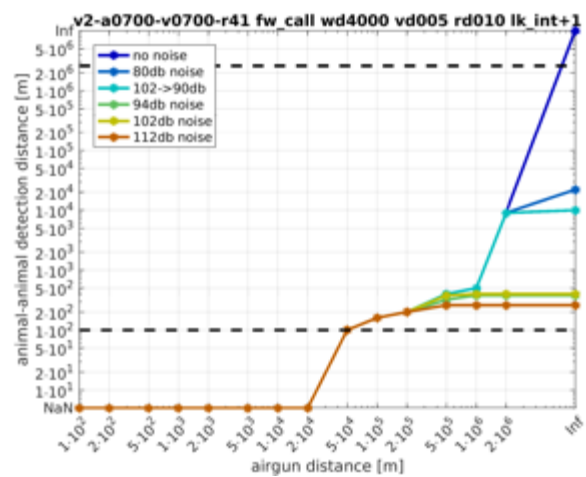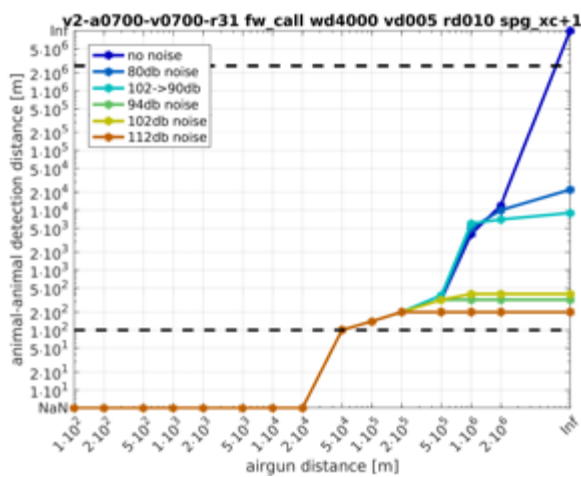
► Receiver depth is 50 m:
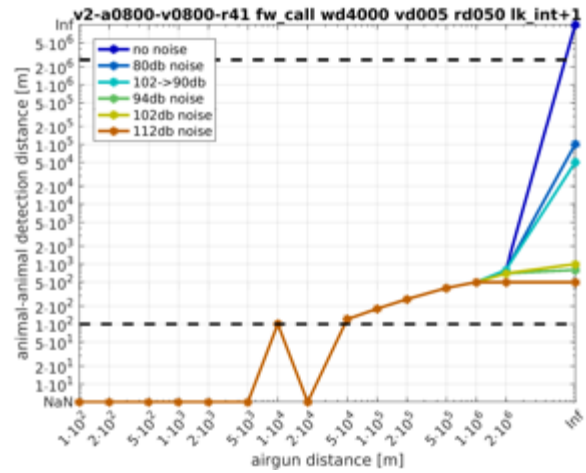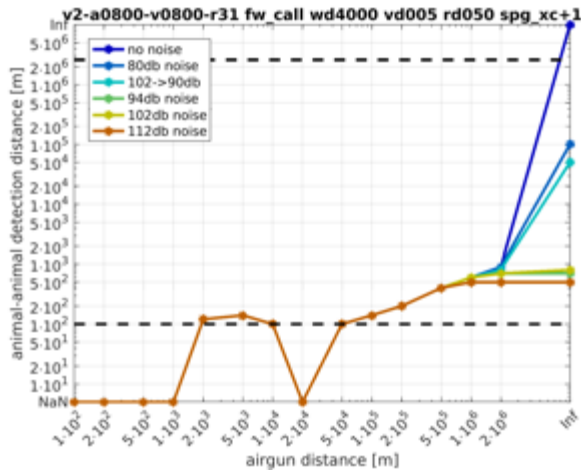
► Receiver depth is 200 m:
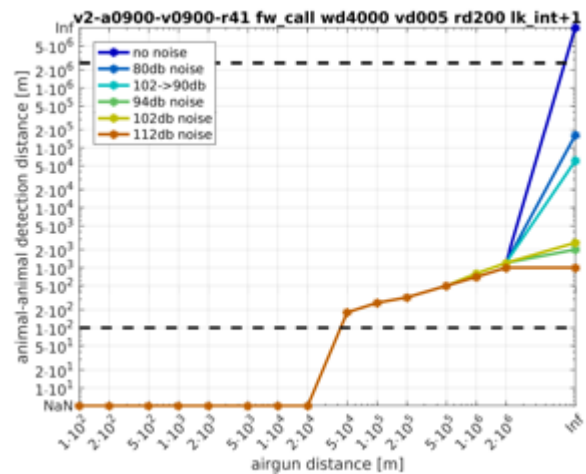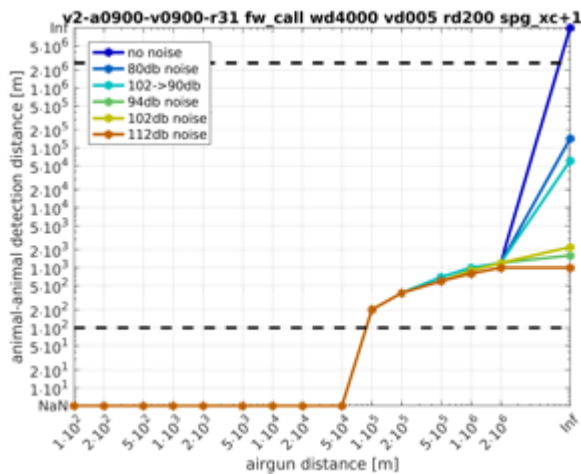
9.1.3.1.2   Vocalization depth is 50 m

9.1.3.1.2.1   Water depth is 500 m

► Receiver depth is 10 m:
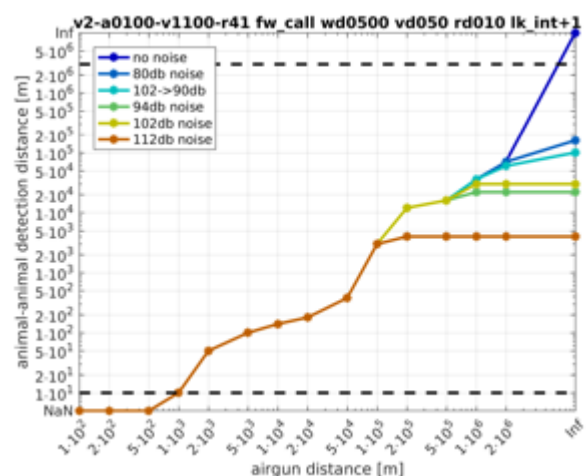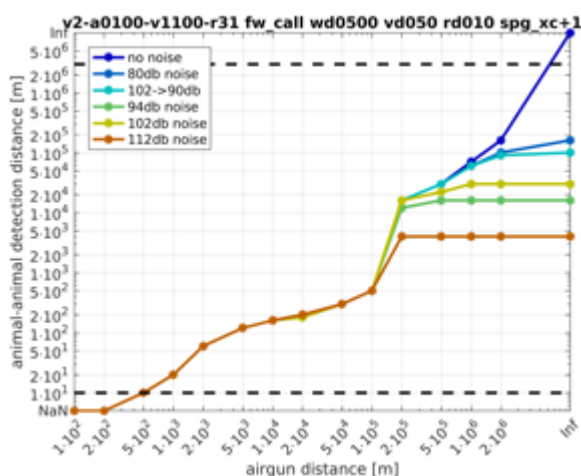
► Receiver depth is 50 m:
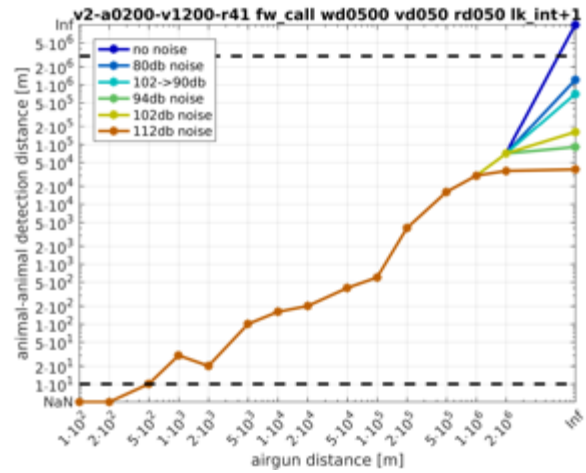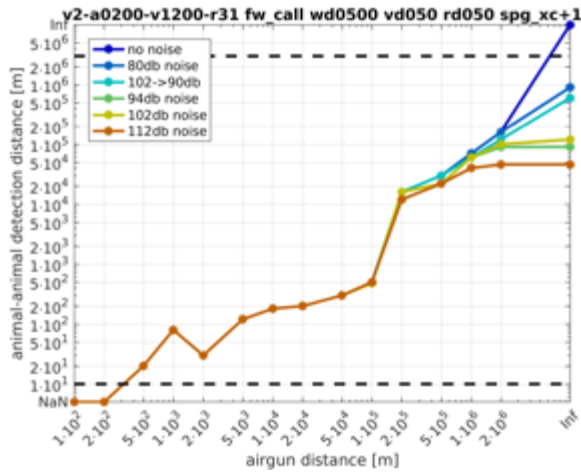
► Receiver depth is 200 m:
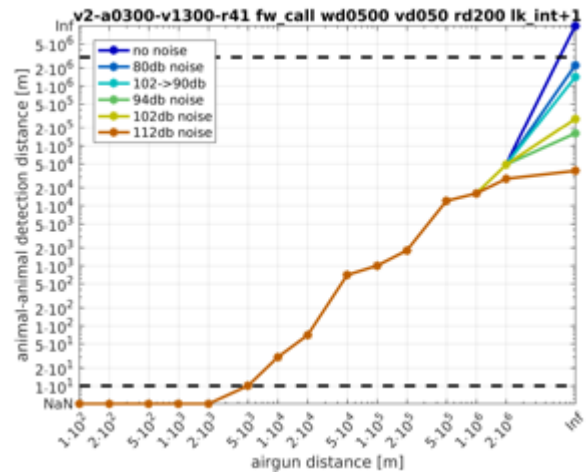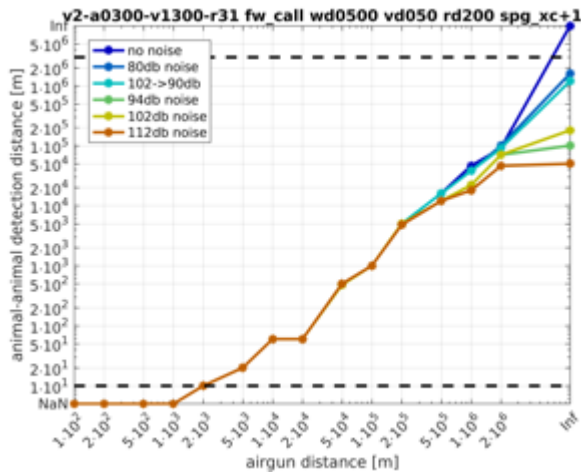
9.1.3.1.2.2   Water depth is 4000 m

► Receiver depth is 10 m:
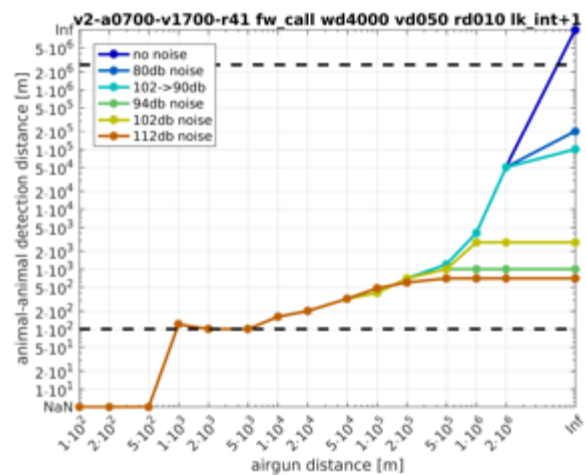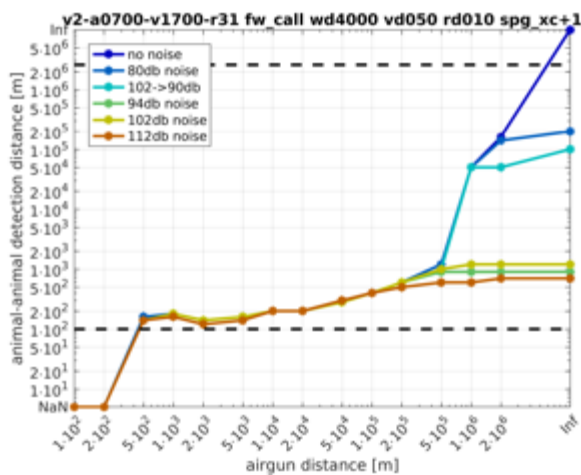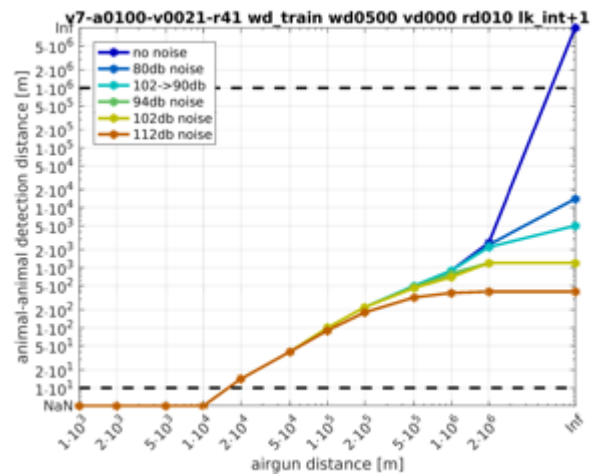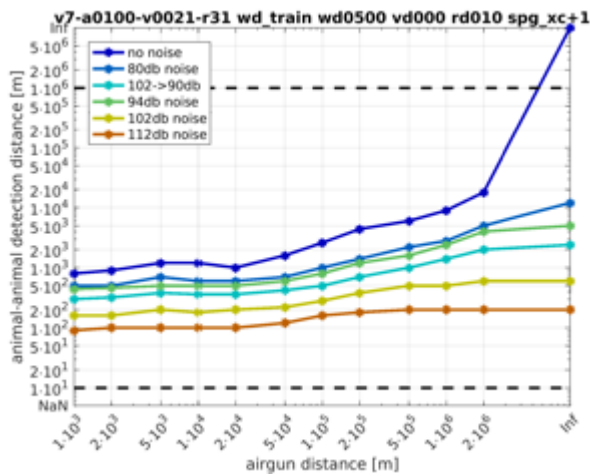

► Receiver depth is 50 m:
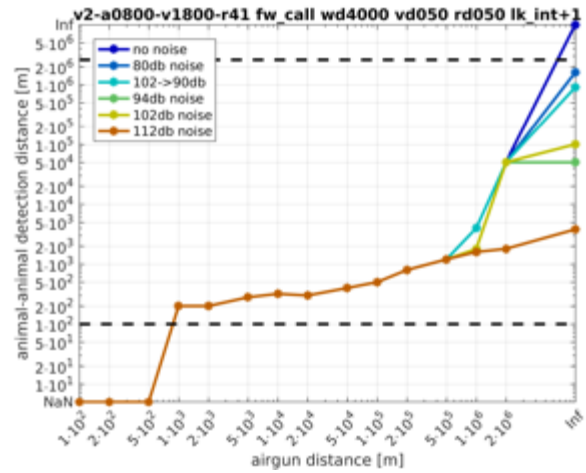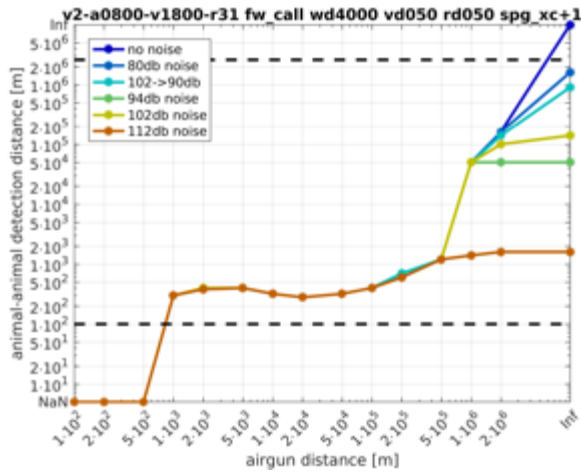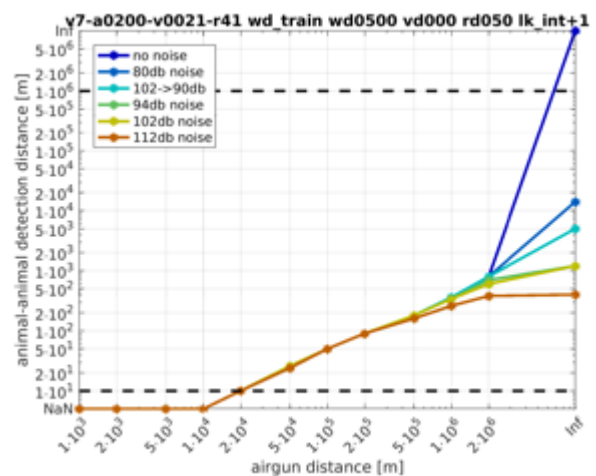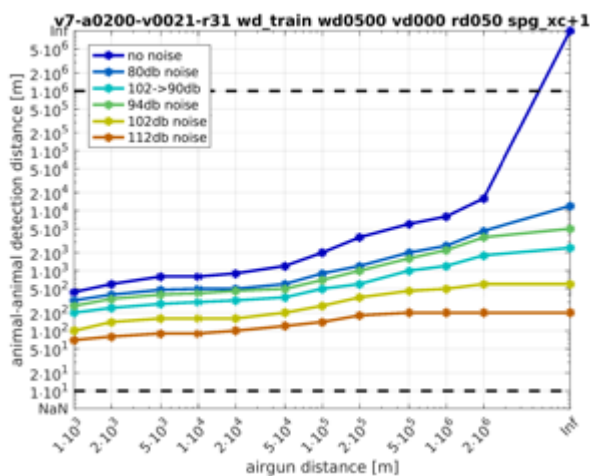
► Receiver depth is 200 m:
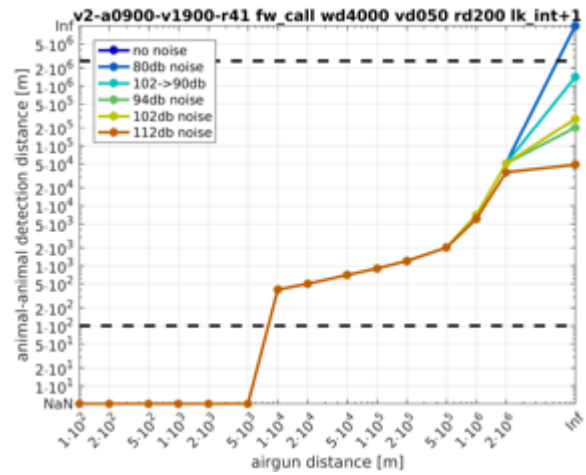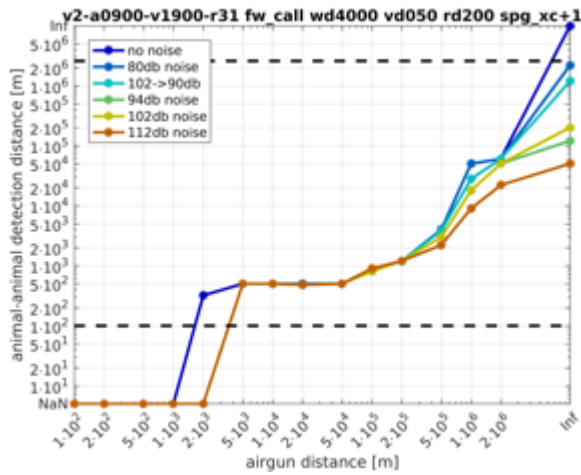
9.1.3.1.3 Propagation of airgun is modelled by numerical transfer functions, propagation of vocalization is modelled assuming spherical spreading

9.1.3.1.3.1 Water depth is 500 m

► Receiver depth is 10 m:

► Receiver depth is 50 m:

174
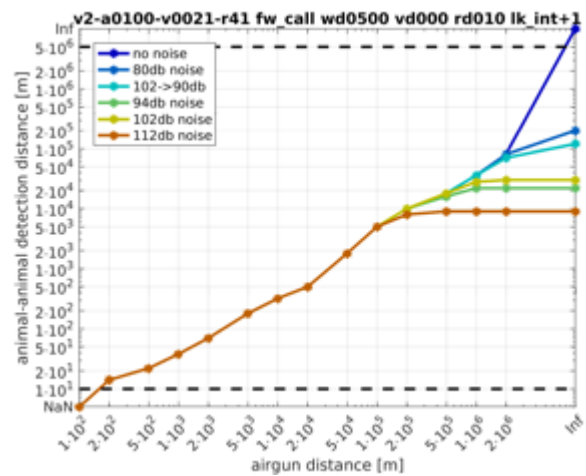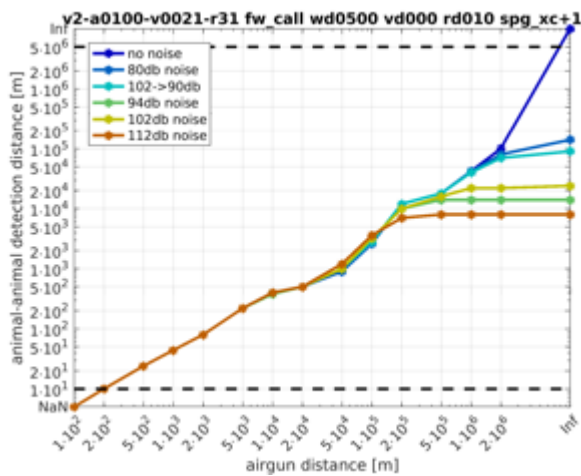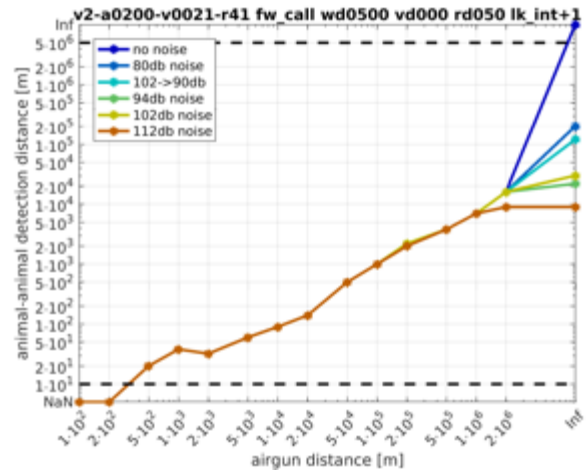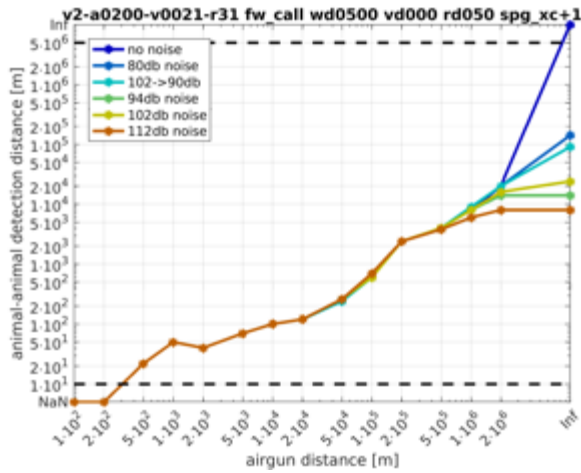
► Receiver depth is 200 m:
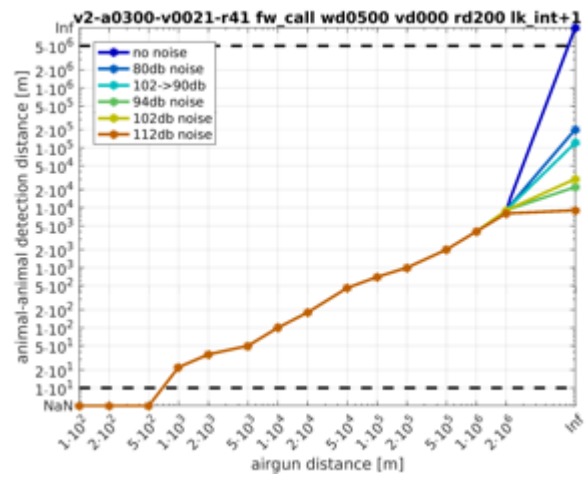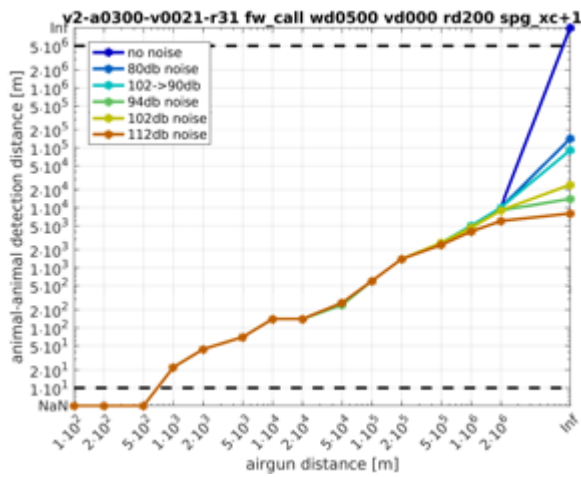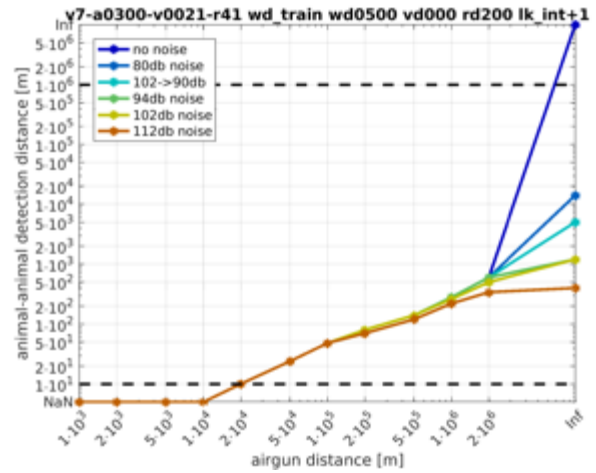

9.1.3.1.3.2 *Water depth is 4000 m*

► Receiver depth is 10 m:
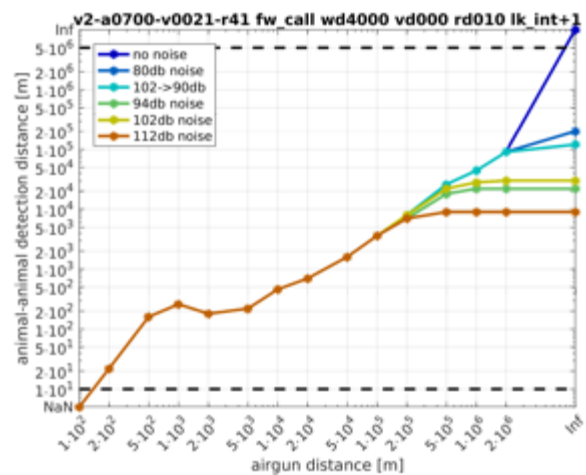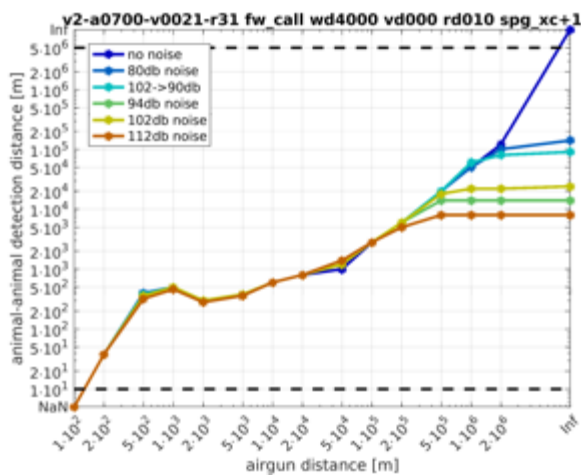
► Receiver depth is 50 m:
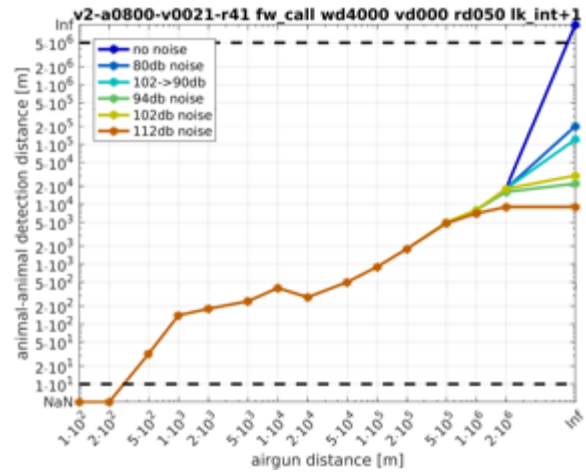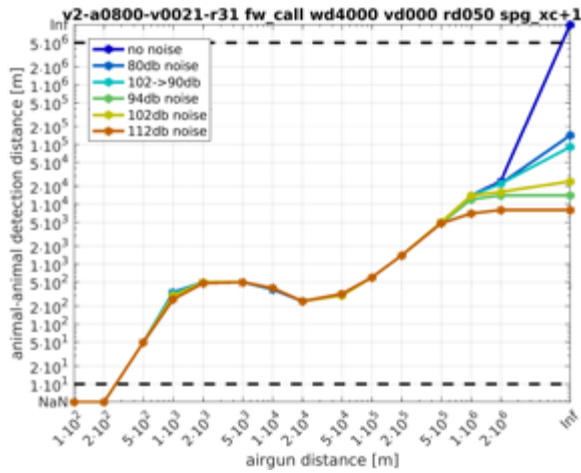
► Receiver depth is 200 m:
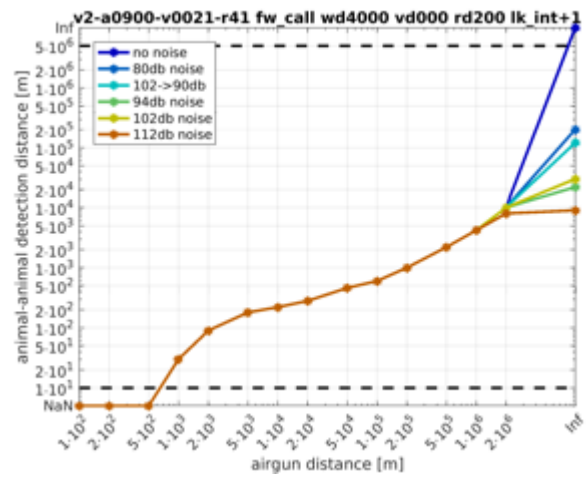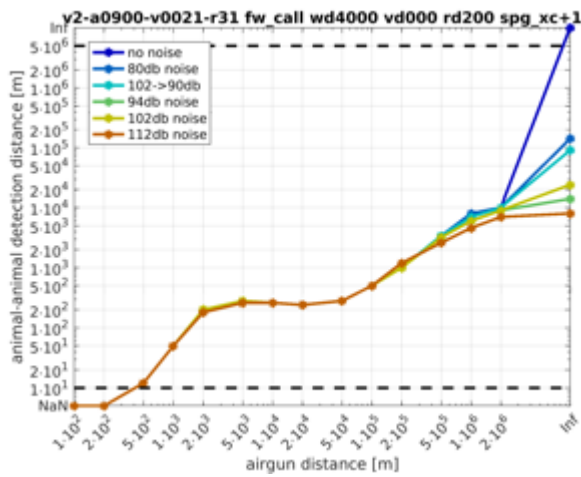
9.1.3.1.4 Propagation of airgun and vocalization is modelled assuming spherical spreading
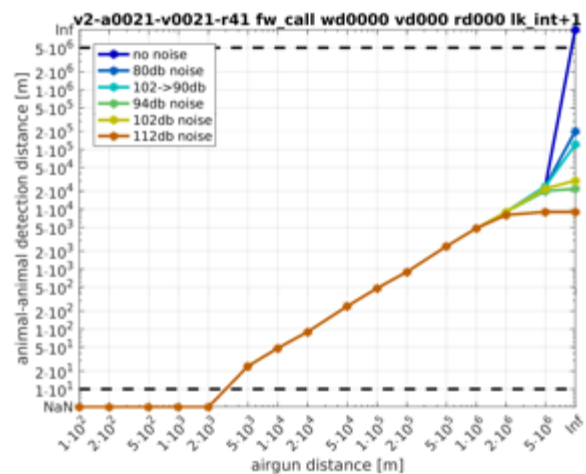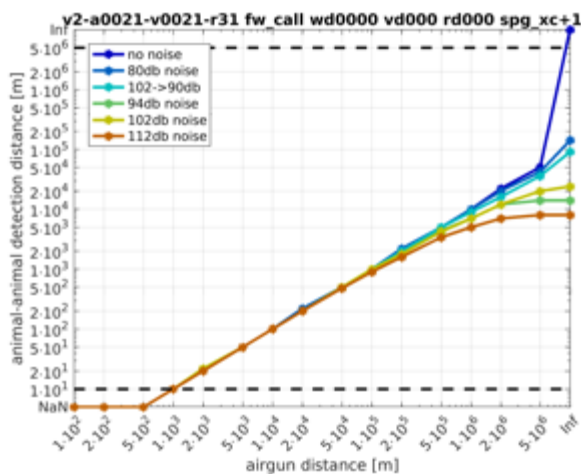
9.1.4   Killer whale multiharmonic call

9.1.4.1   Propagation of both airgun and vocalization are modelled by numerical transfer functions

9.1.4.1.1   Vocalization depth is 5 m

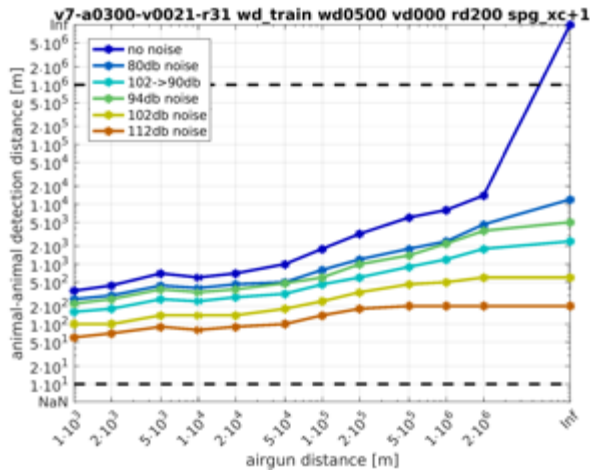*9.1.4.1.1.1   Water depth is 500 m; Full band analysis*

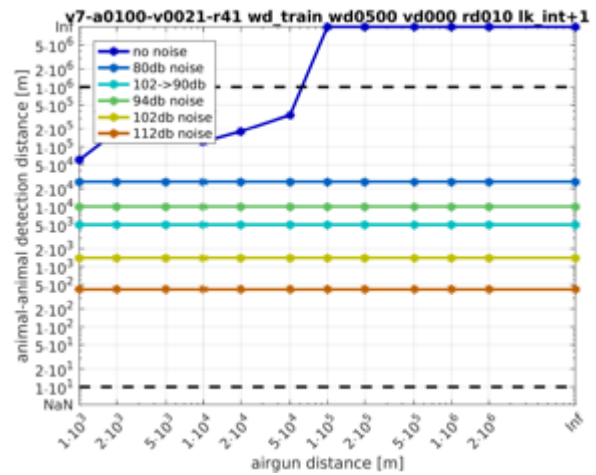► Receiver depth is 10 m:
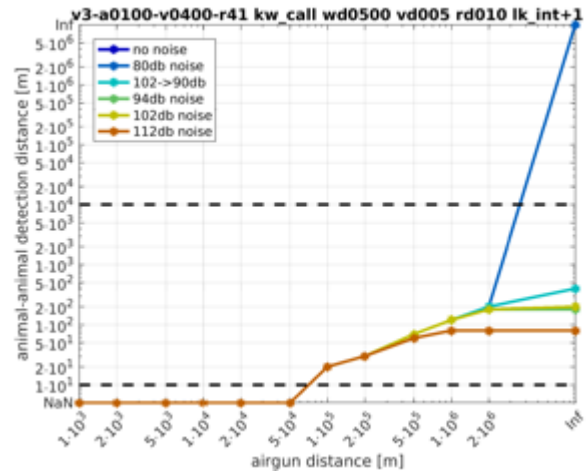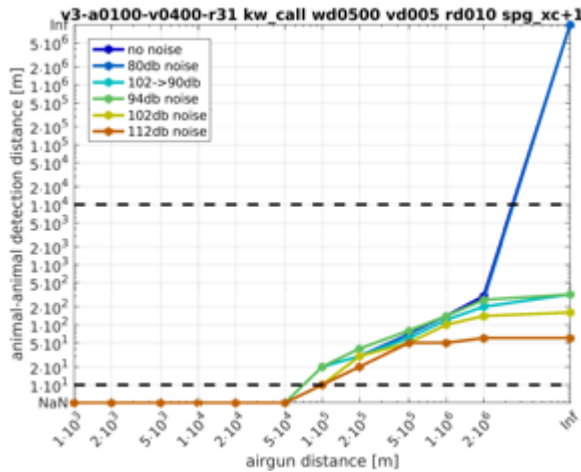
► Receiver depth is 50 m:
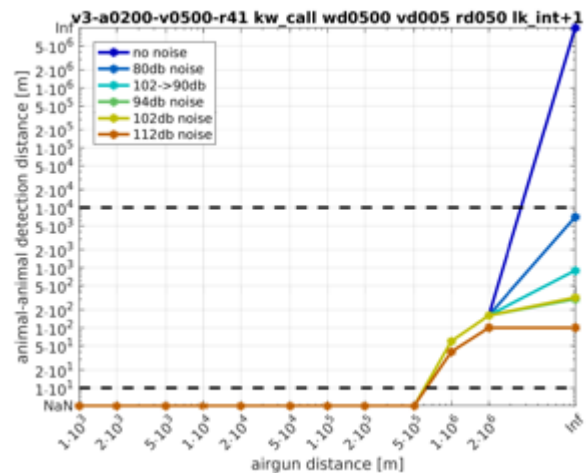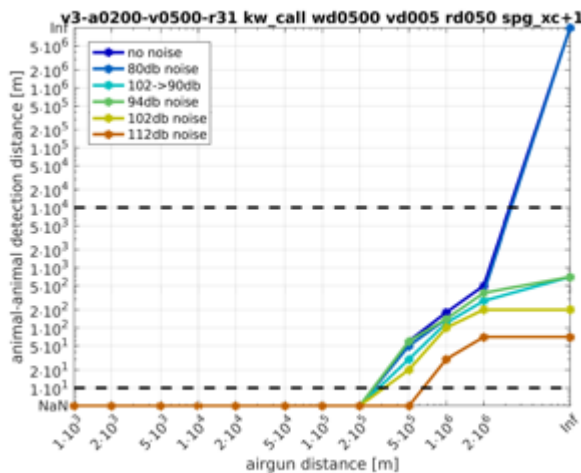
► Receiver depth is 200 m:
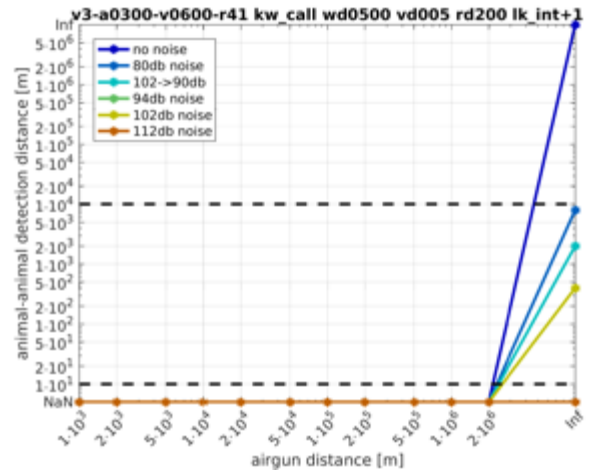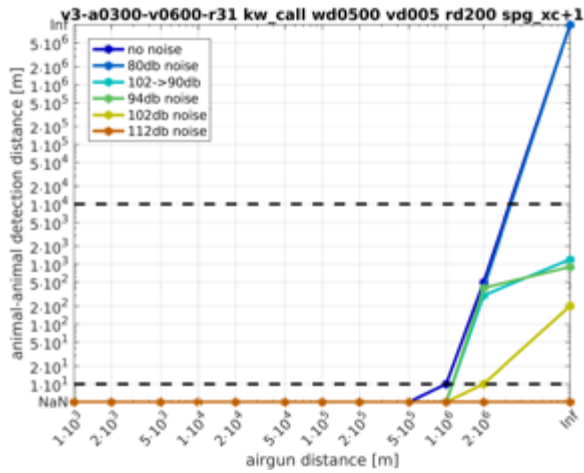
9.1.4.1.1.2   Water depth is 500 m; High pass analysis

► Receiver depth is 10 m:
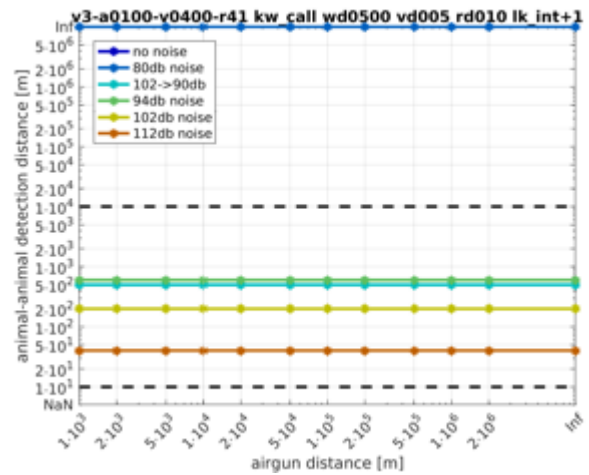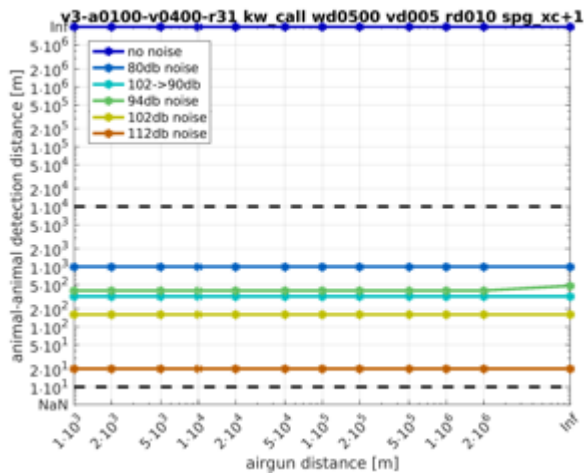
► Receiver depth is 50 m:
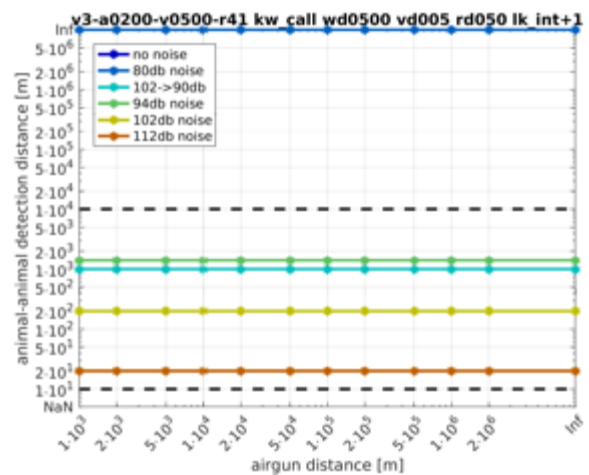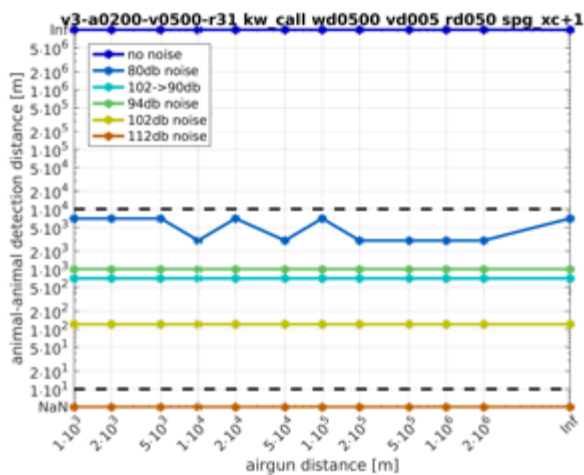
► Receiver depth is 200 m:
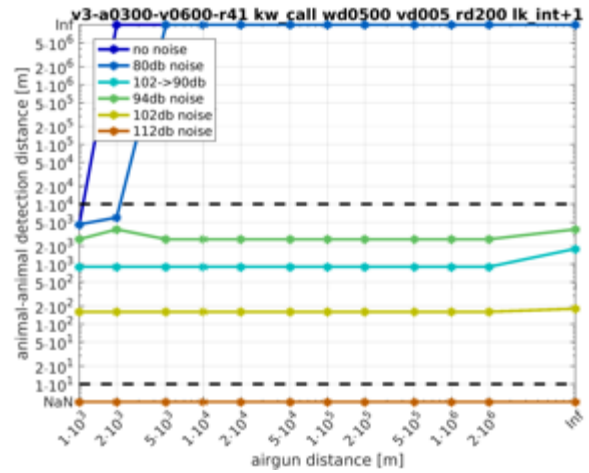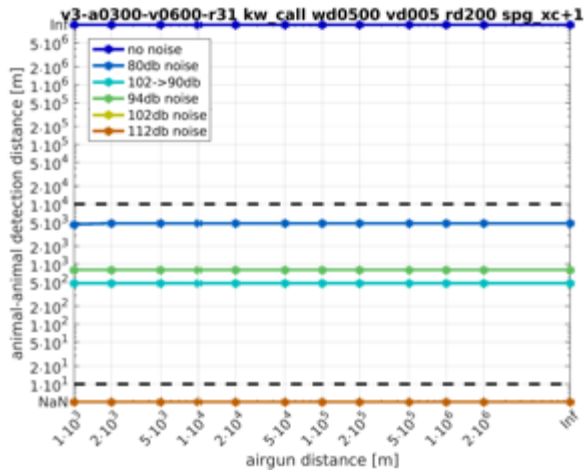
9.1.4.1.2 Vocalization depth is 50 m

9.1.4.1.2.1 Water depth is 500 m; Full band analysis

► Receiver depth is 10 m:
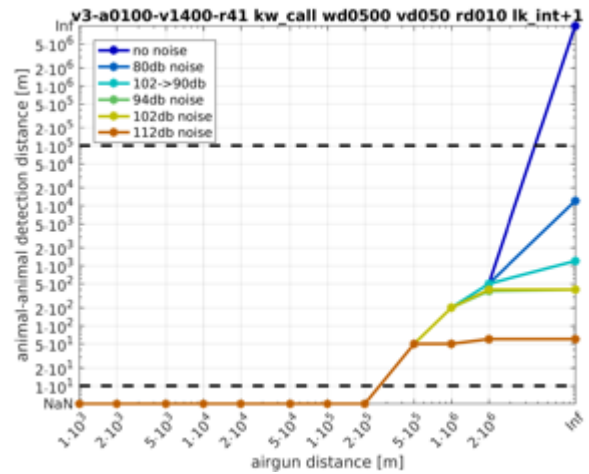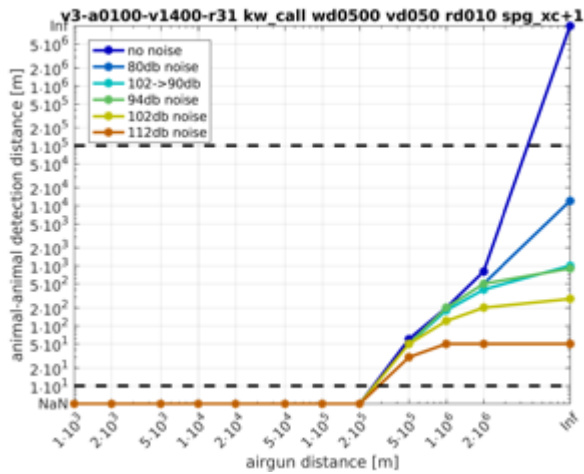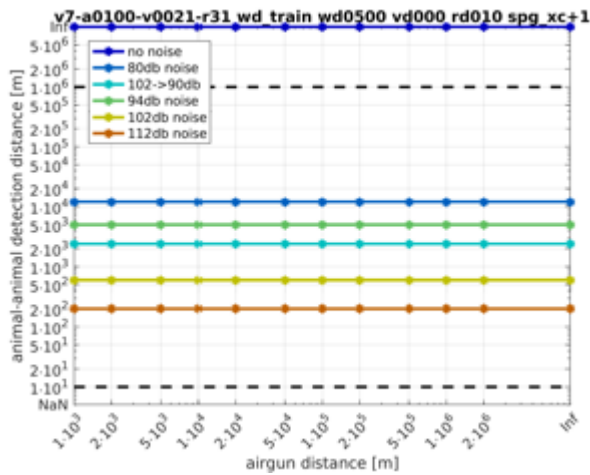

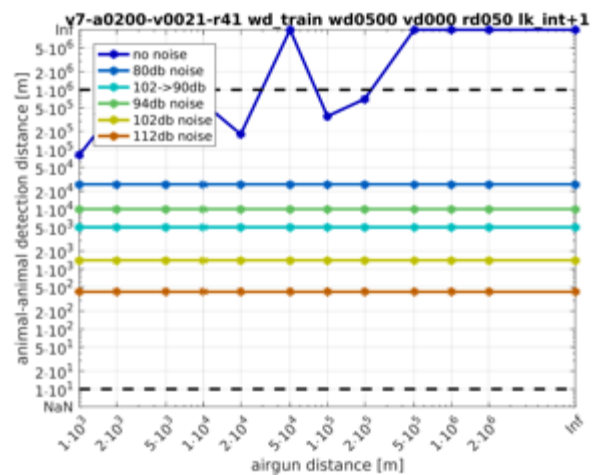► Receiver depth is 50 m:
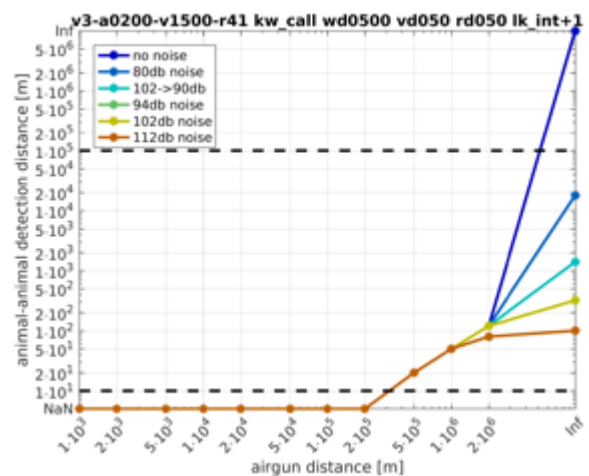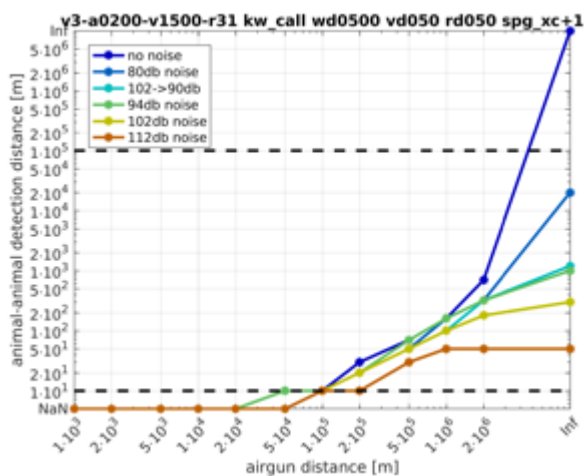
► Receiver depth is 200 m:
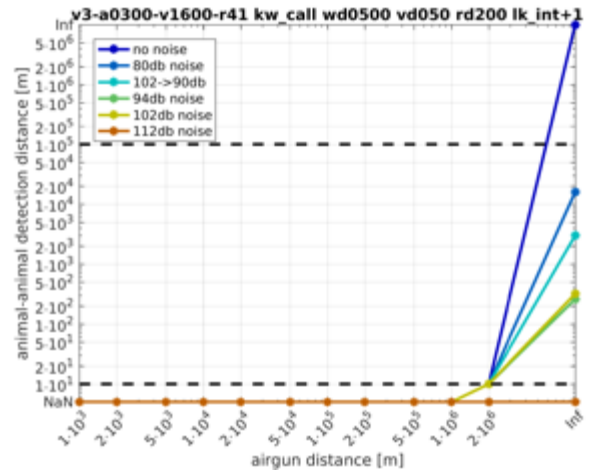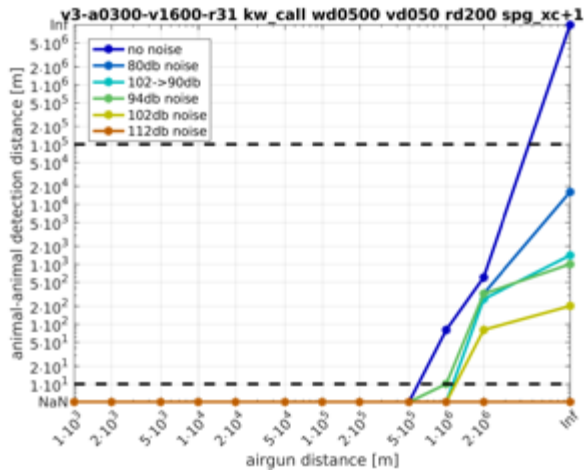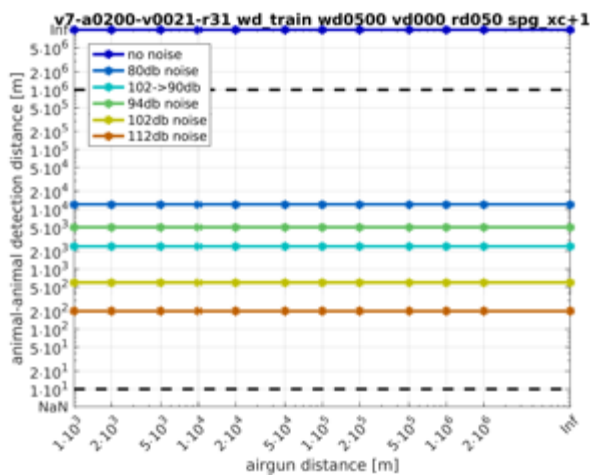
9.1.4.1.2.2   Water depth is 500 m; High pass analysis

► Receiver depth is 10 m:
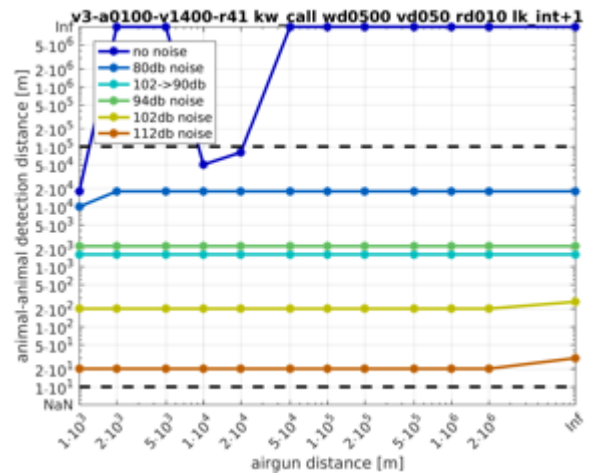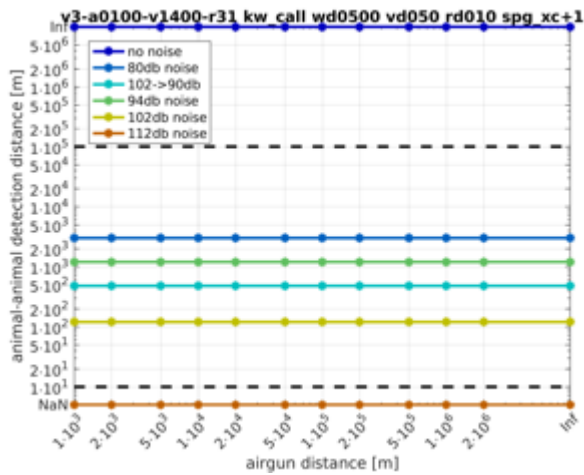
► Receiver depth is 50 m:
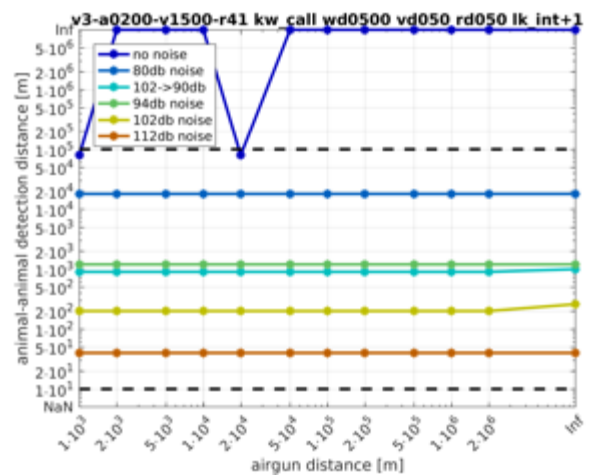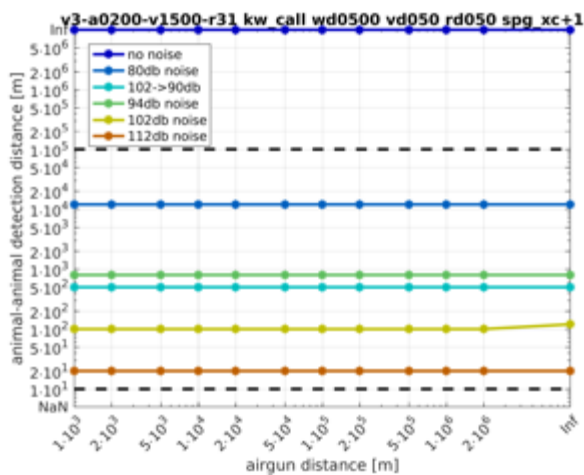
► Receiver depth is 200 m:
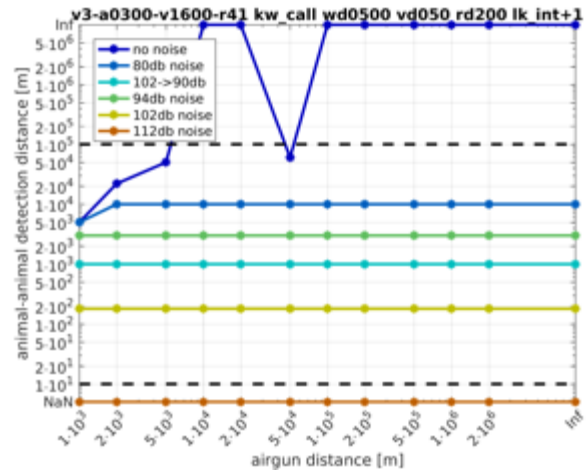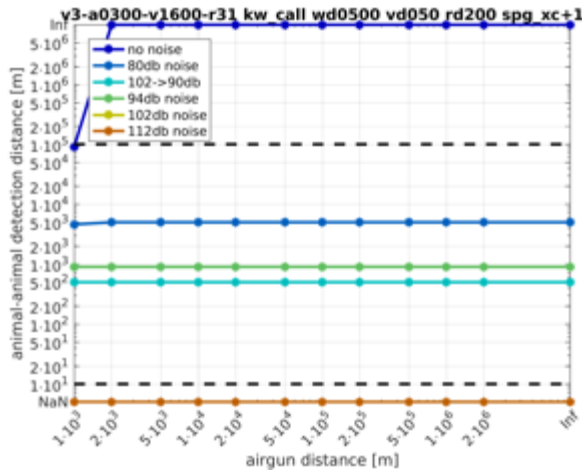
9.1.4.1.3 Propagation of airgun is modelled by numerical transfer functions, propagation of vocalization is modelled assuming spherical spreading

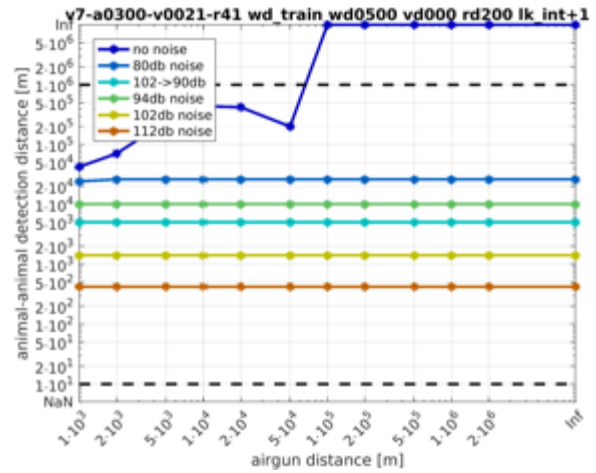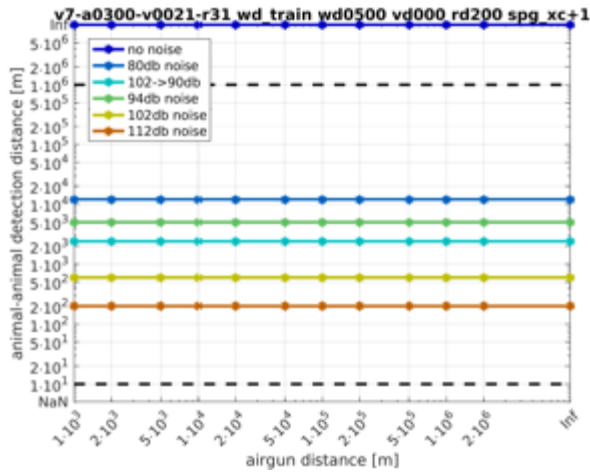*9.1.4.1.3.1 Water depth is 500 m; Full band analysis*

► Receiver depth is 10 m:
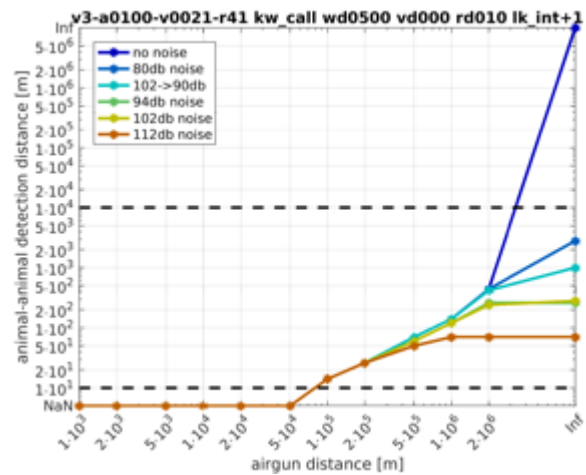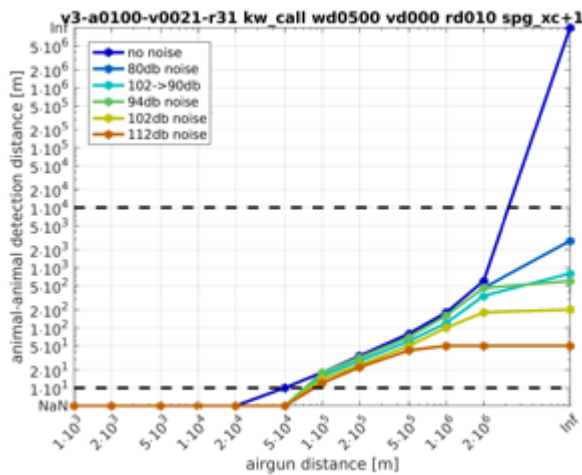
► Receiver depth is 50 m:
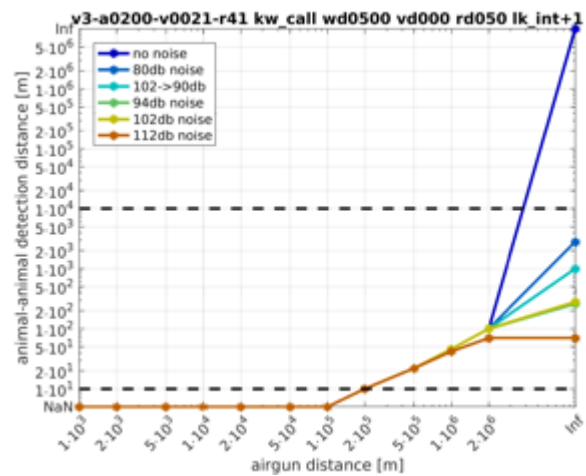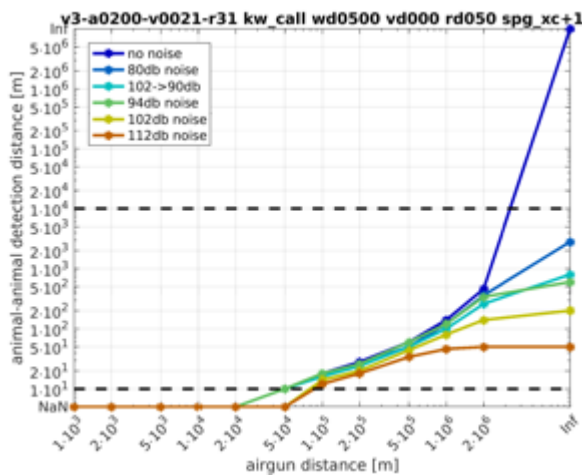
► Receiver depth is 200 m:
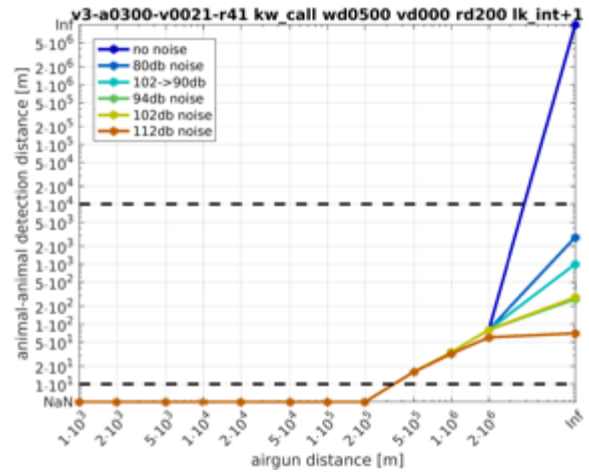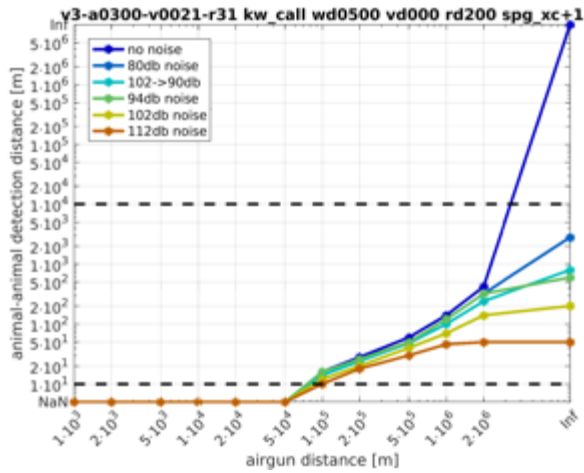
9.1.4.1.3.2   Water depth is 500 m; High pass analysis

► Receiver depth is 10 m:
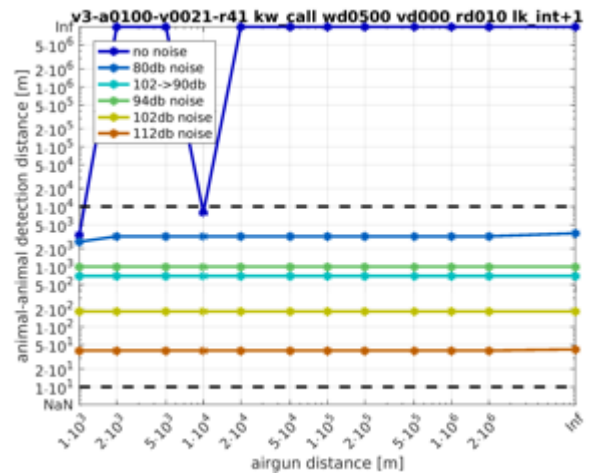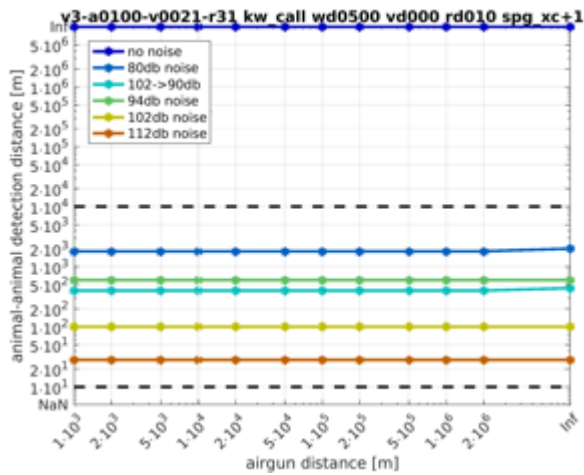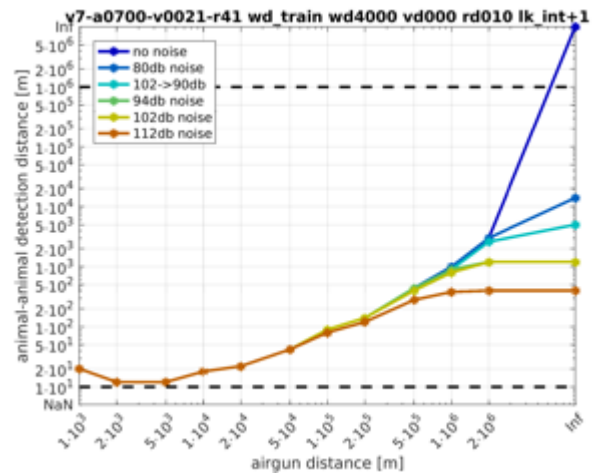

► Receiver depth is 50 m:
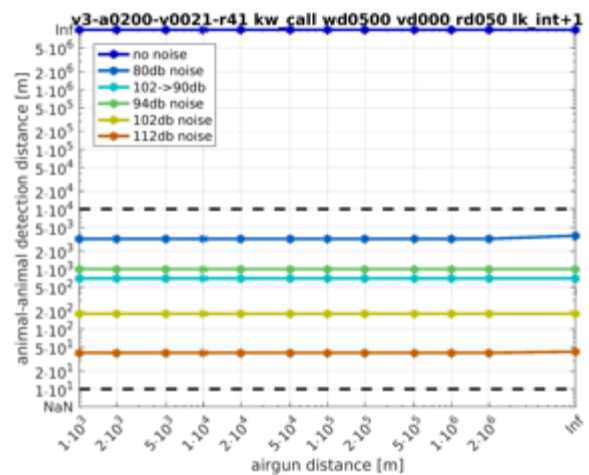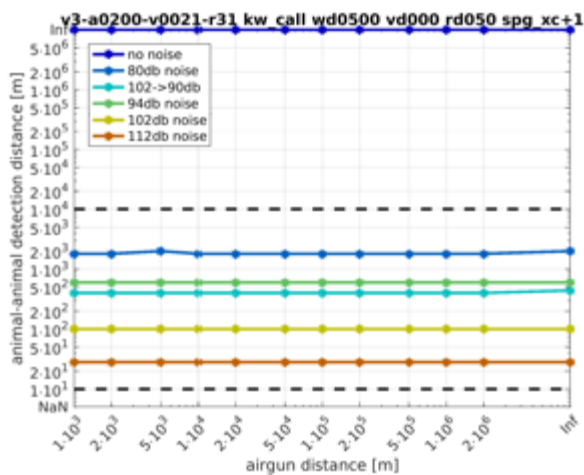
► Receiver depth is 200 m:
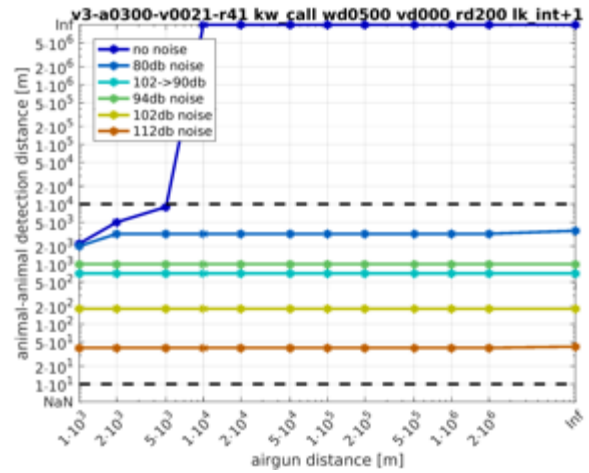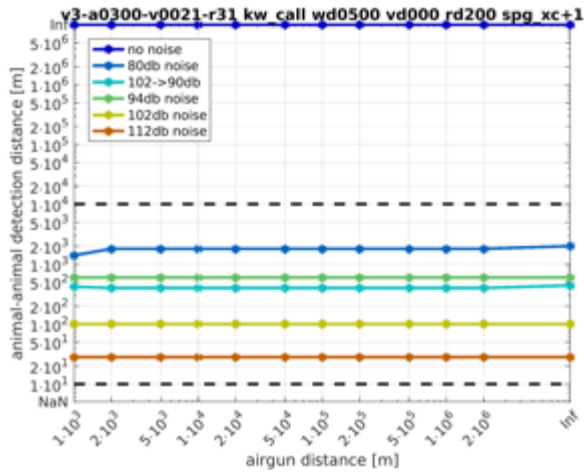
9.1.4.1.3.3 Water depth is 4000 m; Full band analysis

► Receiver depth is 10 m:
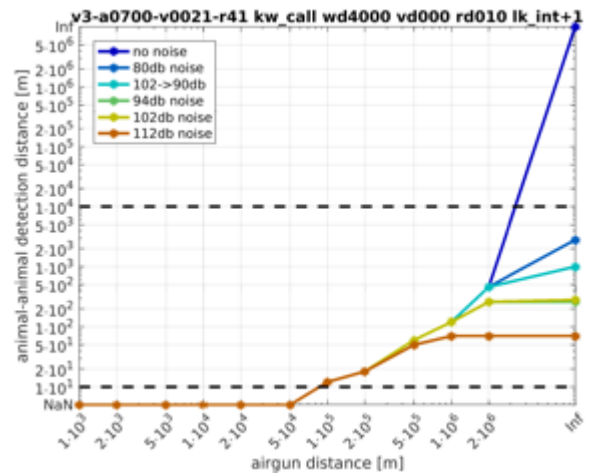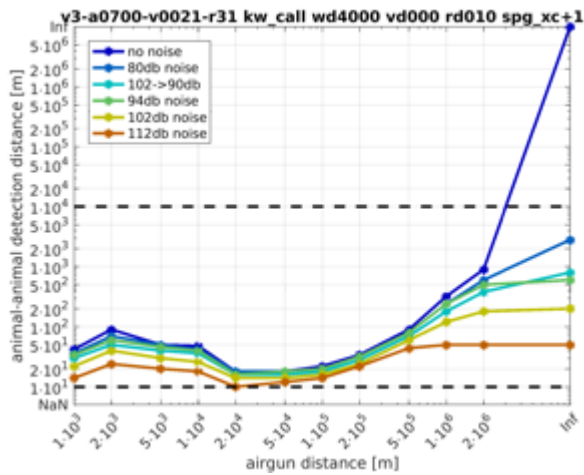
► Receiver depth is 50 m:
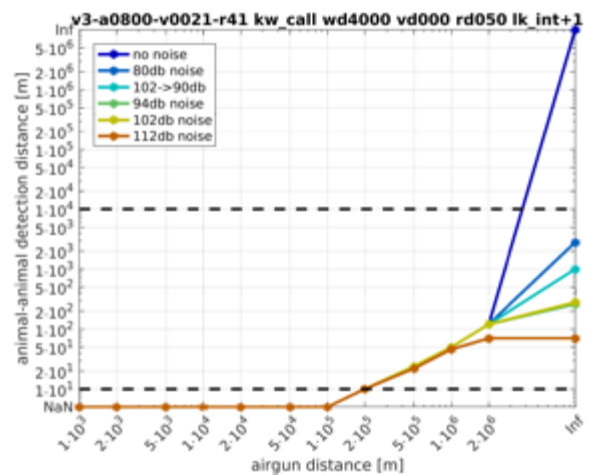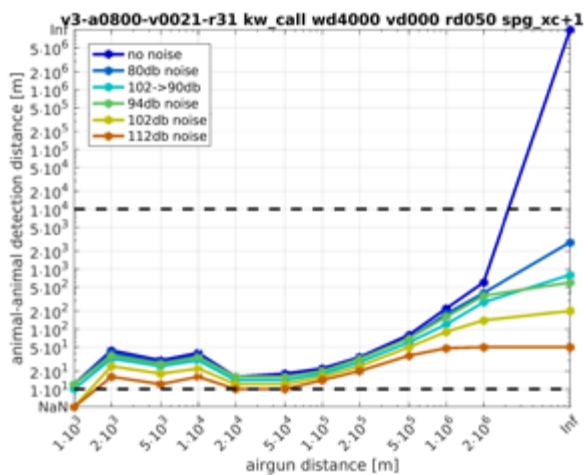
► Receiver depth is 200 m:
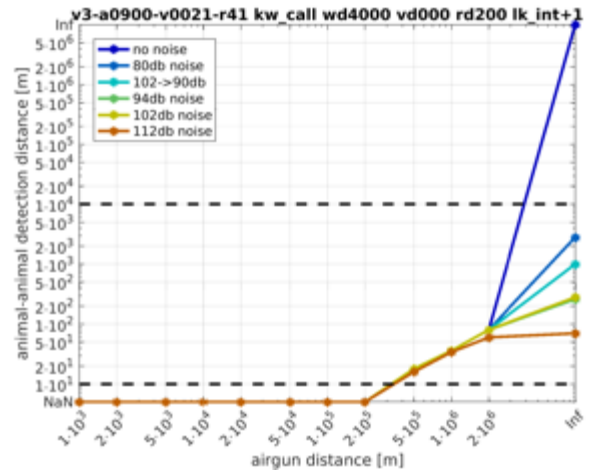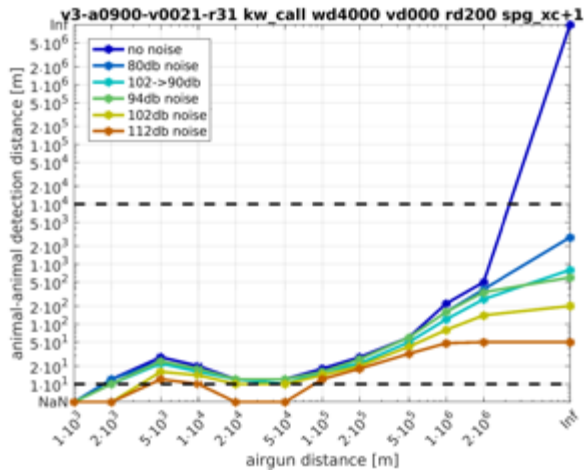
9.1.4.1.3.4 Water depth is 4000 m; High pass analysis

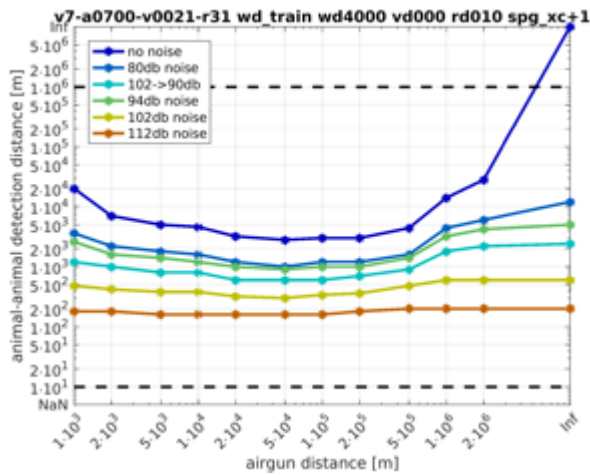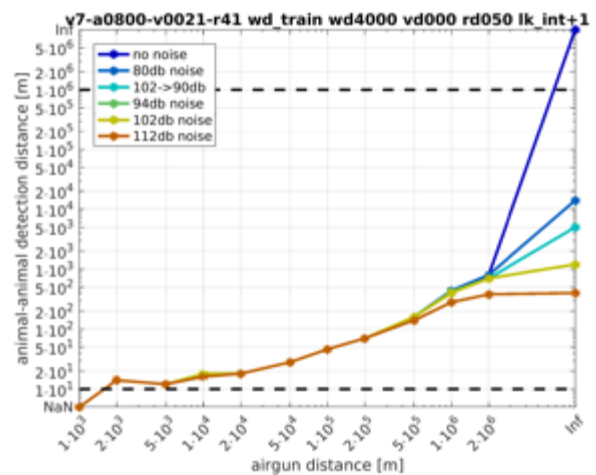► Receiver depth is 10 m:
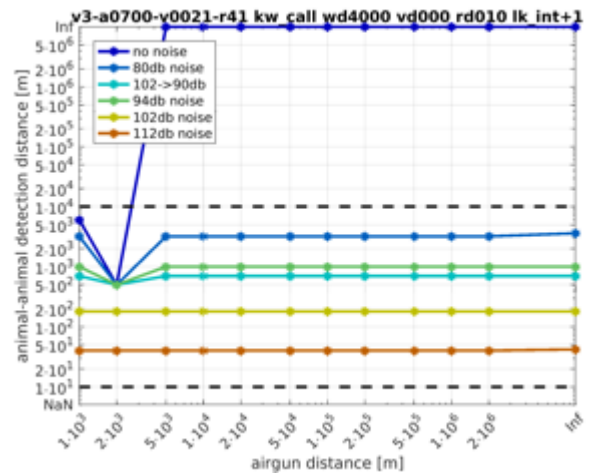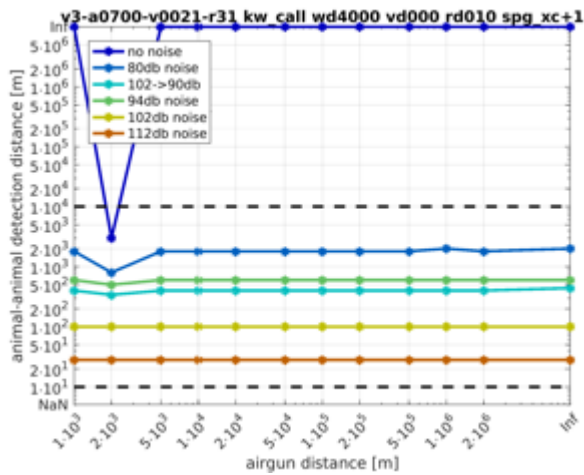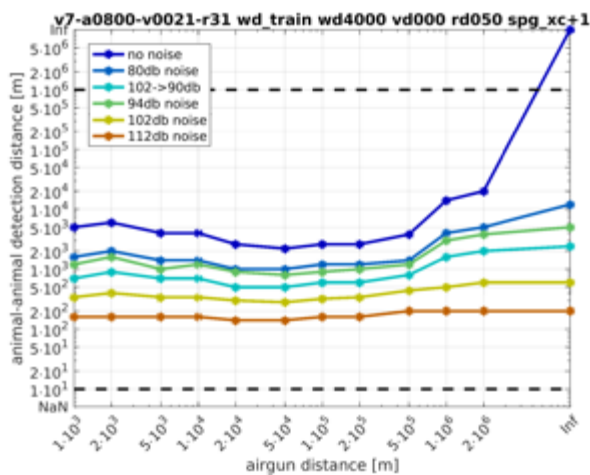

► Receiver depth is 50 m:
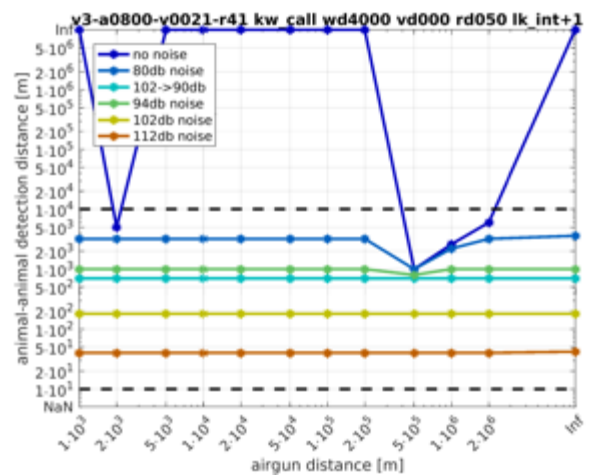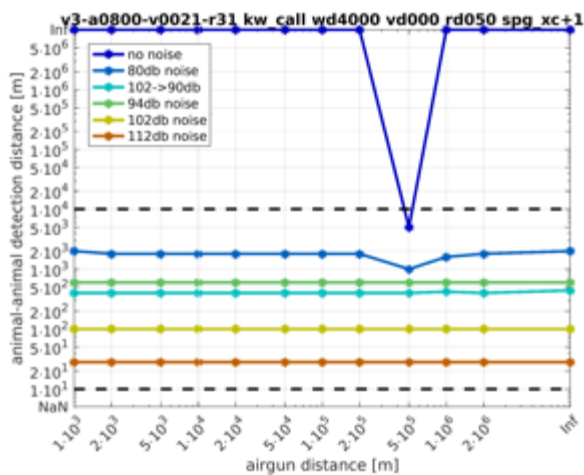
► Receiver depth is 200 m:
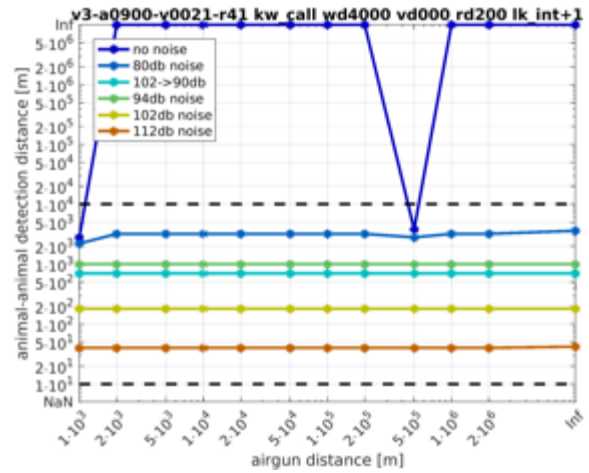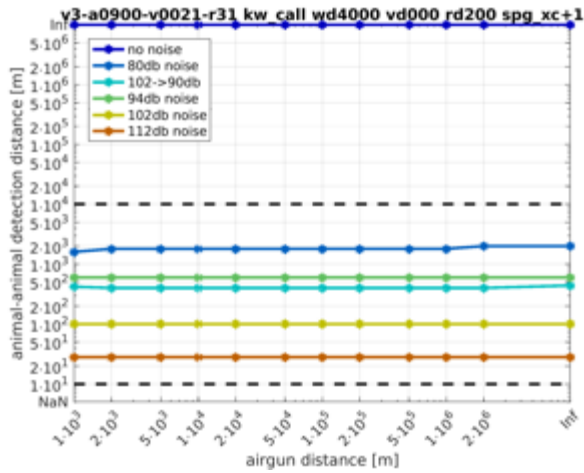
9.1.4.2   Propagation of airgun and vocalization is modelled assuming spherical spreading

9.1.4.2.1   Full band analysis
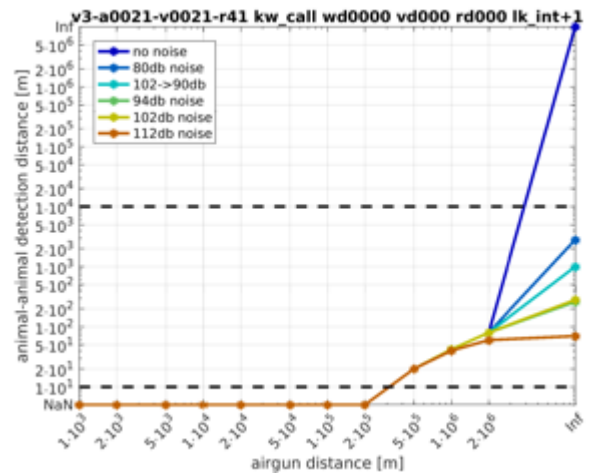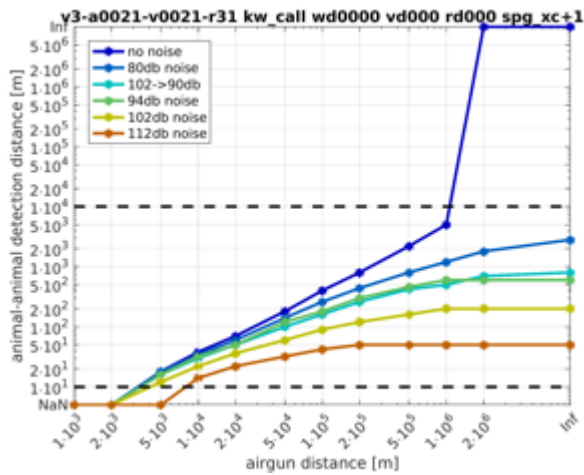
9.1.4.2.2   High pass analysis
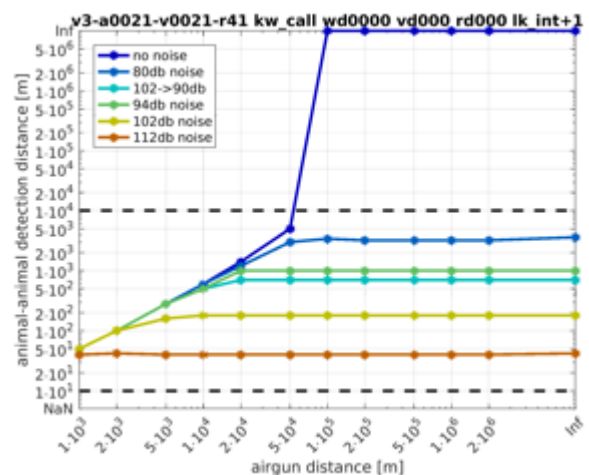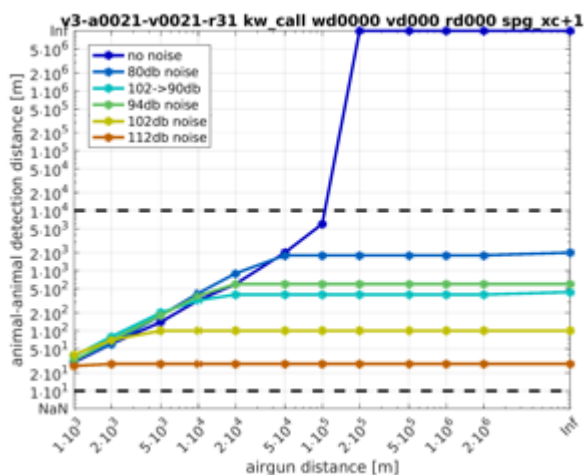
9.1.5   Weddell seal long call

9.1.5.1   Propagation of both airgun and vocalization are modelled by numerical transfer functions

9.1.5.1.1   Vocalization depth is 5 m

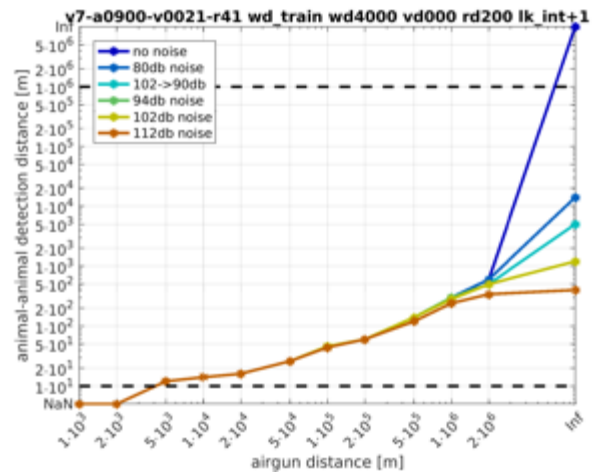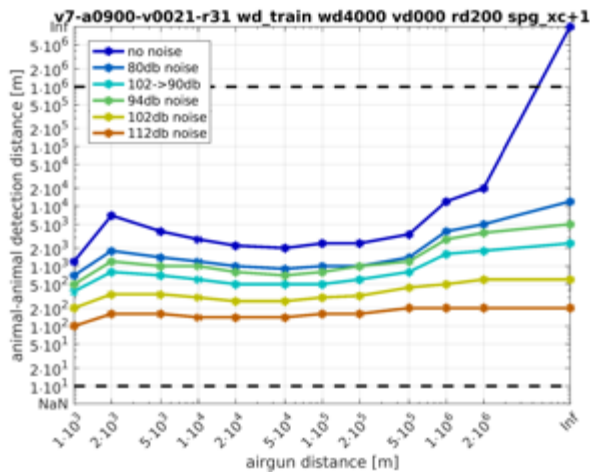*9.1.5.1.1.1   Water depth is 500 m; Full band analysis*

► Receiver depth is 10 m:
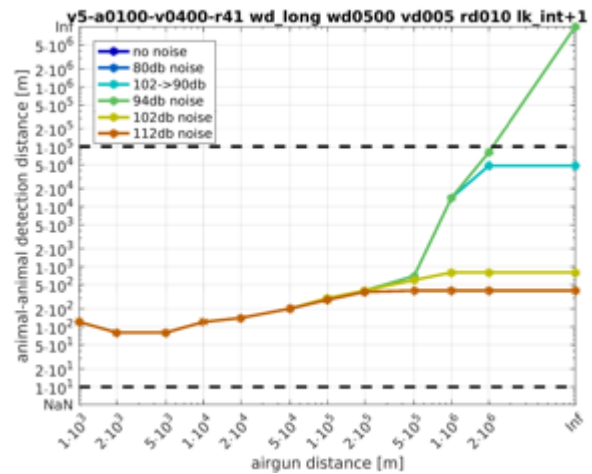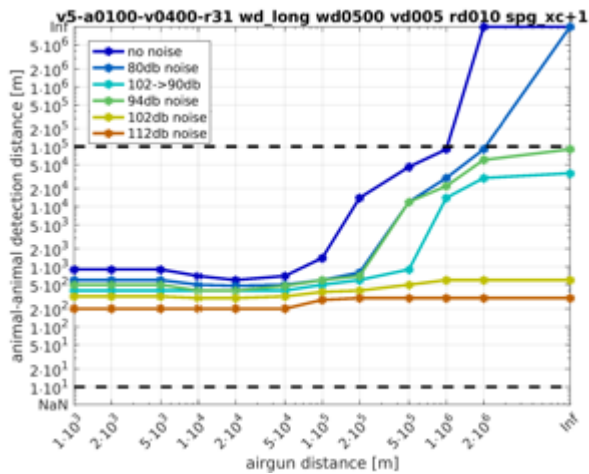
► Receiver depth is 50 m:
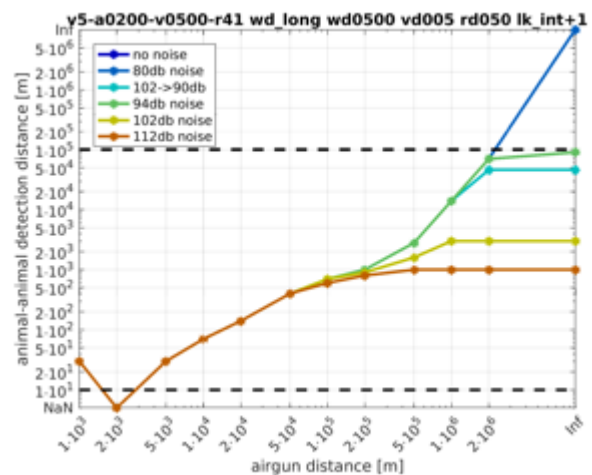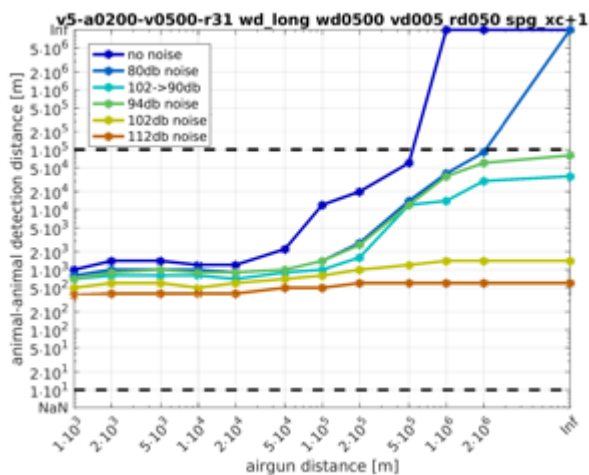
► Receiver depth is 200 m:
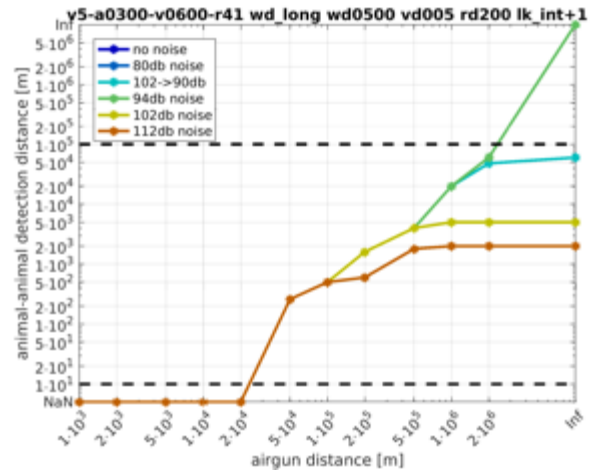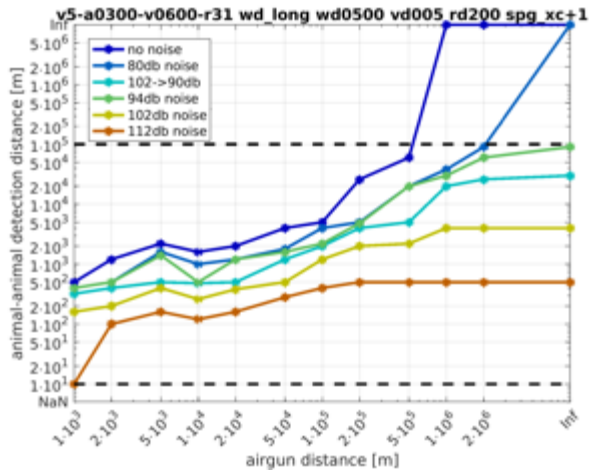
9.1.5.1.1.2 Water depth is 500 m; High pass analysis

► Receiver depth is 10 m:
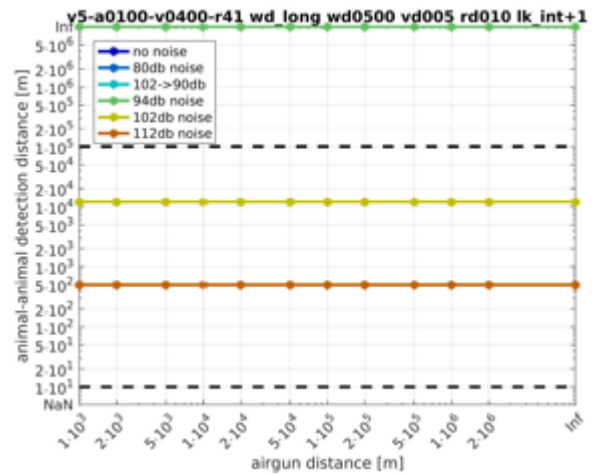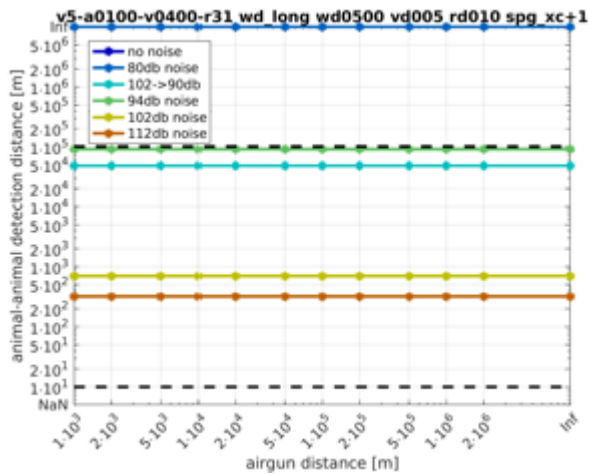
► Receiver depth is 50 m:
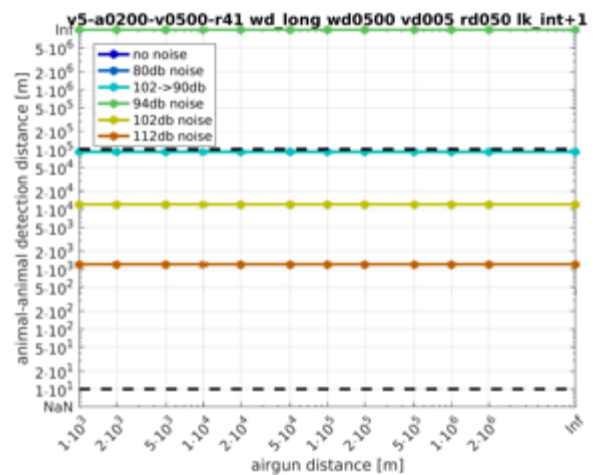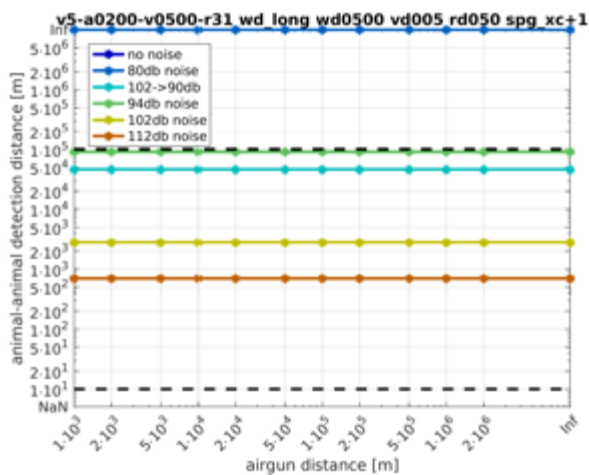
► Receiver depth is 200 m:
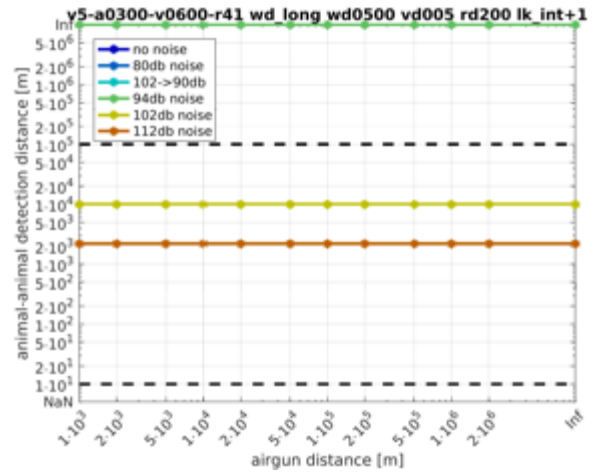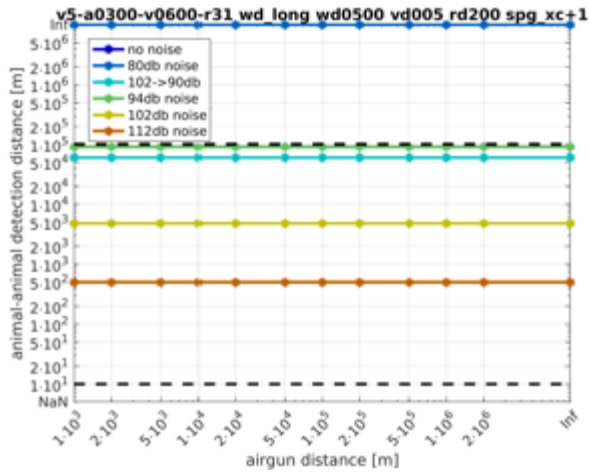
9.1.5.1.2 Vocalization depth is 50 m

9.1.5.1.2.1 Water depth is 500 m; Full band analysis
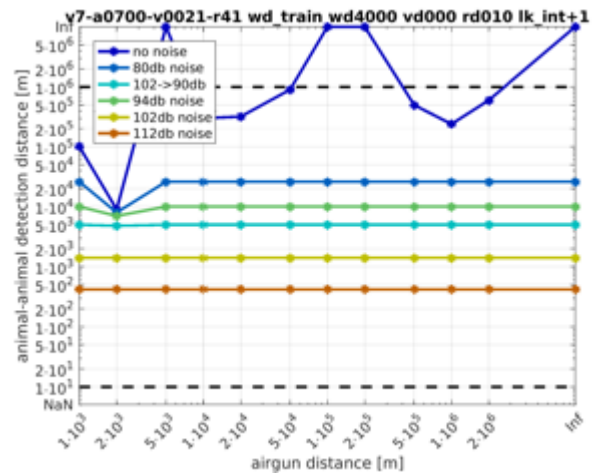
► Receiver depth is 10 m:
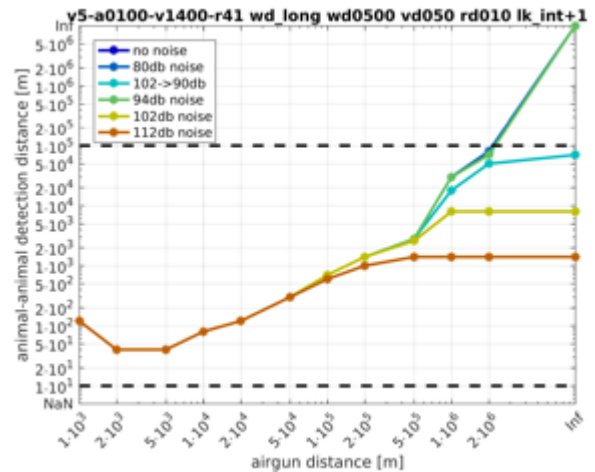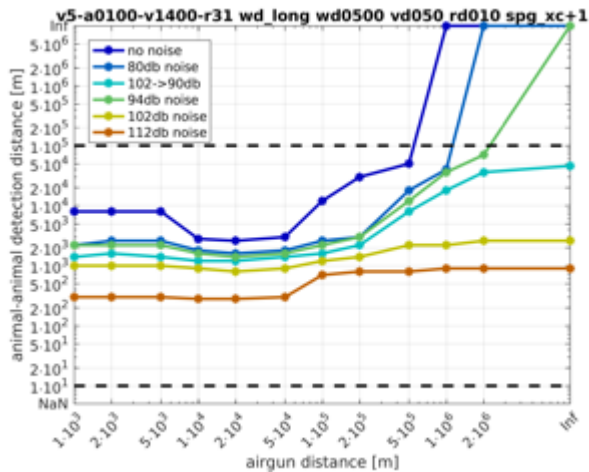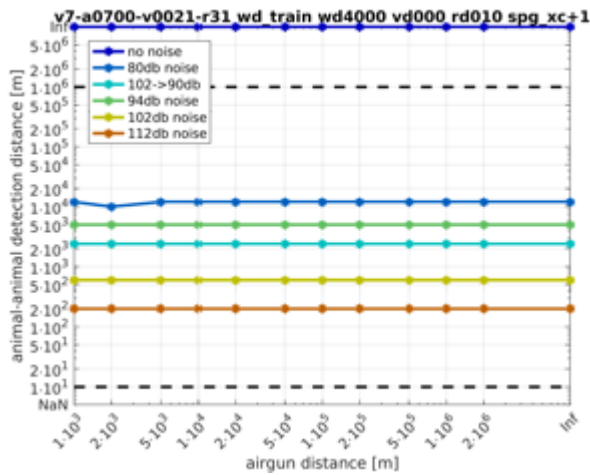

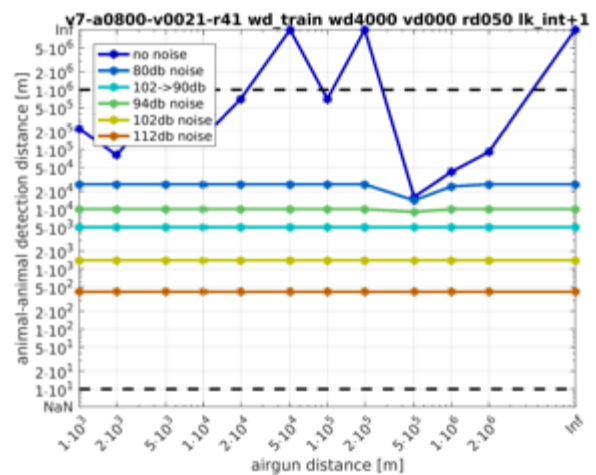► Receiver depth is 50 m:
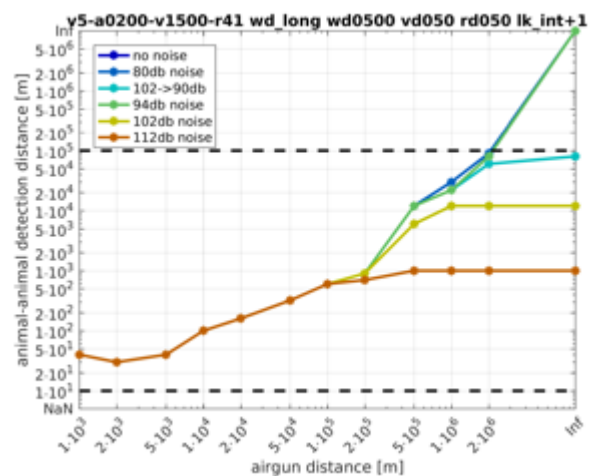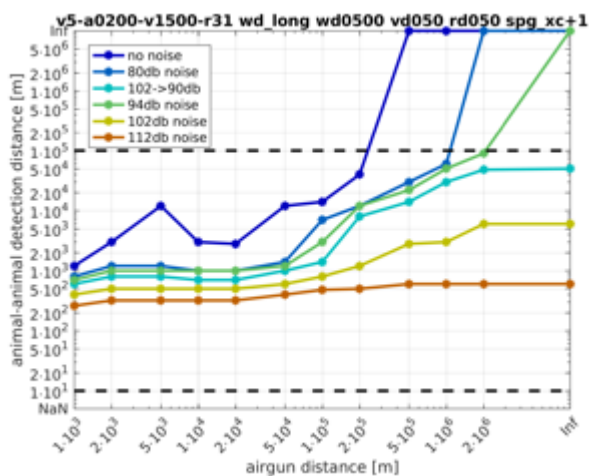
► Receiver depth is 200 m:
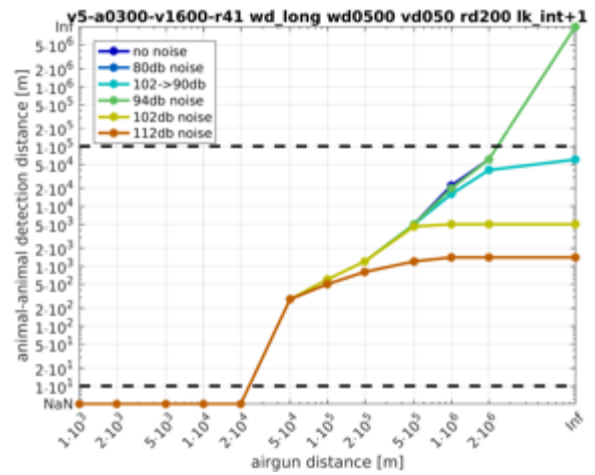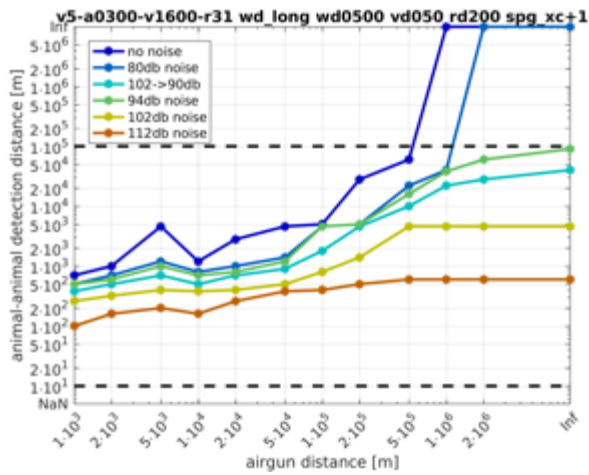
9.1.5.1.2.2 Water depth is 500 m; High pass analysis

► Receiver depth is 10 m:
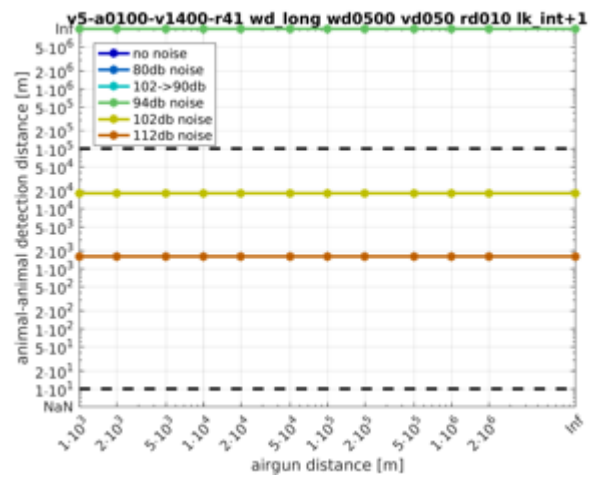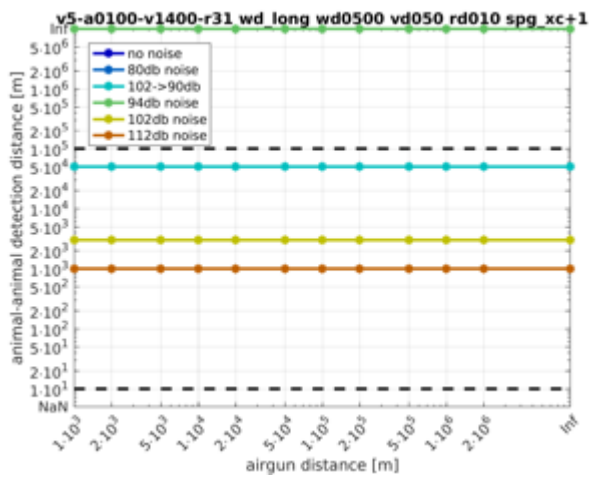
► Receiver depth is 50 m:
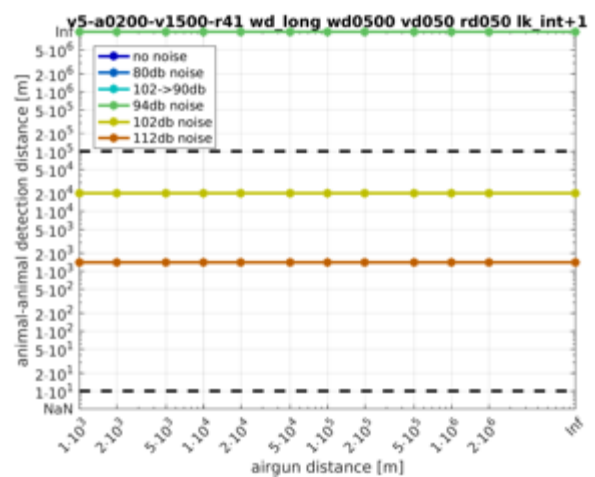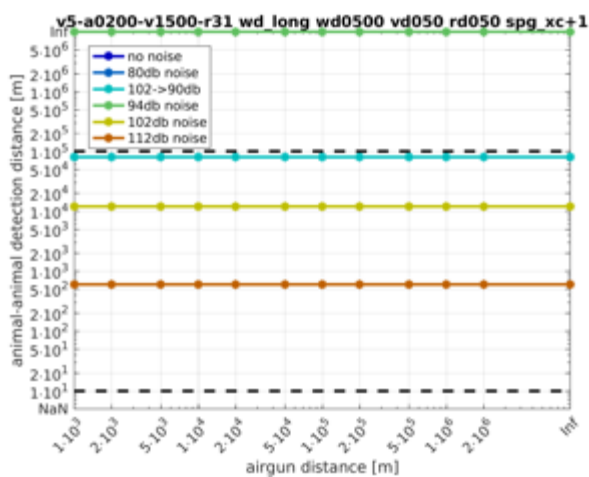
► Receiver depth is 200 m:
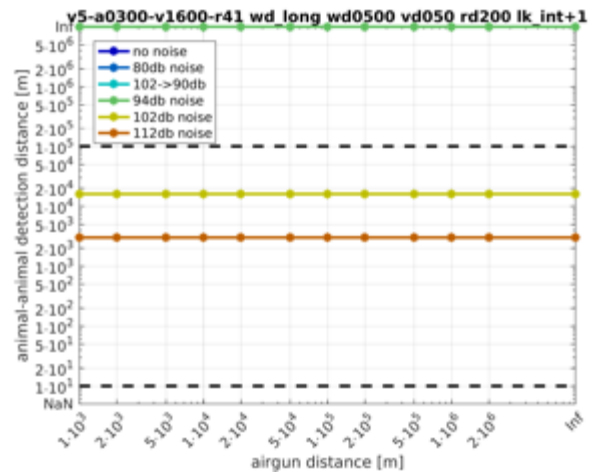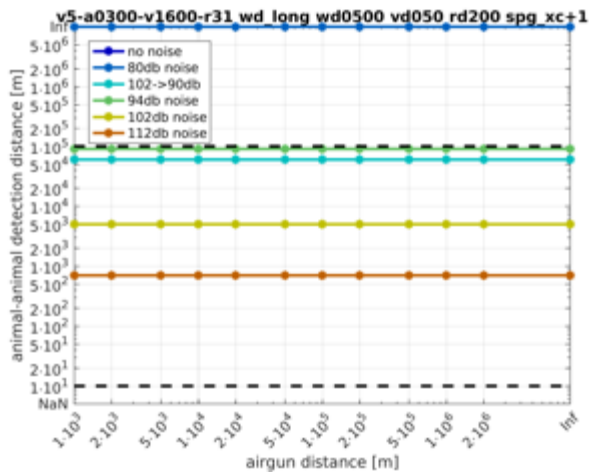
9.1.5.1.3 Propagation of airgun is modelled by numerical transfer functions, propagation of vocalization is modelled assuming spherical spreading

9.1.5.1.3.1 Water depth is 500 m; Full band analysis

► Receiver depth is 10 m:
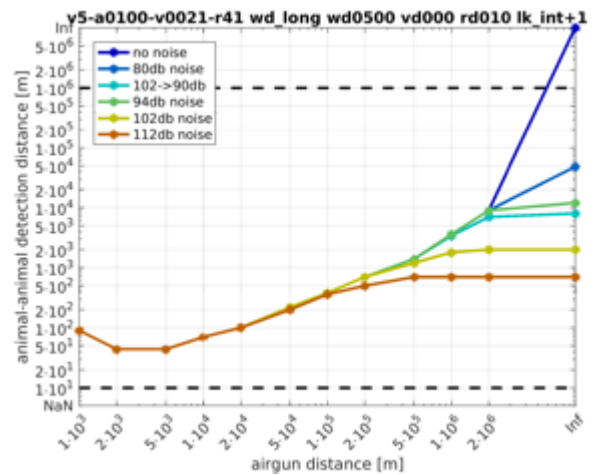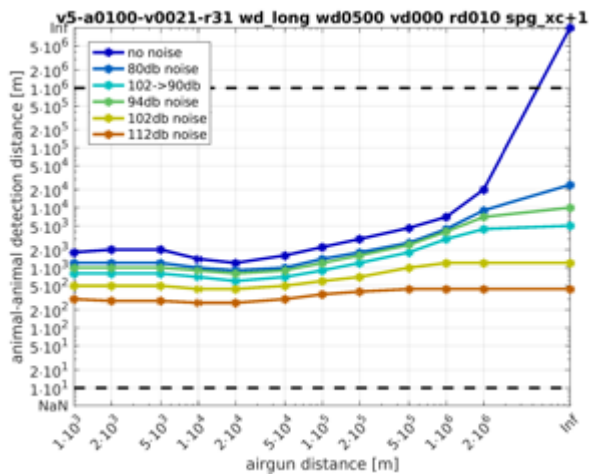
► Receiver depth is 50 m:
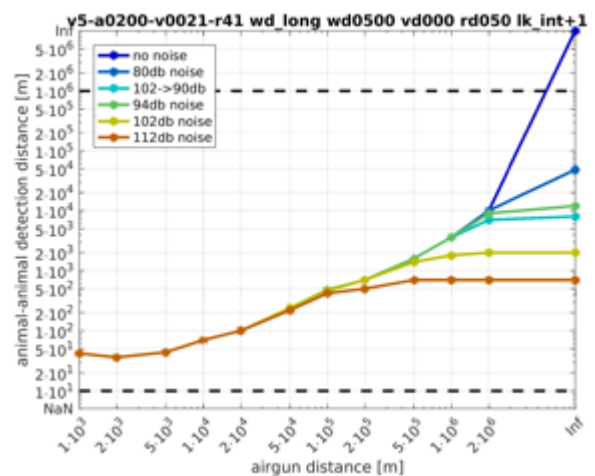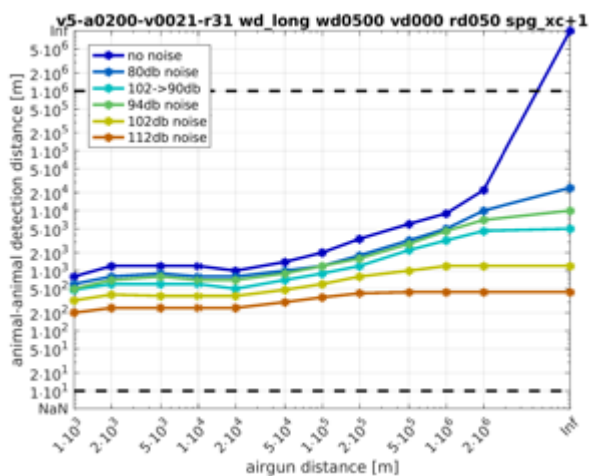
► Receiver depth is 200 m:
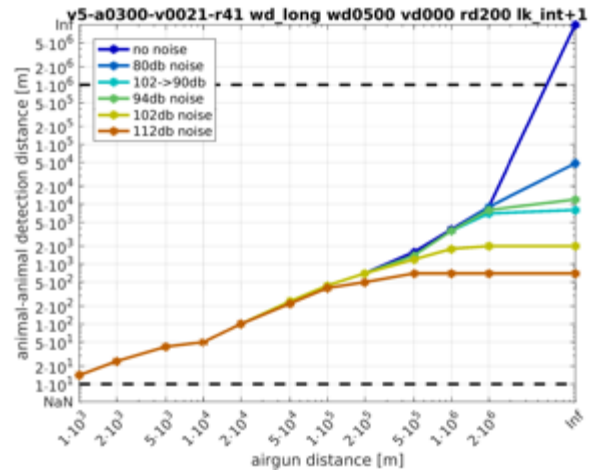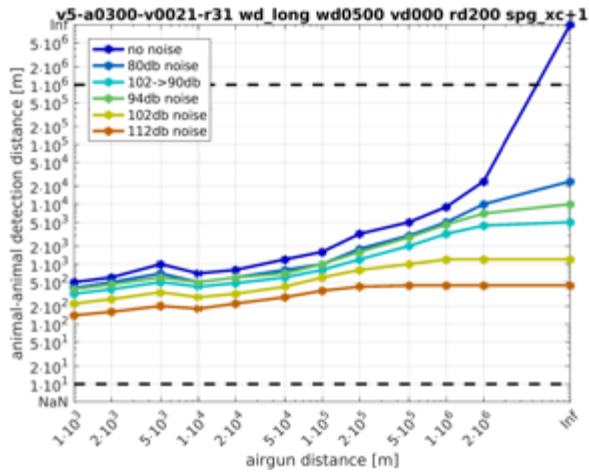
9.1.5.1.3.2 Water depth is 500 m; High pass analysis

► Receiver depth is 10 m:
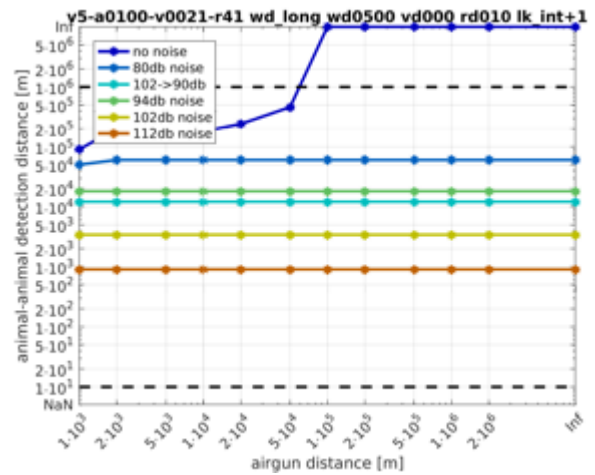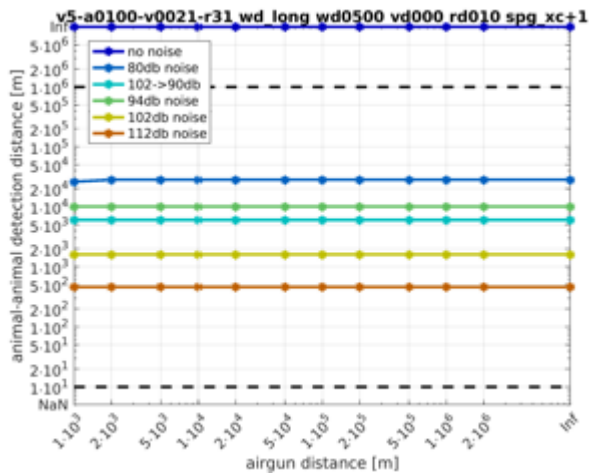
► Receiver depth is 50 m:
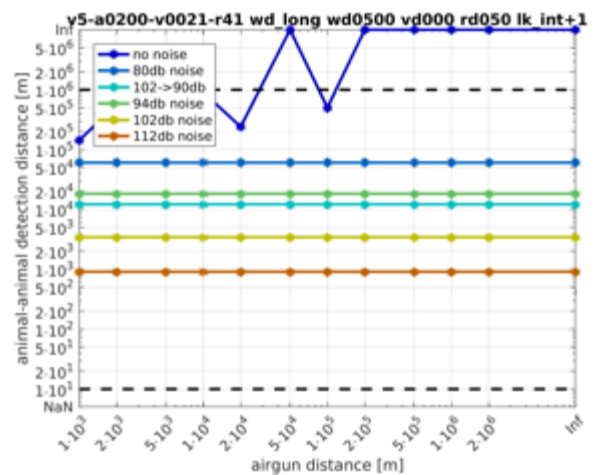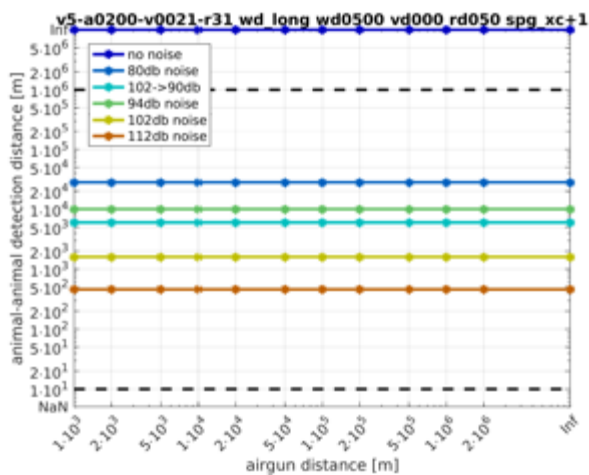
► Receiver depth is 200 m:
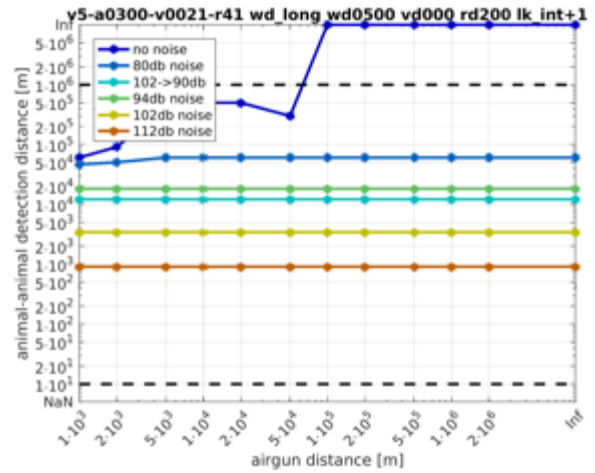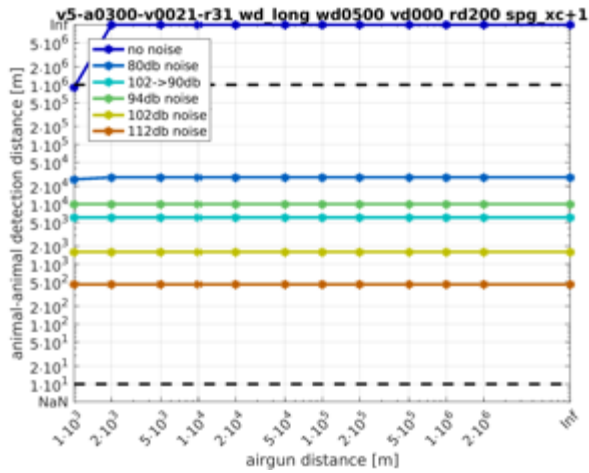
### 9.1.5.1.3.3 Water depth is 4000 m; Full band analysis

► Receiver depth is 10 m:
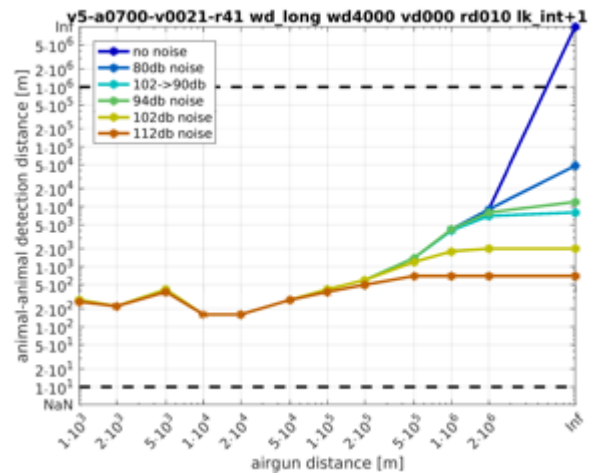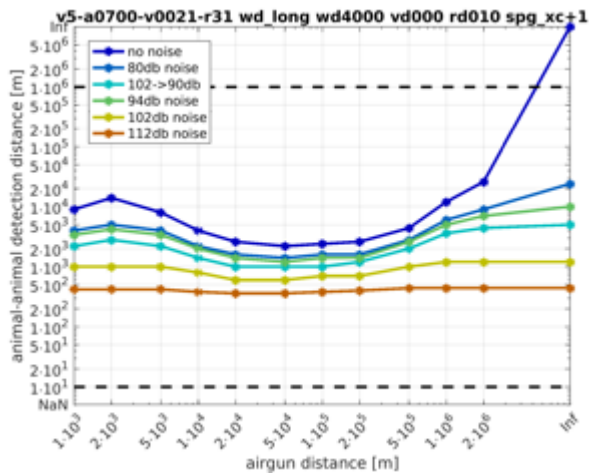
► Receiver depth is 50 m:
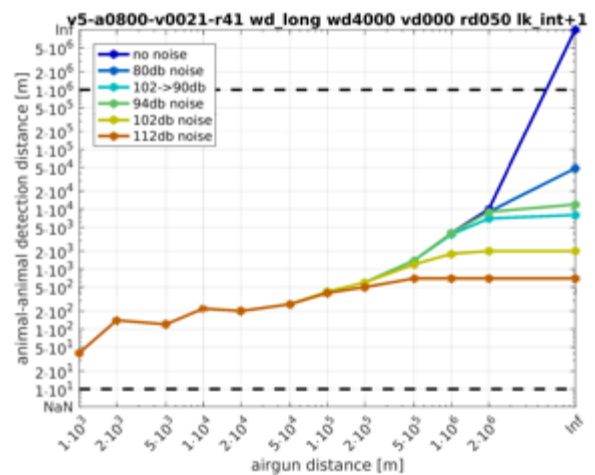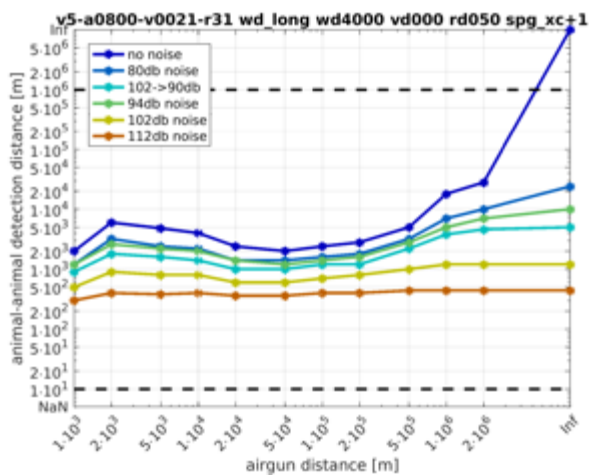
► Receiver depth is 200 m:
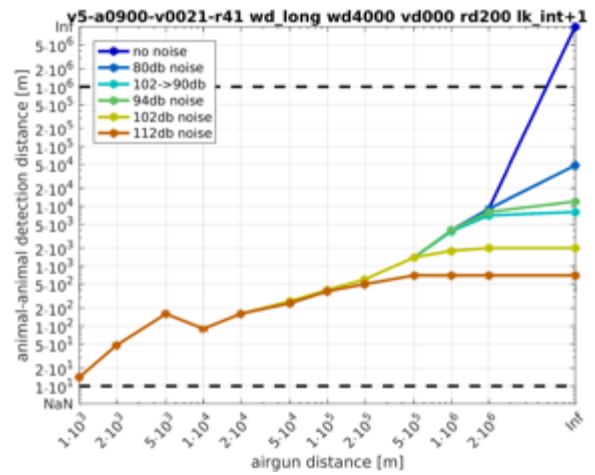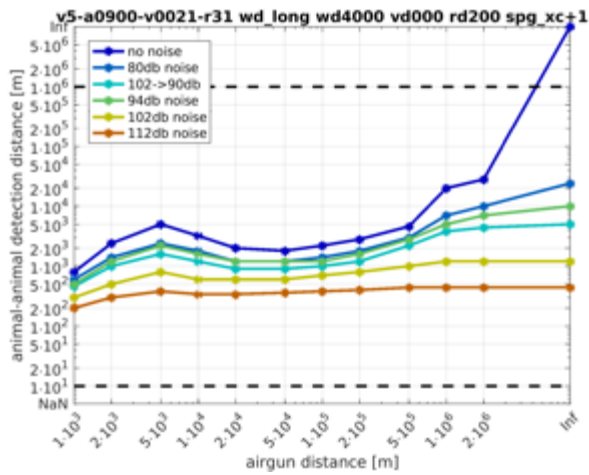
9.1.5.1.3.4   Water depth is 4000 m; High pass analysis

► Receiver depth is 10 m:
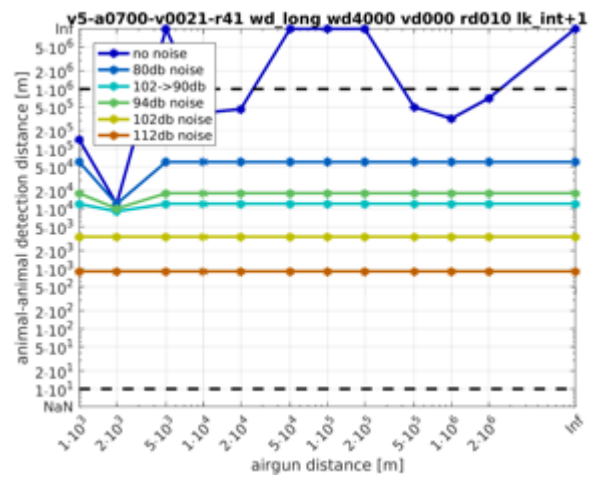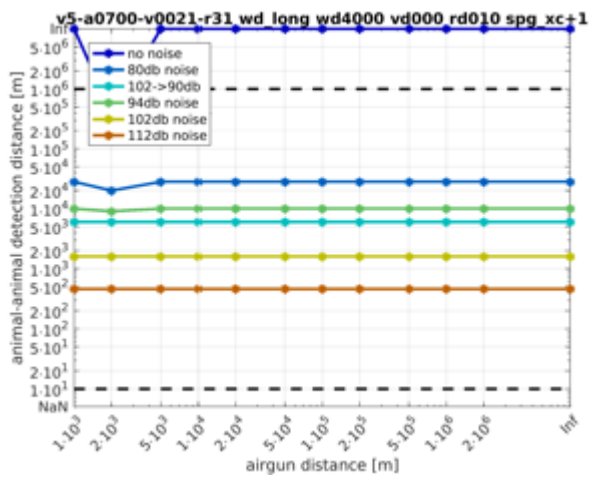

► Receiver depth is 50 m:
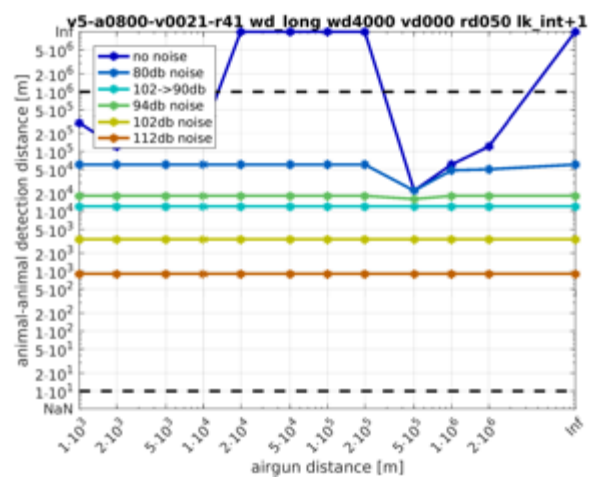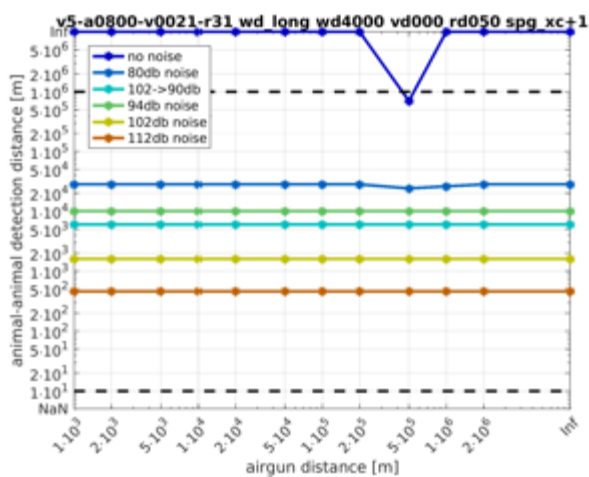
► Receiver depth is 200 m:
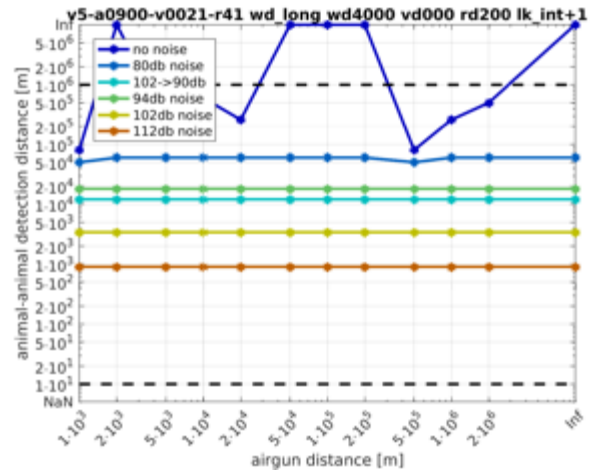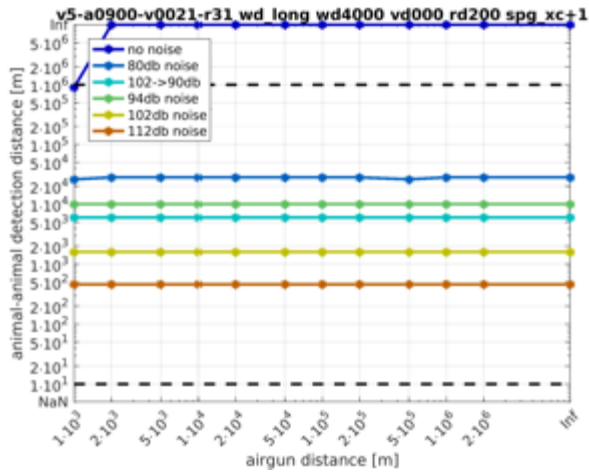
9.1.5.1.4 Propagation of airgun and vocalization is modelled assuming spherical spreading

9.1.5.1.4.1 Full band analysis
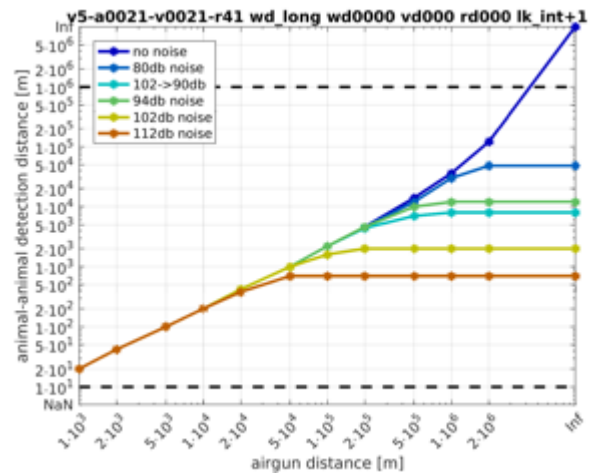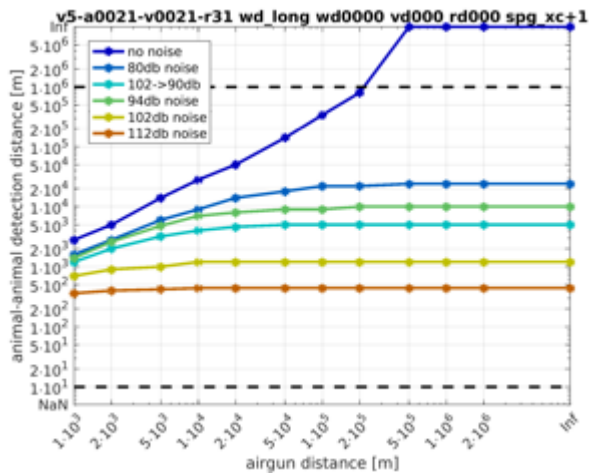
9.1.5.1.4.2 High pass analysis
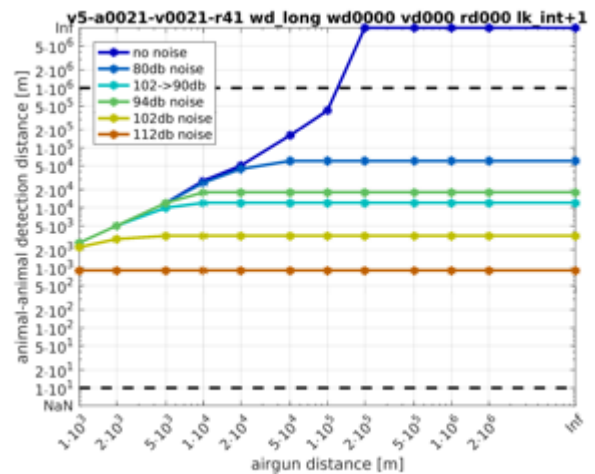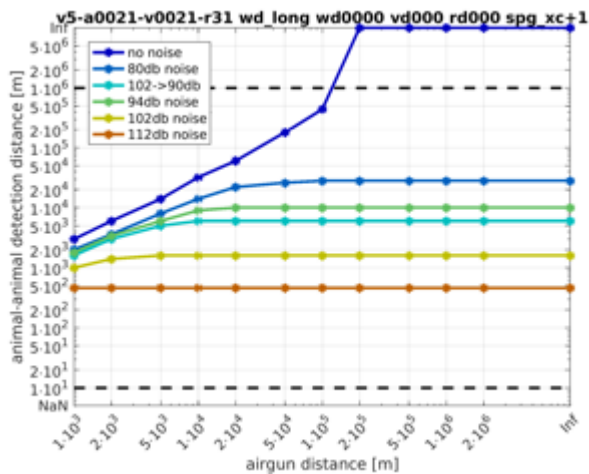
9.1.6 Weddell seal call train

9.1.6.1 Propagation of both airgun and vocalization are modelled by numerical transfer functions

9.1.6.1.1 Vocalization depth is 5 m

9.1.6.1.1.1 Water depth is 500 m; Full band analysis

► Receiver depth is 10 m:
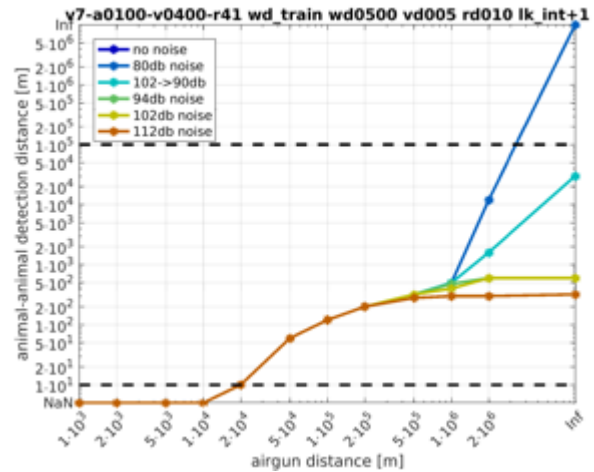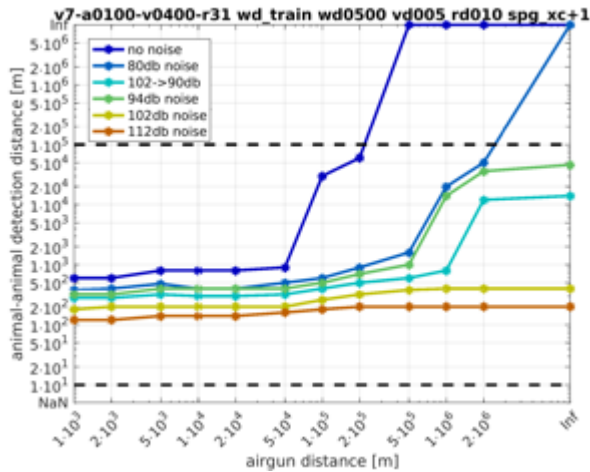

► Receiver depth is 50 m:
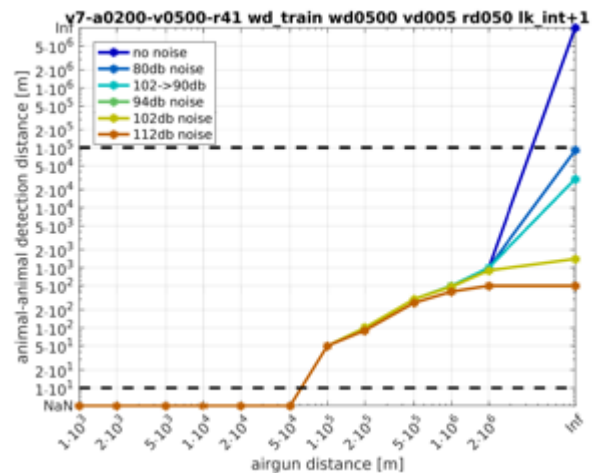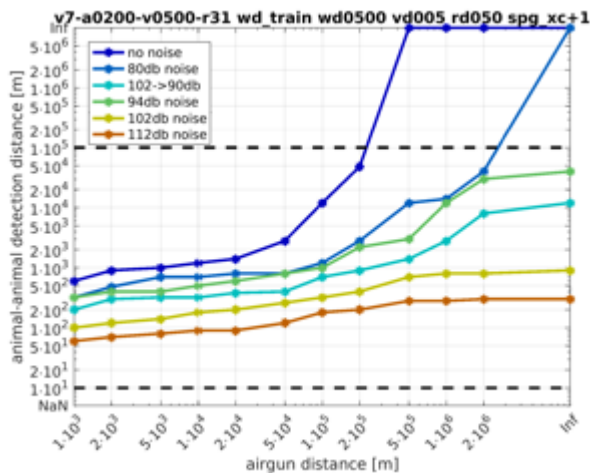
► Receiver depth is 200 m:
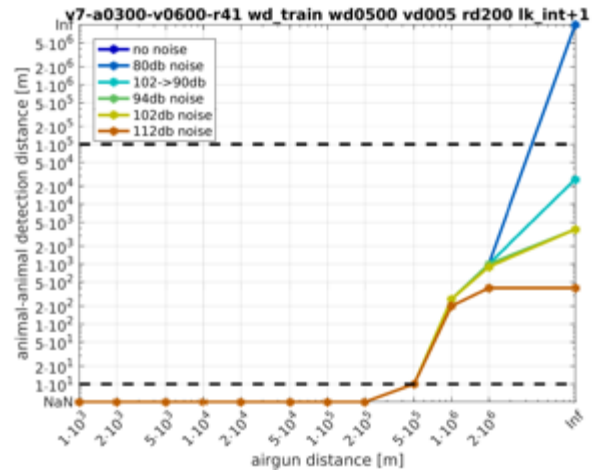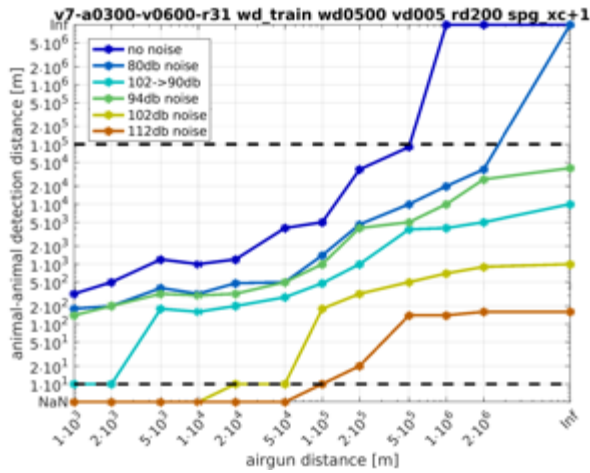
9.1.6.1.1.2 Water depth is 500 m; High pass analysis

► Receiver depth is 10 m:
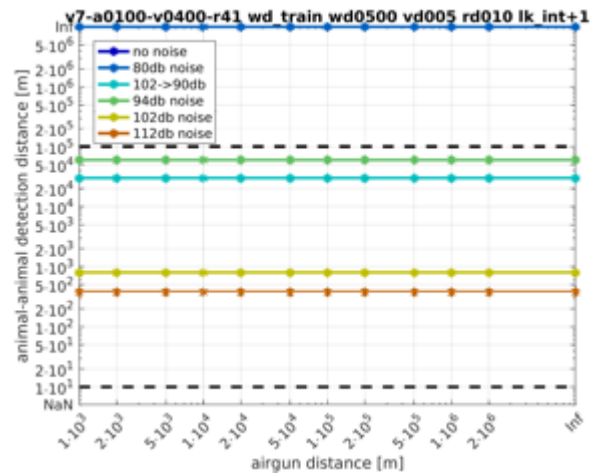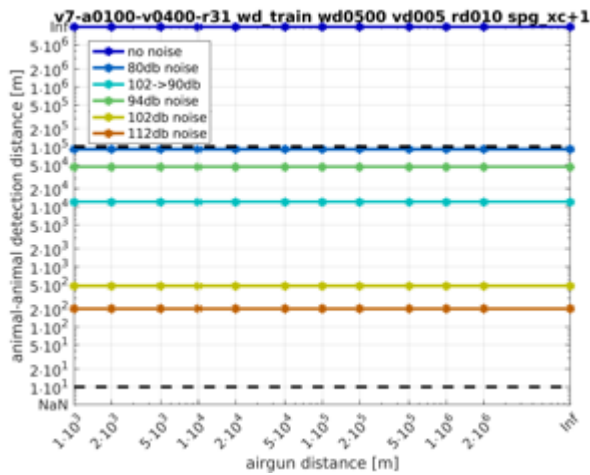

► Receiver depth is 50 m:
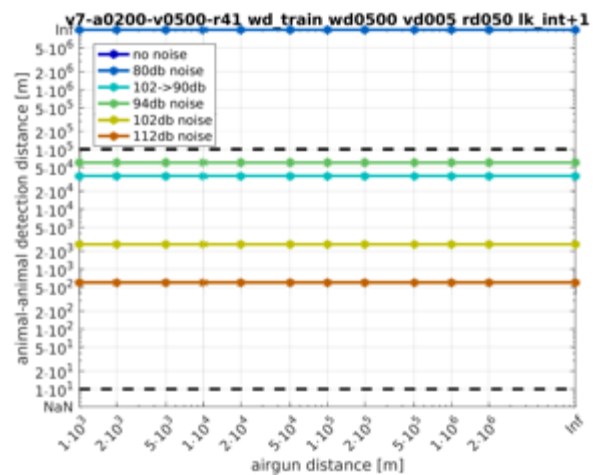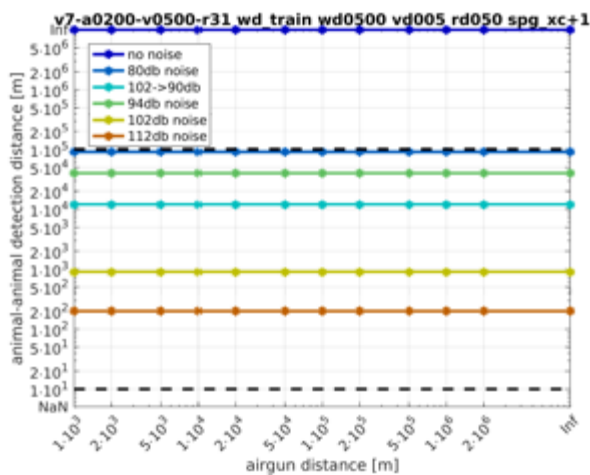
► Receiver depth is 200 m:
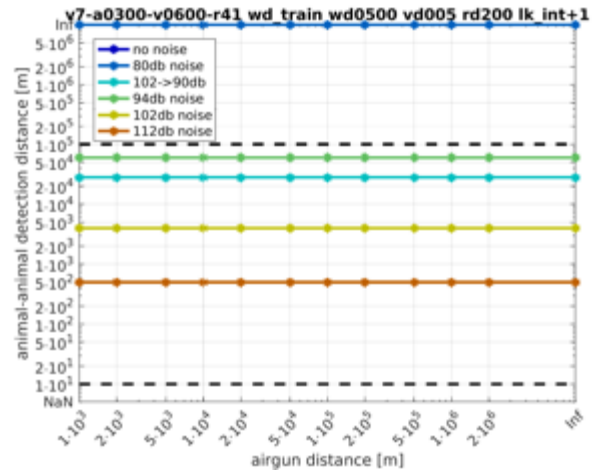
9.1.6.1.2 Vocalization depth is 50 m

9.1.6.1.2.1 Water depth is 500 m; Full band analysis

► Receiver depth is 10 m:

► Receiver depth is 50 m:

► Receiver depth is 200 m:

9.1.6.1.2.2 Water depth is 500 m; High pass analysis

► Receiver depth is 10 m:

► Receiver depth is 50 m:

► Receiver depth is 200 m:

9.1.6.1.3 Propagation of airgun is modelled by numerical transfer functions, propagation of vocalization is modelled assuming spherical spreading

9.1.6.1.3.1 Water depth is 500 m; Full band analysis

► Receiver depth is 10 m:

► Receiver depth is 50 m:

► Receiver depth is 200 m:

9.1.6.1.3.2   Water depth is 500 m; High pass analysis

► Receiver depth is 10 m:

► Receiver depth is 50 m:

► Receiver depth is 200 m:

9.1.6.1.3.3 Water depth is 4000 m; Full band analysis

► Receiver depth is 10 m:

► Receiver depth is 50 m:

► Receiver depth is 200 m:

9.1.6.1.3.4 Water depth is 4000 m; High pass analysis

► Receiver depth is 10 m:

► Receiver depth is 50 m:
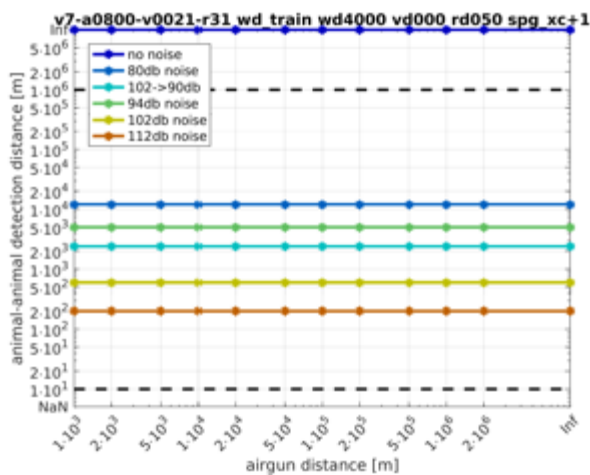
► Receiver depth is 200 m:
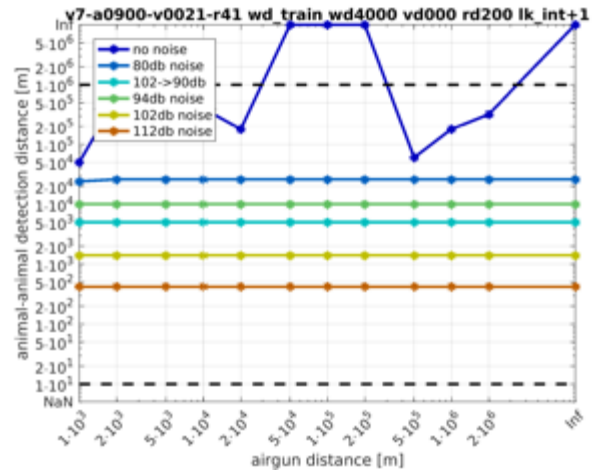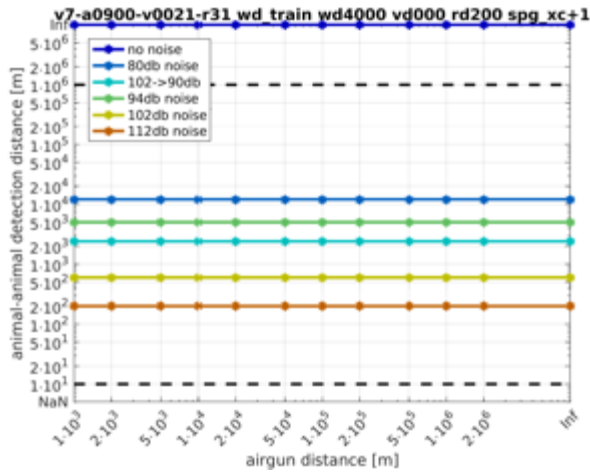
9.1.6.1.4 Propagation of airgun and vocalization is modelled assuming spherical spreading

9.1.6.1.4.1 Full band analysis
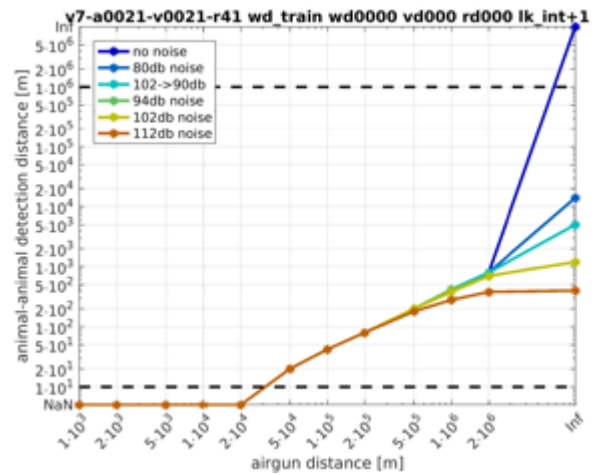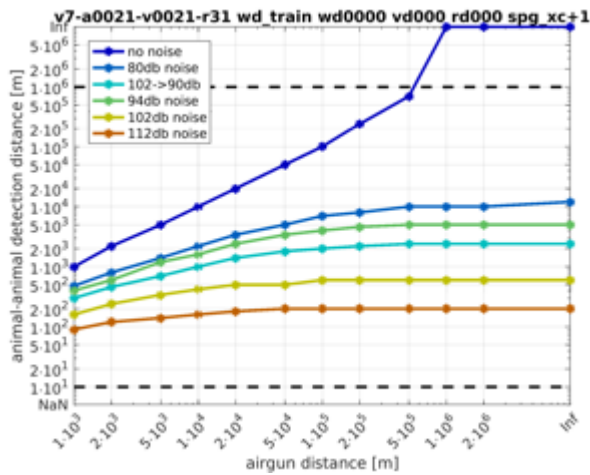
9.1.6.1.4.2 High pass analysis
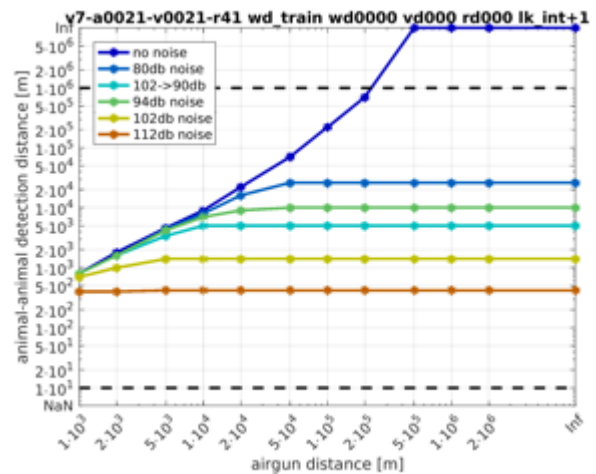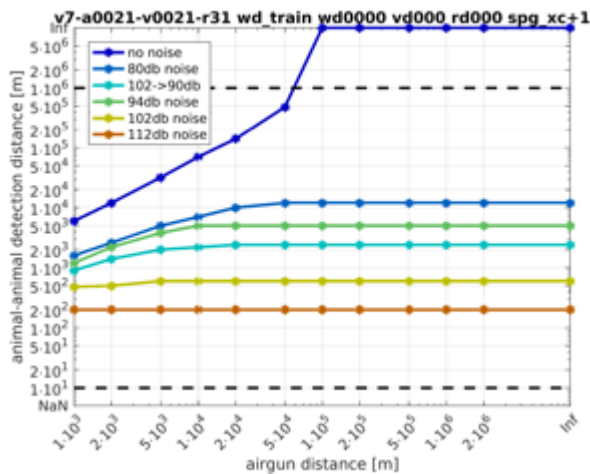
9.2 Appendix: Transfer functions

In the following figures the loss of transmitted total energy (blue line) of a dirac pulse and the reduction of its peak amplitude (black line) as predicted by the numerical propagation models is plotted against

the distance from the sound source. For comparison the energy loss when spherical spreading is assumed (red line) and the energy loss under the assumption of cylindrical spreading (green line) is also plotted.

Figures for the different scenarios are ordered by water depth (500 m or 4000 m), the upper limit of the modelled frequency range (375 Hz or 1500 Hz) and the receiver depth (5 m, 50 m or 200 m). The sound source is located 5 m (figures on the left) or 50 m (figures on the right) below the water surface.

9.2.1 Water depth 500 m

9.2.1.1 Upper limit of frequency range: 375 Hz

9.2.1.1.1 Receiver depth: 10 m
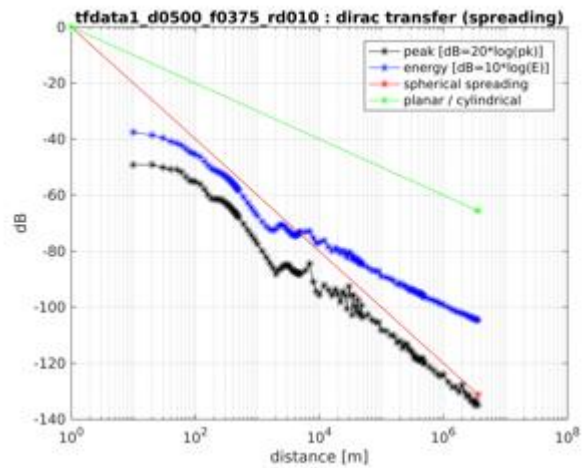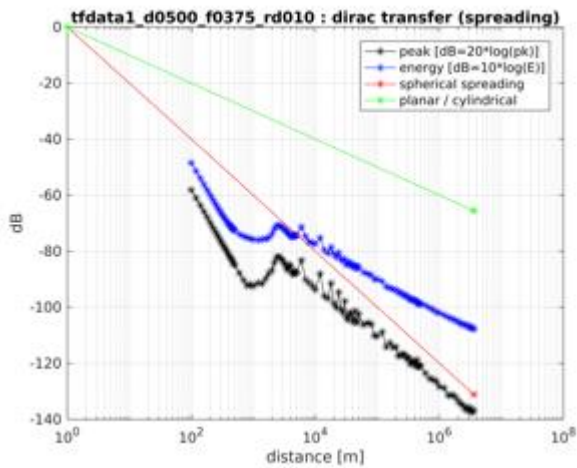
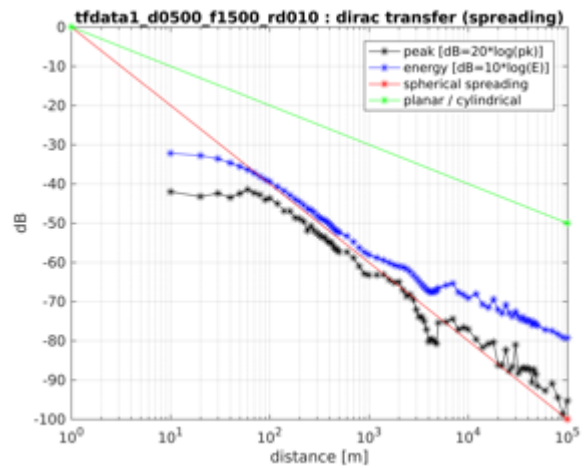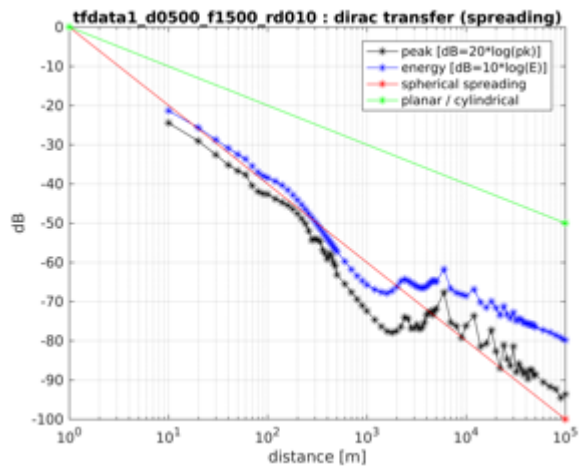##### 9.2.1.1.2 Receiver depth: 50 m
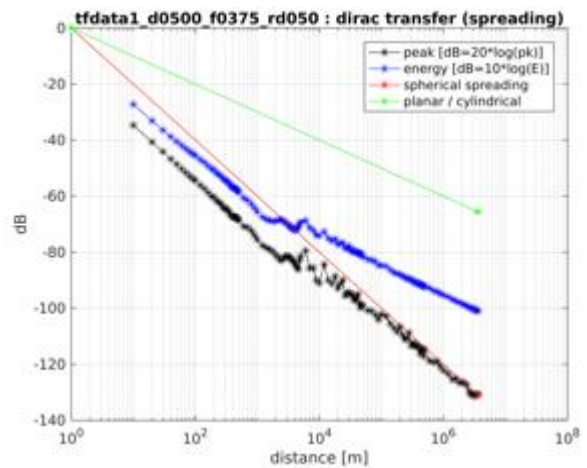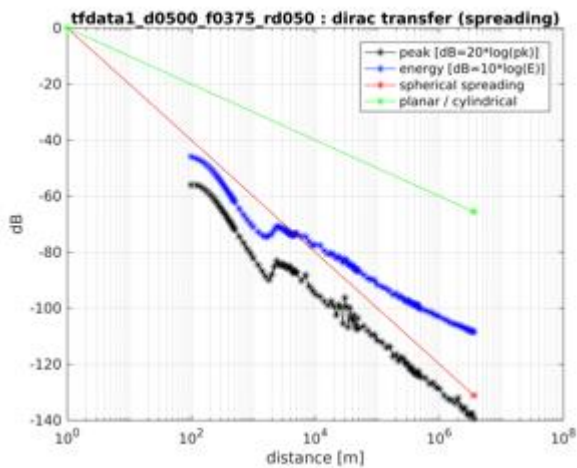
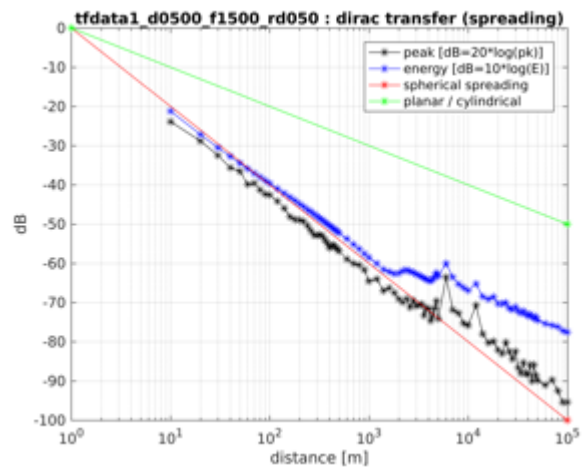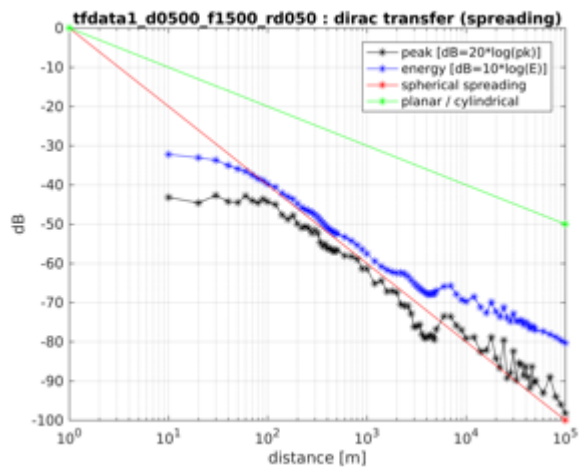### 9.2.1.1.3 Receiver depth: 200 m
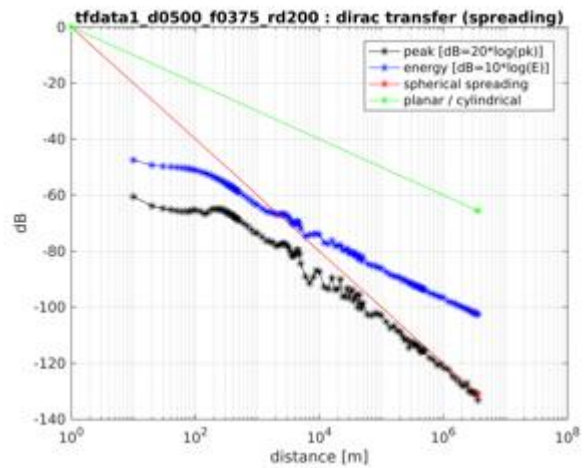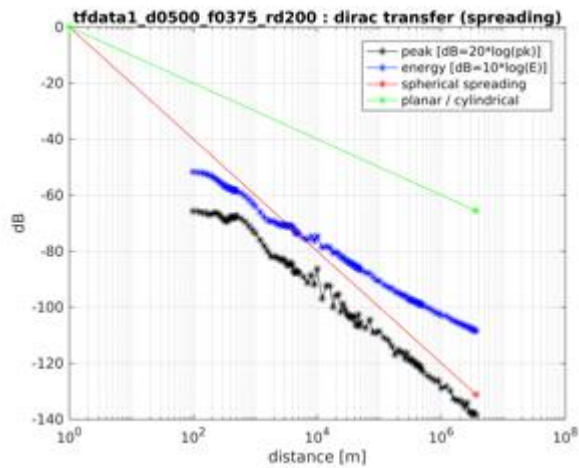
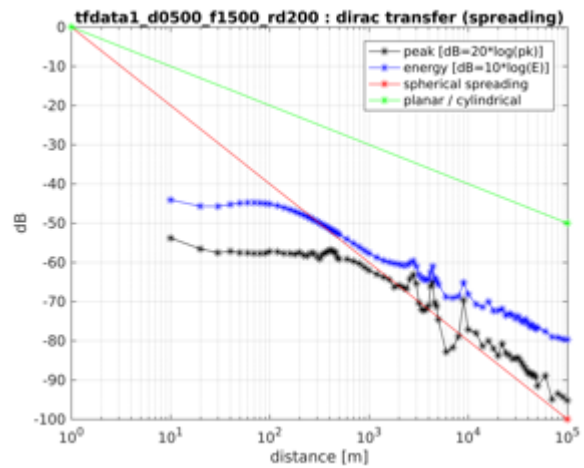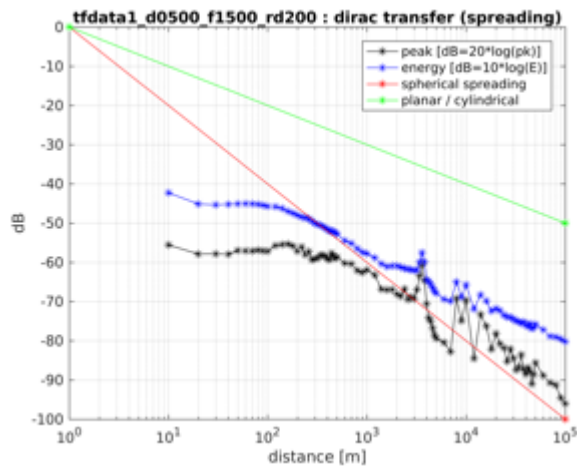### 9.2.1.2 Upper limit of frequency range: 1500 Hz

9.2.1.2.1 Receiver depth: 10 m
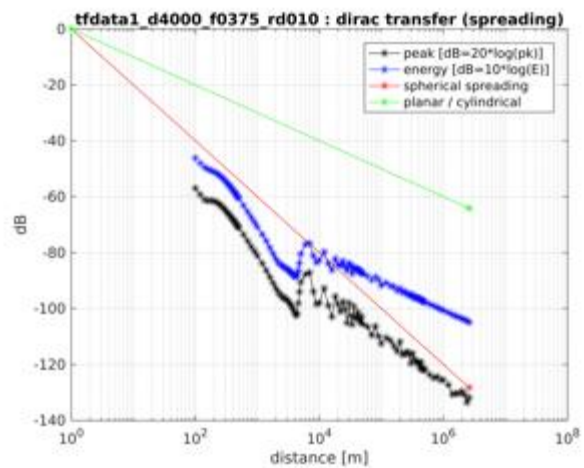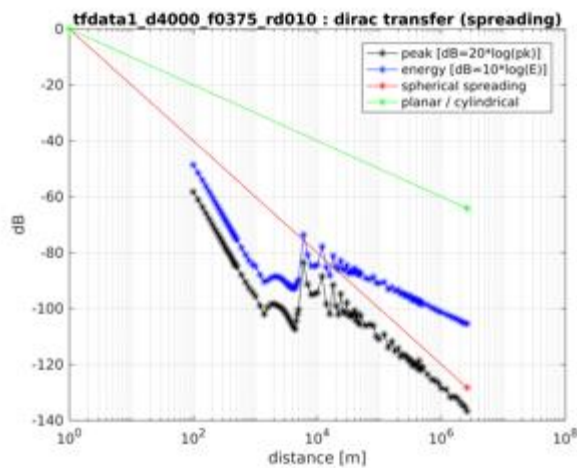

9.2.1.2.2 Receiver depth: 50 m

9.2.1.2.3   Receiver depth: 200 m
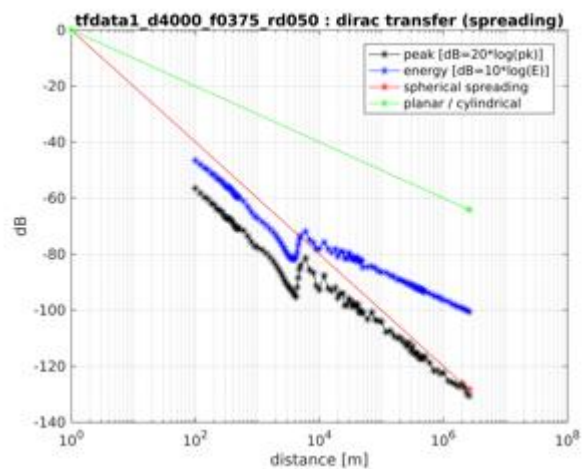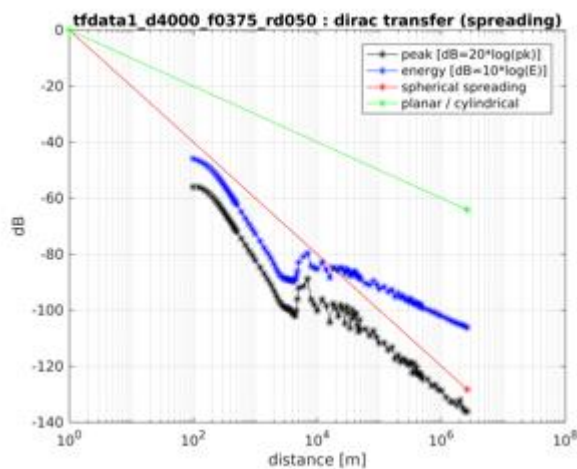

9.2.2   Water depth 4000 m
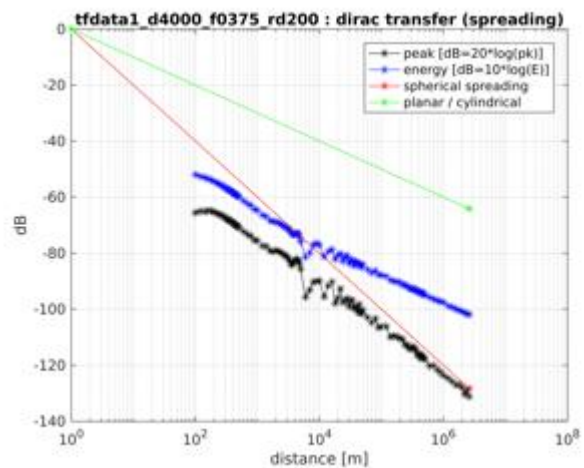
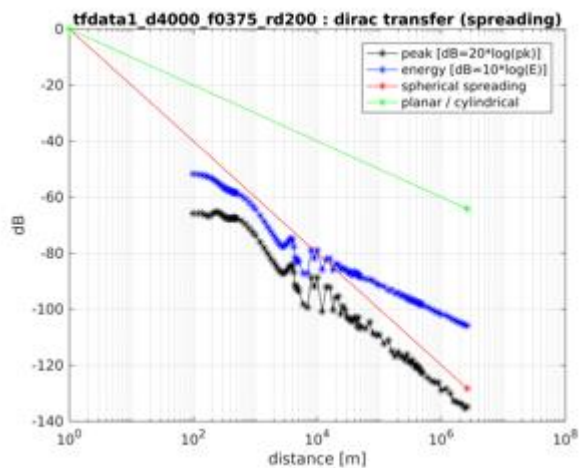### 9.2.2.1   Upper limit of frequency range: 375 Hz

9.2.2.1.1   Receiver depth: 10 m

9.2.2.1.2   Receiver depth: 50 m

9.2.2.1.3   Receiver depth: 200 m

9.3   Appendix: Parameters of the psychophysical model

	Blue Whale Z-Call	Fin Whale	Killer Whale Multiharmonic Call	Weddell Seal Long Call	Weddell Seal Call Train
Vocalisation Parameter					
short name	v1	v2	v3	v5	v7
source level [dB peak]	180	189	160	173	173
call duration [sec]	25	1	0.6	5	4.5
(assumed) repetition cycle [sec]	66	9.25	~(15)	~(15)	~(15)
Analysis Parameters					
Simulation Sampling rate [Hz]	200	200	4000	4000	4000
Spectrogram Correlator					
spg timestep [s]	0.1	0.1	0.025	0.025	0.025
spg frqresolution [Hz]	1	1	8	16	16
spg oversampling	4	4	4	4	4
spg intensity perception exponent	0.6	0.6	0.6	0.6	0.6
pattern vocalisations averaged	50	50	1	1	1
pattern smearing time [sec]	0	0.2	0.1	0.1	0.1
pattern smearing frequency [Hz]	0	1	10	16	16
Bandpass Spectrogram Correlator [Hz]	[15 30]	[12 24]	[10 1980]	[10 1980]	[10 1980]

	Blue Whale Z-Call	Fin Whale	Killer Whale Multiharmonic Call	Weddell Seal Long Call	Weddell Seal Call Train
Bandpass Spectrogram Correlator [Hz]			[500 1980]	[500 1980]	[500 1980]
Time Constant LI [sec]	25	1	0.6	5	4.5
Leaky Integrator					
Bandpass Leaky Integrator [Hz]	[15 30]	[12 24]	[10 1980]	[10 1980]	[10 1980]
Bandpass Leaky Integrator [Hz]			[500 1980]	[500 1980]	[500 1980]
Time Constant Leaky Integrator [sec]	25	1	0.6	5	4.5
Detection Statistics					
Detection Window [s]	120	20	15	15	15
Noise Phases	4	4	4	4	4
Airgun Phases	5	5	5	5	5
Vocalisation phases	7	7	7	7	7
Detection thresholds [dB]	0.1	0.1	0.1	0.1	0.1
ROC Parameters					
ROC AUC Criterion	0.9	0.9	0.9	0.9	0.9

	Blue Whale Z-Call	Fin Whale	Killer Whale Multiharmonic Call	Weddell Seal Long Call	Weddell Seal Call Train